Imperial College
London

Department of Earth Sciences and Engineering
Petroleum Engineering and Rock Mechanics Group

www.imperial.ac.uk/ese

Measurement and Modelling of Asphaltene Precipitation from Petroleum Fluids and the Effect of Resins and Amphiphiles

Lamia Goual

A thesis submitted in fulfilment of the requirements for the degree of Doctor of Philosophy of the University of London and the Diploma of Imperial College

11 August 2003

Copyright Notice

Imperial College of Science, Technology and Medicine
Department of Earth Science and Engineering

Measurement and Modelling of Asphaltene Precipitation from Petroleum Fluids and the Effect of Resins and Amphiphiles

© 2003 Lamia Goual
l.goual@imperial.ac.uk

This publication may be distributed freely in its entirety and in its original form without the consent of the copyright owner.

Use of this material in any other published works must be appropriately referenced, and, if necessary, permission sought from the copyright owner.

Published by: Lamia Goual
Department of Earth Science and Engineering
Imperial College London
South Kensington Campus
Prince Consort Road
London SW7 2BP

11 August 2003

www.imperial.ac.uk/ese

Abstract

This thesis presents a comprehensive experimental and modelling work on the study of asphaltene precipitation from petroleum fluids and the effect of resins and amphiphiles. Eight different petroleum fluids are fractionated into asphaltenes, resins, and oils. An experimental procedure is devised for resin measurement using the dipole moment as a criterion. The ASTM D-2007 adsorption method with some modifications is found to give the true resin amount provided no toluene is used to elute oils. The dipole moment of asphaltenes, resins, and oils is calculated from the Onsager formulation, which relates the dipole moment to the dielectric constant (measured by dielectric spectroscopy), refractive index, density, and molecular weight. The calculated dipole moments are in the range of 3.3–7.0 D (asphaltenes), 2.4–3.2 D (resins), and 0–0.9 D (oils). The effect of resins and dodecyl benzene sulfonic acid (DBSA) amphiphile on precipitation from three petroleum fluids is also examined. Addition of resins to the fluids increases the onset point of precipitation –the increase is more pronounced with the most polar resins– and the amount of precipitation, which is undesirable. When DBSA is mixed with the fluids at different concentrations, an increase then a decrease in the precipitation is observed with increasing DBSA concentration. Thus, the amphiphile is not effective before a certain concentration. The data provide a basis for successful field applications and show that electrostatic and inductive interactions between molecules in petroleum fluids may not be negligible. The experimental results are also used as reference data for the revision of a thermodynamic micellization model. Introduction of inductive forces and a new mixing rule in the PR-EOS allows a high concentration of asphaltene monomers in the bulk liquid. As a result, the effect of various n-alkanes is modelled properly. The predictions at low dilution ratio are improved with a new formulation of the interfacial tension between asphaltene core and surrounding shell. The revised model can be used at both stock tank and reservoir conditions. It also allows the study of the effect of resins on precipitation.

Acknowledgements

Firstly and foremostly, I would like to express my deepest gratitude to Allah for all his love and blessings and for opening the doors to wonderful horizons.

I would like to thank my supervisor Professor Abbas Firoozabadi, Head of the Reservoir Engineering Research Institute (RERI) in Palo Alto and visiting Professor at Imperial College London, for providing the opportunity, guidance, financial support and, most important, encouragement and enthusiasm for good research. I am grateful to my co-supervisor Professor Alain Gringarten for his invaluable help and assistance. I wish to thank Professor George Jackson from Imperial College and Professor Dominique Richon from Ecole des Mines de Paris for serving on my graduate committee. I also would like to acknowledge the kind support and guidance of Professor John Prausnitz from the University of California Berkeley, Professor Masoud Mehdizadeh from Cal Poly San Luis Obispo, and the appreciated help of Huanquan Pan, Tom Tang, Ross Jahanian, and Debbie Rowland from RERI.

To my friends who adopted me in their own families, I would like to thank my dear Roula and Abdallah Harb, Daiana and Kassem Ghorayeb, Dahbia and Sofiene Soukane. I have found in every shelter the warmest love and support. To all my friends in Palo Alto: Jorge Palomino Monteagudo, Mohammad Karimi-Fard, Erik Santiso, Reza Banki, Aditya Darsi, and Renato Santos, I would never thank them enough for always being there when I needed help or just a cheer-up. I am truly grateful to Erik, Jorge, and Mohammad for the nice moments spent together and for sharing their vast knowledge and wisdom. In the college have been a succession of dedicated students and staff– too many to name them all. Special thanks go to my dear Mohammad Piri whom I hold in very high esteem, my faithful friend Moncef Tanfour, my wonderful officemates Widad Al-Wardy and Rifaat Al-Mjeni, Azzan, Al-Yaarubi, Carlos Grattoni, Saifon Daungkaew, Florian Hollaender, Thomas von Schroeter, and many more who made my stay in the college very enjoyable. Thanks to all of whom have made contribution to the realization and critics of this thesis.

I am forever indebted to my dear parents for their continued love, prayers and encouragements, to my brother Jawed and sister Lynda and family for their love and endless support.

Table of contents

Abstract 3

Acknowledgements 4

Table of Contents 5

List of figures 9

List of tables 13

Nomenclature 15

Chapter 1 Introduction 19

1.1 Preamble 19

1.2 Research objectives 22

1.3 Approach 22

1.4 Thesis outline 23

1.5 References 24

Chapter 2 Measurement Asphaltene and resin amounts in petroleum fluids 26

2.1 Introduction 26

2.2 Experimental 29

2.2.1 Asphaltene precipitation 31

2.2.2 Resin precipitation 31

2.2.3 Resin adsorption 34

2.3 Results 34

2.4 Conclusions 39

2.5 References 39

Chapter 3 Molecular size of asphaltenes and resins 42
3.1 Introduction 42
3.2 Theory 44
3.2.1 Absorption 44
3.2.2 Fluorescence emission 45
3.2.2.1 Anisotropic polarization decay 45
3.3 Experimental 49
3.3.1 Sample preparation 49
3.3.2 CARY 500 absorption spectrometer 49
3.3.3 PTI C-72 and A-720 emission spectrometer 50
3.4 Results 52
3.4.1 Absorption spectroscopy 52
3.4.2 Fluorescence emission spectroscopy 53
3.4.2.1 Steady state 53
3.4.2.2 Time resolved 53
3.5 Conclusions 57
3.6 References 57

Chapter 4 Dipole moment of asphaltenes, resins, and oils 59
4.1 Introduction 59
4.2 Theory of dipole moment of molecules 61
4.2.1 The Clausius and Mosotti theory 63
4.2.2 The Debye theory 65
4.2.3 The Onsager theory 68
4.3 Experimental 69
4.3.1 Dielectric constant 69
4.3.2 Refractive index 70
4.3.1 Density 70
4.4 Results 72
4.4.1 Dipole moment verification 72
4.4.2 Dipole moment of asphaltenes, resins, and oils 75
4.5 Conclusions 84
4.6 References 85

Chapter 5 Effect of resins and DBSA amphiphile on precipitation 89
5.1 Introduction 90
5.2 Experimental 93
5.3 Results 94
5.3.1 Solubility of resins 94
5.3.2 Effect of resins on precipitation 96
5.3.2.1 Effect of resin concentration 96
5.3.2.2 Effect of various resins 99
5.3.3 Effect of additional asphaltenes on precipitation 103
5.3.4 Effect of DBSA amphiphile on precipitation 104
5.3.5 Comparison between resins and DBSA 107
5.3.6 Electrostatic and induction vs. dispersion interactions .. 109
5.4 Conclusions 110
5.5 References 111

Chapter 6 Revised thermodynamic micellization model for asphaltene precipitation 114
6.1 Introduction 114
6.2 Model description 121
6.2.1 Characterization of the plus fraction and implementation of different asphaltic species 121
6.2.2 The induction energy 121
6.2.3 The Wong and Sandler Mixing rule in the PR-EOS 125
6.2.3.1 Verification with various mixtures 130
6.2.4 Interfacial tension and asphaltene-core pressure 132
6.2.5 Formulation of the Gibbs free energy 138
6.2.5.1 Standard Gibbs free energy of micellization 139
6.2.5.2 Gibbs free energy of the liquid phase 140
6.2.5.3 Gibbs free energy of the precipitated phase 142
6.2.6 Model parameters 144
6.2.6.1 Interaction coefficients 145
6.2.6.2 Induction energy parameters 146
6.2.7 Minimization of the Gibbs free energy 146

6.3 Results 147
6.3.1 Precipitation from stock tank petroleum fluids 147
6.3.1.1 Effect of nC_5 and nC_7 n-alkanes 147
6.3.1.2 Effect of petroleum resins 152
6.3.2 Precipitation from reservoir fluids 158
6.4 Conclusions 161
6.5 References 162

Chapter 7 Conclusions and recommendations 168
7.1 Introduction 168
7.2 Conclusions from the experimental work 168
7.3 Conclusions from the modelling work 170
7.4 Recommendations 171

Appendix A Characterization of the plus fraction 172

Appendix B Standard Gibbs free energy of micellization 174

Bibliography 178

Publication 1 Measuring Asphaltenes and Resins, and Dipole Moment in Petroleum Fluids 191

Publication 2 Effect of Resins and DBSA on Asphaltene Precipitation from Petroleum Fluids 209

List of figures

Fig. 1.1 Paraffin and asphaltene deposition in flow lines 20

Fig. 1.2 Hydrocarbon group-type distribution for stable and unstable petroleum Fluids. (Carbognani *et al.*, 1999) 20

Fig. 2.1 Procedure for asphaltene precipitation from petroleum fluids 32

Fig. 2.2 Experimental set up for asphaltene precipitation from petroleum fluids 33

Fig. 2.3 Propane test apparatus 33

Fig. 2.4 Photograph of asphaltenes, resins, and oils from petroleum fluid H 37

Fig. 2.5 Increase of the dielectric constant of resins with the amount of toluene in the eluting solvent of oils 38

Fig. 3.1 Plot of the emission spectra for the four smallest aromatic molecules: benzene, naphthalene, anthracene, and tetracene. (Haken *et al.*, 1994) 44

Fig. 3.2 Excitation and fluorescence emission of a spherical molecule, which undergoes anisotropy decay. (Tao, 1969) 46

Fig. 3.3 Schematic of the optical arrangement of the CARY 500 absorption Spectrometer. (Groenzin, 1999) 50

Fig. 3.4 Schematic of the optical arrangement of the PTI C-72 and A720 emission Spectrometer. (Groenzin, 1999) 51

Fig. 3.5 Absorbance spectra of fractions from petroleum fluid H 53

Fig. 3.6 Normalized SSFES spectra of nC_5 asphaltenes and resins from petroleum fluids TK and H at 310 nm (a) and 390 nm (b) excitation wavelengths 54

Fig. 3.7 Normalized SSFES spectra of all the fractions separated from petroleum fluid H at 310 nm excitation wavelength 54

Fig. 3.8 TDFES lifetime spectra of nC_5 asphaltenes H at 365 nm excitation Wavelength (the four time-resolved fluorescence curves) 55

Fig. 3.9 TDFES lifetime spectra of nC_5 asphaltenes H at 365 nm excitation Wavelength (the fits of the difference and the sum curves) 55

Fig. 3.10 The rotational correlation times of nC_5 asphaltenes H and TK and nC_5 resins H vs. emission wavelength 56
Fig. 4.1 Schematic representation of the dielectric constant vs. frequency 63
Fig. 4.2 HP 4284A precision LCR meter connected to the HP 16452A liquid test fixture through HP 16048A test leads 71
Fig. 4.3 HP16452A liquid test fixture 71
Fig. 4.4 Dielectric constant and refractive index vs. concentration of ethanol in toluene 74
Fig. 4.5 Dielectric constant and refractive index vs. concentration of nC_5 asphaltenes, resins and oils in toluene for petroleum fluid H 77
Fig. 4.6 Dielectric constant and refractive index vs. concentration of nC_5 asphaltenes, resins and oils in toluene for petroleum fluid B 78
Fig. 4.7 Dielectric constant and refractive index vs. dipole moment of nC_5 asphaltenes and resins 83
Fig. 5.1 Solubility of resins C in nC_5, oils C and petroleum fluid C 95
Fig. 5.2 Solubility of various resins in petroleum fluids TK and C 95
Fig. 5.3 Precipitation by nC_5 from petroleum fluid U for various concentrations of resins U 97
Fig. 5.4 Precipitation by nC_5 from petroleum fluid TK for various concentrations of resins TK 97
Fig. 5.5 Precipitation by nC_5 from petroleum fluid C for various concentrations of resins C 98
Fig. 5.6 Precipitation by nC_5 from petroleum fluid U for various additional resins .. 101
Fig. 5.7 Precipitation by nC_5 from petroleum fluid TK for various additional resins 101
Fig. 5.8 Precipitation by nC_5 from petroleum fluid C for various additional resins .. 102
Fig. 5.9 Relative increase in the amount of precipitation by nC_5 in petroleum fluids U, TK, and C with additional resins 102
Fig. 5.10 Precipitation by nC_5 from petroleum fluid U for various concentrations of resins and asphaltenes U 103
Fig. 5.11 Precipitation by nC_5 from petroleum fluid U for various concentrations of DBSA 104
Fig. 5.12 Precipitation by nC_5 from petroleum fluid TK for various concentrations of DBSA 105

Fig. 5.13 Precipitation by nC_5 from petroleum fluid C for various concentrations of DBSA 105
Fig. 5.14 Relative increase in amount of precipitation by nC_5 in petroleum fluids U, TK, and C with various concentrations of DBSA 107
Fig. 5.15 Normalized population size distribution (by SSFES) of the precipitate from petroleum fluid U for various concentrations of resins U and DBSA 108
Fig. 6.1 Induced interaction between a dipolar and a non-polar molecule 123
Fig. 6.2 Saturation pressure vs. mole fraction of some organic mixtures. (A) WS parameters from source data, (B) WS parameters from NRTL model 131
Fig. 6.3 Saturation pressure vs. mole fraction of some aqueous mixtures. (A) WS parameters from source data 131
Fig. 6.4 Phase amount vs. pressure of some organic mixtures. (B) WS parameters from the NRTL model 132
Fig. 6.5 Conical section of a spherical inner liquid phase (′) surrounded by an outer liquid phase (″) 133
Fig. 6.6 Effect of the Tolman length parameter ζ on $\sigma(R)$ 135
Fig. 6.7 Variations of $\sigma(R)$, $\sigma_\infty(C)$, $\sigma(R,C)$, and σ (Helfand and Tagami, 1971) with nC_5 dilution ratio for petroleum fluid TK 137
Fig. 6.8 Effect of $\sigma(R)$, $\sigma(R,C)$ and σ (Helfand & Tagami, 1971) on asphaltene precipitation by nC_5 from petroleum fluid TK with the revised model 138
Fig. 6.9 Variation of G with nC_5 dilution ratio for petroleum fluid TK 143
Fig. 6.10 Effect of n-alkanes on asphaltene precipitation from petroleum fluid TK with the original model 148
Fig. 6.11 Effect of the WS mixing rule and the induction energy on the amount of precipitation from petroleum fluid TK 148
Fig. 6.12 Effect of n-alkanes on asphaltene precipitation from petroleum fluid TK ... 149
Fig. 6.13 Effect of n-alkanes on asphaltene precipitation from petroleum fluid C 149
Fig. 6.14 Effect of n-alkanes on asphaltene precipitation from petroleum fluid U 150
Fig. 6.15 Effect of n-alkanes on asphaltene precipitation from petroleum fluid Mex-C 150
Fig. 6.16 Effect of n-alkanes on asphaltene precipitation from petroleum fluid Mex-Y3 150
Fig. 6.17 Effect of n-alkanes on asphaltene precipitation from petroleum fluid

Mex-P 151
Fig. 6.18 Effect of n-alkanes on the core radius and number of micelles in petroleum fluid TK 152
Fig. 6.19 Effect of n-alkanes on the number of asphaltene and resin molecules in the micelles of petroleum fluid TK 152
Fig. 6.20 Effect of n-alkanes on the number of asphaltene and resin monomers in petroleum fluid TK 152
Fig. 6.21 Effect of resins on the dielectric constant of the medium 153
Fig. 6.22 Effect of additional resins from petroleum fluid TK on precipitation from the same petroleum fluid (Resins = 19.9 wt%) 154
Fig. 6.23 Effect of additional resins from petroleum fluid C on precipitation from the same petroleum fluid (Resins = 17.8 wt%) 154
Fig. 6.24 Effect of additional resins from petroleum fluid U on precipitation from the same petroleum fluid (Resins = 22.6 wt%) 155
Fig. 6.25 Effect of resin concentration on asphaltene precipitation from petroleum fluid TK 156
Fig. 6.26 Effect of resin concentration on asphaltene precipitation from petroleum fluid C 156
Fig. 6.27 Effect of resin concentration on asphaltene precipitation from petroleum fluid U 157
Fig. 6.28 Effect of resins from petroleum fluid TK on the core radius and number of micelles in the same petroleum fluid 157
Fig. 6.29 Effect of resins from petroleum fluid TK on the number of asphaltene and resin molecules in the micelles of the same petroleum fluid 158
Fig. 6.30 Effect of resins from petroleum fluid TK on the number of asphaltene and resin monomers in the same petroleum fluid 158
Fig. 6.31 Asphaltene and resin precipitation from the Weyburn petroleum fluid 159
Fig. 6.32 Asphaltene and resin precipitation from the Hirshberg petroleum fluid 160
Fig. 6.33 Pressure at the onset of precipitation and bubble point pressure of the North Sea petroleum fluid 160
Fig. 6.34 Asphaltene and resin precipitation from the North Sea petroleum fluid 160
Fig. B.1 Schematic representation of micelle formation. (Pan and Firoozabadi, 1998) 175

List of tables

Table 2.1 Petroleum fluids 30

Table 2.2 Composition of three selected petroleum fluids at ambient conditions 30

Table 2.3 Amount of asphaltenes precipitated by nC_5, nC_7 and nC_{10} from the petroleum fluids 35

Table 2.4 Amount of asphalt (that is, asphaltenes and resins) precipitated by propane from the petroleum fluids and from the nC_5 deasphaltened fluids ... 35

Table 2.5 Amount of resins adsorbed on clay after elution of oils with nC_5, nC_7 and nC_{10} 36

Table 2.6 Amount of resins adsorbed on clay after elution of oils with various nC_5/ toluene mixtures 36

Table 2.7 Dipole moment (in Debye) of resins 38

Table 2.8 Nitrogen content of oils from petroleum fluids H and C eluted with various nC_5/toluene mixtures 39

Table 3.1 Results of the TDFES measurements 56

Table 4.1 Differentiation methods of Debye equation for binary mixtures of polar solute (species 2) in nonpolar solvent (species 1) 67

Table 4.2 Substances with known dipole moments 73

Table 4.3 Dipole moment of substances from different methods 75

Table 4.4 Dielectric constant, refractive index, density and molecular weight of nC_5 asphaltenes, resins and oils 79

Table 4.5 Dielectric constant and refractive index of asphaltenes and resins reported in the literature 79

Table 4.6 Dipole moment (in Debye) of asphaltenes, resins and oils 81

Table 4.7 Dipole moment (in Debye) of distillation cuts from an asphaltic petroleum fluid and a waxy petroleum fluid 81

Table 4.8 Effect of charge separation on the dipole moment 82

Table 4.9 Effect of heteroatoms on the dipole moment 82

Table 5.1 Concentration of additional resins in petroleum fluids U, TK, and C 98
Table 5.2 Resin precipitation from petroleum fluids U, TK, and C 99
Table 6.1 Selected petroleum fluids 122
Table 6.2 Composition (mole %) of selected petroleum fluids 122
Table 6.3 Activity coefficient at infinite dilution for several solute-solvent systems using the MOSCED model 128
Table 6.4 Volume shift parameters of defined hydrocarbons 129
Table 6.5 Parameters of the modified NRTL model for several binary mixtures 130
Table 6.6 Relevant data of asphaltenes and resins 144
Table 6.7 Gibbs free energy of asphaltene association (kT units) 145
Table 6.8 Binary interaction coefficients between asphaltenes–hydrocarbons and resins–hydrocarbons 145
Table 6.9 Precipitation of additional resins from petroleum fluids and nC_5 154

Nomenclature

a	PR-EOS interaction parameter; molecular cross section area (m^2); area per molecule (m^2 $molecule^{-1}$)
A	Helmoltz free energy (J); Anisotropy constant
b	PR-EOS volume parameter
c	Constant in the WS mixing rule
C	Concentration (mole m^{-3}); capacitance (C^2 J^{-1})
CN	Number of carbon atoms in a molecule
D	Shell thickness (m), diffusion constant
e	Electric charge (C)
E	Magnitude of the electric field vector (C m^{-2})
$\boldsymbol{E}$	Electric field vector (C m^{-2})
f	Fugacity (atm)
F	Electric internal field (C m^{-2}), emission fluorescence
g	Gibbs free energy per molecule (J $molecule^{-1}$)
G	Gibbs free energy (J); calibration factor
$\boldsymbol{G}$	Cavity field vector (C m^{-2})
h	Molar enthalpy (J $mole^{-1}$)
I	Light intensity, ionization potential (J)
k	Boltzmann constant (= 1.381×10^{-23} J K^{-1})
K	Binary interaction coefficient in the PR-EOS
l	Non-randomness parameter in the NRTL model
L	Characteristic length of a molecule (m); inductance (H)
m	Parameter in the PR-EOS; ratio of molecular volumes
$\boldsymbol{m}$	Total dipole moment vector (C m)
M	Molecular weight (amu); Molar weight (g $mole^{-1}$)
n	Number of molecules, refractive index
N	Number density (molecule m^{-3})

N_A Avogadro number (= $6.022.10^{23}$ mol^{-1})

OD Optical density

P Pressure (atm); magnitude of the electric polarization (C m^{-2})

$\boldsymbol{P}$ Electric polarization vector (C m^{-2})

r Distance (m); emission anisotropy

R Radius of the micellar core (m); molecular radius (m); resistance (Ω)

$\boldsymbol{R}$ Reaction field vector (C m^{-2})

R Molar gas constant (J mol^{-1} K^{-1})

s Shift parameter

t Time (s)

T Temperature (K)

$\boldsymbol{u}$ Unit vector

U Potential energy (J)

v Molecular volume (m^3 $molecule^{-1}$)

v Molar volume (m^3 $mole^{-1}$)

$\bar{v}$ Corrected molar volume (m^3 $mole^{-1}$)

V Volume (m^3)

x Optical path length (m)

z Mole fraction

w Weight fraction

Greek symbols

α Polarizability (C^2 m^2 J^{-1}); absorption coefficient (m^2 mol^{-1})

α_v Polarizability volume (m^3)

χ Flory-Huggins interaction parameter

δ Solubility parameter (cal $cm^{-3})^{0.5}$

ε Dielectric constant

ε' Dielectric storage

ε'' Dielectric loss

ε_0 Permittivity of vacuum (= 8.854×10^{-12} C^2 J^{-1} m^{-1} or $1.11\times10^{-10}/4\pi$, F/m)

ϕ Volume fraction

Φ Electrostatic potential (J C^{-1})

φ	Fugacity coefficient
γ	Activity coefficient
η	Viscosity (Pa s)
λ	Wavelength (m)
μ	Magnitude of the dipole moment (C m, 1 D = 3.336×10^{-30} C m)
$\overline{\mu}$	Average magnitude of the dipole moment (C m)
$\boldsymbol{\mu}$	Dipole moment vector (C m)
ν	Frequency (s^{-1} or Hz)
θ	Angle (deg)
σ	Interfacial tension (N m^{-1})
ρ	Mass density (Kg m^{-3})
τ	NRTL binary interaction parameter; rotational correlation time (s)
ω	Acentric factor, solid angle
ζ	Tolman length parameter (m)

Subscripts

0	Standard state; vacuum
1	Asphaltene in micelle; solvent
$1a$	Monomeric asphaltene
$1r$	Monomeric resin
2	Resin in micelle; solute
∞	Infinite pressure; infinite dilution; flat interface
$\parallel, \perp$	Polarized light parallel and perpendicular to excitation plan
a	Asphaltene; absolute
ads	Adsorption
c	Critical
H	Hydrogen bonding
i, j	Component index; asphaltene and resin type index
liq	Liquid phase
m	Micelle
M	Molar
mix	Mixture

o	Resin polar head
oil	Asphalt-free oil
p	Low pressure; resin non-polar tail
r	Resin; reduced property
s	Solvent
x, y, z	Direction of polarization

Superscripts

*	Reference state
0	Pure state
00, Θ	Standard state (infinite dilution)
as	Association
def	Deformation
E	Excess property
f	Fusion property
ind	Induction
int	Interaction
L	Liquid phase
m	Micelle
mix	Mixing
P	Precipitated phase
sh	Shell
ste	Steric
tr	Transfer

Chapter 1

Introduction

1.1 Preamble

A large number of subsurface petroleum reservoirs from various parts of the world experience asphaltene precipitation in the subsurface formation, in the wellbore, in the well, and in the surface facilities and pipelines. Asphaltene precipitation is undesirable because it reduces well productivity and limits fluid flow. In some cases, precipitation can result in complete plugging of flow lines (see Fig. 1.1), fouling, wettability alteration, and coking. The main factors that promote precipitation are pressure, temperature and composition variations due to gas injection, phase separation, mixing of fluid streams.

Paradoxically, the asphaltene precipitation is often observed in petroleum fluids that contain very low asphaltene content (see Fig. 1.2). A heavy petroleum fluid with an asphaltene content of say 20 wt% may not have precipitation problems. On the other hand, a light petroleum fluid with an asphaltene content of less than 0.2 wt% may precipitate asphaltene. Examples are the light petroleum fluid from the Hassi-Messaoud field in Algeria (44 API gravity) with an asphaltene content of 0.1 wt%, which precipitates a considerable amount of deposits in tubings and surface facilities. On the other hand, the heavy petroleum fluid from Boscan in Venezuela (10 API gravity) containing approximately 17 wt% asphaltenes does not encounter asphaltene deposition (Leontaritis and Mansoori, 1988).



Fig. 1.1 – Paraffin and asphaltene deposition in flow lines.
(http://www.bakerhughes.com/bakerpetrolite/oilgas/paraffin.html)

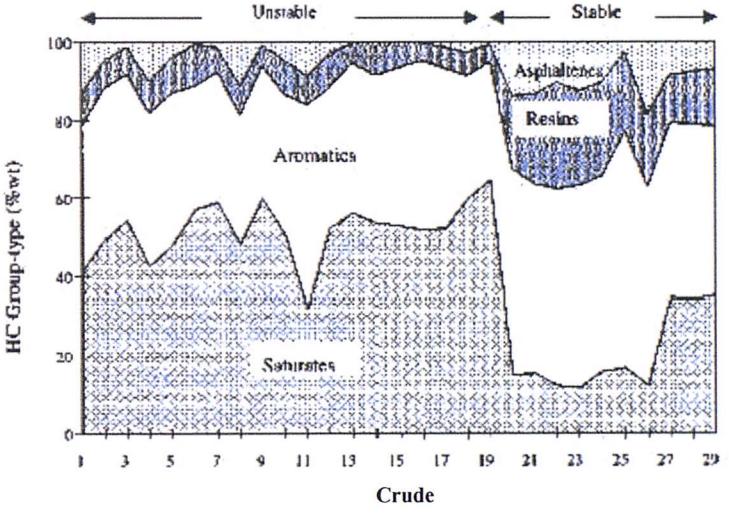


Fig. 1.2 – Hydrocarbon group-type distribution for stable and unstable petroleum fluids. (Carbognani *et al.*, 1999)

It is imperative to be able to predict when and why asphaltene precipitation occurs in order to mitigate production decline in oilfields. Accurate prediction of the precipitation requires a number of input parameters that are not readily defined for asphaltenes and resins. In particular, the amount of resins depends on the method of separation. The disparity in the measured data is due to the lack of definition of the resin fraction. In this thesis, asphaltene and resin molecules are different from the rest of hydrocarbons in the petroleum fluid because of their polar character. Polarity stems

from the presence of heteroatoms and metals in the molecules and may lead to association. The quantification of polarity is not important for hydrocarbon vapor-liquid equilibrium (VLE) calculations, however it is essential for the modelling of asphaltene precipitation. Presently, most models lack in predictive capability because they do not take into account the interactions from polar molecules. There are several means to quantify polarity; among them is the dipole moment which allows the calculation of the van der Waals interactions between asphaltenes, resins, and the medium.

Knowledge of the aggregation and precipitation mechanisms is also fundamental to the development of preventive and curative measures against asphaltene precipitation. Resins act as natural dispersants of asphaltenes. A viable option for the inhibition of asphaltene precipitation is the mixing of resins or some dispersants with the petroleum fluid in a batch process. Field data show that in some cases the resins and dispersants not only do not inhibit precipitation; they may also promote it. The study of the effect of resins and chemical dispersants on precipitation contributes significantly to the understanding of molecular interactions in petroleum fluids. Such interactions are believed to be key elements for a proper modelling of asphaltene precipitation.

Several models have been developed for the prediction of asphaltene precipitation from petroleum fluids. Some completely ignore the complexity of the interactions and use simple concepts such as solubility (Hirshberg et al., 1984), and equation of state (Gupta, 1986; Thomas *et al.*, 1992). Other improved models account for the micellar nature of petroleum fluids and the dispersant effect of resins (Leontaritis and Mansoori, 1987; Pan and Firoozabadi, 1998, 2000). More modern approaches use association equations of state (Wu *et al.*, 1998) and integral equations (Duda and Lira-Galeana, 2002). All of these are valid approaches. However, there is need for a simple model that one can use to predict the asphaltene precipitation with a limited number of input parameters based on few simple measurements. The thermodynamic micellization model by Pan and Firoozabadi (1998, 2000) shows promising results at reservoir conditions however it has some limitations at stock tank conditions. In the same model, a hypothetical path is devised to describe the formation of micelles, which is mainly driven by the polarity of molecules. However, the model cannot predict properly the effect of n-alkanes and resins on precipitation from stock tank

petroleum fluids suggesting that an important component is missing in the model formulation. One of the motivations of this thesis is to find that component, which is believed to be related to the polarity of asphaltenes and resins.

1.2 Research objectives

The main objectives of this research are as follows,

- Devise a suitable method for the measurement of resins and asphaltenes in stock tank petroleum fluids,
- Quantify the polarity of asphaltenes, resins, and oils by measuring their dipole moment,
- Investigate the effect of resins and dodecyl benzene sulfonic acid (DBSA) amphiphile on the precipitation,
- Model asphaltene precipitation from stock tank and reservoir petroleum fluids and the effect of resins on precipitation using thermodynamics of micellization.

1.3 Approach

This thesis comports mainly two parts: experimental and modelling. In the experimental part, asphaltenes, resins, and oils are first separated from eight different petroleum fluids. Several separation methods (propane precipitation, adsorption on clay with various solvents) are considered and the dipole moment is used as a criterion for the selection of the procedure that preserves the resin constituents in the resin fraction. Once the fractions separated, the molecular size of asphaltenes and resins is estimated by fluorescence emission spectroscopy, and the dipole moment of asphaltenes, resins, and oils is calculated from measurements of dielectric constant (by dielectric spectroscopy at radio frequency), refractive index, and density. The dipole moment is used as a measure of polarity. Different theories that correlate the dipole moment to the macroscopic properties are tested using chemicals with known dipole moments. The theory that provides the most accurate data of dipole moment is selected. Next, the effect of resins and DBSA amphiphile on the precipitation from

three petroleum fluids is investigated by first studying the effect of resin concentration then the effect of resin dipole moment on the precipitation. Because of the complex interactions involved, the experiments are conducted by keeping the asphaltenes in their natural environment that is, in the petroleum fluid. In order to corroborate the differences between asphaltene and resin species, solubility tests are performed on resins in different fluids and precipitation tests are carried out on the fluids with additional asphaltenes. The effect of DBSA concentration is further measured on the three petroleum fluids in the same manner as for the resins. In the last part, attempts are made to model the experimental data using thermodynamics of micellization. Accordingly, the formulation proposed by Pan and Firoozabadi (1998, 2000) is revised by taking explicitly into account the effect of polarity and non-ideal mixing. The predicted results are compared to the experimental data in order to validate the revised model.

1.4 Thesis outline

The thesis is divided into seven chapters including the introduction chapter. Chapter 2 contains the comprehensive work undertaken on eight different petroleum fluids in order to devise a procedure for the measurement of asphaltene and resin amounts. Chapter 3 provides the molecular size of some asphaltene and resin samples by fluorescence emission spectroscopy. The method also presents the population size distribution of various asphaltene, resin, and oils fractions. Chapter 4 provides the dipole moment of asphaltenes, resins, and oils. The methodology followed for the determination of the dipole moment is described and the measurement procedures for the dielectric constant, refractive index, and density are included. The results obtained are compared and discussed. Chapter 5 presents the effect of resin concentration and dipole moment on the onset point and the amount of precipitation as well as the effect of DBSA amphiphile at different concentrations on the precipitation from three petroleum fluids. The chapter also outlines the contribution of different types of van der Waals molecular interactions in the precipitation. Chapter 6 models asphaltene precipitation from petroleum fluids using a revised formulation of the thermodynamic micellization model. The main revisions are presented and discussed. The model predictions of the effect of various n-alkanes and resins on precipitation from different stock tank petroleum fluids are compared to the experimental data. The model is also

tested at reservoir conditions. The final chapter reflects on the work carried out in this thesis and considers recommendations and future developments.

1.5 References

Carbognani, L., M. Orea, and M. Fonseca, "Complex Nature of Separated Solid Phases from Crude Oils", *Energy and Fuels*, **13**, 351 (1999).

Duda, Y., and C. Lira-Galeana, "Modelling Asphaltene Precipitation using Integral Equations. An Analytical Solution to the Associative Ornstein-Zernike Integral Equation", *International Conference of Heavy Organic Depositions*, Puerto-Vallarta, Jalisco, Mexico, Nov. 17-21 (2002).

Gupta, A. K., *A Model for Asphaltene Flocculation using an Equation of State*, MSc Thesis, Department of Chemical and Petroleum Engineering, University of Calgary (1986).

Hirschberg, A., L. N. J. de Jong, B. A. Schipper, and J. G. Meijer, "Influence of Temperature and Pressure on Asphaltenes Flocculation", *SPE* paper # 11202 (1984).

Leontaritis, K. J., and G. A. Mansoori, "Asphaltene Flocculation during Production and Processing: A Thermodynamic-Colloidal Model", *SPE* paper # 16258 (1987).

Leontaritis, K. J., A. G. Mansoori, "Asphaltene Deposition: A Survey of Field Experience and Research Approaches", *Journal of Petroleum Science & Engineering*, **1**, 229 (1988).

Pan, H., and A., Firoozabadi, "Thermodynamic Micellization Model for Asphaltene Aggregation and Precipitation in Petroleum Fluids", *SPE Prod. & Facilities J.*, 118 (May 1998).

Pan, H., and A., Firoozabadi, "Thermodynamic Micellization Model for Asphaltene Precipitation from Reservoir Crudes at High Pressures and Temperatures", *SPE Prod. & Facilities J.*, **15**, 1, 58 (2000).

Thomas, F. B., D. B. Bennion, D. W. Bennion, and B. E. Hunter, "Experimental and Theoretical Studies of Solids Precipitation from Reservoir Fluid", *J. Can. Petrol. Technol.*, **31**, 1, 22 (1992).

Wu, J., J. M. Prausnitz, and A. Firoozabadi, "Molecular-Thermodynamic Framework for Asphaltene-Oil Equilibria", *AIChE J.*, **44**, 5, 1188 (1998).

Wu, J., J. M. Prausnitz, and A. Firoozabadi, "Molecular Thermodynamics of Asphaltene Precipitation in Reservoir Fluids", *AIChE J.*, **46**, 1, 197 (2000).

Chapter 2

Measurement of asphaltene and resin amounts in petroleum fluids

A petroleum fluid can be divided into three types of species: 1) asphaltenes, 2) resins, and 3) oils. Different methods for the measurement of asphaltenes in a petroleum fluid give similar results. However, different methods give different results for the resin content. We have embarked on a comprehensive work to measure the amount of asphaltenes and resins in eight different petroleum fluids from various parts of the world. Once asphaltenes separated, resins are measured using two distinct methods: 1) propane precipitation, and 2) ASTM D-2007 adsorption method with different combinations of n-pentane/toluene solvents to elute oils. The dipole moment property is used as a criterion for the determination of resins in petroleum fluids. Results from this chapter show that resin separated from a petroleum fluid by propane is part of the total resin and contains the most polar resin molecules. On the other hand, adsorption methods give the true amount of resins provided no toluene is used to elute the oils.

2.1 Introduction

It is generally recognized that petroleum fluids at atmospheric pressure and ambient temperature are composed of three major constituents: 1) oils (that is, saturates and aromatics), 2) resins, and 3) asphaltenes. This partition is very broad; every part of the

petroleum fluid also consists of a wide range of molecules with varying structures and properties. Oils are often nonpolar or mildly polar, however asphaltenes and resins are polar because they contain heteroatoms (such as S, O, N) and metals (such as V, Ni, Fe). There is evidence that asphaltenes and resins exist in the form of monomers, as well as in micelles (Pfeiffer and Saal, 1940; Swanson, 1942). In a micelle, asphaltenes associate into an aggregate to form the core and resins adsorb onto the core to form a steric shell, which also contains the oils (Firoozabadi, 1999). The properties and the amount of asphaltenes and resins affect the formation of micelles. Considering petroleum fluids as a continuum of several thousands of molecules, it is very difficult to define a cut-off between the asphaltene, the resin and the oils fractions. The diversity of the methods for the measurement of asphaltene and resin amounts in petroleum fluids is related to the operational definition of these fractions. Indeed, asphaltenes are defined as those hydrocarbons insoluble in an excess of n-pentane (or n-heptane). Resins remain soluble when petroleum fluid is mixed with nC_5 (or nC_7) but can adsorb on surface-active materials such as fuller's earths, attapulgus clay, alumina or silica gel (Speight, 1999). In addition, resins are insoluble in an excess of liquid propane, butane(s) and some other chemicals (such as acids, acetates, alcohols, etc).

The standard procedures for asphaltene measurement are similar and generate comparable results. They consist mainly of precipitation by n-alkanes (nC_5 or nC_7). Although acids and heavy paraffins may co-precipitate with asphaltenes (Becker, 2000; Newberry and Barker, 2000), precipitation with n-alkanes is the main separation method of asphaltenes from petroleum fluids. In the IP143 procedure (1957), asphaltenes are separated from petroleum fluids with nC_7; the precipitated phase is then washed for one hour with a reflux of hot heptane to remove waxy constituents. In the ASTM D-3279 method (1978), asphaltenes from petroleum residues are precipitated with nC_7 and filtered after 30 minutes of heating and stirring with a reflux system. In the ASTM D-893 method (1980), asphaltenes are precipitated from lubricating oils by centrifugation in nC_7. Finally, in the Syncrude analytical method (1979), petroleum fluids are mixed with benzene prior to asphaltene precipitation with nC_5. After two-hour settling in the dark, they are filtered and washed.

There are two main methods for the separation of resins from petroleum fluids: 1) precipitation, and 2) adsorption. The precipitation by liquid propane is inspired from refinery processes and has found application in the laboratory by Schwager and Yen (1978), Murzakov *et al.* (1981) and others. Other precipitation methods using chemicals have also been proposed. In the standard ASTM D-2006 procedure (1970), resins are separated from rubber extender and processing oils by precipitation in sulfuric acid. A method prevalent in Germany applied by the German Petroleum Institute advocates the precipitation of asphalt (that is, asphaltenes and resins) from petroleum fluids with ethyl acetate and solubilization of resins from the precipitate with nC_5 (Andersen and Speight, 2001). The adsorption methods have been extensively used and consist of adsorbing resins on surface-active materials. The oils are eluted (that is, washed away from the column) with a nonpolar solvent and the resins remain on the adsorbent until desorbed by a polar solvent. Following this separation scheme, a series of standard procedures have been established. The Syncrude analytical method (1979) separates resins by adsorption on attapulgus clay; oils are eluted with nC_5 and resins are desorbed by successive elution with methyl-ethyl-ketone and tetrahydrofuran/water (95/5 vol/vol). The ASTM D-2007 (1991) uses the same adsorbent and eluting solvent for oils but a mixture of toluene and acetone (50/50 vol/vol) to desorb resins. In the ASTM D-4124 (1991), resins are adsorbed on activated alumina, oils are eluted with nC_7 and toluene (33/67 vol/vol); a mixture of toluene-methanol-trichloroethylene (17/17/66 vol/vol/vol) recovers resins. In all the above methods, oils are eluted by the n-alkane used to precipitate asphaltenes. The separation is time-consuming and it is sometimes found that heavy aromatics are eluted with resins due to the high retention time in the column. This has oriented some to introduce a certain amount of aromatic solvent with n-alkanes to elute the oils. Callen (1976) used 6 vol% dichloromethane in nC_6, Farcasiu (1979) used 15 vol% toluene in nC_7, Moinelo (1988) used 36 vol% benzene in nC_6, and more recently McLean and Kilpatrick (1997) used 32 vol% toluene in nC_7.

Resins recovered by precipitation or adsorption show marked differences in the amount and chemical composition. Even within adsorption methods, discrepancies can be found if adsorbents are different or elution time is varied (Wallace *et al.*, 1987). Currently, resins are defined according to the solvents used for their separation. Considerable effort has been dedicated to the selection of appropriate

polar solvents to desorb resins from surface-active materials with less effort to the choice of nonpolar solvents to elute oils. The principle of resin separation by adsorption assumes that the nonpolar solvent should not dissolve any resin. Yet, aromatic solvents such as toluene or benzene are very good solvents for resins and their use may cause unreliability for resin separation.

The main objective of this chapter is to devise a simple method for proper measurement and separation of resins in petroleum fluids. Simplicity, scale and practicality are considered when choosing the method. The resin content is measured using a precipitation method with liquid propane and an adsorption method according to the modified ASTM D-2007 procedure. In the adsorption method, different nC_5/toluene volume ratios are used to recover the oils in order to accelerate the separation and to ensure that heavy aromatics are washed from the column with oils. Because toluene may elute some resin constituents with oils, one would study the nC_5/toluene volume ratio that separates oils by preserving all the constituents of resins in the resin fraction. This is possible by measuring the dipole moment of resins recovered in each test.

This chapter is structured into three parts. The first part provides the experimental methods and procedures for asphaltene and resin separation from eight different petroleum fluids. In the second part, the results on the amounts of asphaltenes, resins and oils recovered from each petroleum fluid are presented and commented. The main conclusions of this chapter are drawn in the last part.

2.2 Experimental

Eight different petroleum fluids with API gravities in the range of 10 to 56 are used (see Table 2.1). Two of the petroleum fluids are from the Hamaca field in Venezuela, from two different wells. The other petroleum fluids are from various parts of the world. Detailed composition of three petroleum fluids at ambient conditions is available in Table 2.2. In this work, asphaltenes are first precipitated from the petroleum fluids using nC_5, nC_7, and nC_{10}, then resins are separated from the nC_5-deasphaltened petroleum fluids by: 1) precipitation with liquid propane, and

Table 2.1 – Petroleum fluids

Petroleum fluid	Density at 20°C (g/cc)	API gravity at 20°C	Refractive index at 20°C	Description
H	1.0089	9	–	Very heavy
TE	0.9990	10	–	Very heavy
C	0.8588	33	1.487	Medium
TA	0.8372	37	1.479	Medium
TK	0.8520	35	1.488	Medium
S	0.8627	32	1.472	Medium
U	0.8550	34	1.491	Medium
B	0.7554	56	1.431	Very light

Table 2.2 – Composition of three selected petroleum fluids at ambient conditions

Fraction	C		TK		U	
	Component mole%	*M* g/mol	Component mole%	*M* g/mol	Component mole%	*M* g/mol
C_1	0.00	0.00	0.00	0.00	0.00	0.00
C_2	0.00	0.00	0.01	30.1	0.04	30.1
C_3	0.00	0.00	0.15	44.1	0.73	44.1
C_4	0.82	58.1	0.85	58.1	4.15	58.1
C_5	2.12	72.1	2.48	72.1	6.00	72.1
C_6	3.84	86.2	4.91	85.8	8.33	85.8
C_7	5.18	100.2	8.39	95.8	10.35	100.2
C_8	7.32	114.2	11.14	108.5	70.40*	329.5
C_9	6.58	128.3	10.29	123.2		
C_{10}	6.11	142.3	7.83	137.8		
C_{11}	5.77	156.3	5.67	148.3		
C_{12}	4.99	170.3	4.38	154.4		
C_{13}	5.17	184.4	4.46	172.4		
C_{14}	4.81	198.4	3.79	187.9		
C_{15}	4.61	212.4	3.59	197.2		
C_{16}	3.72	226.4	3.02	210.1		
C_{17}	3.63	240.5	2.69	227.1		
C_{18}	3.48	254.5	2.62	240.9		
C_{19}	2.72	268.5	2.42	254.2		
C_{20+}	29.13	433.6	21.31	441.2		
Total	100.00	242.0	100.00	206.1	100.00	256.5

* C_{8+}

2) modified ASTM D-2007 adsorption procedure. In the adsorption method, the oils are eluted with five different nC_5/toluene volume ratios. All the chemicals used are Reagent grade with maximum water content of 0.05% and minimum purity of 99%.

2.2.1 Asphaltene precipitation

From the examination of the various asphaltene precipitation methods and identification of optimum separation conditions (Speight *et al.*, 1984), the Syncrude analytical method (1979) is selected with some modifications. The precipitation sequence includes mixing of the petroleum fluid with toluene (10 ml per g asphaltene in the fluid) followed by addition of nC_5 (50 ml per ml toluene). The settling time is set to twelve hours to allow complete precipitation. Asphaltenes are then filtered under vacuum and the precipitate is extensively washed with nC_5. The sequence is repeated several times to remove resins adsorbed onto asphaltenes until the liquid filtrate is colorless. Fig. 2.1 provides the detailed procedure for asphaltene precipitation from the petroleum fluids.

Apparatus – The experimental set-up is presented in Fig. 2.2 and consists of a filtration flask and funnel connected to a vacuum pump through rubber tubings. To avoid solvent infiltration into the pump, a trap is used at a temperature of – 60°C to liquefy n-pentane from vapor. Asphaltenes are filtered using a Whatman glass microfibre filter paper (7 mm diameter and 1.5 μm pore size). The weight is measured with a Sartorius analytical balance with an accuracy of 0.001g.

2.2.2 Resin precipitation

The resin precipitation is performed using a high-pressure cylinder with piston connected to a high-pressure filter holder at one side, and a water pump at the other side (see Fig. 2.3). The filter holder contains a Whatman glass microfibre (4.7 mm diameter and 0.8 μm pore size) filter paper. Liquid propane from a 1-gallon high-pressure bottle is charged at a low temperature (– 5 to 0°C) into the cylinder containing the deasphaltened oil sample, with a sample to propane ratio of 1/20 (wt/wt). The pressure in the cylinder is increased to 1,400 psia and the mixture is left for 4–6 hours at room temperature. A piston is then used to push the mixture through

the filter. The resins are recovered from the filter as well as the cylinder walls by washing with toluene.

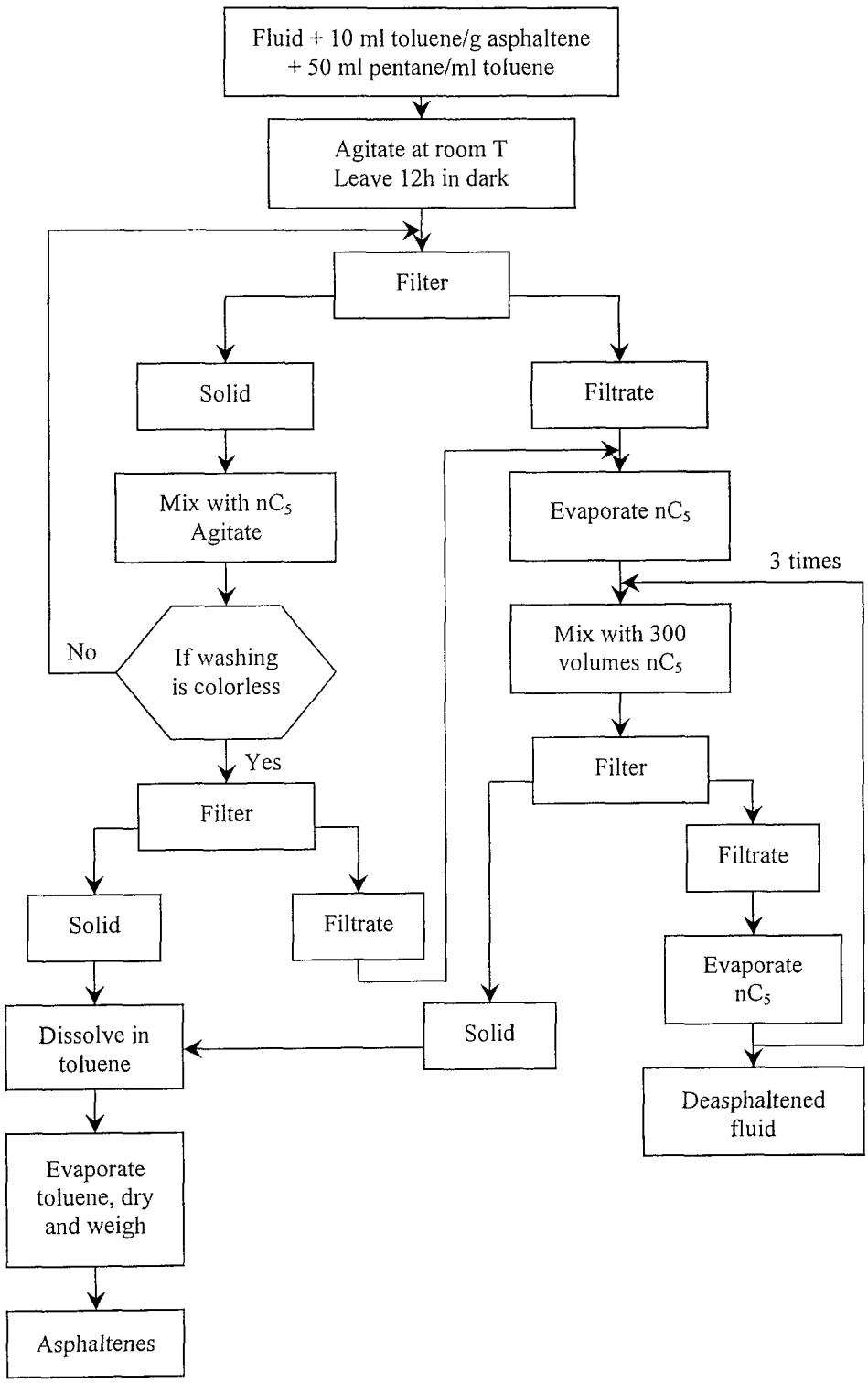


Fig. 2.1 – Procedure for asphaltene precipitation from petroleum fluids

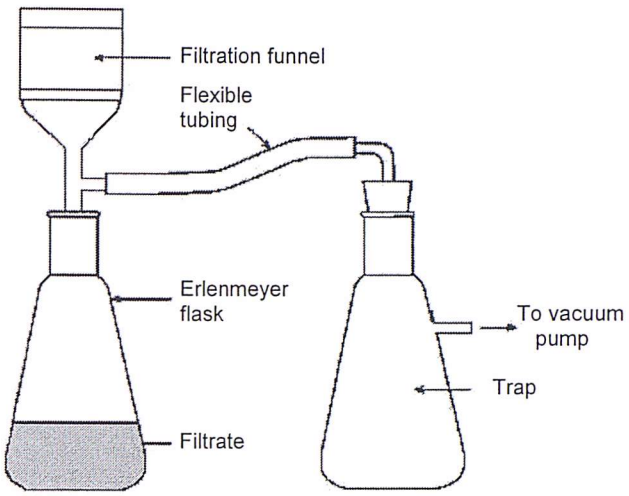


Fig. 2.2 – Experimental set up for asphaltene precipitation from petroleum fluids

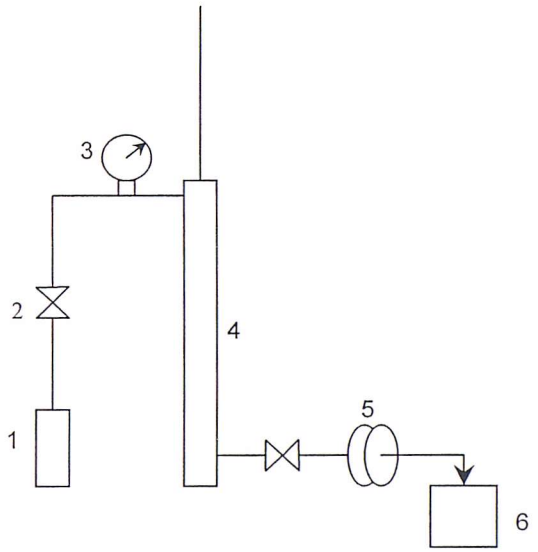


Fig. 2.3 – Propane test apparatus

Apparatus – The cylinder used is made of stainless steel (400 mm long × 20 mm ID) and can stand a maximum pressure of 680 atm. Stainless steel tubings (1/16" ID) are used for connections to the water pump (max pressure 272 atm) and to the high-pressure filter holder. Ball valves (max pressure 136 atm) and needle valves (max pressure 408 atm) allow the control of flow rate. The pressure of water pumped into

the cylinder is read from a pressure gauge (max pressure 272 atm). The filter holder (stainless steel, 47mm size) is designed to stand pressures up to 95 atm.

2.2.3 Resin adsorption

Once asphaltenes are removed, resins are separated from the deasphaltened petroleum fluid using the ASTM D-2007 (1991) method with some modifications. The deasphaltened petroleum fluid is charged into an adsorption column containing the attapulgus clay immersed in nC_5. Saturates and aromatics are then eluted with various proportions of nC_5/toluene mixtures: 100/0, 85/15, 70/13, 50/50 and 0/100 vol/vol. The elution continues until the yellow coloration of the liquid leaving the column sustains (the yellow coloration is attributed to aromatic hydrocarbons in oils). On average, 2 to 3 liters are required to recover oils from 1 g of sample. Once the column is drained from the solvent, resins are desorbed using a 40/40/20 volume mixture of toluene/acetone/methylene chloride. The solvent in the resin solution is then evaporated and the resins are dried and weighed.

Apparatus – The adsorption column (300 mm height × 44 mm diameter) is made of glass and contains the attapulgus clay (250–500 μm pore size) with a sample/clay ratio of approximately 1/20 (wt/wt). Each column has a 125 ml reservoir in the top inside which the eluting solvent is poured. A glass wool plug is placed in the bottom of the column in order to retain the clay inside the column.

2.3 Results

The amount of asphaltenes precipitated with n-alkanes (nC_5, nC_7 and nC_{10}) and resins separated by propane precipitation and the ASTM D-2007 adsorption method with different solvents are presented. Table 2.3 provides the results of asphaltene precipitation with nC_5, nC_7 and nC_{10} from the eight petroleum fluids. On average, five tests are performed on each sample, and the standard deviation is about 1%. The amount of nC_5 asphaltenes varies from 0.05 wt% in petroleum fluid B to 17.7 wt% in petroleum fluid H and decreases with the carbon number of the precipitating n-alkane. Table 2.4 presents the results of asphaltene and resin (that is, asphalt) precipitation by propane. When propane is mixed with the petroleum fluid, C_3 asphaltenes and C_3

resins precipitate. However, when propane is mixed with the nC_5-deasphaltened fluid, C_3-nC_5 asphaltenes and C_3 resins precipitate. Thus, the difference between the two amounts provides the nC_5 asphaltenes in the petroleum fluid (see Table 2.4). The difference compares well with the amounts of nC_5 asphaltenes reported in Table 2.3. The disparity is due to some losses during the separation. Each test is repeated at least three times and the standard deviation is 4%.

Table 2.3 – Amount of asphaltenes precipitated by nC_5, nC_7 and nC_{10} from the petroleum fluids

	H	TE	C	TA	TK	S	U	B
Precipitant	Amount, wt%							
nC_5	17.7	14.8	2.3	0.18	1.33	1.1	2.5	0.05
nC_7	13.5	11.9	1.52	0.10	0.46	0.77	-	0.04
nC_{10}	13.0	11.2	1.42	0.05	0.26	0.63	-	0.03

Table 2.4 – Amount of asphalt (that is, asphaltenes and resins) precipitated by propane from the petroleum fluids and from the nC_5 deasphaltened fluids

	H	TE	C	TA	TK	S	U	B
Precipitation from	Amount, wt%							
Petroleum fluids	38.6	36.3	6.2	3.9	5.7	-	-	-
nC_5-deasphaltened petroleum fluids	19.8	20.0	3.3	3.6	4.2	1.5	-	0.3
Difference	18.8	16.3	2.9	0.2	1.5	-	-	-

Results of resin separation by the modified ASTM D-2007 adsorption method using different solvents are provided in Tables 2.5 and 2.6. Table 2.5 shows the amount of resins recovered after elution of oils with nC_5, nC_7 and nC_{10}. The amount of resins slightly increases with the carbon number of n-alkane used to elute oils, which is consistent with the amounts of asphaltenes precipitated with the n-alkanes. For all the petroleum fluids, the amounts of resins by adsorption are higher than those by propane precipitation. It is also observed that petroleum fluids with high asphaltene content contain substantial amounts of resins. Material balance calculation on the very heavy petroleum fluids reveals minor losses (that is, irreversible adsorption of polar compounds on the clay (< 1 wt%)). It is found that the high quality of the clay assures good selectivity and reproducibility of the tests. Table 2.6 provides the amount of

resins recovered from the nC_5-deasphaltened petroleum fluids after elution of oils with different nC_5/toluene volume ratios of 100/0, 85/15, 70/30, 50/50 and 0/100 (vol/vol). The amount of resins decreases with the volume of toluene in nC_5/toluene mixtures. When using only nC_5 to elute oils, one obtains almost two times more resins than when using only toluene. All the above tests are performed three times and the standard deviation is 3%.

Table 2.5 – Amount of resins adsorbed on clay after elution of oils with nC_5, nC_7 and nC_{10}

	H	TE	C	TA	TK	S	U	B
Elution of oils with					Amount, wt%			
nC_5	30.3	28.6	6.5	6.0	7.5	3.5	8.6	0.56
nC_7	31.1	28.7	7.4	6.2	7.6	3.8	-	0.65
nC_{10}	32.0	30.0	7.8	6.5	7.9	4.0	-	0.68

Table 2.6 – Amount of resins adsorbed on clay after elution of oils with various nC_5/toluene mixtures

	H	TE	C	TA	TK	S	U	B
Elution of oils with nC_5/toluene					Amount, wt%			
100/0 (vol/vol)	30.3	28.6	6.5	6.0	7.5	3.5	8.6	0.56
85/15 "	26.4	24.0	5.9	4.8	5.9	2.7	-	0.45
70/30 "	21.8	19.9	4.9	3.9	5.2	2.2	-	0.37
50/50 "	20.0	18.0	4.2	3.6	4.2	1.5	-	0.30
0/100 "	14.0	13.3	2.9	2.8	2.9	1.1	-	0.25

Fig. 2.4 shows the photograph of the separated asphaltenes and resins from petroleum fluid H. The resins are those separated by adsorption after elution of oils with nC_5. Asphaltenes and resins have very different appearances. Indeed, asphaltenes from all the petroleum fluids are black, shiny and friable solids while resins are dark brown, semi-solid, shiny and gummy. Oils are orange/brown liquids with a density that varies from a petroleum fluid to another. The color of oils changes from orange/brown to red/brown when the proportion of toluene in the nC_5/toluene mixtures is increased. This change in coloration may suggest the presence of polar species in the oils (Becker, 2000).

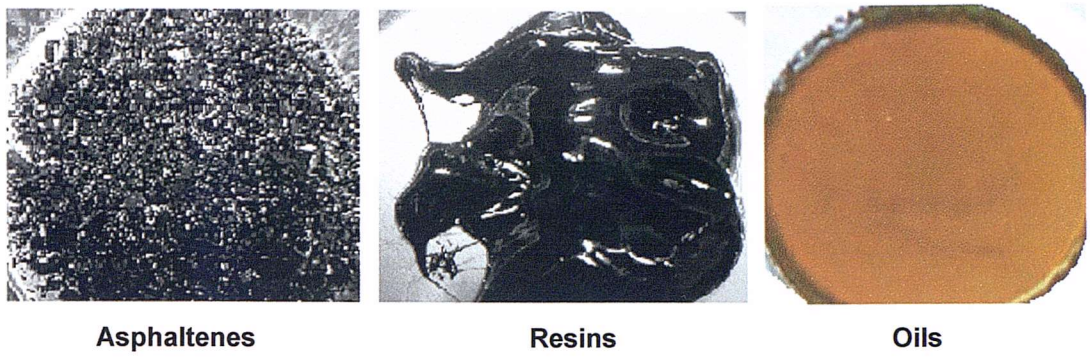


Fig. 2.4 – Photograph of asphaltenes, resins, and oils from petroleum fluid H.

In order to compare the results of this study with other separation techniques, the resin content of petroleum fluid E has been determined in two different laboratories (Durandeau, 1999; Boduszynski, 2000). Durandeau used Thin Layer Chromatography (TLC) and reported a value of 14 wt% while Boduszynski used High Performance Liquid Chromatography (HPLC) and reported a resin content of 25 wt%. In TLC, saturates are eluted with nC_6 and aromatics with toluene while in HPLC, nC_6 is used to elute oils. The solvents used in the two techniques correspond to the extreme proportion of nC_5/toluene volume ratios. The results from HPLC correspond to 100% nC_5 (0% toluene) and the results from TLC correspond to 100% toluene (0% nC_5) when compared with our adsorption method. It is interesting to see that the results from HPLC and TLC for resins which are 25 and 14 wt%, respectively for petroleum fluid TE are in line with our measurements of 28.6 wt% and 13.3 wt%, respectively.

The next step is to define the true resins from the set of fractions recovered. We would like to find the nC_5/toluene volume ratio that separates oils by preserving all the constituents of resins in the resin fraction. This is possible by measuring the dipole moment of the resin fractions. The detailed procedure of the measurements is described in chapter 4. The dipole moment of resins is found to increase gradually with increasing volume of toluene as shown in Table 2.7. In fact, when toluene is introduced into the eluting solvent of oils even at small concentrations, the dielectric constant of resins increases linearly with the amount of toluene in the solvent (see Fig. 2.5).

Table 2.7 – Dipole moment (in Debye) of resins

	H	TE	C	TA	TK	S	U	B
Precipitated by								
C_3	4.0	3.8	4.4	3.5	4.0	4.2	-	3.7
Adsorbed after elution of oils with nC_5/toluene								
100/0 (vol/vol)	2.5	2.4	3.2	3.1	2.8	2.4	2.4	3.0
85/15 "	2.6	2.5	3.3	3.1	3.0	2.5	-	3.1
70/30 "	2.7	2.6	3.5	3.2	3.1	2.6	-	3.2
50/50 "	2.9	2.8	3.6	3.3	3.2	2.7	-	3.4
0/100 "	3.1	2.9	3.7	3.3	3.4	2.8	-	3.5

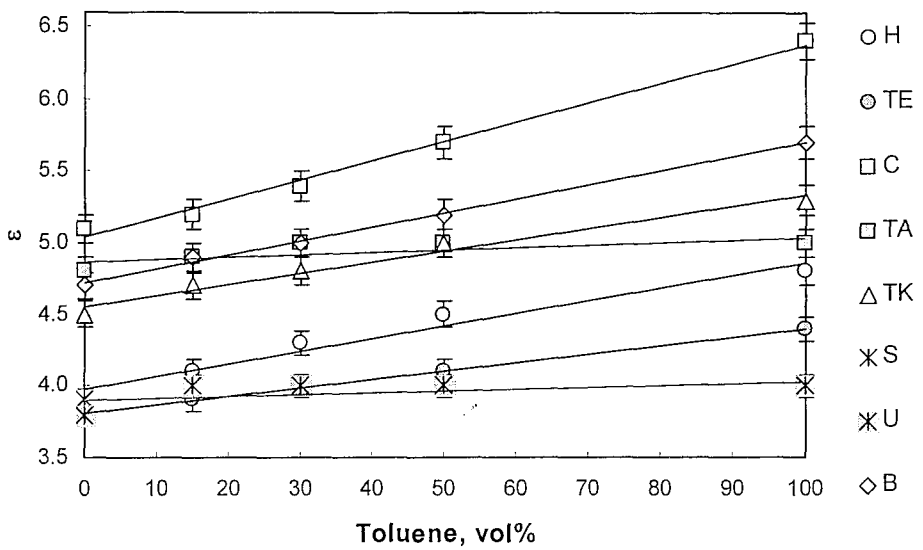


Fig. 2.5 – Increase of the dielectric constant of resins with the amount of toluene in the eluting solvent of oils.

A nitrogen analysis of the oils from petroleum fluids H and C shows that the resins eluted with the oils are those containing nitrogen functions (see Table 2.8). Because heavy aromatics may possess a small polarity (as will be see in chapter 4), one may argue that the increase in dipole moment be attributed to the presence of slightly polar aromatics. However, slightly polar aromatics are distinguished from slightly polar resins in that the polarity of resins stems from the presence of heteroatoms in the molecule. These results imply that toluene does elute some resins with the oils, probably those weakly bound to the clay. Therefore, it is recommended not to use any toluene with nC_5 to separate oils from resins. Table 2.7 also provides the dipole moment of resins by the precipitation method. It is found that resins precipitated by

propane are more polar than resins separated by adsorption. This reveals that propane precipitates only part of the resin fraction containing the most polar molecules.

Table 2.8 – Nitrogen content of oils from petroleum fluids H and C eluted with various nC_5/toluene mixtures

nC_5/toluene, vol/vol	Amount, ppm	
	H	C
100/0	213	250
85/15	655	300
70/30	1100	356
50/50	1700	415

2.4 Conclusions

Based on the extensive work on the separation of asphaltenes and resins from petroleum fluids, the following conclusions are drawn.

1) The Syncrude analytical method allows a good separation of asphaltenes from petroleum fluids by precipitation with n-alkanes. The method is slightly modified to reduce the co-precipitation of heavy resins with asphaltenes.

2) The propane precipitation method separates only part of resins. This part is the most polar fraction of the resins.

3) The total resins can be separated by the ASTM D-2007 adsorption method using nC_5-deasphaltened petroleum fluids. Modifications are introduced into the method to assure consistency of the separation and provide reproducible results. It is found that the use of an aromatic solvent such as toluene with nC_5, even a small quantity, to elute the oils may reduce the amount of the separated resins.

2.5 References

Andersen, S. I., and J. G. Speight, "Petroleum Resins: Separation, and Role in Petroleum", *Petroleum Science and Technology*, **19** (1&2), 1-34 (2001).

Annual Book of ASTM Standards, ASTM D2006, D3279, D893, D2007, D4124, *American Society for Testing and Material* (1970, 1978, 1980, 1991, 1991).

Atkins, P. W., *Physical Chemistry*, Oxford University Press, Oxford (1978).

Becker, H. L., "Asphaltene: To Treat or Not", SPE paper # 59703 presented at the 2000 SPE Permian Basin Oil and Gas Recovery Conference, Midland, TX, 21-23 March (2000).

Boduszynski, M. M., Private Communication, Chevron Technology Company, Richmond, CA (2000).

Callen, R. B., J. G. Bendoraitis, C. A. Simpson, and S. E. Voltz, "Upgrading Coal Liquids to Gas Turbine Fuels 1. Analytical Characterization of Coal Liquids", *Ind. Eng. Chem. Prod. Res. Dev.*, **15**, 4, 223 (1976).

Carbognani, L., and Y. Espidel, "Characterization of Solid Deposits from Production Facilities– Identification of Possible Causes of Deposits Formation", Vision Tecnologica, 3, 1, 35 (1995).

Durandeau, M., Private Communication, Total Elf Fina Research Center, Pau, France (1999).

Farcasiu, M., "Fractionation and Structural Characterization of Coal Liquids", *Fuel,* **56**, 9 (1977).

Firoozabadi, A., *Thermodynamics of Hydrocarbon Reservoirs*, McGraw-Hill, New York (1999).

Leontaritis, K. J., A. G. Mansoori, "Asphaltene Deposition: A Survey of Field Experience and Research Approaches", *Journal of Petroleum Science & Engineering*, **1**, 229 (1988).

McLean, J. D., and P. K. Kilpatrick, "Comparison of Precipitation and Extrography in the Fractionation of Crude Oil Residua", *Energy and Fuels*, **11**, 570 (1997).

Moinelo, S. R., R. M. Menendez, and J. Bermejo, "Fractionation of Coal-derived Liquids by Extrography", *Fuel,* **67**, 682 (1988).

Murzakov, R. M., S. A. Sabanenkov, and Z. I. Syunyaev, "Influence of Petroleum Resins on Colloidal Stability of Asphaltene-containing Disperse Systems", *Khim. Tekhnol. Topl. Masel.*, **10**, 40 (1981).

Newberry, M. E., and K. M. Barker, "Organic Formation Damage Control and Remediation", SPE paper # 58723 presented at the 2000 SPE International Symposium on Formation Damage Control, Lafayette, Louisiana, 23-24 Feb (2000).

Pfeiffer, J. Ph., and R. N. J. Saal, "Asphaltic bitumen as colloid system", *Journal of Physical Chemistry*, **44**, 139 (1940).

Schwager, I., and T. F. Yen, "Coal Liquefaction Products from Major Demonstration Processes 1. Separation and Analysis", *Fuel,* **57**, 100 (1978).

Speight J. G., R. B. Long, and T. D. Trowbridge, "Factors Influencing the Separation of Asphaltenes from Heavy Petroleum Feedstocks", *Fuel,* **63**, 616 (1984).

Speight J. G., *The chemistry and Technology of Petroleum*, Marcel Dekker, New York (1999).

Standards for Petroleum and its Products, "IP 143: Asphaltenes Precipitation with Normal Heptane", *Institute of Petroleum*, London (1957).

Swanson, J. M., "A contribution to the Physical Chemistry of the Asphalts", *Journal of Physical Chemistry*, **46**, 141 (1942).

Syncrude Analytical Method for Oil Sand and Bitumen Processing, Edmonton, Syncrude Canada Ltd (1979).

Wallace D., D. Henry, K. Pongar, and D. Zimmerman, "Evaluation of Some Open Column Chromatographic Methods for Separation of Bitumen Components", *Fuel,* **66**, 44 (1987).

Chapter 3

Molecular size of asphaltenes and resins

This chapter investigates the molecular size of asphaltene and resin species from some of the petroleum fluids in Chapter 2. Three different sets of experiments are performed: 1) absorption spectroscopy, 2) steady state fluorescence emission spectroscopy (SSFES), and 3) time-dependent fluorescence emission spectroscopy (TDFES). In SSFES, the emission intensity correlates with the molecular size. The measured molecular size distributions suggest a decrease in the population of large molecules from nC_7 asphaltenes to nC_5 asphaltenes to C_3 resins to nC_5 resins to petroleum fluids to oils. TDFES uses the theory of anisotropy decay to calculate the molecular size of spherical molecules. The radius of asphaltene molecules by TDFES is found to vary between 2.5 to 5.9 Å depending on the nature of the petroleum fluid.

3.1 Introduction

The molecular size of asphaltenes has been extensively studied over the past years. The emergence of sophisticated measurement techniques unveiled important structural features of the asphaltenes. It is now recognized that asphaltene molecules are substantially smaller in size than it was previously reported. Zajac *et al.* (1994) used scanning tunneling microscopy (STM) to image directly the aromatic components of asphaltenes and reported an average molecular radius of 5 Å.

Liang *et al.* (2000) measured values in the same range by X-ray diffraction. Recently, fluorescence depolarization measurements provided estimates in the range of 5–10 Å (Groenzin and Mullins, 2000; Buenrostro-Gonzales *et al.*, 2001).

In this chapter, fluorescence emission spectroscopy is used to measure the molecular size of asphaltenes and resins that were separated from some petroleum fluids in Chapter 2. The fluorescence emission can be measured under steady state or time-resolved conditions. The steady state fluorescence emission spectroscopy (SSFES) provides a qualitative estimation of the size of chromophore populations that emit at a definite wavelength while the time-dependent fluorescence emission spectroscopy (TDFES) assesses the volume of molecules based on the decay of their fluorescence emission with time. The decay depends on the molecular size; small molecules experience a high anisotropy due to Brownian motion and their decay is sharp and short compared to large molecules. In other words, large molecules emit in the "red" (infra red region) and small molecules emit in the "blue" (ultra violet region) as shown in Fig. 3.1. Because asphaltene fluorescence emission is significant in the range of 400 to 650 nm, the tests are performed at excitation wavelengths in the range of 310 to 400 nm. Prior to the fluorescence emission measurements, the samples are diluted in toluene at very small concentrations. For such small concentrations, it is preferable to measure the sample concentration from its absorbance response rather than using conventional methods. Thus, the absorption spectroscopy (AS) is used for concentration measurements. The AS method can also be used to probe the presence of metals such as Ni or V in the molecule.

This chapter is structured into four parts. In the first part, a brief theory on absorption, fluorescence emission, and anisotropy decay is presented. The second part describes the equipments used and provides the measurement procedures. The third part presents the results of SSFES tests on several samples of asphaltenes, resins, and oils, as well as the results of TDFES test on two asphaltenes and one resin sample. The results are then compared and discussed before drawing in the last part the main conclusions of this chapter.

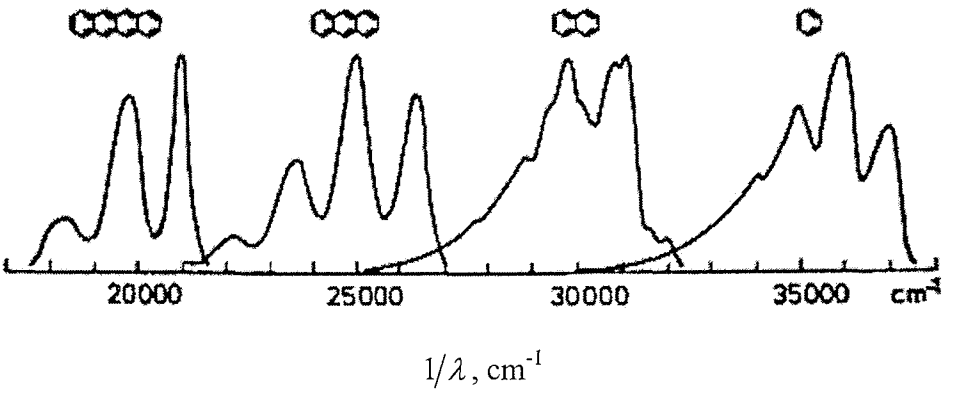


Fig. 3.1 – Plot of the emission spectra for the four smallest aromatic molecules: benzene, naphthalene, anthracene, and tetracene. (Haken *et al.*, 1994)

3.2 Theory

3.2.1 Absorption

Absorption is defined as the transition from the ground level of electronic ground states to the lowest vibrational levels of excited electronic states. For a given wavelength, the absorption intensity can be determined from the Beer-Lambert law,

$$I = I_0 e^{-\alpha x C} \tag{3.1}$$

where I_0 is the incident intensity, C is the concentration of the absorbing material, x the optical path length, and α the absorption coefficient. The optical density (OD) or absorbance is defined as,

$$OD \equiv ln\frac{I}{I_0} = -\alpha x C \tag{3.2}$$

The optical density is directly proportional to the concentration. Thus, one can use the optical density response to measure the small sample concentrations. Another application of the absorbance spectroscopy is the detection of metals such as Ni and V; a Soret band at 389 nm and 409 nm indicates the presence of Ni and V in the sample, respectively (Dolphin, 1978).

3.2.2 Fluorescence emission

Fluorescence emission is defined as the spontaneous radiative transitions between an excited quantum state to any state with a lower energy. Usually, transitions occur between the highest occupied (HO) energy level to the lowest unoccupied (LU) energy level and they depend on the size of the molecule. The observed HO-LU gap of electronic energy levels of large molecules is small compared to that of small molecules. Consequently, large molecules emit at high wavelengths (in the IR region) while small molecules emit at small wavelengths (in the UV region).

The steady state fluorescence spectrum technique is able to obtain the energy difference between the states that participate at the optical transition by measuring the intensity at a wavelength that corresponds to a certain transition. At low temperature, the fluorescence spectrum is the mirror image of the absorption spectrum and is detectable in the UV-VIS-Near IR region. While the steady state fluorescence spectroscopy can locate an optical transition on an energy scale, the time-resolved fluorescence spectrum gains additional information about the excited state of that transition.

3.2.2.1 Anisotropic polarization decay

The theory of anisotropic polarization decay as presented in the following is mainly based on the work of Chuang and Eisenthal (1972). The first formulation of the relationship between fluorescence and rotational Brownian motion was done by Perrin (1926) and extended by several authors such as Tao (1969) who developed the theory of rotational Brownian motion of a free rigid body. The work is partly based on Einstein's theory of Brownian motion (Einstein, 1906), which developed the basic concept of the motion of particles suspended in fluids. We present briefly in the following the spherical model formulated by Perrin-Tao-Chuang (Chuang and Eisenthal, 1972). The state of fluorescence polarization may be characterized by the three polarized components I_x, I_y, I_z, where the subscript gives the direction of polarization (see Fig. 3.2).

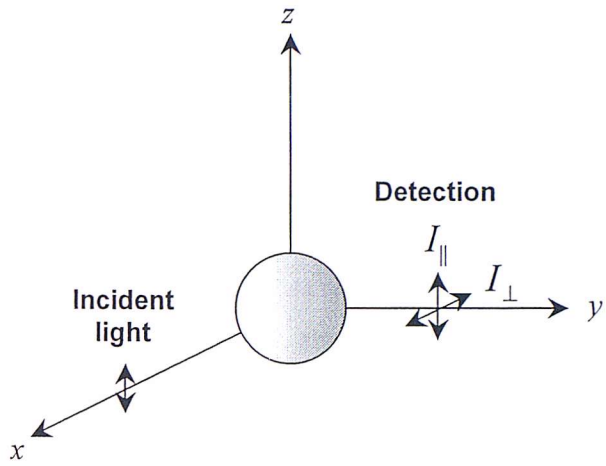


Fig. 3.2 – Excitation and fluorescence emission of a spherical molecule, which undergoes anisotropy decay. (Tao, 1969)

For the exciting light polarized in the z-direction and traveling in the negative x-direction and by observation of the fluorescence along the y-direction, it follows that $I_{\|} = I_z$ and $I_{\perp} = I_x = I_y$, where the subscripts $\|$ and $\perp$ denote a detection of light polarized parallel and perpendicular to the excitation, respectively. In this system, the emission anisotropy is defined as,

$$r(t) = \frac{D(t)}{S(t)} \tag{3.3}$$

where D is the difference between the parallel and perpendicular polarized light and S is the sum of the three polarized components, which represents the magnitude of the intensity emitted by the fluorophore. Therefore, the emission anisotropy can be written for a vertically polarized exciting light as,

$$r(t) = \frac{I_{\|} - I_{\perp}}{I_{\|} + 2I_{\perp}} \tag{3.4}$$

The emission of light by a molecule is characterized by a transition dipole moment, which stays constant in the molecular frame but is time-dependant in the laboratory frame (due to Brownian motion). In the four possible combinations of excitation-emission of light: vertical-vertical (*vv*), vertical-horizontal (*vh*), horizontal-vertical (*hv*) and horizontal-horizontal (*hh*), the transition dipole has to rotate 90° except for *vv*

excitation-emission of light. If one considers a vertical incident light, the *vv* light intensity is equal to $I_{vv} = I_{\parallel}$ for a vertically polarized emission light, and the *vh* light intensity is equal to $I_{vh} = I_{\perp}$ for a horizontally polarized emission light (see Fig. 3.2). The difference between the two intensities provides an estimate of anisotropy.

Emission has two components: 1) fluorescence $F(t)$, and 2) anisotropy $r(t)$. The total emission intensity is $F(t)r(t)$. Assuming an equal distribution of intensity along the three axis, the intensity of each axe will be $F(t)r(t)/3$. For a clockwise rotation of the dipole, one can write,

$$I_{\parallel} = \left[\frac{1}{3}r(t)F(t)\right] + \left[\frac{1}{3}r(t)F(t)\right] + \left[\frac{1}{3}F(t)\right] = \frac{F(t)}{3}\left[1+2r(t)\right] \tag{3.5}$$

$$I_{\perp} = [0] + \left[\frac{1}{3}F(t)\right] - \left[\frac{1}{3}r(t)F(t)\right] = \frac{F(t)}{3}\left[1-r(t)\right] \tag{3.6}$$

Therefore, $S(t) = F(t)$ and $D(t) = r(t)F(t)$. Now let us express the emission anisotropy as a function of $S(t)$ and $D(t)$. The general expression of the emission anisotropy is,

$$r(t) = Ae^{-\frac{1}{\tau}t} \tag{3.7}$$

where A is the anisotropy constant and τ is the rotational correlation time in seconds. Groenzin (1999) derived the following expression for the anisotropy,

$$r(t) = \frac{2}{5}e^{-6Dt} \tag{3.8}$$

where D is the diffusion constant of a sphere of volume V. Based on a method used by Einstein, the diffusion constant is give by,

$$6D = \frac{kT}{V\eta} \tag{3.9}$$

where k is the Boltzman constant, T the temperature, V the volume and η the viscosity of the solvent (η_{toluene} = 0.0005716 Pa.s). Thus, the rotational correlation time is,

$$\tau = \frac{V\eta}{kT} \tag{3.10}$$

The rotational correlation time provides the volume of the molecule and thus the radius for a given molecular shape (spherical) from,

$$R = \left(\frac{3kT\tau}{4\pi\eta} \right)^{1/3} \tag{3.11}$$

Determination of the rotational correlation time is possible through measurement of the difference and sum curves. The data are fitted to exponential curves as follows,

$$D(t) = A_1 e^{-\frac{1}{\tau_1}t} \tag{3.12}$$

$$S(t) = A_2 e^{-\frac{1}{\tau_2}t} + A_3 e^{-\frac{1}{\tau_3}t} \tag{3.13}$$

which is approximated to,

$$S(t) \approx (A_2 + A_3) e^{-\frac{1}{\tau_4}t} \tag{3.14}$$

with

$$\tau_4 = \frac{A_2\tau_2 + A_3\tau_3}{A_2 + A_3} \tag{3.15}$$

The ratio of D over S gives,

$$r(t) = \frac{A_1}{A_2 + A_3} e^{-\left(\frac{1}{\tau_1} - \frac{1}{\tau_4}\right)t} \tag{3.16}$$

Thus, the anisotropy constant and the rotational correlation time can be obtained from,

$$A = \frac{A_1}{A_2 + A_3} \tag{3.17}$$

$$\frac{1}{\tau} = \frac{1}{\tau_1} - \frac{1}{\tau_4} \tag{3.18}$$

3.3 Experimental

The sample preparation is first presented then the experimental setup and procedure is provided for each test.

3.3.1 Sample preparation

A small amount of solute is introduced into a cuvette and toluene is added so that the concentration of the solute in toluene is approximately 0.006 g/l, which corresponds approximately to a solution *OD* of 0.2 at a 237 nm excitation wavelength. During sample preparation, repeated dilutions of the solute in toluene are performed until the desired *OD*-wavelength match is obtained. The solution is then de-irradiated by blowing nitrogen during ten minutes in order to remove oxygen, known to induce quenching effects. The sample is then charged into the emission spectrometer for fluorescence emission measurements.

3.3.2 CARY 500 absorption spectrometer

For all absorption measurements, a UV-VIS-Near IR absorption spectrometer CARY 500 is employed (see Fig. 3.3). The spectrometer is controlled by a PII/200 PC with a software that allows complete control of the measurement parameters such as slit width of the monochromator, scanning range, setting of rear beam attenuator, detector and filter change. To collect the spectra, the default setting with a baseline correction is used. The baseline correction is collected with an empty sample compartment. The range of variation of the source wavelength is set from 600 nm to 300 nm. In the vicinity of 300 nm, the optical density increases considerably due to toluene absorbance in this region.

Procedure – For each measurement, 10 mm path-length cuvettes are used. The cuvettes are hermetically closed to avoid solvent evaporation or any contamination. After use, the cuvette is emptied and thoroughly flushed with acetone. Rests of acetone are dried and acetone vapors are removed by purging with nitrogen.

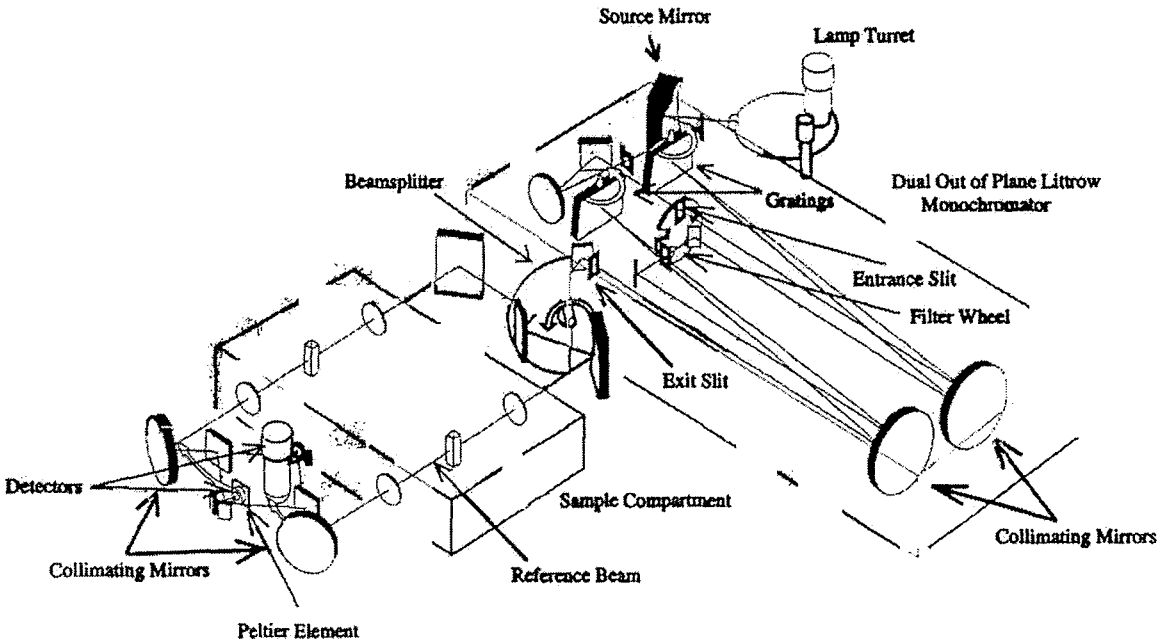
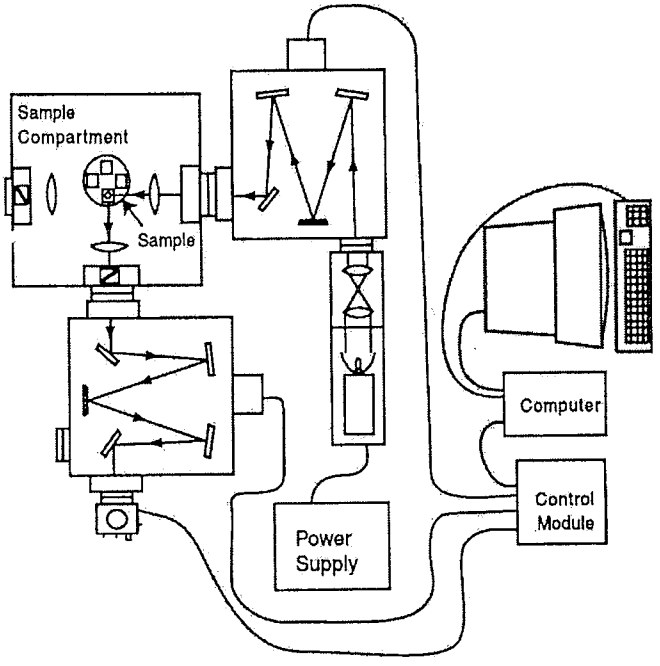


Fig. 3.3 – Schematic of the optical arrangement of the CARY 500 absorption spectrometer. (Groenzin, 1999)

3.3.3 PTI C-72 and A-720 emission spectrometer

For collection of SSFES spectra, the A-720 fluorescence spectrometer is used with a 75 watt Xe compact arc lamp source (see Fig. 3.4a). TDFES data are collected with the (Photon Technology International) PTI C-72 laser system connected to the A-720 fluorescence spectrometer. The PTI C-72 employs a PTI GL-3300 nitrogen laser source along with a PTI GL-302 high-resolution dye laser with a fiber optic coupling to the measurement cell to excite the fluorophore (see Fig. 3.4b). The directions of the excitation and emission light from the cell are oriented 90°C from each other with vertical polarization defined to be perpendicular to this plane. The wavelength of the emission monochromator is fixed while two polarizers (placed before and after the measurement cell) are used to select the polarizations. TDFES curves are collected for four source-emission polarizations: vertical-vertical (*vv*), vertical-horizontal (*vh*), horizontal-vertical (*hv*), and horizontal-horizontal (*hh*). The *vh* curve has a higher intensity than the *hv* curve due to different transmission efficiency through the emission channel of the instrument. A calibration factor G equal to I_{hv}/I_{hh} is introduced in order to compensate this effect.

a) A-720



b) PTI C-72 and A-720

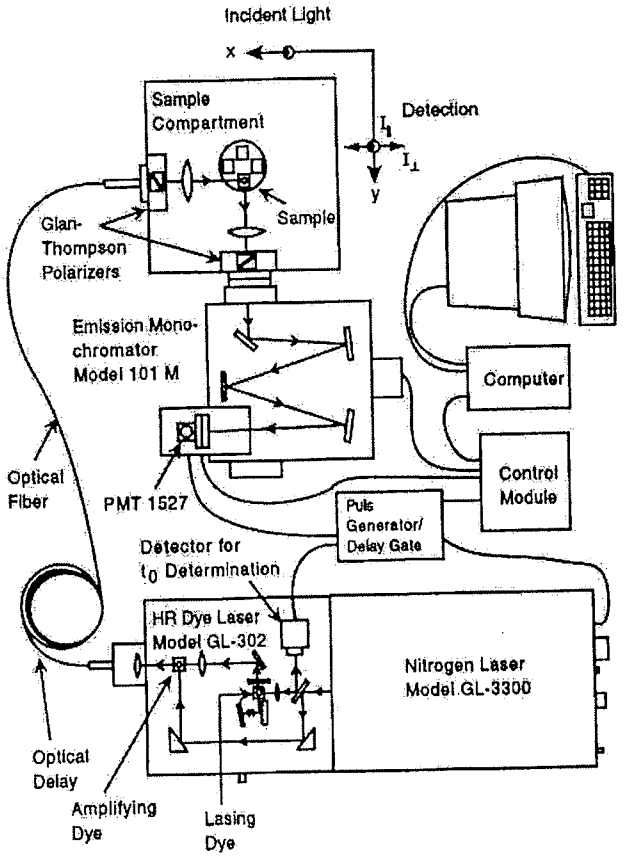


Fig. 3.4 – Schematic of the optical arrangement of the PTI C-72 and A-720 emission spectrometer. (Groenzin, 1999)

Procedure – The steps for the determination of the rotational correlation time τ are,

1) Measure and plot the emission intensity I_{vv}, I_{vh}, I_{hv}, I_{hh}, and $I_{scatterer}$ curves vs. time at different emission wavelengths,
2) Normalize all curves,
3) Correct curves to remove the effect of the scatterer,
4) Calculate the calibration factor *G*,
5) Correct the I_{vh} curve by multiplying by G,
6) Plot the difference curve $D = I_{vv} - I_{vh}G$,
7) Plot the sum curve $S = I_{vv} + 2I_{vh}G$,
8) Fit the difference *D* with an exponential curve,
9) Fit the sum S with the sum of two exponential curves.

3.4 Results

The experimental data obtained from the absorption spectroscopy, steady state and time-dependent fluorescence emission spectroscopy are presented. The selected samples for the SSFES test are the nC_5 asphaltenes, nC_7 asphaltenes, C_3 resins, nC_5 resins, and oils which were separated from petroleum fluids TK and H in Chapter 2. Note that the emission spectra of the other fluids lay between those of petroleum fluids TK and H, and are not presented here. The TDFES test is performed on nC_5 asphaltenes from petroleum fluids H and TK, and on nC_5 resins from petroleum fluid H.

3.4.1 Absorption spectroscopy

The absorption spectra of oils, resins and asphaltenes from our petroleum fluids are measured. All the spectra obtained are similar except those of the very heavy petroleum fluid H. Indeed, a Soret band in the spectrum of nC_5 asphaltenes H and nC_5 resins H at a 406 nm wavelength is detected, suggesting the presence of Vanadium in the fractions (see Fig. 3.5). It is interesting to see that traces of metal are present in both asphaltenes and resins.

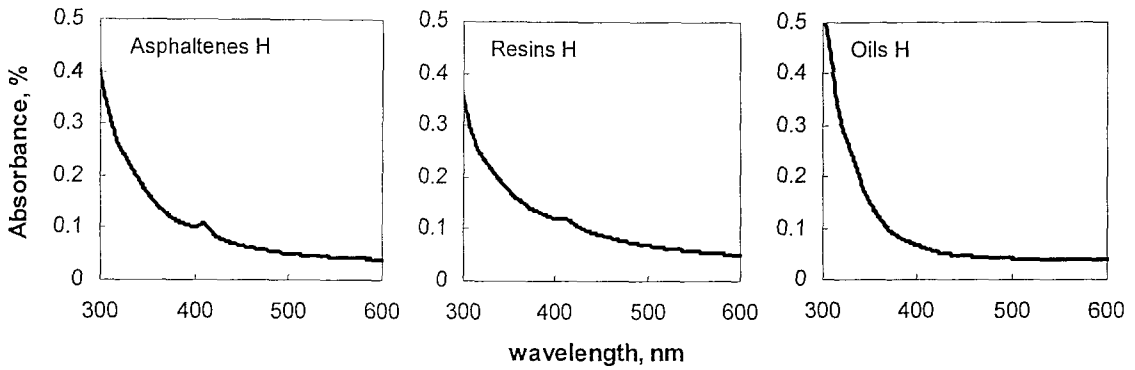


Fig. 3.5 – Absorbance spectra of fractions from petroleum fluid H.

3.4.2 Fluorescence emission spectroscopy

3.4.2.1 Steady state

Fig. 3.6 shows the normalized steady state fluorescence emission spectra of nC_5 asphaltenes and nC_5 resins from petroleum fluids TK and H at two excitation wavelengths (310 nm and 390 nm), and reflects the wide distribution of small and large chromophores in the molecules. Results suggest that the size of asphaltene chromophores from petroleum fluid TK is smaller than that of asphaltene chromophores from petroleum fluid H. On the other hand, the emission spectra of C_5 resins are almost similar; this has also been observed for other petroleum fluids. Fig. 3.7 compares the population size distribution of nC_5 and nC_7 asphaltenes H, C_3 and nC_5 resins H, oils H, and petroleum fluid H at an excitation wavelength of 310 nm. The spectra generated show that the population of large molecules decreases from nC_7 asphaltenes to nC_5 asphaltenes to C_3 resins to nC_5 resins to petroleum fluid to oils.

3.4.2.2 Time resolved

Fluorescence depolarization rates of very dilute solutions of asphaltenes or resins in toluene are analyzed. For each wavelength, the excitation wavelength is about 40 nm shorter than the emission wavelength. Fig. 3.8 provides the TDFES spectra of nC_5 asphaltenes from petroleum fluid H. A complete data set for one excitation and emission wavelength pair corresponds to the acquisition of four time-resolved fluorescence curves *vv*, *vh*, *hv*, and *hh* that are used to generate the anisotropy decay. The initially large difference between *vv* and *vh* curves is due to anisotropy; the reduction of this difference with time is due to rotational diffusion.

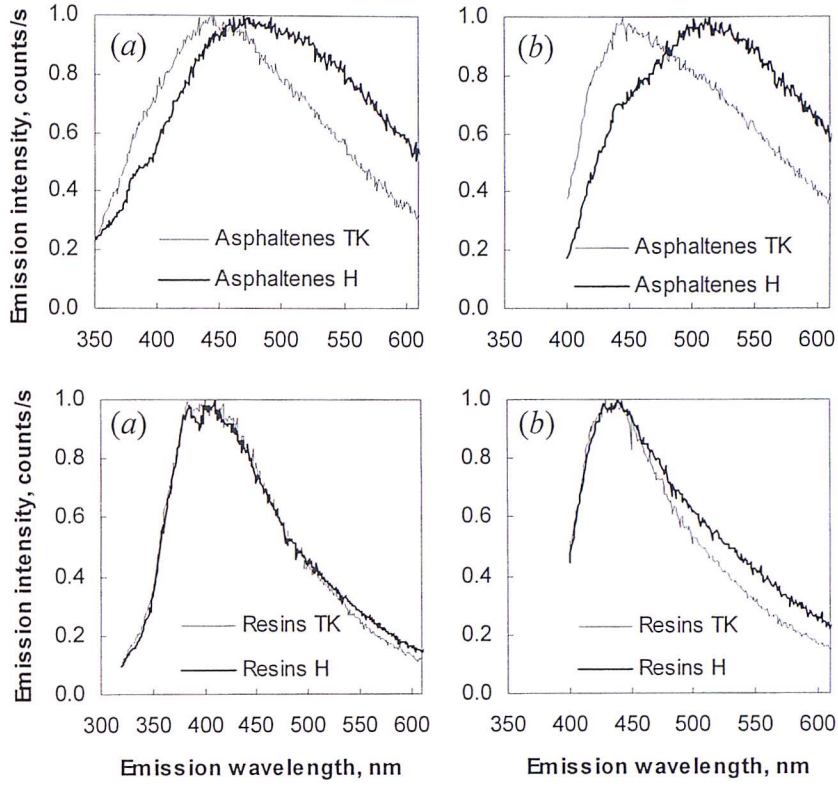


Fig. 3.6 – Normalized SSFES spectra of nC_5 asphaltenes and resins from petroleum fluids TK and H at 310 nm (*a*) and 390 nm (*b*) excitation wavelengths.

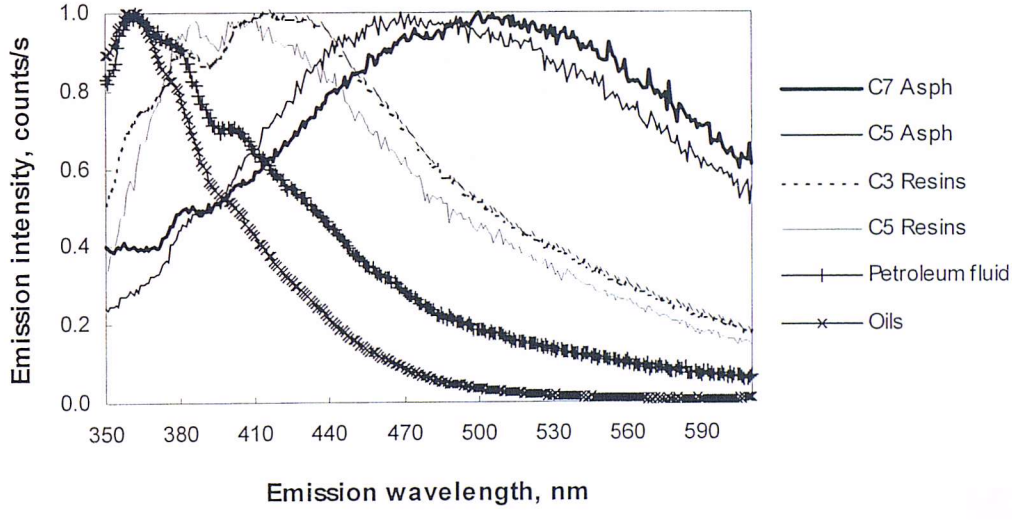


Fig. 3.7 – Normalized SSFES spectra of all the fractions separated from petroleum fluid H at 310 nm excitation wavelength.

The sum and difference curves created from Fig. 3.8 are presented in Fig. 3.9. The fits of the curves are used to calculate the anisotropy constant and the rotational correlation time. The values obtained are reported in Table 3.1 together with the average radius calculated from Eq. (3.11). One can observe that the rotational correlation times of asphaltenes H and resins H are very close. The values vary from 0.01 ns to 0.1 ns as shown in Fig. 3.10. The large variation suggests a wide range of molecular sizes in the asphaltene and resin population of petroleum fluid H, on average the radii are about 5 Å, which is in line with the literature. On the other hand, asphaltenes TK are smaller than asphaltenes H, the rotational correlation times are approximately equal to 0.01 nm giving an average molecular radius of 3 Å (see Table 3.1).

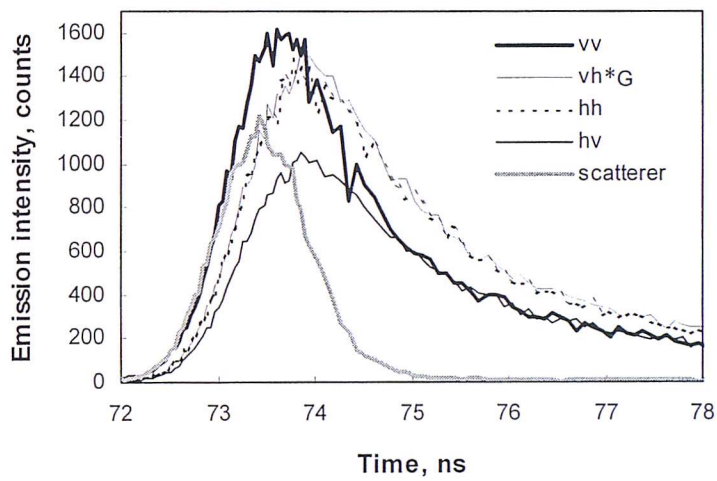


Fig. 3.8 – TDFES lifetime spectra of nC_5 asphaltenes H at 365 nm excitation wavelength (the four time-resolved fluorescence).

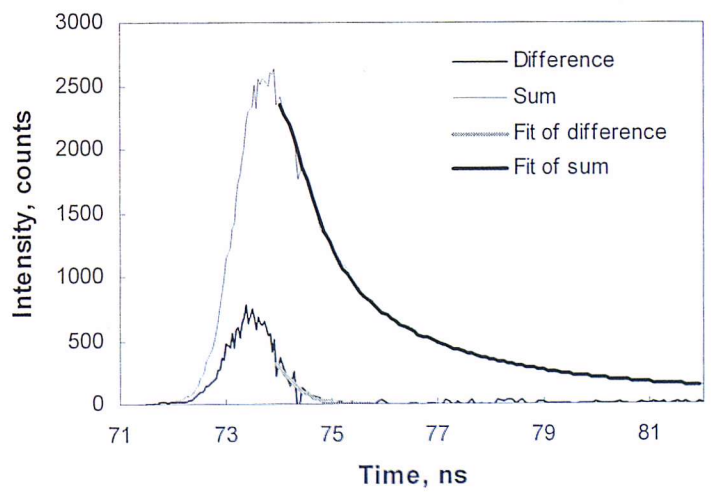


Fig. 3.9 – TDFES lifetime spectra of nC_5 asphaltenes H at 365 nm excitation wavelength (the fits of the difference and the sum curves).

Table 3.1. Results of the TDFES measurements

	λ_{ex}, nm	λ_{em}, nm	τ, ns	A	R, Å
Asphaltenes					
H	600	635	0.1195824	0.271144	5.9
	530	570	0.0967440	0.289565	5.5
	480	520	0.0759931	0.337563	5.1
	440	480	0.0530304	0.315084	4.5
	406	450	0.0403203	0.380936	4.1
	365	410	0.0153176	0.688407	3.0
Average					4.7
TK	600	635	0.016624	0.430692	3.0
	530	570	0.015748	0.48002	2.5
	480	520	0.009496	0.304888	2.9
	406	450	0.015466	0.313558	2.5
	365	410	0.016624	0.430692	2.5
Average					2.7
Resins					
H	440	480	0.062925	0.23987	4.7
	600	635	0.112184	0.199115	5.8
	365	410	0.02822	0.371238	3.6
	406	450	0.053452	0.294846	4.5
Average					4.7

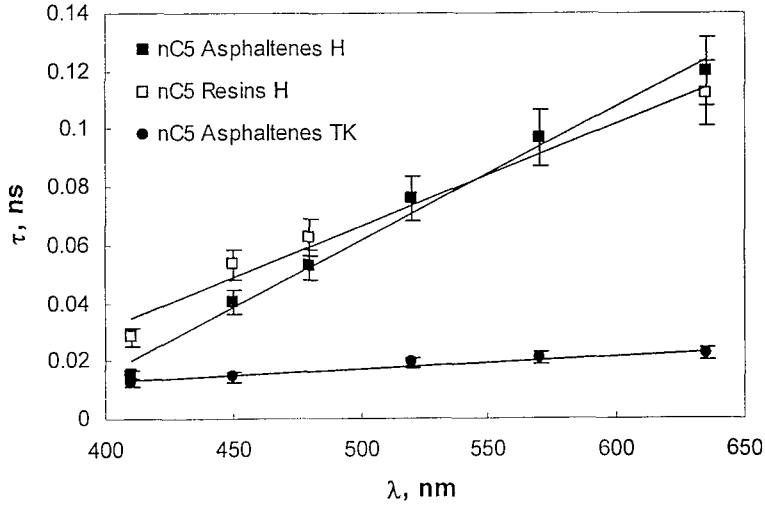


Fig. 3.10 – The rotational correlation times of nC_5 asphaltenes H and TK and nC_5 resins H vs. emission wavelength.

3.5 Conclusions

The conclusions drawn from this chapter are presented in the following points.

1) In a petroleum fluid, the population of large molecules decreases from nC_7 asphaltenes to nC_5 asphaltenes to C_3 resins to nC_5 resins to petroleum fluids to oils.

2) The radii of asphaltenes and resins are in the range of 2.5–6 Å depending on the nature of the petroleum fluid, which is in line with the literature.

3.6 References

Buenrostro-Gonzalez, E., H. Groenzin, C. Lira-Galeana, O. C. Mullins, "The Overriding Chemical Principles that Define Asphaltenes", *Energy and Fuels*, **15**, 4, 972 (2001).

Chuang, T., and K. Eisenthal, "Theory of Fluorescence Depolarization by Anisotropic Rotational Diffusion", *J. of Chem. Physics*, **57**, 5094 (1972).

Dolphin, D., *The Porphyrins*, vol. 3, Academic Press, NY (1978).

Einstein, A., "Zur Theorie der Brownschen Bewegung", *Annalen der Physik*, **19**, 371 (1906).

Groenzin, H, *Resonant Fluorescence Quenching by CS_2 and Asphaltene Molecular Size and Structure Analysis by Fluorescence Anisotropy*, MSc. Thesis, Applied Optics, Rose- Hulman Institute of Technology, Boston (1999).

Groenzin, H., and O. C. Mullins, "Asphaltene Molecular Size and Structure", *J. Phys. Chem. A*, **103**, 11237 (1999).

Groenzin, H., and O. C. Mullins, "Molecular Size and Structure of Asphaltenes from Various Sources", *Energy and Fuels*, **14**, 677 (2000).

Liang, W., G. Que, Y. Chen, and C. Liu, "Chemical Composition and Characteristics of Residues of Chinese Crude Oils", in *Asphaltenes and Asphalts*, 2. Developments

in Petroleum Science, 40B, Chapter 10, Edited by T. F. Yen, and G. V. Chilingarian, Elsevier (2000).

Perrin, F., "Polarisation de la Lumière de Fluorescence. Vie Moyenne des Molecules dans l'Etat Excite", *J. de Physique et le Radium*, **5**, 497 (1926).

Tao, T., "Time-dependent Fluorescence Depolarization and Brownian Rotational Diffusion Coefficients of Macromolecules". *Biopolymers*, **8**, 609 (1969).

Zajac, G. W., N. K. Sethi, and J. T. Joseph, "Molecular imaging of Petroleum Asphaltenes by Scanning-Tunneling-Microscopy- Verification of Structure from C13 and Proton Nuclear-Magnetic-Resonance Data", *Scanning Microscopy*, **8**, 3, 463 (1994).

Chapter 4

Dipole moment of asphaltenes, resins, and oils

Asphaltenes and resins are polar while the rest of the so-called oils are either non- or mildly polar. The interaction between these species has a strong effect on asphaltene precipitation from petroleum fluids. It is believed that the polarity of asphaltenes and resins affects precipitation. The Onsager formulation of dipolar moments is used to measure the dipole moment of asphaltenes, resins, and the oil species in petroleum fluids. The dipole moment is a measure of polarity and is in the range of 3.3–7.0 D for nC_5 asphaltenes, 2.4–3.2 D for resins, and 0.0–0.9 D for oils. The dipole moment of resins is reported for the first time in this thesis. Results reveal that for a given petroleum fluid, asphaltenes have a higher dipole moment than resins. However, resins from one petroleum fluid can have a higher dipole moment than asphaltenes from another petroleum fluid.

4.1 Introduction

In chapter 2, several samples of asphaltenes, resins, and oils have been separated from eight petroleum fluids. The separation procedure allowed the preservation of all the polar constituents of resins in the resin fraction. The polar character of resins plays an important role in the stabilization of asphaltenes in petroleum fluids (Speight, 1999). Also, the polarity of asphaltenes affects the micellar formation and precipitation. This chapter investigates the polarity of asphaltenes, resins, and oils from the measurement of their dipole moments.

There has been very little work on the measurement of asphaltene and resin dipole moment, despite their polar character. To the best of our knowledge, the dipole moment of resins has not yet been reported in the literature. The dipole moment depends on the structure and size of the molecule, and is a guide to the polarity generated by functional groups and metallic elements. The polarity of asphaltenes has often been related to heteroatom or metal content (Nalwaya *et al.*, 1999; Kaminski *et al.*, 1999). Swanson (1942) studied qualitatively the polarity of asphaltenes, resins and oils by dielectric constant measurements in benzene solution at different frequencies. Asphaltenes were found to be highly polar while resins had intermediate polarity between asphaltenes and oils. Conversely, Ese *et al.* (1998) analyzed the adsorptive properties of asphaltenes and resins and concluded that resins were more polar than asphaltenes. Maruska and Rao (1987) investigated the dipole moment of asphaltenes and reported a value of 5.3 D (the symbol for Debye) for a vacuum residue of a heavy petroleum fluid. They used the Onsager theory (1936) to correlate the dipole moment of asphaltenes to the dielectric constant and refractive index. Because asphaltenes are solid, it was not possible to determine directly the dielectric constant by dielectric spectroscopy; instead, Maruska and Rao dissolved asphaltenes in dilute toluene solutions. At low asphaltene concentrations (<10wt%), the dielectric constant and refractive index were found to vary linearly with concentration. The linear variations were then extrapolated to 100 wt% concentration to estimate the properties of pure asphaltenes. Halvorsen (1997) measured the dipole moment of asphaltenes from several North Sea petroleum fluids precipitated by n-pentane. Dielectric constants were determined by dielectric spectroscopy (100 Hz to 15 MHz) and a loop system allowed the circulation of p-xylene solutions from the dielectric cell to the impedance meter. Halvorsen used the Debye theory (1929) to relate the dielectric constant to the dipole moment of asphaltenes and reported values ranging from 4 to 17 D. In this chapter, it will be demonstrated that the Debye theory may not provide reliable results. A study of the dielectric behavior of hydrocarbon mixtures by Sen *et al.* (1992) revealed that the Debye theory can be used for mixtures of nonpolar liquids (such as n-octane in n-hexane) while the Onsager theory can be used for mixtures of polar and nonpolar liquids (such as acetone in n-hexane).

The main objective of this chapter is to measure the dipole moment of asphaltenes, resins, and oils. The theory of dipole moment is briefly reviewed and various methods are compared using chemicals with a known dipole moment. The appropriate method is selected and applied for measuring the dipole moment of asphaltenes and resins. The determination of asphaltene and resin dipole moments is important in that it provides a valuable database for the study of the effect of resin polarity on asphaltene precipitation (see chapter 5), and the calculation of molecular interactions involving asphaltene molecules in a solvent medium (see chapter 6).

4.2 Theory of dipole moment of molecules

In a dipolar molecule, the center of negative charges (say electrons) and the center of positive charges (say protons) do not coincide. In such molecules, the charge times the separation between the centers is called dipole moment (Feynman, 1964). Large molecules containing heteroatoms such as ms-tetraphenylporphine do not necessarily possess a dipole moment when they have a symmetrical structure (Kumler, 1942). For non-symmetrical molecules, the dipole moment is the vector (directed from the negative to the positive charge) that tends to orient a molecule in a polarized dielectric. The dipole moment is generally expressed in Debye (1 D = 3.338×10^{-30}C m); it is given by,

$$\mu = \sum_i e_i \boldsymbol{r}_i \tag{4.1}$$

where i refers to the number of atoms in the molecules, e_i is the charge of an atom in the molecule, and $\boldsymbol{r}_i$ is the distance vector between charges. The charge distribution creates an electric field that tends to line up the individual dipoles to produce a net moment per unit volume called electric polarization. The electric polarization $\boldsymbol{P}$ is given by,

$$\boldsymbol{P} = N\mu \tag{4.2}$$

where N is the number of molecules per unit volume.

One can study the behavior of dielectrics in a condenser to estimate the electric properties. Dielectrics, such as petroleum fluids are insulators; such materials do not conduct electricity, but when placed in an electric field, molecules become polarized. When an electric field is applied, the charges that build on the plates of the condenser are two types: free charges, and polarization charges (of opposite sign) due to polarization; the net charge on the plates will be the difference between the two. The charge density due to polarization is equal to the electric polarization inside the dielectric (Feynman, 1964). The dielectric constant is a characteristic of the dielectric and is given by,

$$\varepsilon = \frac{\varepsilon_a}{\varepsilon_0} \tag{4.3}$$

where ε_a is the absolute permittivity of the dielectric and ε_0 is the absolute permittivity of vacuum. The dielectric constant depends on the frequency ν and is written in the complex space as,

$$\varepsilon(\nu) = \varepsilon'(\nu) - i\varepsilon''(\nu) \tag{4.4}$$

$$\varepsilon(\nu) = \begin{cases} \varepsilon'(0) & \text{at radio } \nu \\ \varepsilon'(\infty) = n^2 & \text{at visible } \nu \end{cases}$$

where ε' and ε'' are the dielectric storage and loss, respectively (see Fig. 4.1). The dielectric storage is the amount of polarization created at a given frequency and helps to determine the nature of the constituent material. The dielectric loss represents the energy of molecules dissipated or lost as heat; it is used to estimate the penetration of the sensing wave into the material (Sen *et al.*, 1992; Pedersen *et al.*, 1999). At radio frequency, the dielectric constant equals the dielectric storage at zero frequency; it is also called static dielectric constant $\varepsilon'(0)$. At visible frequency, the dielectric constant is approximated by the dielectric storage at infinite frequency $\varepsilon'(\infty)$; it is equal to the square root of the refractive index n of the sodium D-line of light (Maxwell, 1954).

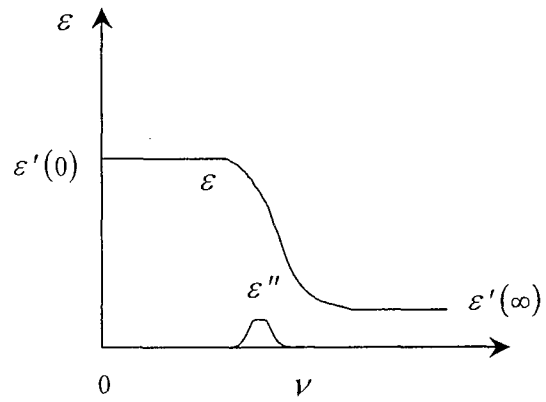


Fig. 4.1 – Schematic representation of the dielectric constant vs. frequency

Using fundamental electrostatic equations, one can readily derive the following expression that relates electric polarization to electric field $\boldsymbol{E}$ (Böttcher, 1952),

$$\boldsymbol{P} = \frac{(\varepsilon - 1)}{4\pi}\boldsymbol{E} \tag{4.5}$$

The dipole moment cannot be measured directly. Several theories exist to relate the dipole moment to macroscopic measurable quantities such as dielectric constant, refractive index and density. The first theory from Clausius and Mosotti (Böttcher, 1952) is applicable to non-polar molecules. Debye (1929) extended the formulation of Clausius and Mosotti to polar gases and liquid solutions. Later, Onsager (1936) advanced the original Clausius and Mosotti theory for polar molecules and proposed a new formulation. A brief review of these theories is presented in the following.

4.2.1 The Clausius & Mosotti theory

Clausius and Mosotti used the notion of internal field to relate the dielectric constant of a non-polar spherical molecule to the density (Böttcher, 1952; Born and Wolf, 1980). While the electric field is the mean field obtained by averaging over a region that contains a large number of molecules, the internal (or effective) field acts on the molecule itself. The difference between the two fields is due to the gaps between molecules (Born and Wolf, 1980). To estimate the internal field, each molecule is considered to be surrounded by a small sphere. For non-polar molecules, molecules inside the sphere do not produce any resulting field at the central molecule and one

may regard the molecule as being situated in a spherical region inside which there is vacuum and outside which there is a homogeneously polarized medium. The internal field is derived by assuming that the field at the spherical hole is equal to the difference between the field at any point in the dielectric and the field due to a spherical plug. The expression for the internal field $\boldsymbol{F}$ is given by,

$$\boldsymbol{F} = \boldsymbol{E} + \frac{4\pi}{3}\boldsymbol{P} \tag{4.6}$$

In vacuum, the internal field equals the electric field but in other materials, it is higher. Clausius and Mosotti assumed that the electric dipole moment induced in a molecule is proportional to the internal field,

$$\mu^{ind} = \alpha_v \boldsymbol{F} \tag{4.7}$$

where α_v is the polarizability volume of the molecule, a macroscopic quantity which has the unit of volume (Smyth, 1955). The polarizability volume is a measure of the strength with which protons in the nucleus attract the electrons and prevent their distortion by the applied field. This parameter increases with increasing atomic number, atomic size, and the ease of excitation of atoms in the molecules (Atkins, 1978). When N molecules are contained in a unit volume, one can write,

$$\frac{4\pi R^3}{3} N = 1 \tag{4.8}$$

where R is the radius of the spherical molecules. Combining Eqs. (4.2), (4.5), (4.6) and (4.7),

$$\frac{\varepsilon - 1}{\varepsilon + 2} = \frac{4\pi}{3} N\alpha_v \tag{4.9}$$

Eq. (4.9) is the general expression of Clausius and Mosotti. From $\varepsilon = n^2$ and combining Eqs. (4.8) and (4.9),

$$\alpha_v = \frac{n^2 - 1}{n^2 + 2} R^3 \tag{4.10}$$

The polarizability volume (also dipole moment) may have two contributions

depending on the nature of the molecule and the frequency of excitation: 1) permanent (orientation) and 2) induced. Polar molecules experience both contributions at very low frequencies (such as radio frequencies) while non-polar molecules experience only the induced one. The induced contribution is the result of two parts: 1) atomic (or distortion) and 2) electronic effects. The former is associated with the molecular vibrations and the latter results from the displacement of the electron cloud by the field in the visible-ultraviolet frequency domain. The atomic polarizability volume is not readily determined and may be neglected on the grounds that it is partially compensated by the use of refractive index of the sodium D-line of light to estimate the electronic polarizability volume (or dipole moment).

Limitations – The Clausius and Mosotti equation applies to gases at moderate pressures but deviations may occur at high pressures when the polarizability volume of molecules is large. There may also be some deviations for liquids especially for mixtures (Böttcher, 1952).

4.2.2 The Debye theory

Debye (1929) borrowed the oldest model of conductive spheres proposed by Clausius and Mosotti. He made the implicit assumption that the average permanent dipole moment of a molecule is proportional to the internal field. In the absence of external forces, the moments of a number of molecules will, on the average, be distributed with the same probability over all directions in space. Therefore, if one considers a small solid angle at a given orientation, the average dipole moment is, according to Debye, equal to the total dipole moment divided by the number of molecules in the direction confined within the solid angle. Debye used the Boltzmann-Maxwell distribution law to calculate the small variations of the number of molecules confined within the solid angle. The final expression of the average dipole moment found is,

$$\overline{\mu} = \left(\alpha_v + \frac{\mu^2}{3kT} \right) F \tag{4.11}$$

where F is the magnitude of the internal field vector. Combining Eqs. (4.2), (4.5), (4.6), (4.8), (4.10) and (4.11) gives the Debye equation,

$$\frac{\varepsilon-1}{\varepsilon+2}=\frac{n^2-1}{n^2+2}+\frac{4\pi N}{9kT}\mu^2 \tag{4.12}$$

It is more convenient to work with molar polarization P_M because of its additivity in mixtures (Debye, 1929; Böttcher, 1952; and Smyth, 1955). The molar polarization is defined by,

$$P_M=\frac{\varepsilon-1}{\varepsilon+2}\frac{M}{\rho} \tag{4.13}$$

From the expression of the number of molecules per unit volume,

$$N=\frac{\rho N_A}{M} \tag{4.14}$$

and combining Eqs. (4.12), (4.13) and (4.14), one can write,

$$P_M=\frac{n^2-1}{n^2+2}\frac{M}{\rho}+\frac{4\pi N_A}{9kT}\mu^2 \tag{4.15}$$

The first term on the right hand side of Eq. (4.15) is the induced molar polarization, and the second term is the orientation molar polarization. Therefore,

$$P_M=P_{ind}+P_\mu \tag{4.16}$$

Limitations – At moderate pressures, the dielectric constant of a gas conforms accurately to the Debye equation. The dipole moment is generally determined from temperature variation. The procedure consists of plotting the molar polarization against $1/T$ and deducing the dipole moment from the slope of the straight line. For polar liquids, the dipole moment is usually overestimated and the theory does not hold. Several authors claimed that the limitations of the Debye equation are due to association between polar molecules (Böttcher, 1952). To overcome this deficiency, it was suggested to work with a very dilute solution of polar solutes in a non-polar solvent. A series of differentiation techniques were proposed to measure the dipole moment of solutions of polar solutes in nonpolar solvents.

Differentiation methods – The Debye theory was recast according to the modifications introduced by various authors. Only the methods in which the electronic molar polarization of the polar molecule is not required are retained. The selected methods are those proposed by Cohen-Henriquez (Böttcher, 1952), LeFèvre (1948), Smyth (1950) and Guggenheim (1951). Measurements are performed with dilute solutions of a polar solute (species 1) in a non-polar solvent (species 2). The methods consider the additivity of molar polarization and molecular weight, and assume linear variations of the dielectric constant, refractive index (and density in some cases) with the mole or weight fraction of the solute as shown in Table 4.1. The authors listed in Table 4.1 expressed the difference between the molar polarization at a low frequency and at visible frequency in order to eliminate the solvent and the electronic polarization of the solute. The expression obtained is then differentiated with respect to mole (or weight) fraction of the solute at very low concentrations; the expressions of the orientation molar polarization of the solute are obtained (see Table 4.1). The equation of Smyth is similar to the one by LeFèvre, except that the density term is neglected. Guggenheim further simplified Smyth's equation by assuming that the dielectric constant of the solvent is approximately equal to the square of its refractive index. Böttcher found that the last three methods give similar results (1951). The Guggenheim version is selected for its simplicity. The Cohen-Henriquez equation is also selected and compared with the one by Guggenheim.

Table 4.1 – Differentiation methods of Debye equation for binary mixtures of polar solute (species 2) in nonpolar solvent (species 1)

Author	Year	Assumptions	Orientation molar polarization	Eq.
Cohen-Henriquez	1935	$\varepsilon = az_2 + \varepsilon_1$ $n = cz_2 + n_1$	$P_{\mu_2} = \frac{3M_1}{\rho_1(n_1^2+2)^2}(a-2n_1c)$	(T1)
LeFèvre	1948	$\varepsilon = \varepsilon_1(aw_2+1)$ $\rho = \rho_1(bw_2+1)$ $n^2 = n_1^2(cw_2+1)$	$P_{\mu_2} = \frac{3M_2}{\rho_1}\left(\frac{(1-b)(\varepsilon_1-n_1^2)}{(\varepsilon_1+2)(n_1^2+2)} + \frac{a\varepsilon_1}{(\varepsilon_1+2)^2} - \frac{cn_1^2}{(n_1^2+2)^2}\right)$	(T2)
Smyth	1950	$\varepsilon = \varepsilon_1(aw_2+1)$ $n^2 = n_1^2(cw_2+1)$	$P_{\mu_2} = \frac{3M_2}{\rho_1}\left(\frac{a\varepsilon_1}{(\varepsilon_1+2)^2} - \frac{cn_1^2}{(n_1^2+2)^2}\right)$	(T3)
Guggenheim	1951	$\varepsilon_1 \approx n_1^2$ $\varepsilon = \varepsilon_1(aw_2+1)$	$P_{\mu_2} = \frac{3M_2}{\rho_1}\frac{\varepsilon_1}{(\varepsilon_1+2)^2}(a-c)$	(T4)

4.2.3 The Onsager theory

Because the internal field depends on the orientation, Onsager (1936) proposed to compute the orienting force-couple for each individual direction of the dipole. Onsager considered the original Clausius and Mosotti theory of the internal field not applicable to permanent dipoles. In his work, the total dipole moment $\boldsymbol{m}$ is the vector sum of the permanent and the induced dipole moments,

$$\boldsymbol{m} = \mu \boldsymbol{u} + \alpha_v \boldsymbol{F} \tag{4.17}$$

where μ is the permanent dipole moment in vacuum (which rotates around a mean orientation) and $\boldsymbol{u}$ is the unit vector in the direction of the dipole axis. In addition, the internal field is the sum of a cavity field and a reaction field.

$$\boldsymbol{F} = \boldsymbol{G} + \boldsymbol{R} \tag{4.18}$$

where $\boldsymbol{G}$ is the cavity field vector and $\boldsymbol{R}$ is the reaction field vector. The reaction field is parallel to the average dipole moment and it is only the cavity field that contributes to the orientation of the polar molecule. Onsager solved the electrostatic problem by combining the results of a dipolar molecule in a non-polarized dielectric with those of a spherical cavity in a polarized dielectric. The internal field is then expressed as (detailed derivations are provided by Onsager (1936)),

$$\boldsymbol{F} = \left(1 + \frac{n^2(\varepsilon - 1)}{2\varepsilon + n^2}\right)\boldsymbol{E} + \frac{\mu}{R^3}\frac{2(\varepsilon - 1)}{2\varepsilon + 1}\frac{(n^2 + 2)(2\varepsilon + 1)}{3(2\varepsilon + n^2)}\boldsymbol{u} \tag{4.19}$$

Eqs. (4.6) and (4.19) are identical for non-polar molecules (for which $\mu = 0$ and $\varepsilon = n^2$). Unlike the induced dipole moment, the permanent dipole moment depends on the orientation of the molecule and its average value is equal to the actual dipole moment times the mean orientation of the molecule. The mean orientation is determined from the Boltzmann-Maxwell formula using the work of orientation. The expression derived by Onsager is then introduced into Eqs. (4.17)–(4.19) to give the Onsager equation,

$$\frac{\varepsilon-1}{\varepsilon+2}=\frac{n^2-1}{n^2+2}+\frac{4\pi N}{9kT}\left(\frac{3\varepsilon\left(n^2+2\right)}{\left(2\varepsilon+n^2\right)\left(\varepsilon+2\right)}\mu^2\right) \tag{4.20}$$

Eqs. (4.12) and (4.20) are identical for $\varepsilon = n^2$. Therefore, the Onsager and Debye equations give similar results for nonpolar molecules. However for polar molecules ($\varepsilon > n^2$), the dipole moments calculated from Debye and Onsager equations are different.

Limitations – The formulation of Onsager is limited to spherical molecules in liquid systems. In addition, the neighborhood of a molecule is considered to be a continuum.

4.3 Experimental

The dipole moment determination is made by measuring the dielectric constant and refractive index of dilute solutions of asphaltenes, resins and oils in toluene. The procedure is similar to Maruska and Rao's (1987), however lower concentrations of polar solutes are used to allow visual reading of the refractive index and to reduce the effect of association. There has been a debate whether nC_5 asphaltenes are less polar than nC_7 asphaltenes or vice-versa (Speight, 1999). The asphaltenes are separated with both n-alkanes to clarify the issue of polarity by measuring the dipole moment. The dipole moment of resins by adsorption after elution of oils with nC_7 is also measured.

4.3.1 Dielectric constant

In a class of substances called insulators or dielectrics, the electrons move a very small distance from the nucleus when the substance is subjected to an electric field. The dielectric constant of a dielectric substance is a measure of chemical composition and density (Feynman, 1964). When a condenser containing a dielectric substance is subjected to an electric field, the dielectric constant is given by $\varepsilon = C/C_0$ where C and C_0 are the capacitance of the condenser filled with the dielectric and air, respectively. In this study, a liquid test fixture is used as a condenser. The determination of capacitance is performed at ambient conditions through impedance measurements (HP impedence measurement handbook, 1999). The electronic circuit comprises the liquid fixture connected to an LCR meter that measures the inductance

L, the capacitance C, and the resistance R of the circuit. The choice of the equipment is driven by the frequency coverage, measurement range, accuracy and ease of operation.

Apparatus – The equipment consist of a precision LCR meter HP 4284A (20Hz to 1MHz frequency range) connected to a liquid test fixture HP 16452A through test leads HP 16048A of 1m- long as shown in Fig. 4.2. The capacity of the liquid test fixture is 3.4 ml. The cell comports four electrodes with 1 mm spacing between plates (see Fig. 4.3). The sensitive areas of the plates are coated with platinum to prevent local polarizability. For accurate reading of capacitance, the equipment is calibrated and a short compensation is performed to account for lead capacitance. Measurements are performed at a frequency of 800 Hz and a voltage level of 1 V.

4.3.2 Refractive index

For a non-absorbing medium, the refractive index is the ratio of the velocity of light in vacuum to the velocity of light in the medium (Bitter, 1956). In the visible range of frequencies, measurements of the refractive index of the sodium D-line of light are possible using a refractometer. The effective speed of light is different in different materials and on this basis, the refractive index depends on the nature of the material (Feynman, 1964).

Apparatus – An Abbe C-10 refractometer is used to measure the refractive index of liquid mixtures to be described later. A built-in thermometer allows the reading of temperature. The range of refractive index covered is 1.300 to 1.700, with an accuracy of 0.0003. Calibration is performed with naphthalene bromide, which has a refractive index of 1.656 at 25°C.

4.3.3 Density

The density of a substance is its mass per unit volume. The density at ambient conditions is usually measured using pycnometers; however digital density-meters, when available, provide more accurate data. In this work, density is measured using 2 types of pycnometers having a fixed volume. Density and refractive index are temperature-dependent.

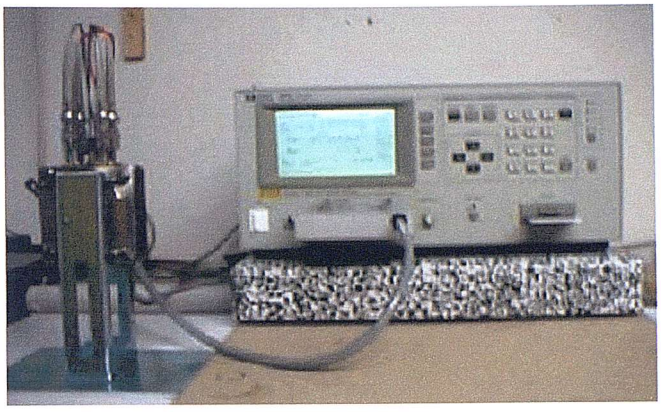
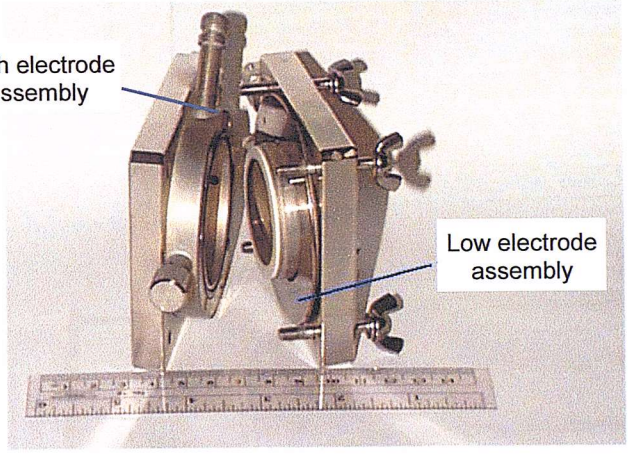


Fig. 4.2 – HP 4284A precision LCR meter connected to the HP 16452A liquid test fixture through HP 16048A test leads



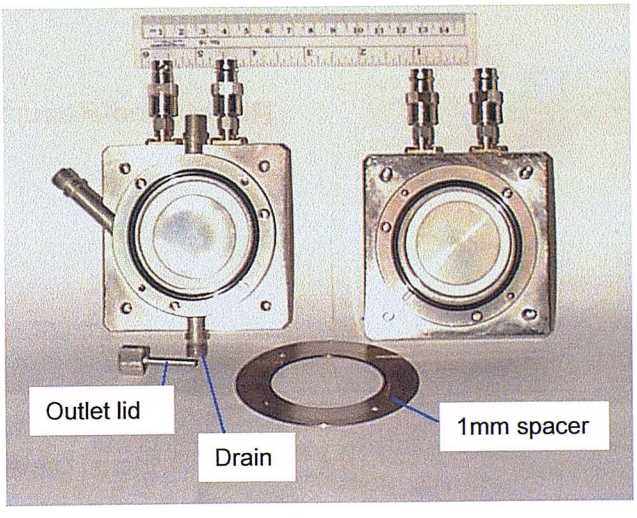


Fig. 4.3 – HP16452A liquid test fixture

Density at a given temperature can be estimated from measurements at another temperature using the correlations of Van Ness and Van Westen (1951).

Apparatus – The density of petroleum fluids is measured using a weld-type pycnometer devised for specific gravity of volatile liquids with an accuracy of 0.001 g/cm^3. The pycnometer made of borosilicate glass, has a capacity of 25 ml and is equipped with a glass stopper and a cap to reduce evaporation of the sample. The density of oils is measured with a Moore-Van Slyke specific gravity bottle with ground-in stopper. The bottles made of borosilicate glass have a capacity of 2 ml.

4.4 Results

The results are presented in two different parts. The first part provides the results of dipole moment calculation from the Debye and Onsager methods for several chemicals with known dipole moments from the literature. In the second part, the Onsager method is selected and applied for the calculation of asphaltene, resin and oils dipole moment. Note that prior to these measurements, the accuracy of the equipment was verified by direct measurement of the dielectric constant and refractive index of pure toluene and water. The difference found between the measured values and the literature data was be less than 1%.

4.4.1 Dipole moment verification

The methods presented for the estimation of the dipole moment of molecules are applied to twelve chemicals with known dipole moments from the literature (Lide and Frederikse, 2000; McClellan, 1963) in Table 4.2. The objective is to verify the validity of the methods; the most accurate method will be used to determine the dipole moment of asphaltenes, resins, and oils. In the selection of the chemicals, we aim to cover a wide range of dipole moments (0 to 4 D) as well as a variety of chemical functions (ketones, alcohols, amines, etc). The dipole moment of toluene, dibutylamine, anisole, ethanol, ethyl acetate, ethyl benzoate and acetone were measured in the vapor phase by the temperature variation procedure in the microwave frequency region, using the Debye equation (Lide and Frederikse, 2000; McClellan, 1963). The dipole moment of the remaining substances were measured in liquid solutions with benzene at 20°C. For instance, the dielectric constant of 2-butanone

solutions in benzene was measured by a Wheatstone bridge method and the dipole moment calculated from LeFèvre (1948) equation. For Dimethylsulfoxide, the dielectric constant was measured by a resonance method and the dipole moment was calculated from the Halverstadt and Kumler (1942) equation. Usually, the dipole moment measurements in the vapor phase are the most reliable (McClellan, 1963).

Table 4.2 – Substances with known dipole moments
(Lide and Frederikse, 2000; McClellan, 1963)

Substance	Formula	M g/mol	$\rho^{20°C}$ g/cm^3	μ D
Toluene	C_7H_8	100.2	0.940	0.37
Dibutylamine	$C_8H_{19}N$	129.2	0.760	1.18
Anisole	C_7H_8O	108.1	1.000	1.36
Ethanol	C_2H_6O	46.1	0.790	1.69
Ethyl acetate	$C_4H_8O_2$	88.1	0.894	1.78
Ethyl benzoate	$C_9H_{10}O_2$	150.2	1.051	1.95
2-Butanone	C_4H_8O	72.1	0.800	2.78
Acetone	C_3H_6O	58.1	0.790	2.88
N,N-Dimethylformamide	C_3H_7NO	73.1	0.944	3.82
Dimethylsulfoxide	C_2H_6OS	78.1	1.096	3.96
3-Methyl-2-cyclopenten-1-one	C_6H_8O	96.1	0.980	4.33

In these measurements, toluene is selected as a solvent although it has a small dipole moment (μ = 0.4 D). The results do not differ significantly when using p-xylene (μ = 0.0 D). Toluene is preferred because of the high solubility of asphaltenes, resins and oils in this solvent. While preparing the solutions, it is important to make sure that all the chemicals are dissolved in toluene. The dipole moment of the substances in Table 4.2 is calculated from various methods, using equations T1 (Cohen-Henriquez) and T4 (Guggenheim) from Table 4.1, and Eq. (4.20) (Onsager). The atomic polarization is neglected in this study. Fig. 4.4 presents results for ethanol solution in toluene. In the Cohen-Henriquez method, the variation of the dielectric constant and refractive index of the solution with the mole fraction of ethanol in toluene is determined. The Guggenheim method requires the determination of $\varepsilon - \varepsilon_1$ and $n^2 - n_1^2$ versus the weight fraction of ethanol in toluene (ε_1 and n_1 are the dielectric constant and

refractive index of toluene, respectively). For the Onsager method, we present the variation of the dielectric constant and refractive index of ethanol solutions as a function of weight percent of ethanol in toluene. In the Cohen- Henriquez and Guggenheim methods, the slope of the straight lines is substituted in the corresponding equations. For the Onsager method, the variations are extrapolated to w_2 = 100 w% to determine the dielectric constant and refractive index of ethanol.

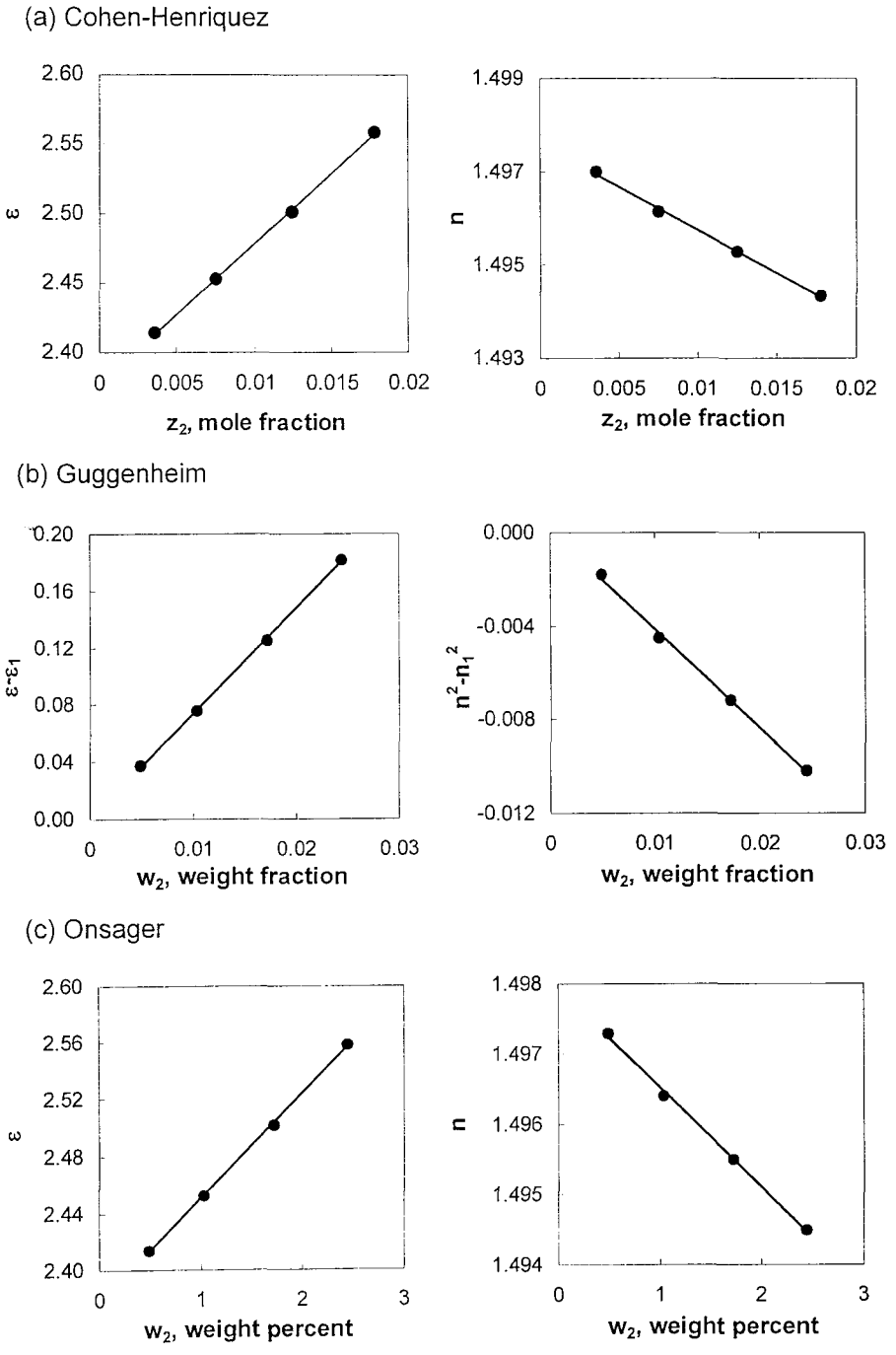


Fig. 4.4 – Dielectric constant and refractive index vs. concentration of ethanol in toluene.

The same procedure is applied to all substances and results are summarized in Table 4.3. For each method, the relative error (%) of the dipole moment and the data from the literature is reported.

Table 4.3 – Dipole moment of substances from different methods
(CH: Cohen-Henriquez, G: Guggenheim, O: Onsager)

	Calculated μ, D					
Substance	CH	Relative error, %	G	Relative error, %	O	Relative error, %
Toluene	0.35	-7	0.53	40	0.36	-3
Dibutylamine	0.86	-27	1.57	33	1.14	3
Anisole	1.57	14	1.93	40	1.13	-16
Ethanol	3.01	78	2.68	58	1.82	8
Ethyl acetate	2.23	25	2.76	55	1.75	-2
Ethyl benzoate	2.45	25	3.01	54	1.67	-14
2-Butanone	3.39	22	4.12	48	2.66	-4
Acetone	3.68	28	4.16	44	2.78	-4
N,N-Dimethylformamide	5.13	34	6.31	65	3.49	-7
Dimethylsulfoxide	5.76	45	7.11	79	3.49	-12
3-Methyl-2-cyclopenten-1-one	6.90	59	7.62	76	4.10	-5

Examination of the results in Table 4.3 reveals that the Cohen-Henriquez and Guggenheim methods overestimate the dipole moment of the substances in Table 4.2. The differences with data in the literature are very high and can be 80%. The error in the estimation becomes large for substances with a high dipole moment. On the other hand, the Onsager equation underestimates the dipole moment. Deviations may arise from the extrapolation technique adopted, which endows some uncertainties in the results especially for refractive indices. Nevertheless, the overall deviation with the Onsager method is small. This method is therefore selected for the determination of the dipole moment of asphaltenes, resins and oils.

4.4.2 Dipole moment of asphaltenes, resins, and oils

Following the above procedure, four different solutions with increasing concentration of solute (that is, asphaltenes, resins or oils) in toluene are prepared. The oils

considered comport only the hydrocarbons that are non-volatile at atmospheric conditions; the light hydrocarbons were removed by evaporation. A small concentration of solutes (<5 wt%) is used in order to allow complete dissolution of asphaltenes and resins in toluene and for accurate reading of refractive indices. For each sample, the tests are repeated two to four times to assure reproducibility of the results.

Among the parameters required in the dipole moment calculation are the molecular weight and density of asphaltenes and resins. The average molecular weights of asphaltenes and resins are 900 amu and 700 amu, respectively (Boduszynski, 1988; Storm *et al.*, 1990). The density is assumed 1.2 g/cc for asphaltenes (Schabron and Speight, 1998; De Hemptinne *et al.*, 1999) and 1.0 g/cc for resins (Wu *et al.*, 2000). For oils, the density and refractive index are measured at 20°C and the molecular weight is calculated using the Riazi and Daubert (1987) correlation.

Figs. 4.5 and 4.6 illustrate the variation of the dielectric constant and refractive index of nC_5 asphaltenes, resins and oils for the very heavy petroleum fluid H and the very light petroleum fluid B, respectively. The linear variations are extrapolated to w_2 (weight fraction in toluene) of 100 wt% to estimate the dielectric constant and refractive index of asphaltenes, resins and oils. The small range of variation of w_2 especially for asphaltenes increases the uncertainty in the extrapolation results. For each asphaltene, resin and oils sample, the tests are repeated three to four times and the standard deviation in the dielectric constant and refractive index is about 2% and 0.5%, respectively. Oils are viscous translucent liquids and their refractive index can be measured directly. The data obtained by direct measurement and extrapolation from oils in toluene solutions compare very well. The dielectric constant and refractive index of asphaltenes, resins and oils are reported in Table 4.4 along with density and molecular weight. The dielectric constant of asphaltenes, resins and oils is in the range of 5.5–18.4, 3.8–5.1, and 2.1–2.6, respectively. The range of variation of the refractive index is 1.638–1.707 for asphaltenes, 1.576–1.608 for resins, and 1.472–1.527 for oils. The refractive indices of asphaltenes are in line with those reported in the literature (see Table 4.5).

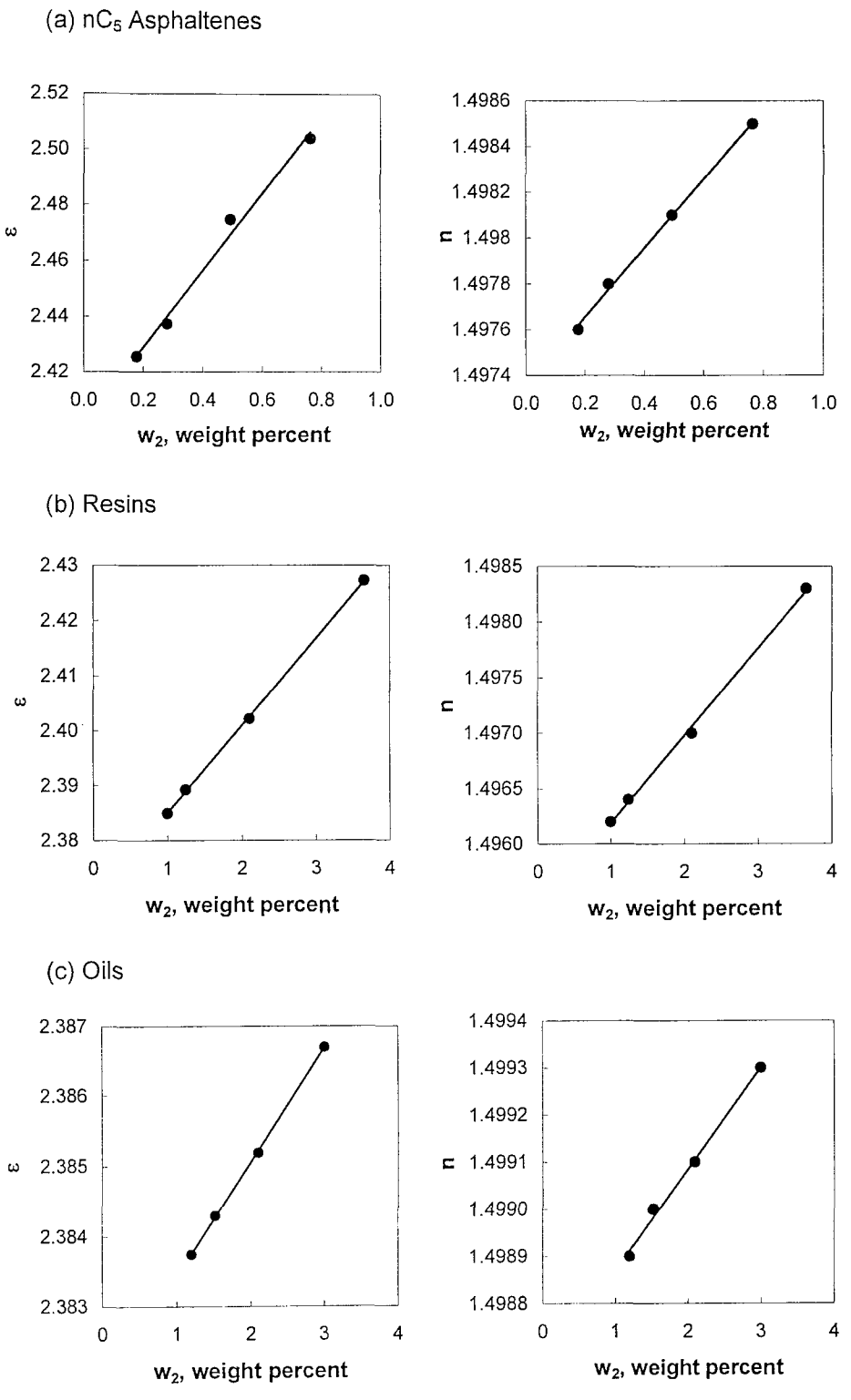


Fig. 4.5 – Dielectric constant and refractive index vs. concentration of nC_5 asphaltenes, resins and oils in toluene for petroleum fluid H.

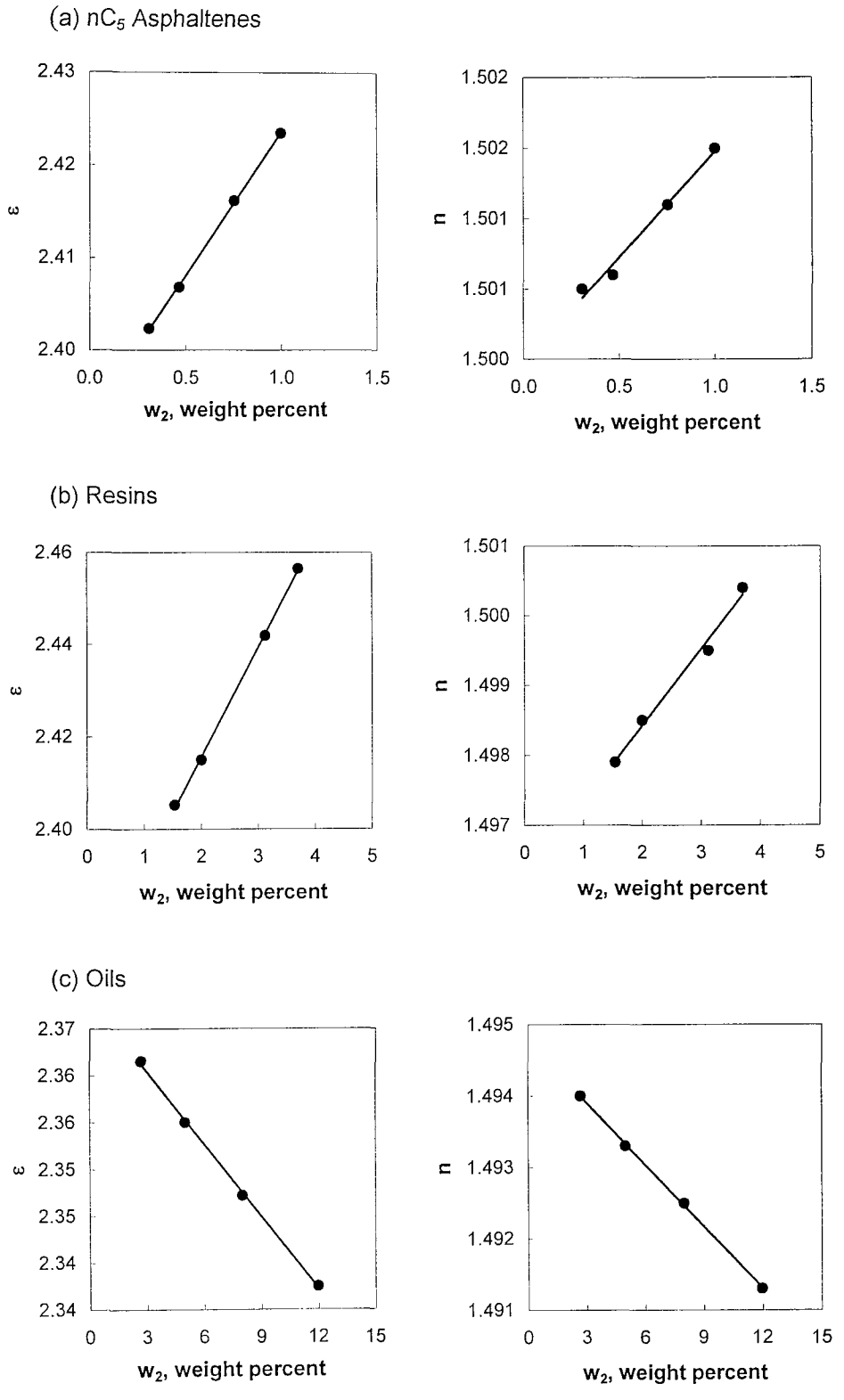


Fig. 4.6 – Dielectric constant and refractive index vs. concentration of nC_5 asphaltenes, resins and oils in toluene for petroleum fluid B.

Table 4.4 – Dielectric constant, refractive index, density and molecular weight of nC_5 asphaltenes, resins and oils

	H	TE	C	TA	TK	S	U	B
				nC_5 asphaltenes				
$n^{20°C}$	1.647	1.707	1.638	1.676	1.706	1.668	1.685	1.650
ε	16.2	18.4	15.2	9.2	10.9	10.1	8.2	5.5
$\rho^{20°C}$, g/cm^3	1.2	1.2	1.2	1.2	1.2	1.2	1.2	1.2
M, g/mol	900	900	900	900	900	900	900	900
				Resins				
$n^{20°C}$	1.576	1.587	1.606	1.585	1.608	1.608	1.595	1.606
ε	3.9	3.8	5.1	4.8	4.5	3.9	3.8	4.7
$\rho^{20°C}$, g/cm^3	1.0	1.0	1.0	1.0	1.0	1.0	1.0	1.0
M, g/mol	700	700	700	700	700	700	700	700
				Oils				
$n^{20°C}$	1.527	1.522	1.487	1.497	1.496	1.498	1.496	1.472
ε	2.6	2.5	2.2	2.3	2.4	2.4	2.4	2.1
$\rho^{20°C}$, g/cm^3	0.935	0.935	0.875	0.876	0.876	0.870	0.881	0.830
M, g/mol	371	389	269	287	300	290	320	196

Table 4.5 – Dielectric constant and refractive index of asphaltenes and resins reported in the literature

Source	Sample	ε	$n^{20°C}$
Oudin (1970)	nC_5 asphaltenes soluble in CCl_4	6.16	-
	nC_5 asphaltenes insoluble in CCl_4	6.92	-
	Resins	5.32	-
Maruska and Rao (1987)	nC_5 asphaltenes	6.80	1.682
Buckley *et al.* (1998)	nC_6 asphaltenes	-	1.720

However, the measured dielectric constants of asphaltenes from all the petroleum fluids (except petroleum fluid B) are high compared to the values reported in Table 4.5. Oudin (1970) measured the dielectric constant of asphaltenes in chloroform at a concentration of 20 g/l and reported a value of 6.2 for asphaltenes soluble in CCl_4 and 6.9 for asphaltenes insoluble in CCl_4. Maruska *et al.* (1987) measured the dielectric

constant of asphaltenes in toluene at a concentration of 1–100 g/l and reported a value of 6.8. The dielectric constant of asphaltenes in toluene is measured at a concentration of 1–8 g/l and dielectric constants in the range of 5.5–18.4 are obtained. In this work, the asphaltene concentrations in toluene are low compared to those used by Maruska *et al.* and Oudin. This suggests that the high dielectric constants measured in this study may not be due to association between molecules.

Table 4.6 provides the dipole moment of asphaltenes, resins and oils calculated with the Onsager equation. The dipole moments are in the range of 3.3–7.0 D for nC_5 asphaltenes. The standard deviation in the calculated values of dipole moment is about 2%. The dipole moment of asphaltenes increases with the carbon number of the precipitating n-alkane. The results show that nC_7 asphaltenes are more polar than nC_5 asphaltenes (note that the same molecular weight is used for both nC_5 and nC_7 asphaltenes). Previous studies by Nighswander *et al.*, 1993; Speight, 1999 and Nalwaya *et al.* (1999) suggest that the molecular weight and the metal content of asphaltenes increases with the carbon number of the precipitating n-alkane; which is consistent with our dipole moment data. In the adsorption method, nC_7 resins are more polar than nC_5 resins because they contain the nC_5-nC_7 fraction of asphaltenes (that is, the fraction of asphaltenes soluble in nC_7 but insoluble in nC_5). The oils eluted by pure nC_5 possess a small dipole moment that does not exceed 1 D (see Table 4.6). In order to elucidate the origin of this dipole moment, distillation cuts from two different petroleum fluids (an asphaltic petroleum fluid and a waxy petroleum fluid) are used. The asphaltic petroleum fluid is heavy and viscous with high sulfur, asphaltene, resin and aromatic content (>50 wt%). The waxy petroleum fluid contains large amount of paraffins and small amount of aromatics. The asphaltene and resin content in waxy petroleum fluids is low (<10 wt%) (Whauquier, 1995). The dipole moment of the distillation cuts is determined and presented in Table 4.7. The cuts from the waxy petroleum fluid are completely apolar while the cuts from the asphaltic petroleum fluid have dipole moments in the same range as the oils listed in Table 4.6. Moreover, it is unlikely that the distillation cuts up to 550 °F contain any traces of asphaltenes or resins. Asphaltic petroleum fluids are characterized by a high amount of aromatic hydrocarbons (Whauquier, 1995) and this may be the precursor of the small polarity measured. Swanson (1942) reported the small polarity of oils and

attributed it to the high electronic and atomic polarizations of heavy aromatic hydrocarbons.

Table 4.6 – Dipole moment (in Debye) of asphaltenes, resins and oils

	H	TE	C	TA	TK	S	U	B
				Asphaltenes				
Precipitated by								
nC_5	6.9	7.0	6.7	4.8	5.2	5.1	4.4	3.3
nC_7	7.2	7.7	7.2	5.8	6.5	6.4	-	4.0
				Resins				
nC_5	2.5	2.4	3.2	3.1	2.8	2.4	2.4	3.0
nC_7	3.5	3.6	3.9	3.4	3.6	3.9	-	3.7
				Oils				
Eluted by								
nC_5	0.9	0.8	0.0	0.4	0.6	0.7	0.7	0.0

Table 4.7 – Dipole moment (in Debye) of distillation cuts from an asphaltic petroleum fluid and a waxy petroleum fluid

Cut, °C	Asphaltic petroleum fluid	Waxy petroleum fluid
177 – 132	0.3	0.0
232 – 288	0.6	0.0
288 – 343	0.7	0.0
343 – 454	0.9	0.0

The results presented above for different petroleum fluids show that the dipole moment is in the range of 3.3–7.0 D for nC_5 asphaltenes, 2.4–3.2 D for resins, and 0.0–0.9 D for oils. Water is a polar substance and its dipole moment is 1.87 D. The dipole moment measurements show that in these petroleum fluids, asphaltenes and to a lesser degree resins are highly polar molecules. Asphaltenes are more polar than resins in the same petroleum fluid, however, resins of one petroleum fluid can be more polar than asphaltenes of another petroleum fluid.

Tables 4.8 and 4.9 show the effect of charge separation and the presence of heteroatoms on the dipole moment of several substances, respectively. The dipole moment slightly increases from toluene to ethyl anthracene in Table 4.8, suggesting

that charge separation does not contribute significantly to the dipole moment of asphaltenes. Table 4.9 provides the dipole moment of some chemicals that have been reported to be part of the asphaltenes (Waldo *et al.*, 1992; Mitra-Kirtley *et al.*, 1993). The presence of certain groups (such as sulfoxide) in a molecule has a significant effect on the dipole moment.

Table 4.8 – Effect of charge separation on the dipole moment
(Lide and Frederikse, 2000; McClellan, 1963)

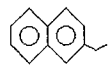
Molecule	Formula	μ, D
Toluene		0.4
Ethyl benzene		0.6
2-Methyl naphthalene		0.4
2-Ethyl naphthalene		0.6
2-Methyl anthracene		0.5
2-Ethyl anthracene		0.6

Table 4.9 – Effect of heteroatoms on the dipole moment
(Lide and Frederikse, 2000; McClellan, 1963)

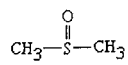
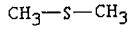
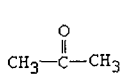
Molecule	Formula	μ, D
1.H-Pyrrole		1.7
Pyridine		2.2
Dimethyl sulfoxide		4.0
Thiophene		0.6
Dimethyl sulfide		1.6
Phenol		1.2
Acetone		2.9

Fig. 4.7 illustrates the variation of the dielectric constant and refractive index of nC_5 asphaltenes and resins vs. the dipole moment. There is a linear relationship between the dielectric constant and dipole moment for both asphaltenes and resins. However, no correlation is observed between the refractive index and the dipole moment of these fractions.

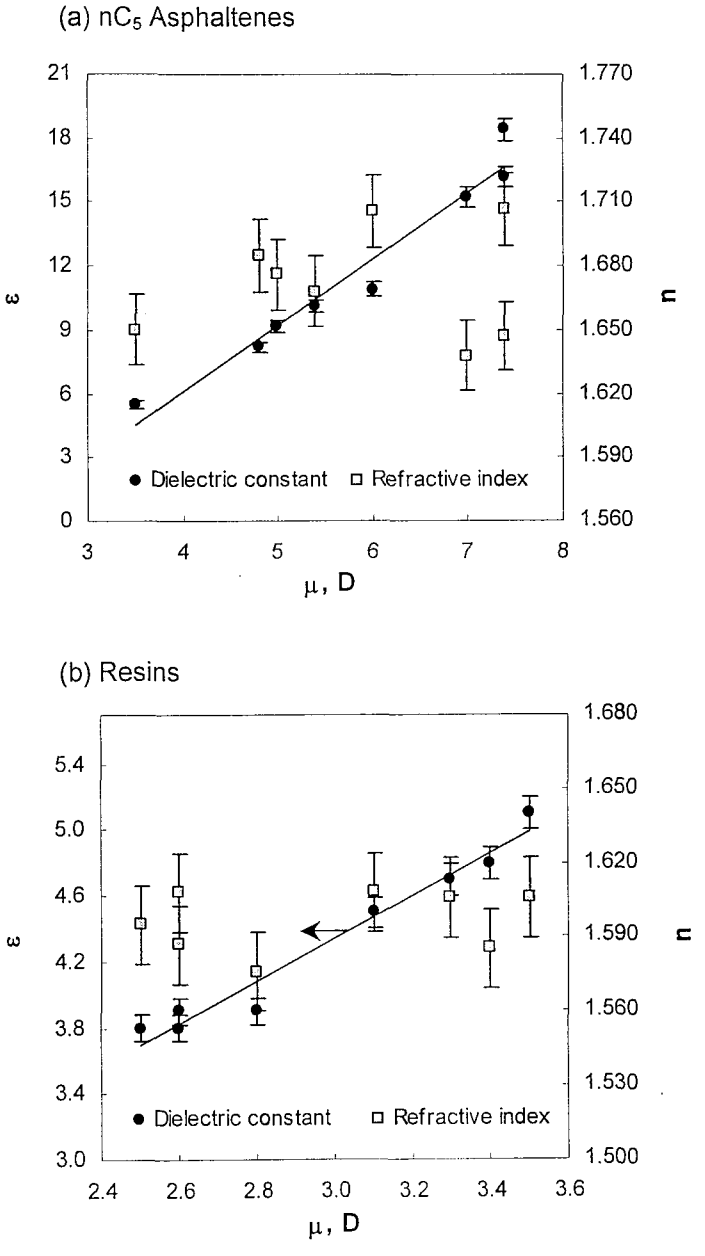


Fig. 4.7 – Dielectric constant and refractive index vs. dipole moment of nC_5 asphaltenes and resins.

A closer examination of Fig. 4.7 shows that the refractive index is around 1.68 for asphaltenes and 1.60 for resins. This might indicate that molecules with a same refractive index are not similar if their dipole moment is different. The refractive index has been previously used to determine the onset point of asphaltene precipitation from petroleum fluids (Buckley *et al.*, 1998) and was concluded that asphaltene precipitation is dominated by London dispersion interactions. Chapter 5 of this thesis demonstrates that the effect of resins on asphaltene precipitation is a function of their dipole moment. In the same chapter, the onset point of asphaltene precipitation is found to increase when resins or surfactants are added to the petroleum fluid; the magnitude of the increase as well as the amount of precipitation depend on the dipole moment of the added resin/surfactant. These measurements suggest that the interactions involving polar molecules should be included in the study of asphaltene precipitation from petroleum fluids.

4.5 Conclusions

The measurement of the dipole moment of asphaltenes, resins, and oils leads to the following conclusions,

1) Asphaltenes precipitated by heavy normal alkanes are more polar than asphaltenes precipitated by light normal alkanes; nC_{10} asphaltenes are more polar than nC_7 asphaltenes and nC_7 asphaltenes are more polar than nC_5 asphaltenes.

2) For a variety of petroleum fluids used in this study, the dipole moment of resins and nC_5 asphaltenes are in the range of 2.4–3.2 D and 3.3–7.0 D, respectively.

3) For all the petroleum fluids used in this study, the asphaltenes are more polar than the resins in the same petroleum fluid. However, resins from one petroleum fluid could be more polar than the asphaltenes in another petroleum fluid.

4) The oil fraction (that is, the atmospheric crude minus the asphaltenes and resins and volatiles) can be slightly polar with a dipole moment of less than 1 D.

4.6 References

Atkins, P. W., *Physical Chemistry*, Oxford University Press, Oxford (1978).

Bitter, F., *Currents, Fields and Particles*, The Technology Press of Massachusetts Institute of Technology and John Wiley & Sons, Inc., NY (1956).

Boduszynski, M. M., "Composition of Heavy Petroleums. 2. Molecular Characterization", *Energy & Fuels*, **2**, 597 (1988).

Born, M., and E. Wolf, *Principles of Optics*, Pergamon Press (1980).

Böttcher, C. J. F., *Theory of Electric Polarization*, Elsevier, Amsterdam (1952).

Buckley, J. S., G. J. Hirasaki, Y. Liu, S. Von Drasek, J-X. Wang, and B. S. Gill, "Asphaltene Precipitation and Solvent Properties on Crude Oils", *Petroleum Science and Technology Int.*, **16**, 3-4, 251 (1998).

Debye, P., *Polar Molecules*, Dover Publications Inc., NY (1929).

De Hemptinne, J-C., A. Aubertin-Couvreur, I. Fondio, and D. Broseta, "Viscosity Prediction of Heavy Crudes in Hydrotreatment Conditions", Paper presented at the International Conference on Petroleum Phase Behavior and Fouling, Houston, March 14-18 (1999).

Ese, M. -H., X. Yang, and J. Sjoblom, "Film Forming Properties of Asphaltenes and Resins. A Comparative Langmuir-Blodgett Study of Crude Oils from North Sea, European Continent and Venezuela", *Colloid Polymer Science*, **276**, 800 (1998).

Feynman, R. P., R. B. Leighton, and M. Sands, *The Feynman Lectures on Physics*, Vol. 2, Addison-Wesley Publishing Company, Redwood City, CA (1964).

Firoozabadi, A., *Thermodynamics of Hydrocarbon Reservoirs*, McGraw-Hill, New York (1999).

Groenzin, H., and O. C. Mullins, "Molecular Size and Structure of Asphaltene from Various Sources", *Energy & Fuels*, **14**, 3, 677 (2000).

Guggenheim E. A., "The Computation of Electric Dipole Moments", *Trans. Faraday Soc.*, **47**, 573 (1951).

Halverstadt, I. F., and W. D. Kumler, "Solvent Polarization Error and its Elimination in Calculating Dipole Moments', *J. Am. Chem. Soc.*, **64**, 2988 (1942).

Halvorsen, K., *Dipole Moments and Molecular Weights for Alkane Precipitated Solid Fractions for Some North-Sea Oils*, MSc Thesis, Institute of Chemistry, University of Bergen, Norway (1997).

Hewlett Packard, *The Impedance Measurement Handbook: A guide to Measurement, Technology and Techniques*, Hewlett Packard, Hyogo- Japan (1999).

Kaminski, T. J., H. S. Fogler, and A. Mairal, "Classification of Asphaltenes via Fractionation and the Effect of Heteroatom Content on Dissolution Kinetics", Paper presented at the International Conference on Petroleum Phase Behavior and Fouling, Houston, March 14-18 (1999).

Kumler, W. D., "The Dipole Moment of ms-Tetraphenylporphirine", *J. Am. Chem. Soc.*, **64**, 2993 (1942).

LeFèvre, R. J. W., *Dipole Moments*, 2nd Edition, London (1948).

Lian, H., J. R. Lin, and T. F. Yen, "Peptization Studies of Asphaltene and Solubility Parameter Spectra," *Fuel,* **73**, 423 (1994).

Lide, D. R., and H. P. R. Frederikse, *Handbook of Chemistry and Physics*, 81st Edition 2000-2001, CRC Press, Boca Raton, FL (2000).

Maruska, H. P., and B. M. L Rao, "The Role of Polar Species in the Aggregation of Asphaltenes", *Fuel Science & Technology Int'L*, **5**, 2, 119 (1987).

Maxwell, J. C., *A Treatise on Electricity and Magnetism*, Oxford University Press, Vol. 2, Third edition, Dover Publications, New York (1954).

McClellan, A. L., *Tables of Experimental Dipole Moments*, Vol. 1, W.H Freeman and Company, San Francisco (1963).

Mitra-Kirtley, S., O. C. Mullins, J. Van Elp, S. J. George, J. Chen, and S. P. Cramer, "Determination of the Nitrogen Chemical Structures in Petroleum Asphaltenes using XANES Spectroscopy", *J. Am. Chem. Soc.*, **115**, 1, 252 (1993).

Murzakov, R. M., S. A. Sabanenkov, and Z. I. Syunyaev, "Influence of Petroleum Resins on Colloidal Stability of Asphaltene-containing Disperse Systems", *Khim. Tekhnol. Topl. Masel.*, **10**, 40 (1981).

Nalwaya, V., V. Tangtayakom, P. Piumsomboon, and S. Fogler, "Studies on Asphaltenes through Analysis of Polar Fractions", *Ind. Eng. Chem. Res.*, **38**, 964 (1999).

Nighswander, J. A., H. Kaira, and A. Majeed, "Effect of Low Molecular Weight Hydrocarbons on the Onset Concentration and Bulk Properties of Asphaltenes at in-Situ Temperature and Pressure Conditions", presented at the AIChE Spring National Meeting, March 28- April 1 (1993).

Onsager, L., "Electric Moments of Molecules in Liquids", *J. Am. Chem. Soc.*, **58**, 1486 (1936).

Oudin, J. L., "Analyse Géochimique de la Matière Organique Extraite des Roches Sédimentaires I. Composés Extractibles au Chloroforme", *Revue de l'Institut Français du Pétrole*, **25**, 1, 4 (1970).

Pedersen, C., and S. I. Andersen, "Dielectric Properties of Asphaltenes and Oils", presented at the AIChE Spring National Meeting, Houson, TX, March 14-18 (1999).

Pfeiffer, J. Ph., and R. N. J. Saal, "Asphaltic bitumen as colloid system", *Journal of Physical Chemistry*, **44**, 139 (1940).

Riazi, M. R., and T. E. Daubert, "Improved Characterization of Wide Boiling Range Undefined Petroleum Fractions", *Ind.& Eng. Chem. Res.*, **26**, 3, 629 (1987).

Schabron, J. F., and J. G. Speight, "Solubility and Three-Dimensional Structure of Asphaltenes", *Petroleum Science and Technology*, **16**, 3-4, 361 (1998).

Sen, A. D., V. G. Anicich, and T. Arakelian, "Dielectric Constant of Liquid Alkanes and Hydrocarbon Mixtures", *Journal of Physics D: Applied Physics*, **25**, 3, 516 (1992).

Smyth, J.W., "Some Developments of Guggenheim's Simplified Procedure for Computing Electric Dipole Moments", *Trans. Faraday Soc.*, **46**, 394 (1950).
Smyth, C. P., *Dielectric Behavior and Structure*, McGraw-Hill, Amsterdam (1955).

Speight, J. G., *The chemistry and Technology of Petroleum*, Marcel Dekker, New York (1999).

Storm, D. A., S. J. DeCanio, M. M. DeTar, and V. P. Nero, "Upper Bound on Number Average Molecular Weight of Asphaltenes", *Fuel*, **69**, 735 (1990).

Swanson, J. M., "A contribution to the Physical Chemistry of the Asphalts", *Journal of Physical Chemistry*, **46**, 141 (1942).

Waldo, G. S., O. C. Mullins, J. E. Penner-Hahn, and S. P. Cramer, "Determination of the Chemical Environment of Sulphur in Petroleum Asphaltenes by X-ray Absorption Spetroscopy", *Fuel*, 71, 53 (1992).

Wu, J., J. M. Prausnitz, and A. Firoozabadi, "Molecular Thermodynamics of Asphaltene Precipitation in Reservoir Fluids", *AIChE J.*, **46**, 1 (2000).

Chapter 5

Effect of resins and DBSA amphiphile on asphaltene precipitation

This chapter examines the effect of various resins and dodecyl benzene sulfonic acid (DBSA) amphiphile on asphaltene precipitation from different petroleum fluids. Various resins are added to three different petroleum fluids to measure precipitation with n-pentane. Results show that the dipole moment of resins (which is a measure of polarity) has a strong effect on precipitation. Resins with a high dipole moment are more effective than resins with a low dipole moment. The effectiveness is defined in terms of the increase in the onset point of precipitation. However, addition of resins to a petroleum fluid increases the amount of precipitated asphaltenes. This is the first report of such a behavior in the literature; the increase is less pronounced with the most polar resins. Addition of asphaltenes to a petroleum fluid results in a high amount of precipitation. As expected, the onset point of precipitation from asphaltene addition to a petroleum fluid is different from that of resins. When the DBSA amphiphile is mixed with the petroleum fluid at different concentrations, a retrograde phenomenon is observed. The amount of precipitated asphaltene increases first with increasing DBSA concentration. Beyond a certain concentration, there is a decrease in precipitation. At higher concentrations, DBSA proves to be very effective to move the onset point of precipitation. The data show the complex interactions between various species in petroleum fluids.

5.1 Introduction

The description of the structure and properties of asphaltenes has been a challenge over the past decades. More recently, a growing interest has developed towards the study of resins with the recognition of their effect on the stability of asphaltenes in petroleum fluids. The stabilizing effect is related to the association of resins with asphaltenes to form micelles (Swanson, 1942). In chapter 4, the dipole moment of asphaltenes, resins and oils was investigated for eight petroleum fluids. The dipole moment was found to increase sharply from oils (0.0–1.0 D) to resins (2.4–3.2 D) to asphaltenes (3.3–6.9 D). Polar species with a high dipole moment (greater than 2.0 D) affect molecular interactions in the petroleum fluid and result in the formation of micelles. The interactions involved in micellar formation and stabilization are not yet well defined.

Generally, molecular interactions are classified into two types: 1) short-range, and 2) long-range interactions. Hydrogen bonding, charge transfer, and repulsion are short-range interactions while van der Waals interactions are long-range (Ratajczak and Orville-Thomas, 1980). The difference between short- and long-range interactions is mainly in the bond distance between interacting molecules. Short-range interactions occur when the bond distance between molecules is smaller than the sum of the van der Waals radii, resulting in an overlap between the electron clouds and the formation of molecular complexes (Ratajczak and Orville-Thomas, 1980). Hydrogen bonding consists of the sharing of a proton between the proton acceptor of a molecule and the anion derived from the proton donor of another molecule; charge transfer consists of the transfer of electrons between an electron donor and electron acceptor of two molecules (Huyskens *et al.*, 1991). The repulsion interaction is orientation-dependent and occurs when the electronic orbital of two approaching molecules begin to overlap noticeably (Israelachvili, 1991). The main contributions to the van der Waals interactions are: 1) electrostatic (Keesom or orientation or dipole-dipole), 2) induction (Debye or dipole-induced dipole), and 3) dispersion (London or induced dipole-induced dipole) interactions (Maitland *et al.*, 1981). In electrostatic interactions, the rotating dipoles of two polar molecules interact by aligning into a favorable arrangement. Hydrogen bonding is no more than a particularly strong type of directional dipole-dipole interaction (Israelachvili, 1991). In induction interactions,

the permanent dipole of a polar molecule distorts the electron charge distribution of a non-polar molecule and an induced dipole moment is created. In dispersion interactions, the instantaneous positions of the electrons around the nucleus protons of a molecule create a finite dipole moment, which in turn generates an electric field that polarizes a nearby molecule, inducing a dipole moment in it (Israelachvili, 1991).

It is believed that dispersion interactions affect asphaltene flocculation (Buckley *et al.*, 1998; Rogel, 2000). Electrostatic and induction interactions, on the other hand, help stabilize the asphaltenes in the petroleum fluid (Moschopedis and Speight, 1976; Bardon *et al.*, 1996; Li *et al.*, 1997). Murgich (2002) presented a comprehensive analysis on the intermolecular forces in aggregates of asphaltenes and resins and stated that the main contributions involved are the electrostatic, repulsion, and dispersion interactions. In this chapter, it will be shown that electrostatic interactions between asphaltenes and resins affect the precipitation. In order to understand the mechanism of asphaltene precipitation, it is primordial to analyze the effect of resins on asphaltenes and to define the main interactions involved.

Very few studies have delved into the effect of resins on asphaltene precipitation. The limited studies center around the effect of resins on the onset point of precipitation. In addition, the effect of resins on asphaltene precipitation is usually assessed after asphaltenes have been precipitated from petroleum fluids and solubilized in aromatic solvents. Murzakov *et al.* (1981) investigated the micellar stability of asphaltenes in benzene solutions by means of gravimetric sedimentation analysis and found that the addition of resins (2–8 wt%) to the solution decreased the amount of asphaltene precipitated by nC_7. Lian *et al.* (1994) performed nC_5 precipitation tests from asphaltene/toluene solutions and found as well that addition of resins to the solution decreased the amount of precipitated asphaltenes. Hammami *et al.* (1998) measured the onset point of asphaltene precipitation at ambient temperature and high pressure (690 kPa) and found that addition of resins with high content of basic functions to the petroleum fluid increased significantly the onset point of asphaltene precipitation by nC_5. Recently, Carnahan *et al.* (1999) reported that resins from Boscan petroleum fluid could increase considerably the onset point of asphaltene precipitation from Hamaca petroleum fluid, suggesting that resins from Boscan petroleum fluid are more effective than resins from Hamaca petroleum fluid.

However, the reasons underlying this phenomenon were not discussed.

Structural investigations of the resin fractions have not been carried out to the same extent as those of the asphaltene fractions. Because asphaltenes and resins are two contiguous classes of components separated from a continuum of molecules, they may have a similar structure. However the difference in size, aromaticity, polarity, and physical appearance confer to asphaltenes and resins different properties (Speight, 1999). Spectroscopic investigations indicate the presence of hydroxyl groups, as well as ester, acid, and carbonyl functions in the resin fractions (Speight, 1999). It has been postulated that resins contain long paraffinic chains connected to naphtenic and aromatic rings with polar functions (Wu *et al.*, 1998; Firoozabadi, 1999). This might confer to resins some of the properties of surfactants. By definition, a surfactant is a substance that lowers the surface tension of the medium in which it is dissolved (Hiemenz, 1986). Amphiphiles are the surfactants with molecules consisting of two parts: a polar head and a nonpolar long-chain hydrocarbon tail, each part has an affinity for different phases (Hiemenz, 1986). There have been several studies on the effect of amphiphiles on asphaltene precipitation. Chang and Fogler (1994) analyzed the effect of the structure of amphiphiles such as p-nonylphenol (NP) and dodecyl benzene sulfonic acid (DBSA) on asphaltene stabilization. They found that the polarity of the head and the length of the tail affect the effectiveness of the amphiphile and selected DBSA as the most effective stabilizer for asphaltenes. The effect of DBSA on asphaltene precipitation has been reported to be successful in some studies (Permukarome *et al.*, 1997; Rogel *et al.*, 2001; Al-Sahhaf *et al.*, 2002) and not so successful by others (Clarke and Pruden, 1998). Recently, Al-Sahhaf *et al.* (2002) investigated the effect of resins and various amphiphiles on the onset point of asphaltene precipitation. They confirmed the observations of Chang and Fogler and reported the effectiveness of dodecyl resorcinol (DB) and DBSA amphiphiles. The same authors also reported that larger amounts of resins are required to produce the same effect on the onset point as low concentration of amphiphiles.

The main objective of this chapter is to examine the effect of resins with different concentrations and dipole moments on asphaltene precipitation from the three petroleum fluids U, TK, and C using nC_5 as a precipitant. Due to the complexity of interactions between asphaltenes and resins in a petroleum fluid, this study is

conducted by keeping asphaltenes in their natural environment (i.e. in the petroleum fluid). The effect of DBSA amphiphile on asphaltene precipitation from the same petroleum fluids is also studied at different concentrations. The effects of resins and DBSA are compared and discussed. Another objective of this chapter is to unveil the differences between asphaltenes and resins in a petroleum fluid. Accordingly, solubility tests on resins in different media are performed and the effect of asphaltene addition to a petroleum fluid on precipitation from the same petroleum fluid is examined.

5.2 Experimental

We use the three petroleum fluids: U, TK, and C to investigate the effect of resins and DBSA on asphaltene precipitation. The resins are separated by adsorption liquid chromatography according to the procedure described in Chapter 2, and are named after the respective petroleum fluids. The dipole moments of the resins and the corresponding nC_5 asphaltenes are provided in Chapter 4. Resins C have the highest dipole moment while resins U have the lowest dipole moment. The effectiveness of resins is evaluated from the onset point of asphaltene precipitation as well as the precipitation amount. Precipitation data are measured with nC_5/petroleum fluid ratios varying from 1 vol/vol to 20 vol/vol. The resins are added to the petroleum fluids at three different concentrations. Prior to the precipitation tests, the solubility of resins C is measured in nC_5, oils C and petroleum fluid C, as well as the solubility of resins TK and C in petroleum fluids TK and C, respectively. The effect of asphaltenes U on precipitation by nC_5 from petroleum fluid U is also measured and compared to that of resins U. In addition, precipitation measurements are performed with DBSA at concentrations of 0.3 wt%, 0.5 wt%, 1.0 wt%, 3.0 wt%, and 5.0 wt% in the petroleum fluid. It was not possible to determine the dipole moment of DBSA by dielectric spectroscopy because of strong association in toluene even at very small concentrations.

Procedure – Resins and DBSA are first transferred in equal amounts (approximately 1g) into eight different flasks. The weight of resins and DBSA is measured and an appropriate quantity of petroleum fluid is added to each flask. The mixture is left for 24 hours after 1h steering then nC_5 is added in different proportions.

The concentration of nC_5 is varied to provide the nC_5/petroleum fluid ratios of 1, 2, 4, 6, 8, 10, 15 and 20 vol/vol. After standing overnight, the mixtures are filtered according to the procedure described in Chapter 2. The procedure used to measure the amount of resins soluble in different fluids consists of mixing resins with each fluid at various concentrations (from 1 to 20 wt%) and recording, after several days, the amount of resins soluble in the fluid as a percent of total resins. The amount of insoluble resins is measured by taking into account the portion of resins that remain on the wall of the test tube as well as the amount filtered from the petroleum fluid. Note that the filtrate has the appearance of resins (brown, shiny and non-friable).

5.3 Results

The results of resin solubility in different fluids are first presented. Once the solubility behavior of resins is defined, the effect of resins U, TK and C on precipitation from petroleum fluids U, TK and C at three concentrations is presented. To better illustrate the difference between asphaltenes and resins, the effect of asphaltenes U on nC_5 precipitation from petroleum fluid U is also described. The effect of DBSA amphiphile on precipitation from the same petroleum fluids is also measured. The results are discussed and compared with those obtained with resins. All precipitation measurements are repeated a minimum of three times.

5.3.1 Solubility of resins

Fig. 5.1 presents the solubility of resins C in three different fluids: nC_5, oils C, and petroleum fluid C. The oils C represent the non-volatile fraction of saturates and aromatics in petroleum fluid C; this fraction is only 40% of the total oils. For all the three fluids, the amount of soluble resins increases with the fluid concentration. The measurements were repeated twice and the average value is plotted in Fig. 5.1. For petroleum fluid and oils concentration higher than 90 wt%, resins are completely soluble, however resins become partially soluble for lower petroleum fluid and oils concentrations. Data show that when resins are mixed with a petroleum fluid or with oils at a concentration of 20 wt%, 4% of the resins are insoluble in the petroleum fluid and 2% are insoluble in oils. Resins are generally believed to be soluble in nC_5 but our results show that this is not the case even at a low resin concentration. Indeed,

when 80 g of nC_5 is mixed with 20 g of resins, about 70% of the resins are soluble, that is only 14 g.

Fig. 5.2 depicts the solubility of resins U, TK and C in petroleum fluid TK as well as the solubility in petroleum fluid C. Resins C are more soluble in the petroleum fluids than resins TK and U. In addition, resins U show the same solubility behavior as resins TK. This may imply that resins with a high dipole moment are more soluble in petroleum fluids than resins with a low dipole moment. In all cases, additional resins revealed to be completely soluble in the petroleum fluid at a concentration lower than 7 wt%. The solubility tests are repeated three times and the standard deviation is about 0.5%.

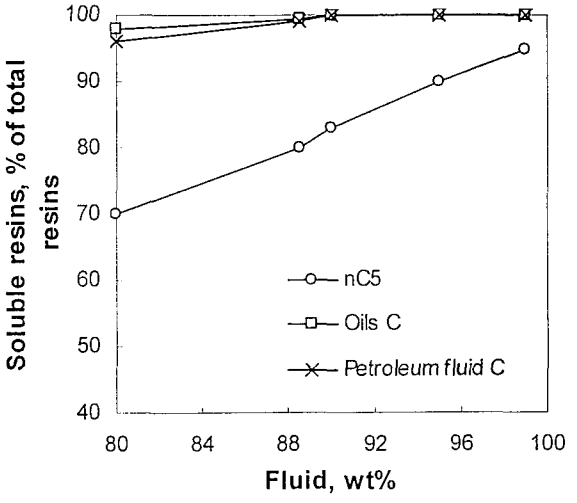


Fig. 5.1 – Solubility of resins C in nC_5, oils C and petroleum fluid C.

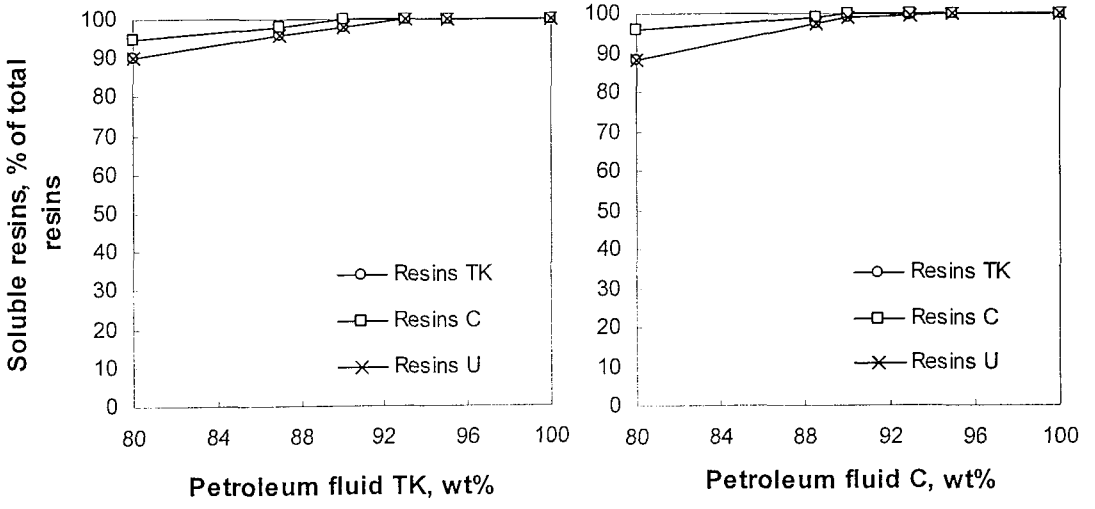


Fig. 5.2 – Solubility of various resins in petroleum fluids TK and C.

5.3.2 Effect of resins on precipitation

The effect of resins is presented in two separate sections. The first section presents the effects of resin concentration on precipitation by nC_5 from the three petroleum fluids U, TK, and C. The second section provides the effect of various resins with different dipole moments on precipitation from the same petroleum fluids.

5.3.2.1 Effect of resin concentration

Figs 5.3, 5.4 and 5.5 show the effect of resin amounts on precipitation by nC_5 from petroleum fluids U, TK, and C. Resins are added to each petroleum fluid at three concentrations (see Table 5.1). In Figs 5.3–5.5, the thick solid curves represent the precipitation of asphaltenes from the petroleum fluids without resin addition. Examination of the data in Table 5.1 and Fig. 5.2 suggests that resins added at the two first concentrations are completely soluble in the petroleum fluid while resins added at the highest concentration are partially soluble in the petroleum fluid. Indeed, asphaltene precipitated upon addition of low resin concentration do not have the same appearance as asphaltene precipitated upon addition of high resin concentration. In the first case, the precipitate is black, shiny and friable and resembles the asphaltenes precipitated from the petroleum fluids without resin addition. In the second case, the precipitate is brown, shiny and non-friable which reveals the presence of some resins with asphaltenes. Nevertheless, high resin concentrations are considered in order to examine the effect on the onset point of precipitation and the amount of precipitate. The main observation from Figs 5.3–5.5 is that the additional resins at low concentration increase the onset point of precipitation as well as the amount precipitated. The effect of resins on the onset point of precipitation at low concentration is in line with published data (Hammami *et al.*, 1998; Carnahan *et al.*, 1999). However, the increase in the amount of precipitation was not expected and has not been reported in the literature, to the best of our knowledge. Previous studies (Murzakov *et al.*, 1981; Lian *et al.*, 1994) examined the effect of resins on solutions of asphaltenes in aromatic solvents. This study examines the effect of additional resins on precipitation from petroleum fluids. The results obtained reveal that asphaltenes interact differently with resins according to the medium in which they are present.

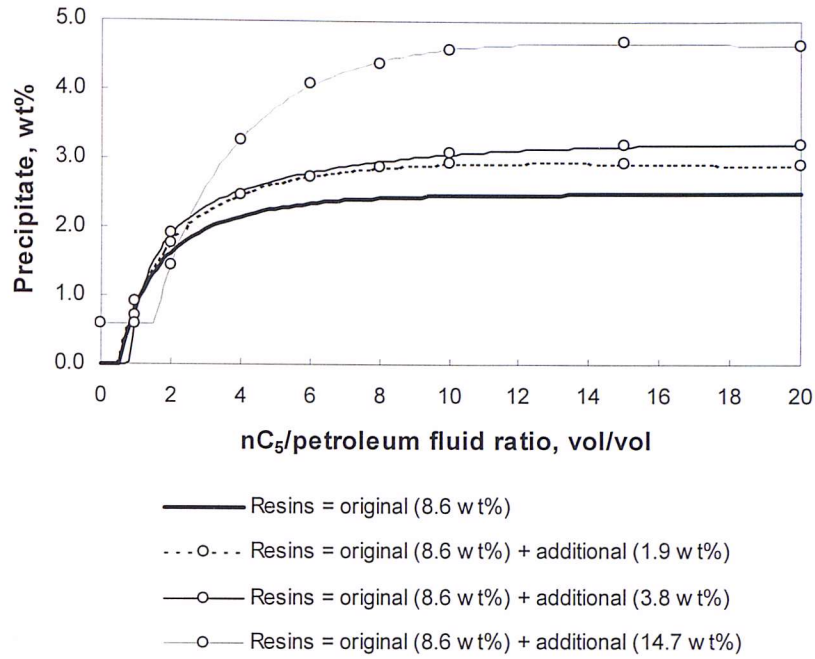


Fig. 5.3 – Precipitation by nC_5 from petroleum fluid U for various concentrations of resins U.

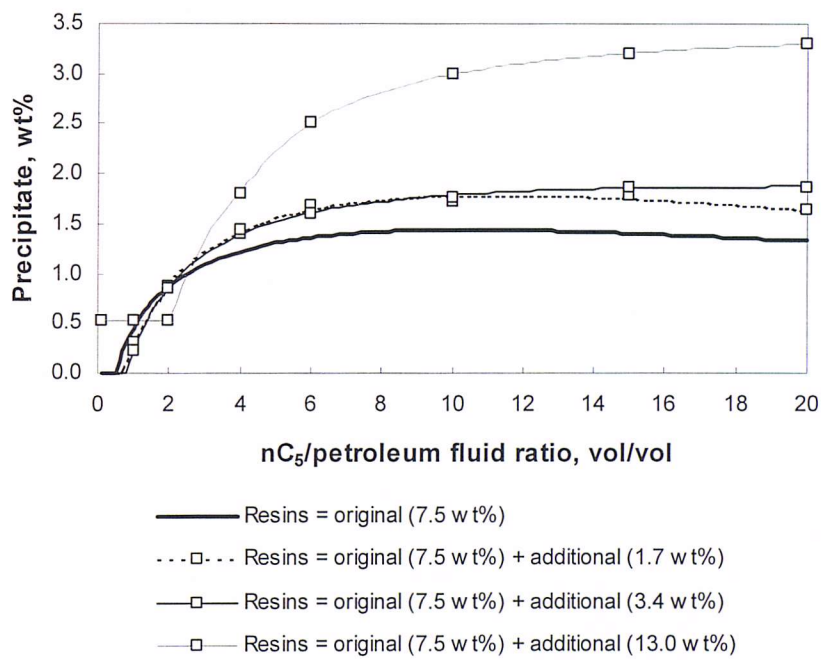


Fig. 5.4 – Precipitation by nC_5 from petroleum fluid TK for various concentrations of resins TK.

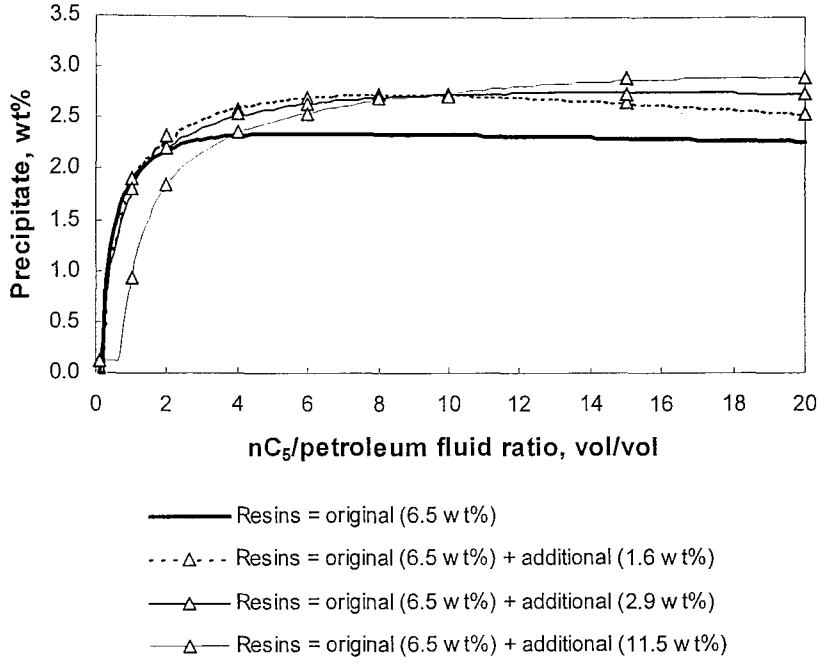


Fig. 5.5 – Precipitation by nC_5 from petroleum fluid C for various concentrations of resins C.

Table 5.1 – Concentration of additional resins in petroleum fluids U, TK, and C

Additional resins, wt%			Total resins, wt%		
U	TK	C	U	TK	C
0.0	0.0	0.0	8.6	7.5	6.5
1.9	1.7	1.6	10.5	9.2	8.1
3.8	3.4	2.9	12.4	10.9	9.4
14.7	13.0	11.5	23.3	20.5	18.0

Fig. 5.3 shows the effect of different concentrations of resins U on precipitation by nC_5 from petroleum fluid U. The increase in the amount of precipitation is proportional to the concentration of additional resins and becomes substantial (about 89% difference) when the total concentration of resins in the petroleum fluid is 23.3 wt% instead of 8.6 wt% in the original petroleum fluid. On the other hand, the high resin concentration causes early precipitation. The precipitate is mainly composed of resins that are not soluble in the petroleum fluid (see Table 5.2).

Fig. 5.4 portrays the effect of different concentrations of resins TK on precipitation by nC_5 from petroleum fluid TK. The same behavior as in Fig. 5.3 is observed; the maximum precipitation of 3.3 wt% occurs with 13 wt% additional resins TK as

compared to 1.3 wt% in the original petroleum fluid. At the high concentration, precipitation occurs upon resin addition.

Fig. 5.5 depicts the effect of different concentrations of resins C on precipitation by nC_5 from petroleum fluid C. One can observe the high slope of the precipitation curve with the addition of small concentrations of resins, which increases the uncertainty in the reading of the onset points. Nevertheless, the effect of resins in increasing the onset point of precipitation is not substantial at low resin concentration. Also, the amount of precipitation does not increase appreciably with the addition of 11.5 wt% resins. At this concentration, the percent of soluble resins in the petroleum fluid is 99% for resins C and 97% for resins TK and U, leading to 0.3 wt% precipitated resins TK and U and 0.1 wt% precipitated resins C in petroleum fluid C as shown in Table 5.2. In other words with low resin concentration, the onset is moved to the right in Fig. 5.5, however at high concentration the onset is moved to the left, similar to the results in Figs 5.3 and 5.4. This is also the first report in the literature of the effect of resins at high concentration on the amount of precipitation.

Table 5.2 – Resin precipitation from petroleum fluids U, TK, and C

	Petroleum fluid U			Petroleum fluid TK			Petroleum fluid C		
	Additional resins			Additional resins			Additional resins		
	U	TK	C	U	TK	C	U	TK	C
Additional resins, wt%	14.7	14.7	14.7	13.0	13.0	13.0	11.5	11.5	11.5
Petroleum fluid, wt%	85.3	85.3	85.3	83.0	83.0	83.0	88.5	88.5	88.5
				Resin precipitate					
% of additional resins*	4.0	4.0	2.0	4.0	4.0	2.0	2.5	2.5	1.0
wt% "	0.6	0.6	0.3	0.5	0.5	0.3	0.3	0.3	0.1

* Determined from Fig. 5.2

5.3.2.2 Effect of various resins

Figs 5.6, 5.7 and 5.8 present the effect of additional resins on precipitation by nC_5 from the three petroleum fluids, at different concentrations (see Table 5.1). Fig. 5.6 presents the precipitation results for petroleum fluid U after addition of various resins at two concentrations. The maximum increase in precipitation amount is with resins U and the minimum increase is with resins C. Thus, resins with a high dipole moment result in less precipitation than resins with a low dipole moment. In addition, the onset

point of precipitation is higher upon addition of resins C and it is lower upon addition of resins TK and U. This suggests that resins with high dipole moment are more effective than resins with relatively low dipole moment in increasing the onset point of precipitation at low resin concentrations.

Fig. 5.7 presents the precipitation results for petroleum fluid TK by the addition of resins at two concentrations. The same correlation between the amount/onset point of precipitation and the dipole moment of resins is found as with petroleum fluid U. At the two concentrations of resins, comparable effects on the amount of precipitate are observed for resins U and TK and for resins C; the highest amount of precipitate corresponds to addition of resins with the lowest dipole moment (i.e. resins U). The effect of resin dipole moment on the onset point is also noted. A gradual increase in the onset point is obtained with increasing dipole moment of resins and a maximum value of about 1.8 vol/vol is found upon addition of 1.6 wt% of resins C as compared to 0.3 vol/vol in the original petroleum fluid.

Fig. 5.8 depicts the precipitation results for petroleum fluid C after addition of resins at two concentrations. Petroleum fluid C contains approximately the same amount of nC_5 asphaltenes as petroleum fluid U; however, the effect of resins on the two petroleum fluids is different. The first observation is the contrast in the amount of precipitation between resins TK and U and resins C. Addition of 11.5 wt% resins C to petroleum fluid C slightly increases the amount of precipitation, however the amount becomes significant with resins TK and C and reaches 4.9 wt% with resins U. It is also found that resins U do not affect much the onset point of precipitation when added at low concentration.

Comparison of the results reveals that the difference in the amount precipitated with the addition of resins at low concentration increases from petroleum fluid U to petroleum fluid TK to petroleum fluid C as shown in Fig. 5.9. Thus, the increase in precipitation is more pronounced when the dipole moment of asphaltenes in the petroleum fluid is high. On the other hand, resins C (with the highest dipole moment) are the most effective with respect to the change on the onset point of precipitation in all petroleum fluids, and result in the least increase in precipitation.

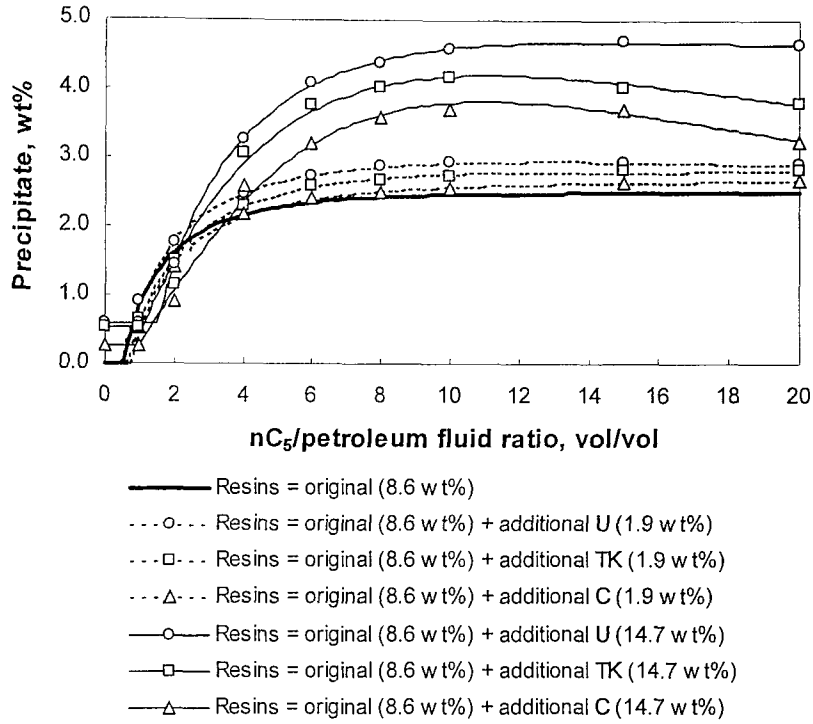


Fig. 5.6 – Precipitation by nC_5 from petroleum fluid U for various additional resins.

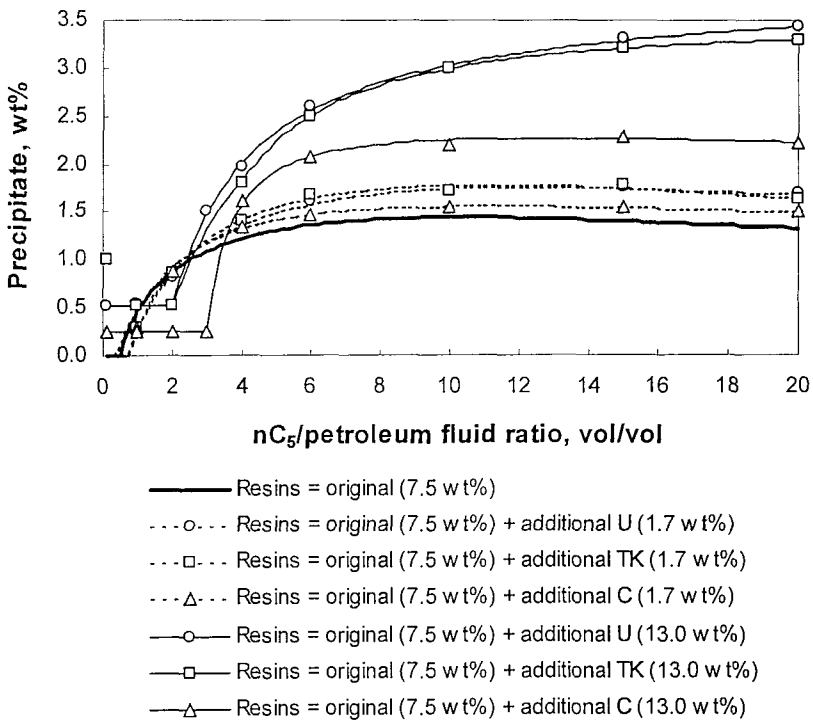


Fig. 5.7 – Precipitation by nC_5 from petroleum fluid TK for various additional resins.

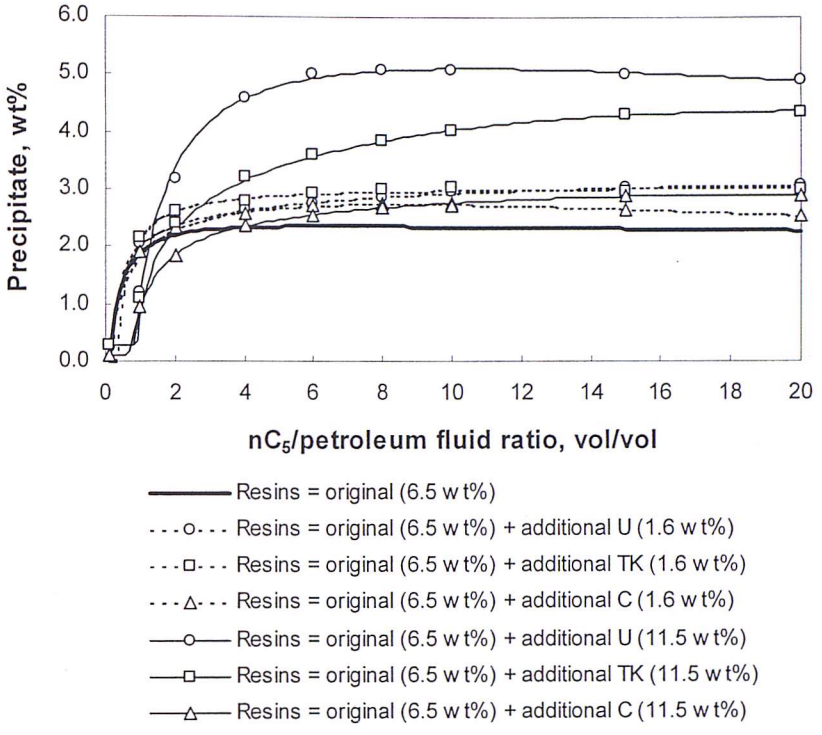
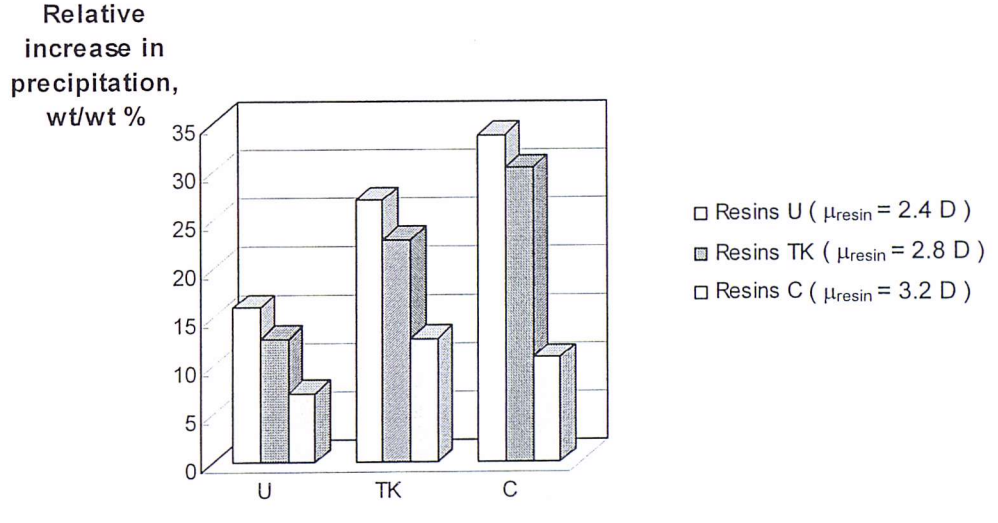


Fig. 5.8 – Precipitation by nC_5 from petroleum fluid C for various additional resins.



Additional resins, wt%	1.9	1.6	1.7
μ_{asph}, D	4.4	5.2	6.7

Fig. 5.9 – Relative increase in the amount of precipitation by nC_5 (nC_5/petroleum fluid ratio = 20 vol/vol) in petroleum fluids U, TK and C with additional resins. [Increase = 100 × (precipitate in fluid with additional resins – precipitate in original fluid) / precipitate in original fluid]

5.3.3 Effect of additional asphaltenes on precipitation

Fig. 5.10 shows the effect of adding asphaltenes U on precipitation from petroleum fluid U. Results are shown for two concentrations of additional asphaltenes: 0.6 wt% and 4.8 wt%. For comparison purposes, the same figures include the results of resin addition at two concentrations: 1.9 wt% and 14.7 wt%. In Fig. 5.10, the addition of 0.6 wt% of asphaltenes increases the amount of nC_5 precipitate from 2.5 to 3.3 wt%, which is 12% higher than the amount precipitated with the addition of 1.9 wt% of resins. For higher concentration of asphaltenes (i.e. 4.8 wt% asphaltene increase), results are substantially different. Prior to nC_5 dilution, only 56% of additional asphaltenes are soluble in the petroleum fluid, that is 2.7 wt%. The amount of precipitate by nC_5 is about 7.5 wt%, almost three times higher than the original amount in the petroleum fluid and considerably higher than the amount obtained with the addition of 14.7 wt% of resins. The addition of asphaltenes and resins at low concentration to a petroleum fluid has an opposite effect on the onset point of asphaltene precipitation. These observations along with solubility analyses corroborate the differences between asphaltenes and resins in the petroleum fluid.

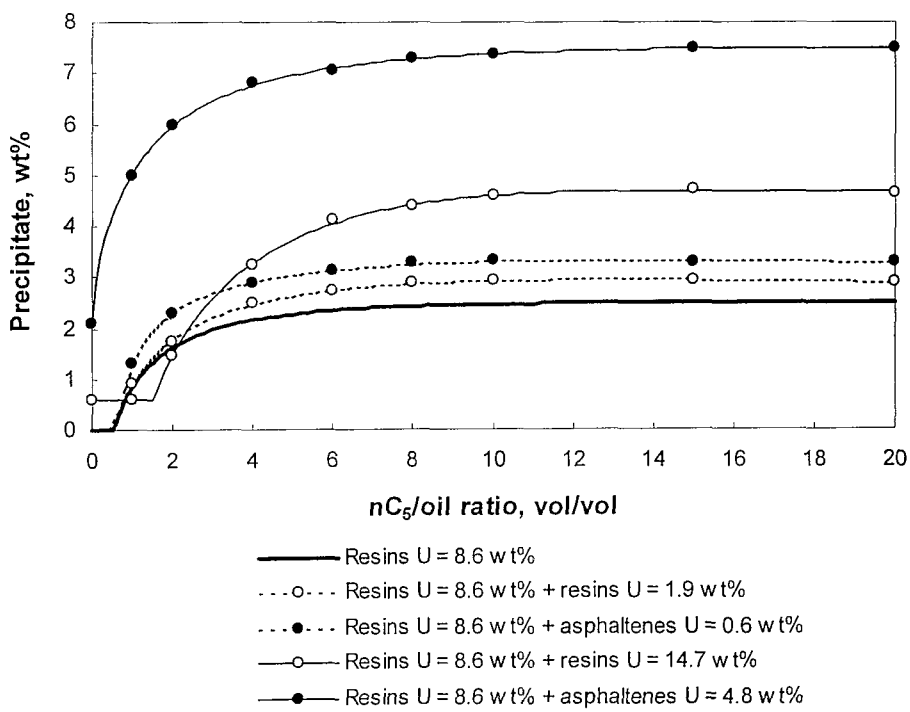


Fig. 5.10 – Precipitation by nC_5 from petroleum fluid U for various concentrations of resins and asphaltenes U.

5.3.4 Effect of DBSA amphiphile on precipitation

Figs 5.11–5.13 present the effect of DBSA on asphaltene precipitation from petroleum fluids U, TK and C, respectively. For each petroleum fluid, five precipitation measurements are made with nC_5 at five different concentrations of DBSA. For high concentrations of DBSA, it is important to observe that the mixing of petroleum fluids with DBSA and an excess of nC_5 generates very small dark black and dispersed particles that deposit on the bottom of the flask. The filtration of the precipitate does not require extensive washing with nC_5 indicating that micelles are almost resin-free. All measurements with resins and DBSA amphiphile are repeated three times and the standard deviation in the amount of precipitation is about 2%.

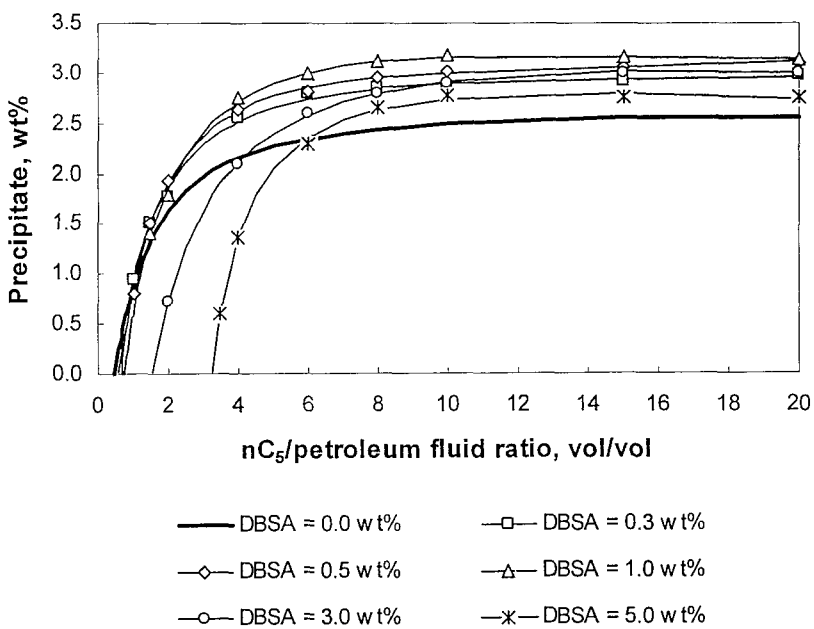


Fig. 5.11 – Precipitation by nC_5 from petroleum fluid U for various concentrations of DBSA.

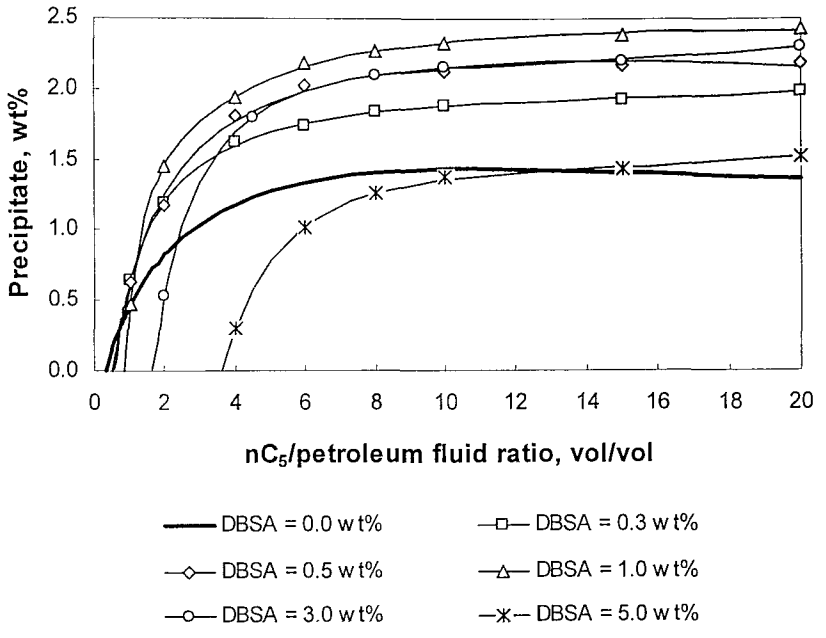


Fig. 5.12 – Precipitation by nC_5 from petroleum fluid TK for various concentrations of DBSA.

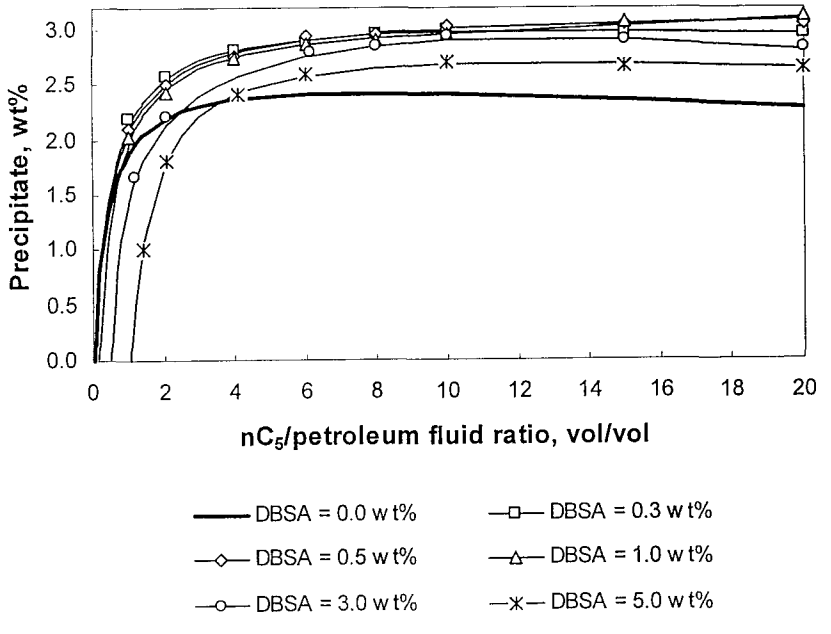


Fig. 5.13 – Precipitation by nC_5 from petroleum fluid C for various concentrations of DBSA.

Fig. 5.11 presents the effect of DBSA on asphaltene precipitation from petroleum fluid U. It appears that the amount precipitated depends on the concentration of DBSA in the petroleum fluid. At concentrations less than 1.0 wt%, the effect is

similar to that of resins. Addition of 0.3, 0.5 and 1.0 wt% DBSA increases the amount of precipitate from 2.5 wt% to approximately 3.0 wt%. At these concentrations, the onset point of precipitation increases slightly with the concentration of DBSA. However, for concentrations above 1.0 wt%, the effect of DBSA on precipitation is different. The precipitation amount decreases with DBSA concentration to only 2.4 wt% when using 5.0 wt% amphiphile. Moreover, increasing the concentration of the amphiphile above 1.0 wt% has a significant effect on the onset point of precipitation. DBSA concentration of 3.0 and 5.0 wt% increases the onset point of precipitation from 0.4 vol/vol, to about 1.6 and 3.3 vol/vol, respectively. Thus, DBSA is a suitable stabilizer for asphaltenes at high concentrations.

Fig. 5.12 presents the effect of DBSA on asphaltene precipitation from petroleum fluid TK, which follows the same pattern as in petroleum fluid U. At 1.0 wt% DBSA concentration in the petroleum fluid, the increase in the amount of precipitation is maximal and is almost two times higher than the original amount in the petroleum fluid. Conversely, a concentration of 5.0 wt% DBSA reduces precipitation considerably to 1.52 wt%, only 10% higher than the original amounts. As for the onset point of precipitation, DBSA shows high stabilization towards asphaltenes at increasing concentrations. The onset point increases significantly from 0.3 to 3.6 vol/vol at 5.0 wt% DBSA.

Fig. 5.13 shows the effect of DBSA on asphaltene precipitation from petroleum fluid C. The effect of DBSA on precipitation is similar to that in petroleum fluid U. At different concentrations, the variation in precipitation is not high. The precipitation data are very close to each other especially when the concentration of DBSA is less than 1.0 wt%. In addition, the data show approximately the same onset point of precipitation. However at 3.0 wt% and 5.0 wt% DBSA, the onset point is increased from 0.05 vol/vol, to about 0.5 and 1.0 vol/vol, respectively.

Comparison of the amount of precipitation from the three petroleum fluids is presented in Fig. 5.14. One can observe the increase in precipitation with increasing concentration of DBSA amphiphile first and then decrease in precipitation. Differences with original amounts are approximately the same for petroleum fluids U and C, but much higher for petroleum fluid TK.

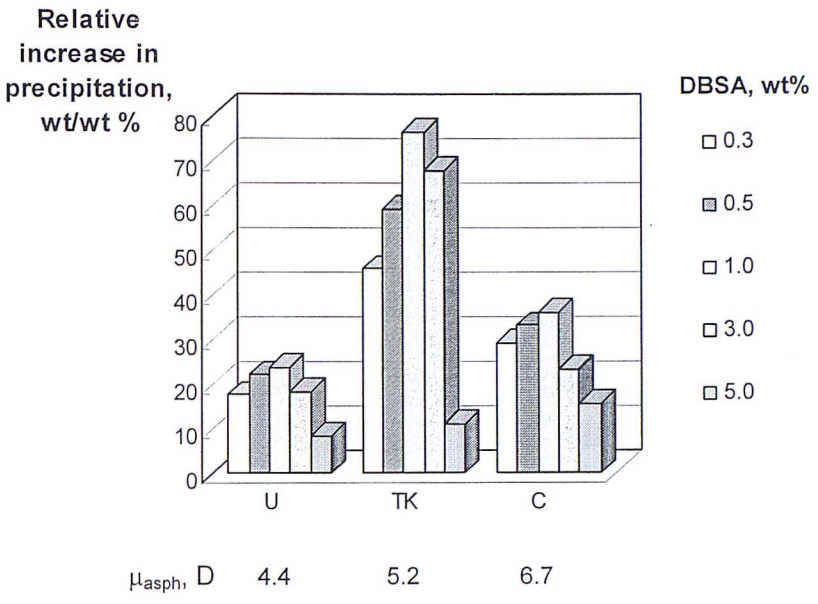


Fig. 5.14 – Relative increase in the amount of precipitation by nC_5 (nC_5/petroleum fluid ratio = 20 vol/vol) in petroleum fluids U, TK and C with various concentrations of DBSA. [Increase = 100 × (precipitate in fluid with DBSA – precipitate in original fluid) / precipitate in original fluid]

5.3.5 Comparison between resins and DBSA

In an attempt to investigate the nature of the precipitate and compare the effects of resins and DBSA on precipitation, fluorescence emission spectroscopy – SSFES – tests (see Chapter 3) are run on the precipitate from petroleum fluid U at three resin concentrations: 8.6 wt% (which is the original resin content in the fluid), 10.5 wt%, and 23.3 wt%. Another set of emission tests is undertaken on the precipitate from the same petroleum fluid at two DBSA concentrations: 1.0 wt% and 5.0 wt%.

Fig. 5.15 provides the normalized population size distribution of the precipitate for an excitation wavelength of 310 nm. The bold continuous line represents the distribution of asphaltenes precipitated by nC_5 from petroleum fluid U. It is seen that addition of a small amount of resins to the fluid does not modify appreciably the population size distribution of the precipitate. The distribution is slightly stretched towards the left indicating the presence of a larger proportion of molecules that emit at relatively short wavelengths, as compared to the original distribution. This may imply that the additional precipitate is solely composed of small asphaltene molecules that were not previously precipitated by nC_5. However, addition of a large amount of

resins shifts the population size distribution of the precipitate towards that of the resins, suggesting the presence of both asphalltenes and resins in the precipitate, which is in agreement with the visual observations.

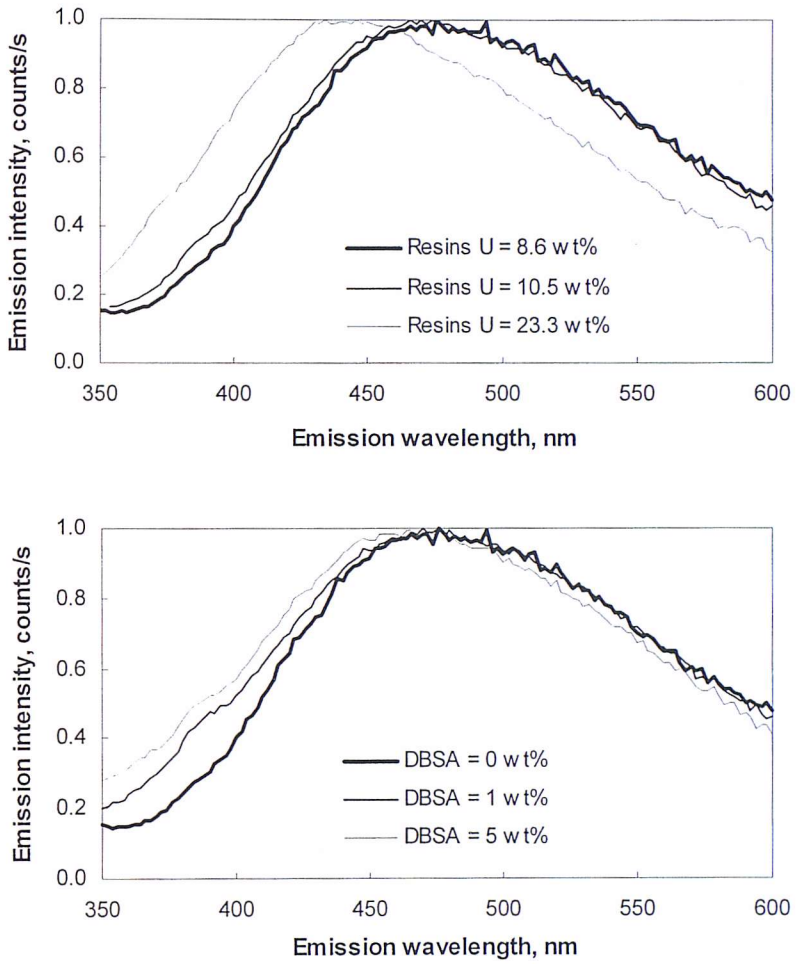


Fig. 5.15 – Normalized population size distribution (by SSFES) of the precipitate from petroleum fluid U for various concentrations of resins U and DBSA.

The population size distribution obtained with DBSA is very interesting. The distribution spans a relatively large proportion of molecules that emit at short wavelengths indicating that DBSA is able to precipitate a higher number of small asphaltene molecules than resins do. This ability is enhanced with increasing amphiphile concentration. On the other hand, the retrograde precipitation obtained with increasing amphiphile concentration demonstrates that DBSA molecules may interact with themselves and with resins and asphaltenes through a complex

mechanism. The reasons underlying the effect of DBSA amphiphile on asphaltenes in petroleum fluids are the subject for future studies.

5.3.6 Electrostatic and induction vs. dispersion interactions

A new finding in this work from the effect of dipole moment of resins and asphaltenes on precipitation is that, the electrostatic and induction interactions may not be negligible. Let us calculate the relative contribution of the electrostatic, induction and dispersion interactions between asphaltene molecules in a solvent medium using the van der Waals interaction energy U derived from the McLachlan theory and given by (Israelachvili, 1991),

$$U_{a-a}(r) = -\left\{ 3kT\left(\frac{\varepsilon_a - \varepsilon_s}{\varepsilon_a + 2\varepsilon_s}\right)^2 + \frac{\sqrt{3}h\nu_e}{4}\frac{\left(n_a^2 - n_s^2\right)^2}{\left(n_a^2 + 2n_s^2\right)^{3/2}} \right\}\frac{R_a^6}{r^6} \tag{5.1}$$

and between asphaltene and resin molecules in a solvent medium given by (Israelachvili, 1991),

$$U_{a-r}(r) = -\left\{ 3kT\left(\frac{\varepsilon_a - \varepsilon_s}{\varepsilon_a + 2\varepsilon_s}\right)\left(\frac{\varepsilon_r - \varepsilon_s}{\varepsilon_r + 2\varepsilon_s}\right) + \frac{\sqrt{3}h\nu_e}{2} \frac{\left(n_a^2 - n_s^2\right)\left(n_r^2 - n_s^2\right)}{\left(n_a^2 + 2n_s^2\right)^{1/2}\left(n_r^2 + 2n_s^2\right)^{1/2}\left(\left(n_a^2 + 2n_s^2\right)^{1/2} + \left(n_r^2 + 2n_s^2\right)^{1/2}\right)} \right\}\frac{R_a^3 R_r^3}{r^6} \tag{5.2}$$

where the subscripts a, r, and s refer to asphaltenes, resins and solvent, respectively, ε is the dielectric constant, n is the refractive index, R is the molecular radius, r is the distance between polar molecules (asphaltenes or resins) and solvent interacting molecules, k is the Boltzmann constant, h is the Planck constant, T is the absolute temperature and ν_e is the absorption frequency. The product $h\nu_e$ is called ionization potential I, and a typical value of I in the UV range is 2×10^{-18} J (Israelachvili, 1991). It is assumed here that asphaltenes, resins, and the solvent medium have the same absorption frequency. In the brackets, the first term in the right-hand side of Eqs. (5.1) and (5.2) represents the electrostatic and induction interactions and the second term represents the London dispersion interactions. The contribution of each term in the total van der Waals interactions will be calculated and compared. At a temperature of

298 K, the dielectric constant of asphaltenes can be as high as 18.0, and the refractive index is approximately equal to 1.7, the dielectric constant of resins is about 4.5, and the refractive index is equal to 1.6, the dielectric constant and refractive index of the petroleum fluid are approximately equal to 2.0 and 1.49, respectively (see Chapter 4). Considering these values in Eqs. (5.1) and (5.2) then the first term in the right-hand side representing electrostatic and induction interactions is equal to 0.65×10^{-20} J in Eq. (5.1) and 0.26×10^{-20} J in Eq. (5.2), and the second term representing London dispersion interactions is equal to 1.96×10^{-20} J in Eq. (5.1) and 1.036×10^{-20} J in Eq. (5.2). The sum of these two terms is equal to 2.61×10^{-20} J and 1.29×10^{-20} J in Eqs. (5.1) and (5.2), respectively, and the ratio of the first term (electrostatic and induction interactions) to the sum of the two terms is 0.25 for Eq. (5.1) and 0.20 for Eq. (5.2). Thus, electrostatic and induction interactions represent 25% of the total van der Waals interactions between asphaltene molecules, and 20% of the total van der Waals interactions between asphaltene and resin molecules; which is significant and may not be neglected.

5.4 Conclusions

Based on the extensive and careful measurements reported in the paper, the following conclusions are drawn.

1) The solubility of resins in petroleum fluids is limited. A common belief in the literature is that resins are completely soluble in nC_5. The results presented in this chapter show that this is not the case.

2) Addition of resins to a petroleum fluid increases the amount of precipitation. Reported data in the literature indicate that resins decrease the amount of asphaltene precipitation. The reasons underlying the observed behavior are presented in the next chapter.

3) The effect of various resins on precipitation depends on the resin dipole moment. Resins with a high dipole moment do not increase the amount of precipitation significantly.

4) The effectiveness of resins on precipitation decreases with asphaltenes having a high dipole moment.

5) The addition of the DBSA amphiphile on precipitation by nC_5 shows two different trends on the amount of precipitation. At low concentrations of DBSA, the amount of precipitation increases with increasing amphiphile concentration. This trend reverses with higher concentration (that is, as DBSA concentration increases, the amount of precipitation decreases). Therefore, before a certain concentration, the amphiphile is not effective.

6) Electrostatic and induction interactions between polar molecules such as asphaltenes and resins in a solvent medium are not negligible in comparison to dispersion interactions. This may explain why resins with distinct dipole moments affect the precipitation differently.

5.5 References

Al-Sahhaf, T. A., A. F. Mohammed, and A. S. Elkilani, "Retardation of Asphaltene Precipitation by Addition of Toluene, Resins, Deasphalted Oil and Surfactants", *Fluid Phase Equilibria*, **194**, 1045 (2002).

Bardon, Ch.; L. Barre, D. Espinat, V. Guille, M. H. Li, J. Lambard, J. C. Ravey, E. Rosenberg, and T. Zemb, "The Colloidal Structure of Crude Oils and Suspensions of Asphaltenes and Resins", *Fuel Science & Technology International*, **14**, 1-2, 203 (1996).

Buckley, J. S., G. J. Hirasaki, Y. Liu, S. Von Drasek, J-X. Wang, and B. S. Gill, "Asphaltene Precipitation and Solvent Properties on Crude Oils", *Petroleum Science and Technology Int.*, **16**, 3-4, 251 (1998).

Carnahan, N. F.; J. L. Salager, R. Anton, and A. Davila, "Properties of Resins Extracted from Boscan Crude Oil and their Effect on the Stability of Asphaltenes in Boscan and Hamaca Crude Oils", *Energy & Fuels*, **13**, 2, 309 (1999).

Chang, C., and H. S. Fogler, "Stabilization of Asphaltenes in Aliphatic Solvents using Alkylbenzene-derived Amphiphiles. 1. Effect of the Chemical Structure of Amphiphiles on Asphaltene Stabilization", *Langmuir*, **10**, 6, 1753 (1994).

Clarke, P. F., and B. B. Pruden, "Asphaltene Precipitation from Cold Lake and Athabasca Bitumens", *Petroleum Science and Technology*, **16**, 3-4, 287 (1998).

Firoozabadi, A., *Thermodynamics of Hydrocarbon Reservoirs*, McGraw-Hill, New York (1999).

Hammami, A., K. A. Ferworn, J. A. Nighswander, S. Overa, and E. Stange, "Asphaltenic Petroleum fluid Oil Characterization: An Experimental Investigation of the Effect of Resins on the Stability of Asphaltenes", *Petroleum Science and Technology*, **16**, 3-4, 227 (1998).

Hiemenz, P. C., *Principles of Colloid and Surface Chemistry*, Marcel Dekker Inc., New York (1986).

Huyskens, P. L., W. A. P. Luck, and T. Zeegers-Huyskens, *Intermolecular Forces: An Introduction to Modern Methods and Results*, Springer-Verlag, Berlin (1991).

Israelachvili, J. N., *Intermolecular and Surface Forces*, Academic Press, San Diego (1991).

Li, S., C. Liu, G. Que, W. Liang, and Y. Zhu, "A Study of the Interactions Responsible for Colloidal Structures in Petroleum Residua", *Fuel*, **76**, 14/15, 1459 (1997).

Lian, H., J. –R. Lin, and T. F. Yen, "Peptization Studies of Asphaltene and Solubility Parameter Spectra", *Fuel*, **73**, 3, 423 (1994).

Maitland, G. C., M. Rigby, E. B. Smith, and W. A. Wakeham, *Intermolecular Forces: Their Origin and Determination*, Clarendon Press, Oxford (1981).

Moschopedis, S. E., and J. G. Speight, "Investigation of Hydrogen Bonding by Oxygen Functions in Athabasca Bitumen", *Fuel*, **55**, 3, 187 (1976).

Murgich, J., "Intermolecular Forces in Aggregates of Asphaltenes and Resins", *Petroleum Science and Technology*, **20**, 9-10, 983 (2002).

Murzakov, R. M., S. A. Sabanenkov, and Z. I. Syunyaev, "Influence of Petroleum Resins on Colloidal Stability of Asphaltene-containing Disperse Systems", *Z. I. Khim. Tekhnol. Topl. Masel*, **10**, 40 (1981).

Permsukarome, P., C. Chang, and H. S. Fogler, "Kinetic Study of Asphaltene Dissolution in Amphiphile/Alkane Solutions", *Industrial & Engineering Chemistry Research*, **36**, 9, 3960 (1997).

Ratajczak. H., and W. J. Orville-Thomas, *Molecular Interactions*, Vol. 1, John Wiley & Sons, Bath, UK (1980).

Rogel, E., "Simulation of Interactions in Asphaltene Aggregates", *Energy & Fuels*, **14**, 566 (2000).

Rogel, E., O. Leon, J. Espidel, and Y. Gonzales, "Asphaltene Stability in Crude Oils", SPE paper 72050 presented at the SPE Production & Facilities Conference (2001).

Speight, J. G., *The Chemistry and Technology of Petroleum*, Marcel Dekker, NY (1999).

Swanson, J. M., "A contribution to the Physical Chemistry of the Asphalts", *Journal of Physical Chemistry*, **46**, 141 (1942).

Wu, J., J. M. Prausnitz, and A. Firoozabadi, "Molecular-Thermodynamic Framework for Asphaltene-Oil Equilibria", *AIChE journal*, **44**, 5, 1188 (1998).

Chapter 6

Revised thermodynamic micellization model for asphaltene precipitation

The thermodynamic micellization model by Pan and Firoozabadi (1998, 2000), which has sound predictive features at reservoir conditions, lacks predictive capability at stock tank conditions. Specifically, the model predicts the complete precipitation of asphaltenes at high dilution ratios with normal alkanes, and cannot predict the effect of resins. The revised formulation includes the effect of inductive forces and accounts for the change of the interfacial tension between the liquid asphaltene in the micellar core and the surrounding shell with curvature. The first modification allows a high concentration of asphaltene monomers in the bulk liquid. As a result, the effect of various normal alkanes is predicted. The second modification allows a better prediction at low n-alkane/petroleum fluid dilution ratio. A number of other modifications are also made in the revised model. As a result, the model can be used for both stock tank and reservoir conditions. It also allows the study of the effect of resins on precipitation.

6.1 Introduction

Gradual progress has been made in the modelling of asphaltene precipitation from petroleum fluids in the last two decades. The modelling approaches can be classified into five different categories: 1) solubility, 2) equation of state, 3) colloidal, 4)

thermodynamic micellization, and 5) molecular thermodynamics. A brief review of the modelling approaches is presented with their main limitations.

The solubility model

This model was first proposed by Hirshberg *et al.* (1984) and further applied by several authors (Burke *et al.*, 1990; Kokal *et al.*, 1992; Cimino *et al.*, 1995). Two sequential phase equilibrium calculations are performed: a vapor-liquid equilibrium using a cubic equation of state, and a liquid-liquid equilibrium in which the deasphalted petroleum fluid (called solvent) is treated as a single component. The reversible liquid-liquid equilibrium is governed by activity coefficients that are calculated from the Flory-Huggins polymer solution theory in order to account for the non-ideality of asphaltene and resin molecules. The activity coefficients depend on solubility parameters derived from the Hildebrand regular solution theory. Another group of authors (Chung, 1992; MacMillan *et al.*, 1995) used a similar approach but considered asphaltenes as a solid component. The fugacities in both phases are equal at equilibrium, and expressed in terms of solubility, activity coefficient, and pure phase fugacity. The general equation that relates the solid to the liquid fugacity of pure asphaltenes depends on temperature and fusion properties (Firoozabadi, 1999). The activity coefficient is derived from the Flory-Huggins theory, which expresses the excess Gibbs free energy of mixing in terms of molar volumes and solubility parameters. The solubility model is simple and useful for reproducing n-alkane-based titration tests, yet it does not include the effect of pressure, which is necessary at reservoir conditions (Park, 1989). The performance of the model depends essentially on the molar volume and solubility parameter of the solvent, resins, and asphaltenes. One limitation of the model is its high sensitivity to small variations in the solubility parameter, which is difficult to calculate accurately for complex molecules such as asphaltenes and resins (Monteagudo *et al.*, 2001). Recently, Andersen and Speight (1999) made a critical review of several methods based on the solubility model and concluded that the methods lack predictability because they require a large number of adjustable parameters.

The equation of state model

This model was established by Gupta (1986) and Thomas *et al.* (1992), and later modified by Nghiem *et al.* (1993, 2000). It is also referred to as the solid model. The

precipitated asphaltene phase is represented by a pure solid component while the liquid and vapor phases are modeled with an equation of state (EOS). The fugacity of the solid asphaltene is calculated from the fugacity of pure liquid asphaltene (Firoozabadi, 1999). Nghiem *et al.* (1993) applied this model to live petroleum fluids and attributed the success of their approach to the division of the heavy petroleum fluid residue into a non-precipitating and a precipitating pseudo-component. The Peng-Robinson EOS was used to calculate the asphaltene precipitation by assigning different values of binary interaction coefficients to the precipitating and non-precipitating pseudo-components with light components. The model is easy to implement however it requires tuning of many parameters to match experimental data. Moreover, Thomas *et al.* (1992) observed that the model does not exhibit the correct behavior with increasing concentration of the precipitating solvent. A serious limitation of the solubility and equation of state models is that the micellar nature of asphaltenes and resins in petroleum fluids is neglected. Thus, there are two main factors controlling asphaltene precipitation that are not addressed in these models: one is the association of asphaltenes and the other is the peptizing effect of resins.

The colloidal model

This model was initially proposed by Leontaritis and Mansoori (1987) and later revised by Park and Mansoori (1988). The model assumes that asphaltenes exist in the petroleum fluid as solid-like particles in suspension, stabilized by resins adsorbed onto their surface. The model comports two parts: a static model to calculate the resin chemical potential, and a dynamic model to predict the streaming potential for the asphaltene precipitate. The static model calculates the onset point of precipitation from the chemical potential of resins. A vapor-liquid flash calculation is first performed using an EOS to determine the composition of the liquid phase. Based on experimental measurements of the onset of precipitation, a critical chemical potential for resins is estimated using the Flory-Huggins theory. This chemical potential corresponds to the coverage of asphaltenes with a single layer of resins. It is then the chemical potential of resins in the solid and liquid phases that determine the split between the two phases. Asphaltene flocculation occurs when the chemical potential of resins becomes lower than the critical value. The dynamic model calculates the amount of asphaltene deposition in pipes under the influence of a streaming potential. A set of equations based on the streaming potential are derived from which the

generated minimum streaming potential during deposition is calculated. The method requires input parameters such as electrical conductivities, total charge densities, mean charge of asphaltene particles. The colloidal model shows promising results at stock tank and reservoir conditions, however it requires a set of experimental and field data that may not be readily available. Nevertheless, this approach can describe the role of resins adhering onto asphaltene surface and assess the possibility of precipitation even though it does not explicitly consider details of the micellar structure and shape.

The thermodynamic micellization model

The model proposed by Pan and Firoozabadi (1998, 2000) calculates the total Gibbs free energy of a system composed of 1) a bulk liquid phase containing oil, asphaltene, and resin monomers, 2) micelles, and 3) a precipitated liquid or solid phase. The micelles consist of an asphaltenic core surrounded by a solvating shell containing both resin and oil molecules. A hypothetical path is devised to describe the formation of micelles in the petroleum fluid (Firoozabadi, 1999) and the phase equilibrium is calculated using the Peng-Robinson equation of state (PR-EOS). The total Gibbs free energy of the system, expressed as a function of several variables and subject to material balance constraints, is minimized using the feasible sequential quadratic programming (Zhou *et al.*, 1997). There are different contributions in the Gibbs free energy of the system, namely the standard, interaction, mixing, precipitation, and micellization free energies. An important feature of the model is that it can capture the micellar nature of petroleum fluids; however it does not predict properly the effect of precipitants such as n-alkanes and aliphatic mixtures on asphaltene precipitation; the model predicts a very low concentration of asphaltene and resin monomers in the bulk liquid as almost all transfer into micelles upon titration with n-alkanes. Because the entire asphaltene content in the petroleum fluid precipitates at a high dilution with various n-alkane precipitants, one cannot properly predict the precipitation amount without forcing different asphaltene fractions to precipitate by different n-alkanes. In addition, the model does not predict properly the effect of resins on precipitation. The onset point of precipitation is increased with additional resins however the amount of precipitation remains unchanged.

The molecular thermodynamic model

This model developed by Wu *et al.* (1998, 2000) and was used by Buenrostro-Gonzalez *et al.* (2002). Both asphaltenes and resins are represented by pseudo-pure components while all other components form a continuous medium. Asphaltene precipitation is considered as a liquid-liquid equilibrium process and the Helmholtz free energy of the system is derived from the hard sphere perturbation theory and the theory for chain molecules (Prigogine *et al.*, 1957). The model uses the statistical associating fluid theory (SAFT) in the framework of the McMillan-Mayer theory to calculate the chemical potential of asphaltenes and resins (Chapman *et al.*, 1988; Lee, 1988). The approach is similar to the SAFT model for association and chain molecules (Chapman *et al.*, 1990; Ghonasgi and Chapman, 1994). Large hard spheres represent the asphaltenes while small ones correspond to the resin chain segments. The model considers hard-sphere repulsion, association and dispersion interactions (Wu *et al.*, 1998). The dispersion interaction is computed from van der Walls potential of mean force. The effect of the medium on asphaltene and resins interactions is taken into account through its density and dispersion force properties. Buenrostro-Gonzalez *et al.* (2002) applied the same approach and used the SAFT model with variable-ranged potentials, which is believed to describe rigorously the intermolecular interactions (Gil-Villegas et al, 1997; Galindo *et al.*, 1998). The molecular thermodynamic model has been applied successfully to stock tank and reservoir petroleum fluids, however it requires some fitting parameters. The strength of the model resides in its ability to describe the intermolecular interactions in petroleum fluids, and the explicit effect of the fluid density, which may not be taken into account in the other approaches. Another method is to apply an integral equation approach using statistical mechanical theory (Duda and Lira-Galeana, 2002). The flocculation depends on the interactions between asphaltenes, resins and the medium and one can solve the associative Ornstein-Zernike integral equation (Varakin *et al.*, 1997) to obtain the structure factor from which the compressibility and other thermodynamic properties can be deduced. The model requires molecular parameters that are estimated from experimental data. This approach is still in the primitive stage and is being investigated for more practical applications.

Among the modelling approaches presented above, the thermodynamic micellization model is selected because it is complete and does not require excessive tuning of parameters. The model considers the micellar nature of petroleum fluids without restraining the deasphalted fluid to a single component. It also allows the study of the peptizing effect of resins and surfactants on precipitation, which is very important for the inhibition of precipitation in the field.

The main goal of this chapter is a revised formulation of the original micellization model by Pan and Firoozabadi (1998, 2000) in order to improve the predictions. Extensive sensitivity studies on various contributions to the Gibbs free energy affecting the precipitation amount helped us to target the main contributions missing in the original formulation. Special attention was given to the energy of interaction, mixing and interfacial properties. In the description of energy of interaction between asphaltenes, resins and the other hydrocarbons, it is important to consider all the interactions that may arise from the presence of polar molecules in a petroleum fluid. While dispersion interactions mainly affect asphaltene flocculation, electrostatic and induction interactions are believed to stabilize polar molecules in the bulk liquid phase (Israelachvili, 1991). The calculation of the interaction energy is complex and not very tractable for large solvated molecules such as asphaltenes and resins. Pan and Firoozabadi (1998) used the mean field approximation to calculate the Gibbs free energy of interaction between all molecules in the petroleum fluid. This chapter offers new insights into the nature of molecular interactions in petroleum fluids and demonstrates the importance of the induction energy between asphaltenes and the medium, which may not be properly represented by the mean field approximation.

Polarity affects the non-ideal mixing of asphaltene and resin molecules in the petroleum fluid. The accuracy of the predictions from the PR-EOS depends on the mixing rule. Quadratic mixing rules may not be appropriate for mixtures containing polar asymmetric molecules; instead, methods based on suitable excess energy models are used. Among these methods, the Wong and Sandler (1992) mixing rule has found wide use in successfully representing the behavior of polar multicomponent mixtures with only binary parameters. We propose to introduce this mixing rule into the PR-EOS. In addition, the volume-translation concept of Peneloux *et al.* (1982) is applied to improve density predictions.

The above considerations along with better characterization of the asphaltene species should allow precipitation predictions from petroleum fluids upon composition alteration. An important parameter that affects the slope of the precipitation curve as well as the onset point of precipitation is the interfacial tension between the asphaltene liquid phase in the core and the liquid phase outside the core in the micelle. Because micelles are nanoparticles (typically the radius of the micellar core is 20-30 Å), the curvature dependence of interfacial tension may be important. Thus, the interfacial tension is considered to be function of both concentration and curvature. Moreover, the curvature of the core surface results in a pressure difference in the bulk phases. The pressure difference is proportional to the interfacial tension and should be considered in fugacity calculations.

Another important aspect to model is the effect of petroleum resins on precipitation. It has been shown in chapter 5 that petroleum resins may not be a suitable inhibitor for asphaltenes as they increase the amount of precipitation. To the best of our knowledge, no attempt has yet been made in the literature to model properly the effect of resins on precipitation. In the original formulation (Pan and Firoozabadi, 1998), increase in resin concentration increases the onset point of precipitation without changing the amount of precipitate. It will be shown in the revised formulation that resins alter the dielectric properties of the medium, which in turn affect the molecular interactions in petroleum fluids and therefore both the onset and the amount of precipitation are affected.

This chapter is structured into three parts. In the first part, a thorough description of the revised model is presented and the modifications are outlined. The second part applies the revised formulation to several petroleum fluids at ambient conditions and the main results on the effect of n-alkanes and resins on precipitation are presented and discussed. Several examples of precipitation from reservoir fluids are also considered, and the effect of composition and pressure is studied. The last part draws the main conclusions of this chapter.

6.2 Model description

This section first explains the characterization of the plus fractions and the implementation of different asphalt species, then presents the main contributions introduced into the model, that is, the van der Waals induction energy, the Wong and Sandler mixing rule as applied to PR-EOS, and the effect of interfacial tension and core pressure. Following these modifications, a revised formulation of the Gibbs free energy of the system is provided and the main parameters used in the model are given. A brief description of the optimization algorithm is also given in the last section.

6.2.1 Characterization of the plus fraction and implementation of different asphaltic species

The Whitson method (1983) is used to characterize the deasphalt plus fraction. Molar and mass distributions are generated from a gamma function and the resulted components are lumped into several pseudo-components of equal weight (see Appendix A). The asphaltenes are also characterized by subdividing them into three different fractions: 1) C_3-nC_5, 2) nC_5-nC_7, and 3) nC_7 asphaltene, according to their solubility in various n-alkanes: propane (C_3), n-pentane (nC_5) and n-heptane (nC_7). It is assumed that the total asphaltene in a petroleum fluid can be precipitated by C_3 while only a portion is precipitated by heavier n-alkanes. Table 6.1 presents the stock tank petroleum fluids and their asphaltene and resin contents. Table 6.2 lists the chemical composition of these petroleum fluids. In this study, only one fraction of resins is considered with average properties. However, when resins are added to the petroleum fluid, a second resin fraction is included in the model.

6.2.2 The induction energy

In the condensed state, the induction interactions may be significant when molecules with free charges or with strong intrinsic dipole moments are present (Israelachvili, 1991). Emphasize is put on the contribution of the induction interaction or the induction energy between dipolar and nonpolar molecules, as it is believed to play an important role in the stabilization of asphaltene monomers in petroleum fluids.

Table 6.1 – Selected petroleum fluids

Petroleum fluid	Petroleum fluid		C_{8+} fraction		Asphaltenes, wt%			Resins, wt%
	M, g/mol	$\rho^{20°C}$, g/cc	Amount, wt%	*M*, g/mol	C_3-nC_5	nC_5-nC_7	nC_7	
TK	206.1	0.852	0.832	230.1	1.07	0.87	0.46	7.5
C	242.0	0.859	0.880	262.9	0.90	0.78	1.52	6.5
U	256.5	0.855	0.704	329.5	0.90	0.98	1.52	8.6
Mex-C	238.1	0.857	0.952	245.7	0.80	0.72	3.08	13.4
Mex-Y3	220.2	0.861	0.914	232.6	0.75	0.54	2.71	11.4
Mex-P	267.7	0.847	0.954	276.0	1.07	0.70	0.73	9.4

Table 6.2 – Composition (mole %) of selected petroleum fluids

Fraction	C	TK	U	Mex-C	Mex-Y3	Mex-P
C_1	0.00	0.00	0.00	0.00	0.00	0.00
C_2	0.00	0.01	0.04	0.00	0.00	0.00
C_3	0.00	0.15	0.73	0.00	0.00	0.00
C_4	0.82	0.85	4.15	0.04	0.00	0.00
C_5	2.12	2.48	6.00	0.21	0.01	0.14
C_6	3.84	4.91	8.33	1.29	2.48	0.72
C_7	5.18	8.39	10.38	3.30	4.84	3.69
C_8	7.32	11.14	70.37*	6.21	7.60	5.95
C_9	6.58	10.29		8.07	9.25	8.32
C_{10}	6.11	7.83		8.59	9.19	7.03
C_{11}	5.77	5.67		7.70	7.57	7.41
C_{12}	4.99	4.38		6.75	7.03	6.08
C_{13}	5.17	4.46		5.89	5.89	4.92
C_{14}	4.81	3.79		5.06	6.26	4.83
C_{15}	4.61	3.59		4.81	4.29	3.10
C_{16}	3.72	3.02		4.07	4.02	4.08
C_{17}	3.63	2.69		3.45	3.29	3.31
C_{18}	3.48	2.62		3.19	2.89	2.81
C_{19}	2.72	2.42		3.07	3.00	3.17
C_{20}+	29.13	21.31		28.36	21.16	34.43
M C_{20}+ g/mol	433.6	441.2	329.5*	425.5	451.2	464.2

* C_{8+}

Let us consider the configuration shown in Fig. 6.1. The dipolar molecule gives rise to an electrostatic potential Φ and consequently to a small electric field $\boldsymbol{F}$. The electric field polarizes the neighboring non-polar molecule and the induced dipole moment is proportional to the field,

$$\mu^{ind} = \alpha F \tag{6.1}$$

where α is the molecular polarizability related to the polarizability volume α_v presented in Chapter 4 by $\alpha = 4\pi\varepsilon_0\alpha_v$. The potential energy of the induced dipole is then,

$$U^{ind} = -\int_0^F \mu^{ind} dF = -\frac{\alpha F^2}{2} \tag{6.2}$$

The expression of the electric field can be derived from the electrostatic potential created by the dipolar molecule (Maitland *et al.*, 1981),

$$\Phi = \frac{1}{4\pi\varepsilon_0\varepsilon}\frac{\mu\cos\theta}{r^2} \tag{6.3}$$

where μ is the permanent dipole moment of the dipolar molecule contained in a medium of dielectric constant ε. From $F = \left[\left(\partial\Phi/\partial r\right)^2 + \left(\partial\Phi/r\partial\theta\right)^2\right]^{1/2}$,

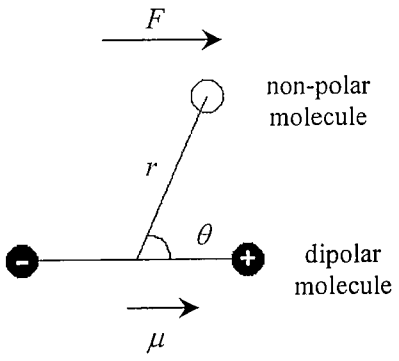


Fig. 6.1 – Induced interaction between a dipolar and a non-polar molecule

$$F = \frac{\mu}{4\pi\varepsilon_0\varepsilon r^3}\left[3\cos^2\theta + 1\right]^{1/2} \tag{6.4}$$

Combining Eqs. (6.2) and (6.4),

$$U^{ind} = -\frac{\alpha\mu^2}{2\left(4\pi\varepsilon_0\varepsilon\right)^2 r^6}\left[3\cos^2\theta + 1\right] \tag{6.5}$$

The mean potential energy is obtained by averaging over all possible angles, giving each angle the Boltzmann weight $e^{-U/kT}$,

$$U^{ind} = -\frac{\alpha\mu^2}{\left(4\pi\varepsilon_0\varepsilon\right)^2 r^6} \tag{6.6}$$

The total induction energy of the dipolar molecule with all the surrounding non-polar molecules is therefore given by,

$$g^{ind} = \int_R^\infty U^{ind} N 4\pi r^2 dr = -\frac{N\alpha\mu^2}{12\pi\left(\varepsilon_0\varepsilon\right)^2 R^3} \tag{6.7}$$

where N is the number density of non-polar molecules (that is, the number of non-polar molecules per unit volume), related to α and ε through the Clausius-Mosotti equation (see Eq. 4.9),

$$\frac{\varepsilon - 1}{\varepsilon + 2} = \frac{4\pi}{3} N\alpha_v = \frac{1}{3}\frac{N\alpha}{\varepsilon_0} \tag{6.8}$$

Combining Eqs. (6.7) and (6.8) gives,

$$g^{ind} = -\frac{\mu^2\left(\varepsilon - 1\right)}{4\pi R^3\varepsilon_0\varepsilon^2\left(\varepsilon + 2\right)} \tag{6.9}$$

6.2.3 The Wong and Sandler Mixing rule in the PR-EOS

The Wong and Sandler (WS) mixing rule is introduced into PR-EOS in order to account for non-ideal mixing of the polar asphaltenes and resins in the medium. The expression of the PR-EOS is,

$$P = \frac{kT}{v-b} - \frac{a}{v(v+b)+b(v-b)} \tag{6.10}$$

where a and b are the interaction and volume parameters, respectively. The basic equations that completely define the parameters a and b in the Wong and Sandler mixing rule allow a high-density limit consistent with experiment and a correct low-density limit according to,

$$A_{\infty}^{E} = -\frac{a}{b} + \sum_{i} z_i \frac{a_i}{v_i} \tag{6.11}$$

$$b - \frac{a}{RT} = \sum_{i}\sum_{j} z_i z_j \left(b - \frac{a}{kT} \right)_{ij} \tag{6.12}$$

Eq. (6.11) is obtained by equating the excess Helmholtz free energy at infinite pressure A_{∞}^{E} to the excess Gibbs free energy at low pressure G_{P}^{E}, which is calculated from an activity coefficient model (Wong and Sandler, 1992). Eq. (6.12) results from the Taylor expansion of the second virial coefficient in terms of the PR-EOS parameters and assuming a quadratic composition dependence of the coefficient. Combining the above equations gives,

$$a = \frac{QD}{1-D} kT \tag{6.13}$$

$$b = \frac{Q}{1-D} \tag{6.14}$$

with D given by Eq. (6.20) and Q defined as,

$$Q = \sum_{i}\sum_{j} z_i z_j \left(b - \frac{a}{kT} \right)_{ij} \tag{6.15}$$

The composition-independent second cross virial coefficient $(b-a/kT)_{ij}$, obtained from the PR-EOS is related to those of pure components by (Orbey and Sandler, 1995),

$$\left(b-\frac{a}{kT}\right)_{ij}=\frac{b_i+b_j}{2}-\frac{\sqrt{a_i a_j}}{kT}\left(1-K_{ij}\right) \tag{6.16}$$

where K_{ij} are the composition-independent interaction coefficients between species i and j, a_i and b_i are the pure component parameters of the PR-EOS given by,

$$a_i=0.457235\frac{R^2T_{c_i}^2}{P_{c_i}}\left[1+m_i\left(1-\sqrt{T_{r_i}}\right)\right]^2 \tag{6.17}$$

$$b_i=0.077796\frac{RT_{c_i}}{P_{c_i}} \tag{6.18}$$

$$m_i=\begin{cases}0.37464+1.54226\omega_i-0.26992\omega_i^2 & \left(0.0<\omega_i<0.5\right)\\ 0.3796+1.485\omega_i-0.1644\omega_i^2+0.01667\omega_i^3 & \left(0.1<\omega_i<2.0\right)\end{cases} \tag{6.19}$$

T_{c_i}, P_{c_i}, and ω_i are the critical temperature, pressure, and acentric factor, respectively. T_{r_i} is the reduced temperature, equal to T/T_{c_i}.

D is defined as,

$$D=\sum_i z_i\frac{a_i}{b_i kT}+\frac{A_\infty^E}{ckT} \tag{6.20}$$

where c is a constant equal to $ln\left(\sqrt{2}-1\right)/\sqrt{2}$ and A_∞^E is the excess Helmholtz free energy at infinite pressure equal to the excess Gibbs free energy at low pressure G_P^E which can be calculated from the modified NRTL model proposed by Huron and Vidal (1979),

$$G_P^E=kT\sum_i z_i\left[\frac{\sum_j z_j G_{ji}\tau_{ji}}{\sum_k z_k G_{ki}}\right] \tag{6.21}$$

with

$$G_{ji} = b_j e^{-l_{ij}\tau_{ji}} \tag{6.22}$$

l_{ij} is the non-randomness parameter and τ_{ji} is the NRTL binary interaction parameter. There are several methods to evaluate τ_{ji} according to polarity.

- For non-polar molecules, l_{ij} is set to zero and τ_{ji} can be calculated from,

$$\tau_{ji} = \frac{c}{kT}\left[\frac{\sqrt{a_i a_j}\left(1-K_{ij}\right)}{b_{ij}} - \frac{a_i}{b_i}\right] \tag{6.23}$$

- For polar molecules, l_{ij} is set to 0.1 and τ_{ji} and τ_{ij} are determined by solving the following system of equations,

$$\begin{cases} \tau_{ji} = ln\gamma_i^{\infty} - \tau_{ij}\dfrac{b_i}{b_j}e^{-l_{ij}\tau_{ij}} & (6.24) \\ \tau_{ij} = ln\gamma_j^{\infty} - \tau_{ji}\dfrac{b_j}{b_i}e^{-l_{ji}\tau_{ji}} & (6.25) \end{cases}$$

γ_i^{∞} and γ_j^{∞} are the infinite dilution activity coefficients of each species in the other, calculated from the modified separation of cohesive energy density MOSCED model (Thomas and Eckert, 1984) which is an extension of regular solution theory to polar and associating mixtures. In this model, asphaltene and resin molecules are considered as acids and alcohols, respectively with an approximate carbon atom number of 50. In order to verify the validity of the MOSCED model, the method is applied to several binary mixtures whose dispersion, induction, and polar parameters are available (Thomas and Eckert, 1984). The calculated activity coefficients at infinite dilution are in good agreement with experimental data, as shown in Table 6.3.

Table 6.3 – Activity coefficient at infinite dilution for several solute-solvent systems using the MOSCED model

Solute	Solvent	γ^{∞} (data)*	γ^{∞} (model)	Abs. error, %
Ethanol	n-Heptane	49.00	46.10	6
Acetone	Carbon tetrachloride	3.00	2.60	13
n-Pentane	Benzene	2.30	2.10	9
n-Hexane	Aniline	25.70	24.20	6
Acetonitrile	p-Xylene	2.16	1.80	17
Ethyl acetate	Hexadecane	2.80	2.89	-3
Nitroethane	Isooctane	18.90	16.00	15
Ethylbromide	Quinoline	1.27	1.29	-2
Dichloromethane	Squalane	0.79	0.81	-3
Hexane	Methanol	27.00	23.60	13
Phenol	Octane	8.89	9.30	-5

* Source: Thomas and Eckert (1984).

The fugacity coefficient of the components in the mixture can now be calculated from,

$$ln\varphi_i = \int_v^{\infty}\left[\frac{1}{kT}\left(\frac{\partial P}{\partial n_i}\right)_{T,v,n_j} - \frac{1}{v}\right]dv - ln\left(\frac{Pv}{kT}\right) \tag{6.26}$$

Integrating this equation and replacing the expressions of the EOS parameters a and b according to Wong and Sandler mixing rule gives,

$$ln\varphi_i = -ln\frac{P(v-b)}{RT} + \frac{1}{b}\left(\frac{\partial nb}{\partial n_i}\right)\left(\frac{Pv}{kT}-1\right)$$

$$+\frac{1}{2\sqrt{2}}\left(\frac{a}{bkT}\right)\left[\frac{1}{a}\left(\frac{\partial n^2 a}{n\partial n_i}\right)-\frac{1}{b}\left(\frac{\partial nb}{\partial n_i}\right)\right]ln\frac{v+b\left(1-\sqrt{2}\right)}{v+b\left(1+\sqrt{2}\right)} \tag{6.27}$$

with,

$$\frac{\partial nb}{\partial n_i} = \frac{1}{1-D}\left(\frac{\partial n^2 Q}{n\partial n_i}\right) - \frac{Q}{(1-D)^2}\left(1-\frac{\partial nD}{\partial n_i}\right) \tag{6.28}$$

$$\frac{\partial n^2 a}{n\partial n_i} = kT\left[D\left(\frac{\partial nb}{\partial n_i} \right) + b\left(\frac{\partial nD}{\partial n_i} \right) \right] \tag{6.29}$$

in which,

$$\frac{\partial n^2 Q}{n\partial n_i} = 2\sum_j x_j \left(b - \frac{a}{kT} \right)_{ij} \tag{6.30}$$

$$\frac{\partial nD}{\partial n_i} = \frac{a_i}{b_i kT} + \frac{1}{c}\left[\frac{\sum_j x_j \tau_{ji} G_{ji}}{\sum_k x_k G_{ki}} + \sum_j \frac{x_j G_{ij}}{\sum_k x_k G_{kj}} \left(\tau_{ij} - \frac{\sum_l x_l \tau_{lj} G_{lj}}{\sum_k x_k G_{kj}} \right) \right] \tag{6.31}$$

To improve the volumetric predictions of the PR-EOS, the volume-translation concept is used (Peneloux *et al.*, 1982; Jhaveri and Youngren, 1988). The volume-translation parameter of each component is defined as $\bar{v}_i = s_i b_i$, where s_i is a dimensionless shift parameter, well defined for components lighter than n-heptane (see Table 6.4). For heavier n-alkanes, it is given by $s_i = 1 - 2.258/M^{0.1823}$. The mixture parameter is related through a linear mixing rule to the parameters $\bar{v}_i$ of each component ($\bar{v} = \sum_i z_i \bar{v}_i$) and the translated volume is equal to $v - \bar{v}_i$.

Table 6.4 – Volume shift parameters of defined hydrocarbons

Component	s
C_1	-0.1540
C_2	-0.1002
C_3	-0.08501
C_4	-0.06413
C_5	-0.04183
C_6	-0.01478
C_7	0.01174

6.2.3.1 Verification with various mixtures

To verify the method, several non-ideal mixtures are investigated (Wong and Sandler, 1992; Orbey and Sandler, 1995; Sandler, 1999; and Poling *et al.*, 2001). The binary interaction coefficient in the PR-EOS is available for each mixture and is obtained by fitting to experimental vapor-liquid data. For non-polar organic mixtures, τ_{ji} is calculated from the modified NRTL model described above, and for aqueous and polar organic mixtures, the parameters available in the literature are used (see Table 6.5).

Table 6.5 – Parameters of the modified NRTL model for several binary mixtures

Binary mixture	K_{12}	l_{12}	τ_{12}	τ_{21}
Ethanol / n-heptane	-0.2	1.7204	1.7204	2.3972
Carbon dioxide / propane	0.37	0.30	1.26	-0.18
2-Propanol / water	0.2529	0.2893	0.1509	1.8051
Acetone / water	0.189	0.2862	0.1835	2.0009

Source: Poling *et al.*, 2001; Wong and Sandler, 1992; Orbey and Sandler, 1995

Fig. 6.2 compares measured and calculated bubble point pressure vs. mole fraction of some organic systems (ethanol/n-heptane, carbon dioxide/propane, methane/n-decane, n-hexane/n-octane/n-hexadecane). Fig. 6.3 provides similar results for aqueous systems (2-propanol/water, acetone/water). In addition, the phase (vapor or liquid) amount vs. mole fraction for different mixtures (n-butane/n-hexane, methane/n-heptane, and methane/n-butane/n-heptane/n-decane) is shown in Fig. 6.4. In all examples, the predicted results are in good agreement with experimental data and thus validate the method.

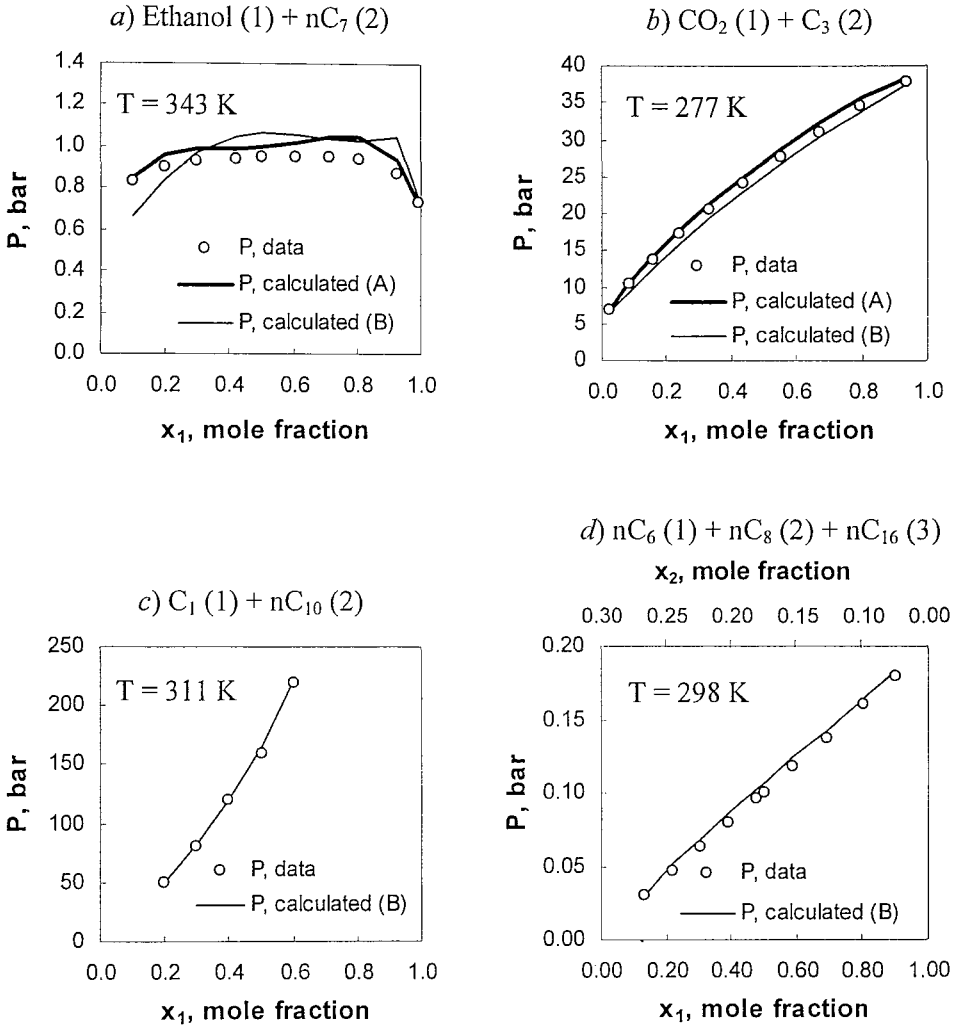


Fig. 6.2 – Saturation pressure vs. mole fraction of some organic mixtures. (A) WS parameters from source data, (B) WS parameters from NRTL model. Source: Wong and Sandler (1992); Sandler (1999); Poling *et al.* (2001).

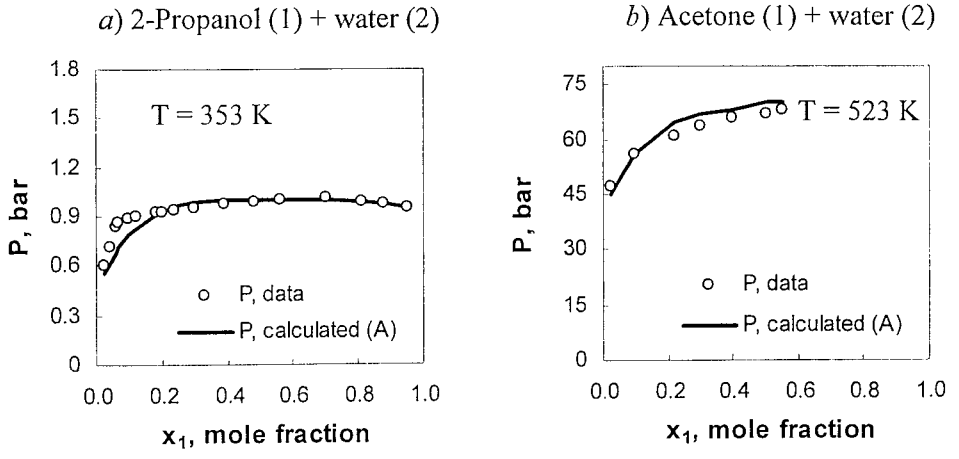


Fig. 6.3 – Saturation pressure vs. mole fraction of some aqueous mixtures. (A) WS parameters from source data. Source: Orbey and Sandler (1995), Sandler (1999).

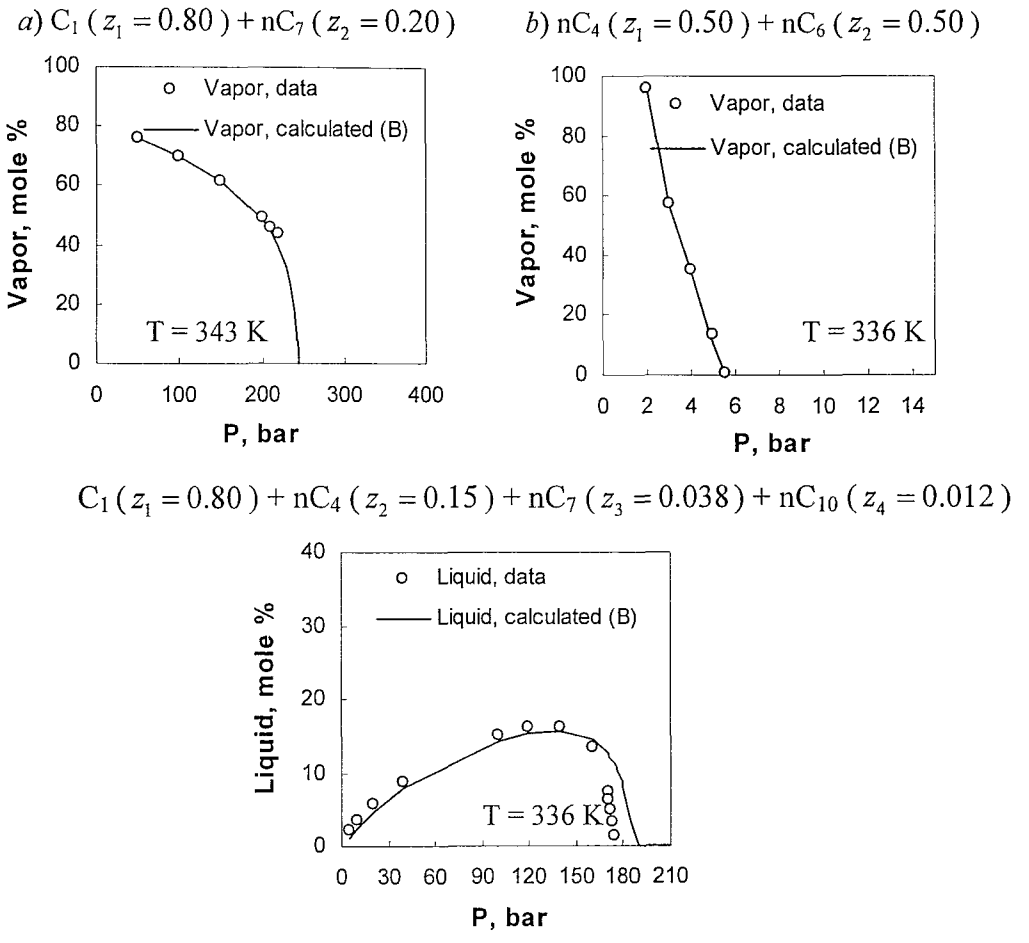


Fig. 6.4 – Phase amount vs. pressure of some organic mixtures. (B) WS parameters from the NRTL model.

6.2.4 Interfacial tension and asphaltene-core pressure

Let us consider a spherical inner liquid phase (′) surrounded by an outer liquid phase (″). The two phases are considered homogeneous up to an imaginary geometrical surface that divides the two phases (called the dividing surface).

In the following, let us consider a small part contained in a conical vessel as indicated in Fig. 6.5. In this figure, ω is the solid angle and R denotes the location of the dividing surface. The work associated with an increase $d\omega$ of the solid angle is given by (Ono and Kondo, 1960; Gibbs, 1961),

$$dW = -\eta d\omega = P' dV' + P'' dV'' - \sigma dA \tag{6.32}$$

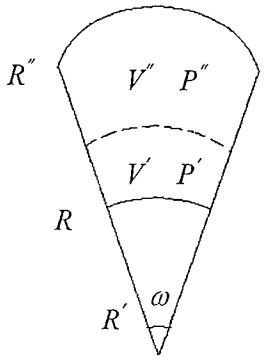


Fig. 6.5 – Conical section of a spherical inner liquid phase (') surrounded by an outer liquid phase (").

where η is an intensive variable conjugate to the extensive variable ω, V' is the volume of the drop $\left(V' = \omega\left(R^3 - R'^3\right)/3\right)$, V'' is the volume of the surrounding liquid $\left(V'' = \omega\left(R''^3 - R^3\right)/3\right)$, σ is the interfacial tension, and A is the area of the dividing surface ($A = \omega R^2$). Replacing the expressions of V', V'', and A into Eq. (6.32) gives,

$$\sigma = \frac{R}{3}\left(P' - P''\right) + \frac{1}{R^2}\left(\eta + P''R''^3 - P'R'^3\right) \tag{6.33}$$

Differentiating Eq. (6.33) with respect to R,

$$P' - P'' = \frac{2\sigma}{R} + \left(\frac{\partial \sigma}{\partial R}\right) \tag{6.34}$$

This is the generalized Laplace equation. For the surface of tension (that is the surface for which $\left(\partial\sigma/\partial R\right) = 0$), the generalized Laplace equation reduces to,

$$P' - P'' = \frac{2\sigma_s}{R_s} \tag{6.35}$$

The subscript s stands for the surface of tension, thus R_s denotes the location of the surface of tension. The Laplace equation provides the condition of mechanical equilibrium of the curved interface. It shows that the pressure in the inner phase (here, the asphaltene micellar core) is higher than the pressure in the surrounding liquid

(here, the liquid in the shell); the difference in pressure is directly proportional to the interfacial tension.

Let us now derive the expression of the interfacial tension as a function of concentration and curvature. For this, the Gibbs-Duhem equation for the interface is (Onon and Kondo, 1960),

$$n_s\, d\mu + A_s\, d\sigma_s = 0 \tag{6.36}$$

where n_s is the number of molecules at the interface. The surface for which n_s is equal to zero is called the equimolar dividing surface, corresponding to the radius R_{EDS}. For isothermal variations, the Gibbs-Duhem relations for the homogeneous phases (′) and (″), are (Ono and Kondo, 1960),

$$d\mu = \frac{V'}{n'} dP' = \frac{V''}{n''} dP'' \tag{6.37}$$

Combining Eqs. (6.35)–(6.37),

$$\frac{d\ln\sigma_s}{d\ln R_s} = \frac{\left(\dfrac{2n_s/A_sR_s}{V'/n'-V''/n''}\right)}{1+\left(\dfrac{2n_s/A_sR_s}{V'/n'-V''/n''}\right)} \tag{6.38}$$

Tolman (1949) defined the length parameter ζ as the difference between the radius of the surface of tension and the radius of the equimolar dividing surface ($\zeta = R_{EDS} - R_s$). From $n_s/A_s = \zeta\left(V'/n'-V''/n''\right)$, Eq. (6.38) becomes (Ono and Kondo, 1960),

$$\frac{d\ln\sigma_s}{d\ln R_s} = \frac{2\zeta/R_s}{1+2\zeta/R_s} \tag{6.39}$$

For simplification, let us represent σ_s and R_s by σ and R. Assuming a constant ζ, integration of Eq. (6.39) leads to,

$$\sigma(R,C) = \frac{\sigma_\infty(C)}{1+2\zeta/R} \tag{6.40}$$

where σ_∞ is the interfacial tension at a planar interface between the asphaltene core and liquid. The interfacial tension $\sigma_{oil,\infty}$ at the asphaltene-petroleum fluid flat interface is assumed to be 0.035 N/m; which is within the range of interfacial tension between the petroleum fluid and water and petroleum fluid and air (Pan and Firoozabadi, 1998). For micelles with a radius of 20–30 Å, the interfacial tension is found to vary from 0.028 to 0.034 N/m when ζ varies between 0.5 and 2.5 Å (see Fig. 6.6). Sorensen (1982), Puvvada and Blankenstein (1992) used a value of 1–2 Å, thus a value of 1.5 Å is considered in the revised model for ζ.

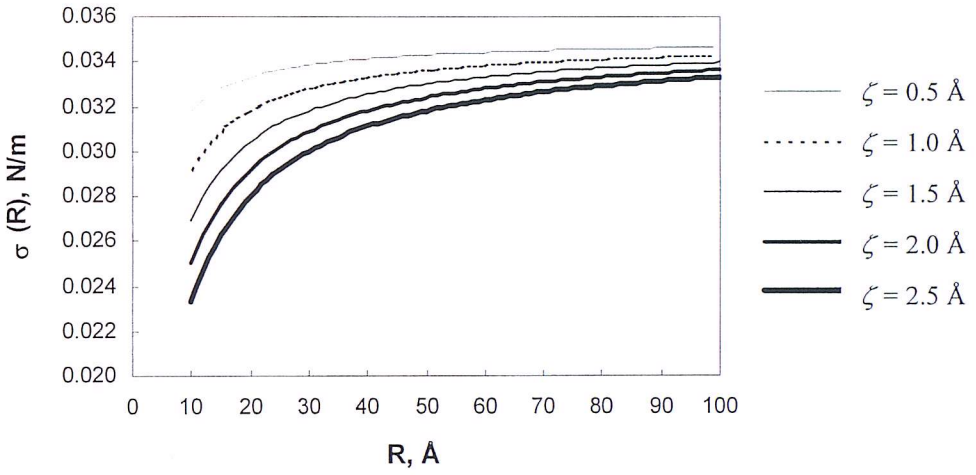


Fig. 6.6 – Effect of the Tolman length parameter ζ on $\sigma(R)$

The interfacial tension at the planar interface σ_∞ depends on the liquid composition; it is expected to increase when the petroleum fluid is diluted with n-alkanes because the density difference between the core and the liquid increases. There is limited literature on the dependence of interfacial tension on composition. Nagarajan and Ruckenstein (1991) calculated the interfacial tension between hydrophobic surfactant tails and water in terms of their surface tension. Helfand and Tagami (1971) derived an expression of the interfacial tension between two symmetric polymers within the framework of the mean-field approximation, and related the interfacial tension to composition through liquid solubility parameter and molar volume. The same formulation as Helfand and Tagami is used with slight modifications. Considering that the interfacial tension in petroleum micelles is lower than that in pure polymer systems, the two exponents in Helfand and Tagami's equation have been modified

from 2 to 1 and from 1/2 to 1/6. The interfacial tension at the planar interface between asphaltene core and liquid in the micelle becomes,

$$\sigma_{\infty}(C) = \frac{kT}{L}\left(\frac{\chi}{6}\right)^{1/6} \tag{6.41}$$

where L is the characteristic length of the liquid molecule (equals to $v_{liq}^{1/3}$) and χ is the Flory-Huggins interaction parameter,

$$\chi = \frac{v_a}{kT}\left(\delta_{liq} - \delta_a\right)^2 \tag{6.42}$$

δ_{liq} , v_{liq} and δ_a, v_a are the solubility parameter and molecular volume of the liquid phase molecules and asphaltene molecules, respectively. At constant temperature, σ_{∞} can be expressed as a function of $\sigma_{oil,\infty}$ from,

$$\sigma_{\infty}(C) = \sigma_{oil,\infty}\left(\frac{T}{T_0}\right)^{5/6}\left(\frac{v_{oil}}{v_{liq}}\right)^{1/3}\left(\frac{\delta_{liq} - \delta_a}{\delta_{oil} - \delta_a}\right)^{1/3} \tag{6.43}$$

The solubility parameter of the liquid is calculated from (Firoozabadi, 1999),

$$\delta_{liq} = \left[\frac{1}{2\sqrt{2}bv_{liq}}\left(a - T\frac{da}{dT}\right)ln\frac{v_{liq} + \left(\sqrt{2}+1\right)b}{v_{liq} - \left(\sqrt{2}-1\right)b}\right]^{1/2} \tag{6.44}$$

with,

$$\frac{da}{dT} = \frac{RTQD}{(1-D)}\left[\frac{1}{D(1-D)}\left(\frac{dD}{dT}\right) + \frac{1}{Q}\left(\frac{dQ}{dT}\right) + \frac{1}{T}\right] \tag{6.45}$$

$$\frac{dD}{dT} = \sum_i -\frac{z_i}{b_i RT}\left[\frac{2m_i a_i}{\sqrt{T_{c_i}T}}\left(1 + m_i\left(1 - \sqrt{T_{r_i}}\right)\right) + \frac{a_i}{T}\right] \tag{6.46}$$

$$\frac{dQ}{dT} = \sum_i\sum_j \frac{z_i z_j\left(1 - K_{ij}\right)}{RT^2}\sqrt{a_i a_j}\left(1 - \sqrt{T_{r_i}}\right) \tag{6.47}$$

And the solubility parameter of asphaltenes is given by (Hirshberg *et al.*, 1984),

$$\delta_a = 9.54\left[-9.1\times10^{-4}\left(T-298.15\right)\right] \tag{6.48}$$

Fig. 6.7 depicts the variations of $\sigma(R)$ $(=0.035/(1+2\zeta/R))$, $\sigma_\infty(C)$, $\sigma(R,C)$, and σ (original model) with nC_5 dilution ratio for petroleum fluid TK. The effect of curvature on the interfacial tension is important at low dilution ratios. The modification of the Helfand and Tagami's equation limits the variation of σ to 0.03–0.04 N/m instead of 0.04–0.15 N/m when the petroleum fluid is diluted with n-alkanes.

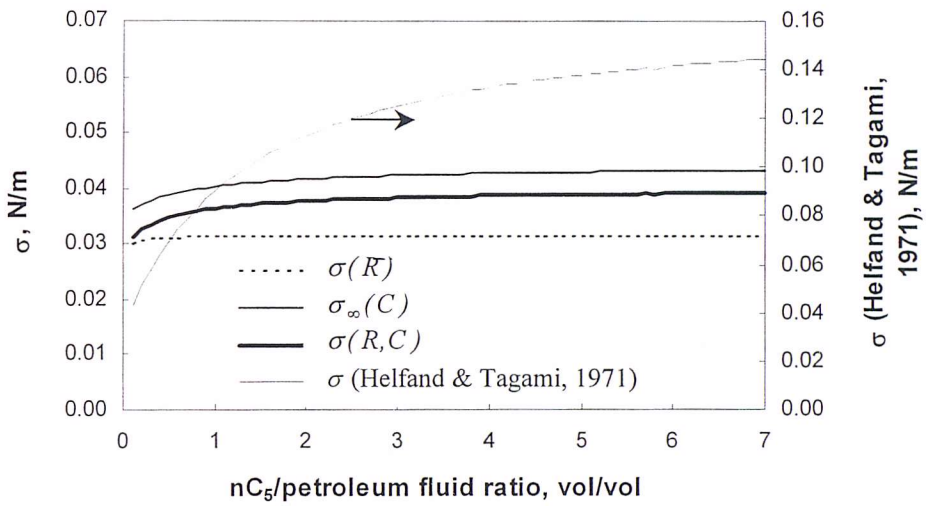


Fig. 6.7 – Variations of $\sigma(R)$, $\sigma_\infty(C)$, $\sigma(R,C)$, and σ (Helfand and Tagami, 1971) with nC_5 dilution ratio for petroleum fluid TK.

Fig. 6.8 shows the effect of $\sigma(R)$, $\sigma(R,C)$, and σ (original model) on asphaltene precipitation from petroleum fluid TK with the revised formulation. The slope of the precipitation curve is improved with the new equations of interfacial tension. At high n-alkane dilution, σ has no effect on the amount of precipitation provided the n-alkane used to precipitate the asphaltenes is the same.

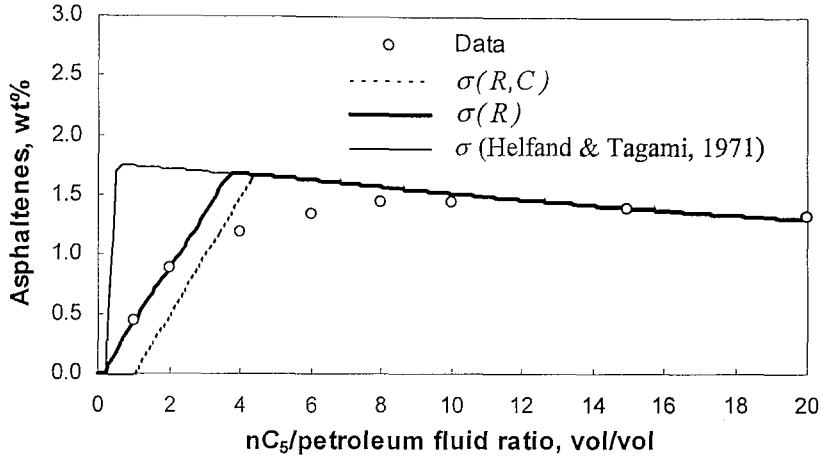


Fig. 6.8 – Effect of $\sigma(R)$, $\sigma(R,C)$ and σ (Helfand & Tagami, 1971) on asphaltene precipitation by nC_5 from petroleum fluid TK with the revised model.

6.2.5 Formulation of the Gibbs free energy

In a mixture comprised of various molecules, the Gibbs free energy is expressed as a function of: 1) the number of asphaltene molecules in the micellar core $n_{1,i}$, 2) the number of resin molecules in the micellar shell $n_{2,j}$, 3) the thickness of the shell D, 4) the number of micelles n_m, 5) the number of asphaltene and resin monomers in the bulk liquid phase $n_{1a,i}$, $n_{1r,j}$, and 6) the number of asphaltene molecules in the precipitated phase $n_{a,i}^P$, assuming that resins do not precipitate at atmospheric conditions. Note that when resins are added to a petroleum fluid in large amounts, the insoluble resin in the fluid is considered as a precipitate. The amount of insoluble resin is calculated from solubility data (see chapter 5). The indices i (i = 1, 2, 3) and j (j = 1, 2) stand for the different types of asphaltenes and resins, respectively.

The total Gibbs free energy is expressed as the sum of different contributions in the liquid and precipitated phases (Pan and Firoozabadi, 1998; Firoozabadi, 1999).

$$G = G^L + G^P \tag{6.49}$$

The next section presents the expression of G as a function of the 15 variables and subject to the following material balance equations,

$$n_{a,i} = \left(n_{1a,i} + n_{1,i} n_m \right) + n_{a,i}^P = n_{a,i}^L + n_{a,i}^P \qquad i = 1, 3 \tag{6.50}$$

$$n_{r,j} = n_{1r,j} + n_{2,j} n_m = n_{r,j}^L \qquad j = 1, 2 \tag{6.51}$$

The total number of molecules in the system is,

$$n = \sum_{k=1}^{n-5} n_k^L + \sum_{i=1}^{3} n_{a,i} + \sum_{j=1}^{2} n_{r,j} \tag{6.52}$$

6.2.5.1 Standard Gibbs free energy of micellization

The standard Gibbs free energy of micellization represents the standard Gibbs free energy difference between asphaltene and resin molecules in the micelle and those in an infinitely diluted petroleum fluid mixture.

$$\Delta G_m^{00} = \mu_m^{\Theta} - \sum_i n_{1,i} \mu_{1a,i}^{\Theta} - \sum_j n_{2,j} \mu_{1r,j}^{\Theta} \tag{6.53}$$

Pan and Firoozabadi (1998) devised a four-step hypothetical path to describe the formation of micelles in a petroleum fluid (see Appendix B) and the final expression of the Gibbs free energy of micellization is,

$$\frac{\Delta G_m^{00}}{kT} = \sum_{i=1}^{3} n_{1,i} \left[\frac{\Delta g_{a,i}^{as}}{kT} + ln \frac{\varphi_{a,i}^{l} z_{a,i}^{m}}{\varphi_{a,i}^{\infty}} + \frac{1}{2} \left(\frac{R^2}{m_{a,i} L_{oil}^2} + \frac{2 m_{a,i}^{1/2} L_{oil}}{R} - 3 \right) \right] + 4 n_{2,2} +$$

$$\sum_{j=1}^{2} n_{2,j} \left[\frac{\sigma \left(a - a_{o,j} \right)}{kT} + ln \frac{\varphi_{r,j}^{m} z_{r,j}^{m}}{\varphi_{r,j}^{\infty}} + \Delta h_{r,j}^{ads} - ln \left(1 - \frac{a_{p,j}}{a} \right) + \frac{1}{2} \left(\frac{D^2}{m_{r,j} L_{oil}^2} + \frac{2 m_{r,j}^{1/2} L_{oil}}{D} - 3 \right) \right] \tag{6.54}$$

with,

$$R = \left(\frac{3}{4\pi} \sum_{i=1}^{3} n_{1,i} V_a \right)^{1/3} \tag{6.55}$$

$$a = \frac{4\pi R^2}{\sum_{j=1}^{2} n_{2,j}} \tag{6.56}$$

$$z_{r,j}^{m} = \frac{n_{2,j}}{n_{oil}^{m} + \sum_{j} n_{2,j}} \tag{6.57}$$

n_{oil}^{m} is the number of oil molecules in the micellar shell,

$$n_{oil}^{m} = \frac{V^{sh} - \sum_{j} n_{2,j} v_{r,j}}{v_{oil}} \tag{6.58}$$

where V^{sh} is the volume of the shell given by $V^{sh} = 4\pi\left[(R+D)^3 - R^3\right]/3$.

6.2.5.2 Gibbs free energy of the liquid phase

The bulk liquid phase is composed of oil, asphaltene, and resin monomers as well as micelles. The Gibbs free energy of each type of components is expressed separately.

$$G^{L} = G_{oil}^{L} + G_{1a}^{L} + G_{1r}^{L} + G_{m}^{L} \tag{6.59}$$

The Gibbs free energy of oil monomers is,

$$G_{oil}^{L} = \sum_{k=1}^{n-5} n_k^{L} \mu_k^{L} \tag{6.60}$$

with

$$\mu_k^{L} = \mu_k^{0} + kT\, ln\frac{f_k}{f_k^{0}} = \mu_k^{*} + kT\, ln\varphi_k P + kT\, ln z_k \tag{6.61}$$

$$\mu_k^{*} = \mu_k^{0} - kT\, ln f_k^{0} \tag{6.62}$$

The Gibbs free energy of asphaltene monomers has three contributions: 1) standard state, 2) mixing, and 3) interaction.

$$G_{1a}^{L} = G_{1a}^{L,\Theta} + G_{1a}^{L,mix} + G_{1a}^{L,int} \tag{6.63}$$

where

$$G_{1a}^{L,\Theta} = \sum_i n_{1a,i}^L \mu_{1a,i}^{\Theta} = \sum_i \left(n_{a,i}^L - n_{1,i} n_m \right) \mu_{1a,i}^{\Theta} \tag{6.64}$$

$$G_{1a}^{L,mix} = kT \sum_i n_{1a,i}^L \ln z_{1a,i} \tag{6.65}$$

$$G_{1a}^{L,int} = kT \sum_i \left(n_{a,i}^L \ln \gamma_{a,i} + n_{1a,i}^L g_a^{ind} \right) \tag{6.66}$$

In the right-hand side of Eq. (6.66), the first term represents dispersion interactions that are estimated using the mean field approximation (Pan and Firoozabadi, 1998), and the second term represents the induction energy between solvent and asphaltene monomers (see Eq. (6.9)).

From $\mu_{a,i} = \mu_{a,i}^* + kT \ln z_{a,i} \varphi_{a,i} P = \mu_{a,i}^{\Theta} + kT \ln z_{a,i} \gamma_{a,i}$, one can write,

$$\ln \gamma_{a,i} = \frac{\mu_{a,i}^* - \mu_{a,i}^{\Theta}}{kT} + \ln \varphi_{a,i} P \tag{6.67}$$

The Gibbs free energy of asphaltene monomers becomes,

$$\frac{G_{1a}^L}{kT} = \sum_i \left[n_{a,i}^L \left(\frac{\mu_{a,i}^*}{kT} + \ln \varphi_{a,i} P \right) + n_{1a,i}^L \left(\ln z_{1a,i} + g_a^{ind} \right) - \frac{n_{1,i} n_m \mu_{1a,i}^{\Theta}}{kT} \right] \tag{6.68}$$

Similarly, the Gibbs free energy of resin monomers is,

$$\frac{G_{1r}^L}{kT} = \sum_j \left[n_{r,j}^L \left(\frac{\mu_{r,j}^*}{kT} + \ln \varphi_{r,j} P \right) + n_{1r,j}^L \ln z_{1r,j} - \frac{n_{2,j} n_m \mu_{1r,j}^{\Theta}}{kT} \right] \tag{6.69}$$

In the above equation, the induced interaction between solvent and resin monomers is neglected due to relatively small values of resin dielectric constant, approximately equal to 4.7 (see chapter 4).

The Gibbs free energy of micelles is,

$$\frac{G_m^L}{kT} = n_m \mu_m^{\Theta} + n_m \ln z_m \tag{6.70}$$

Therefore, the Gibbs free energy of the liquid phase is,

$$\frac{G^L}{kT}=\frac{1}{kT}\left[\sum_{k=1}^{n-5}n_k^L\mu_k^*+\sum_{i=1}^{3}n_{a,i}^L\mu_{a,i}^*+\sum_{j=1}^{2}n_{r,j}^L\mu_{r,j}^*\right]+\sum_{k=1}^{n}n_k^L\ln\varphi_k P+n_m\frac{\Delta G_m^{00}}{kT}$$

$$+\left[\sum_{k=1}^{n-5}n_k^L\ln z_k+\sum_{i=1}^{3}n_{1a,i}^L\ln z_{1a,i}+\sum_{j=1}^{2}n_{1r,j}^L\ln z_{1r,j}\right]+\sum_{i=1}^{3}n_{1a,i}^L g_a^{ind} \qquad (6.71)$$

6.2.5.3 Gibbs free energy of the precipitated phase

The state of the precipitated phase depends on pressure and temperature conditions. At atmospheric conditions, the precipitated phase from stock tank petroleum fluids is assumed to be solid, and at reservoir conditions, it is assumed to be liquid (Firoozabadi, 1999). When the precipitated asphaltenes do not self-associate, the Gibbs free energy of the precipitate is,

$$\frac{G^P}{kT}=\sum_{i=1}^{3}n_{a,i}^P\frac{\mu_{a,i}^P}{kT}=\sum_{i=1}^{3}n_{a,i}^P\left(\frac{\mu_{a,i}^*}{kT}+\ln f_{a,i}^P\right) \qquad (6.72)$$

- At stock tank fluid conditions, an ideal solid solution is assumed and thus,

$$f_{a,i}^P=z_{a,i}^P f_{a,i}^{P,0} \qquad (6.73)$$

The fugacity of pure solid asphaltene can be calculated from the fugacity of pure liquid asphaltene (Pan and Firoozabadi, 1998),

$$f_{a,i}^{P,0}=f_{a,i}^{L,0}\,exp\left[1-\frac{\Delta h_{a,i}^f}{kT}\left(1-\frac{T}{T_{a,i}^f}\right)\right] \qquad (6.74)$$

- At reservoir conditions, the fugacity of liquid asphaltenes is calculated from the equation of state for nonideal mixtures.

Thus, the final expression of the Gibbs free energy of the system can be written in kT units as,

$$G=G^{int}+G^{mix}+n_m\Delta G_m^{00}+G^P \qquad (6.75)$$

with,

$$G^{int} = \sum_{k=1}^{n} n_k^L \ln \varphi_k P + \sum_{i=1}^{3} n_{1a,i}^L g_a^{ind} \tag{6.76}$$

$$G^{mix} = \sum_{k=1}^{n-5} n_k^L \ln z_k + \sum_{i=1}^{3} n_{1a,i}^L \ln z_{1a,i} + \sum_{j=1}^{2} n_{1r,j}^L \ln z_{1r,j} \tag{6.77}$$

$$G^P = \sum_{i=1}^{3} n_{a,i}^P \ln f_{a,i}^P \tag{6.78}$$

Note that $\sum_{k=1}^{n} n_k \mu_k^* / kT$ is a constant and thus is not considered in the minimization of G. To provide an appreciation of various contributions to the total Gibbs free energy of the two-phase system, Fig. 6.9 presents the variation of G^{mix}, G^{int}, $n_m \Delta G_m^{00}$, and G^P with nC_5/petroleum fluid dilution ratio for petroleum fluid TK. Various parameters used in the calculation of Fig. 6.9 will be discussed next.

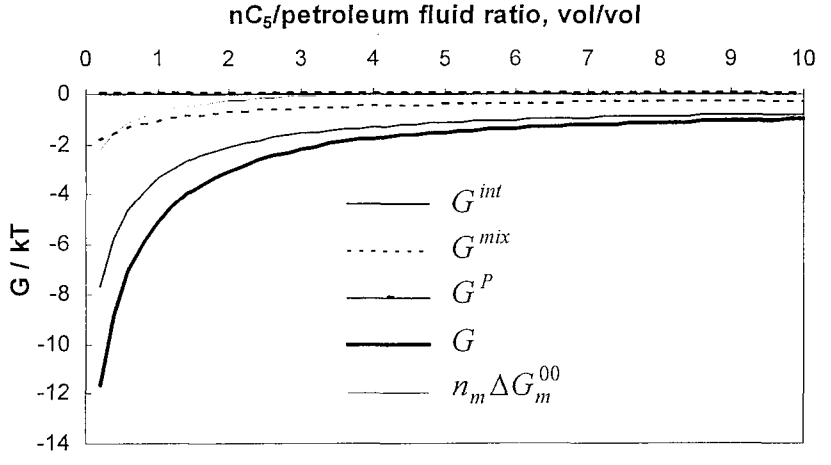


Fig. 6.9 – Variation of G with nC_5 dilution ratio for petroleum fluid TK.

$$G = G^{int} + G^{mix} + n_m \Delta G_m^{00} + G^P$$

6.2.6 Model parameters

The parameters used in the model are presented in this section. The parameters of asphaltenes and resins are provided along with the volume shift parameters of defined hydrocarbons, the molar volume and refractive index of hydrocarbons. In addition, the PR-EOS binary interaction coefficients between petroleum fluid components are presented.

Table 6.6 provides the relevant parameters of asphaltenes and resins, namely the molecular weight, molar volume, density, critical constants and acentric factor, and the fusion temperature and enthalpy. The Gibbs free energy of asphaltene association is found by fitting the onset point of precipitation to experimental data. Table 6.7 shows that Δg_a^{as} is about – 10 kT, which is consistent with values previously reported for a residue (Storm and Sheu, 1995). In addition, the nC_7 asphaltenes have a lower energy of association than C_3-nC_5 asphaltenes; which is in line with their dipole moment values measured in chapter 4. Note that the Gibbs free energy of association in Table 6.7 is provided at stock tank conditions, it is set to – 10 kT at reservoir conditions. Among the micellization parameters, the adsorption enthalpy of resins onto asphaltene core $\Delta h_{r,j}^{ads}$ is approximated to the enthalpy of formation of the hydrogen bond (Δh_H = – 11.2×10^3 J/mol). The cross-sectional areas of resin polar head $a_{o,j}$, and non-polar tail $a_{p,j}$ are set to 40 Å^2 and 21 Å^2, respectively (Nagarajan and Ruckenstein, 1991).

Table 6.6 – Relevant data of asphaltenes and resins

				Critical			Fusion	
	M	v	ρ	T_c	P_c	ω	T_f	Δh_f
	g/mol	cm^3/mol	g/cm^3	K	bar		K	cal/mol
nC_7 Asphaltenes	1100	900.0	1.20	1074	8.1	2.1	680	10500
nC_5-nC_7 "	1000	850.0	1.15	1045	8.2	2.0	583	8500
C_3-nC_5 "	900	800.0	1.10	1017	8.3	1.9	533	7500
Resins	700	700.0	1.00	953	8.8	1.8	350	3500

Table 6.7 – Gibbs free energy of asphaltene association (kT units)

Petroleum fluid	Asphaltenes		
	C_3-nC_5	nC_5-nC_7	nC_7
TK	-8.0	-9.0	-10.0
C	-10.0	-11.3	-12.5
U	-9.7	-12.3	-13.3
Mex-C	-9.4	-11.5	-12.3
Mex-Y3	-9.0	-10.0	-12.0
Mex-P	-9.0	-10.0	-12.0

6.2.6.1 Interaction coefficients

The binary interaction coefficients between CO_2 and hydrocarbons are set to 0.125 and between CO_2 and N_2 to – 0.02. The interaction coefficients between N_2 and hydrocarbons are equal to 0.12. The assigned interaction coefficients between C_1 and C_2/C_3, defined components, pseudo-components are 0, 0.02 and 0.025, respectively. For all other non-polar hydrocarbons, the interaction coefficients are set to 0.01. The interaction coefficients between asphaltenes and resins are considered to be zero, and the interactions with pseudo-components are set to 0.03 for asphaltenes and 0.02 for resins. Table 6.8 provides the interaction coefficients between defined hydrocarbons and asphaltenes, resins. These parameters might be slightly adjusted at reservoir conditions to match saturation pressure data.

Table 6.8 – Binary interaction coefficients between asphaltenes–hydrocarbons and resins–hydrocarbons

Component i	$K_{a,i}$	$K_{r,i}$
C_1	0.12	0.08
C_2	0.11	0.07
C_3	0.10	0.06
C_4	0.08	0.04
C_5	0.07	0.02
C_6	0.05	0.02
C_7	0.04	0.02

6.2.6.2 Induction energy parameters

In the induction energy expression given by Eq. (6.9), the average values of the asphaltene molecular radius and dipole moment are approximated to 2.7 Å (Sheu and Mullins, 1995) and 5.5 D (see chapter 4), respectively. The dielectric constant of the medium is equal to 2, however it increases with additional resins. The Clausius-Mosotti mixing rule (Sihvola, 1999) is used to calculate the average dielectric constant of the medium ε upon resin addition,

$$\frac{\varepsilon-1}{\varepsilon+2}=\phi_r\frac{\varepsilon_r-1}{\varepsilon_r+2}+\left(1-\phi_r\right)\frac{\varepsilon_s-1}{\varepsilon_s+2} \tag{6.79}$$

where ϕ_r and ε_r are the volume fraction and dielectric constant of resins, respectively. The average dielectric constant of resins is approximated to 4.7 as measured in chapter 4.

6.2.7 Minimization of the Gibbs free energy

The calculation of phase equilibrium involves the minimization of the total Gibbs free energy of the system. A feasible sequential quadratic programming (FSQP) algorithm (Zhou *et al.*, 1996) is used to minimize the objective function G with respect to 15 independent variables and subject to 5 material balance constraints. The objective function is given by Eqs. (6.75)–(6.78). The independent variables are $n_{1,i}$, $n_{2,j}$, D, n_m, $n_{1a,i}^L$, $n_{1r,j}^L$, $n_{a,i}^P$ (i = 1,2,3 and j = 1,2), and the dependent variables are R, a, and $z_{r,j}^m$. The fugacity coefficients and molar volumes are computed directly from the PR-EOS at a given pressure and temperature, the other parameters are input in the model.

The problem corresponds to globally minimizing the Gibbs free energy function while satisfying the material balance constraints given by Eqs. (6.50) and (6.51). One needs to provide the gradients of the constraints, and the upper and lower boundaries of the variables. The choice of the variables assures symmetry in the gradients of the constraints used in the minimization algorithm and allows numerical stability of the model. The algorithm generates sequences of *feasible* iterates (that is, satisfying all the constraints) and uses penalty functions to maintain the feasibility on the linear constraints. The convergence of FSQP is sensitive to the initial input of variables and

the model uses the previous results as the input for the current initial values. The global minimum provides the micellar size, the phase(s), and the composition.

6.3 Results

The revised thermodynamic micellization model is used to predict the precipitation from six stock tank petroleum fluids (see Tables 6.1–6.2) and three reservoir fluids. The compositional analyses of the reservoir fluids, including asphaltene and resin contents, are available in the literature (Firoozabadi, 1999; Pan and Firoozabadi, 2000). The results are presented in two distinct parts. The first part examines the precipitation of asphaltenes from stock tank petroleum fluids by nC_5 and nC_7 as well as the effect of resins on precipitation from the three first petroleum fluids in Table 6.1. In the last part, the results for the three reservoir fluids are presented. Because resin precipitation at reservoir conditions may not be negligible, the model allows for resin precipitation but considers only one type of asphaltene to avoid numerical problems in the algorithm that may arise when too many variables are considered. In each part, results are discussed and compared with experimental data.

6.3.1 Precipitation from stock tank petroleum fluids

6.3.1.1 Effect of nC_5 and nC_7 n-alkanes

In asphaltene precipitation with n-alkanes, the amount of precipitation decreases with the n-alkane carbon number. The original formulation by Pan and Firoozabadi (1998) does not predict such a behavior as all the asphaltenes precipitate when the petroleum fluid is mixed with various n-alkanes (see Fig. 6.10). In the revised formulation, it has been shown that in a system with polar molecules, the interaction parameter a in PR-EOS which reflects the strength of attraction between two molecules is better represented by the WS mixing rule. Application of the new mixing rule to petroleum fluids results in a higher number of asphaltene monomers kept in the bulk liquid phase as compared to the original formulation. Consequently, the amount of precipitation slightly decreases as shown in Fig. 6.11. A much further decrease in the amount is obtained when the induction energy is considered (see Fig. 6.11) and the precipitation profile becomes very close to that obtained experimentally. The magnitude of the induction energy calculated from Eq. (6.9) and from the induction energy parameters

presented above, is – 2.5 *kT*. Thus, the induction energy represents an important component of the interaction energy. One can notice that the effect of the induction energy is relatively important in maintaining the asphaltene monomers in solution.

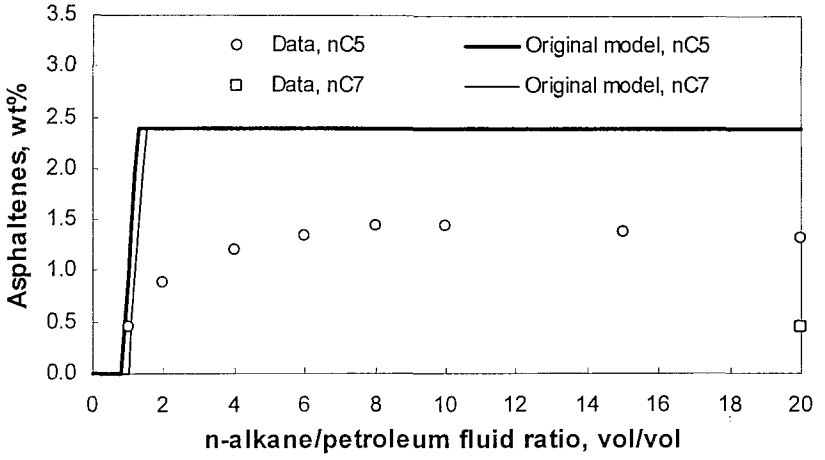


Fig. 6.10 – Effect of n-alkanes on asphaltene precipitation from petroleum fluid TK with the original model.

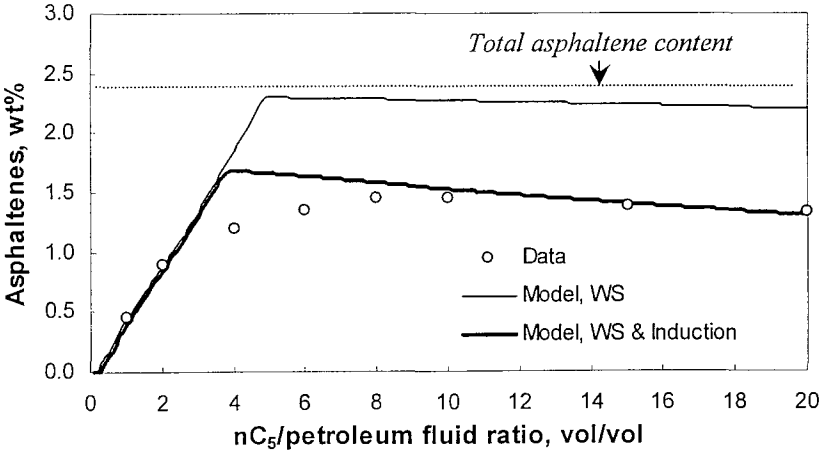


Fig. 6.11 – Effect of the WS mixing rule and the induction energy on the amount of precipitation from petroleum fluid TK.

Figs. 6.12–6.17 depict the amount of precipitated asphaltenes vs. n-alkane (nC_5, nC_7) dilution ratio for the six stock tank petroleum fluids in Tables 6.1–6.2. The predicted amounts are in agreement with the measured data for both n-alkanes. The main difference between precipitation by nC_5 and nC_7 is the difference in n-alkane molar volume. The n-alkane molar volume also affects the interfacial tension between asphaltene core and liquid. As the molar volume increases, the interfacial tension

decreases, which explains the slightly higher onset point of precipitation by nC_7, as compared to precipitation by nC_5. For most cases, the slope of the precipitation curves fits to some extent the experimental data. In addition, the maximum amount of precipitation is observed between a dilution ratio of 2 and 6 vol/vol. From this point, the amount of precipitation slightly decreases with further increase in dilution with n-alkanes and then becomes constant at high dilution ratios. This decrease in the amount of precipitation is due to the high n-alkane dilution for a relatively small increase in the precipitation amount.

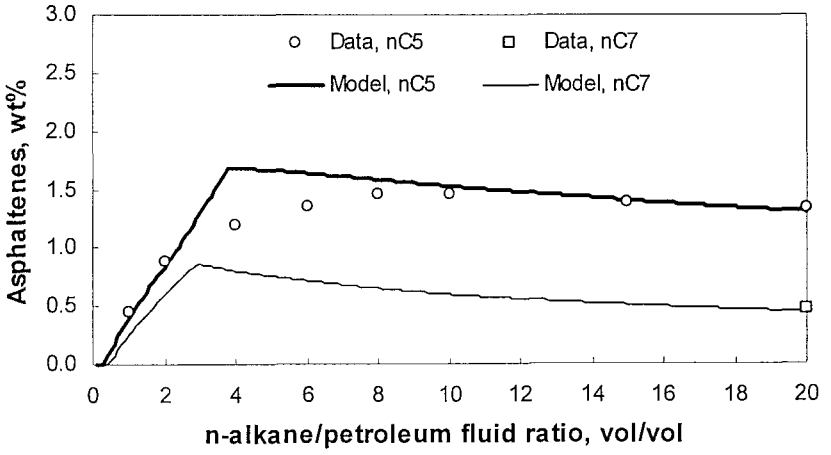


Fig. 6.12 – Effect of n-alkanes on asphaltene precipitation from petroleum fluid TK.

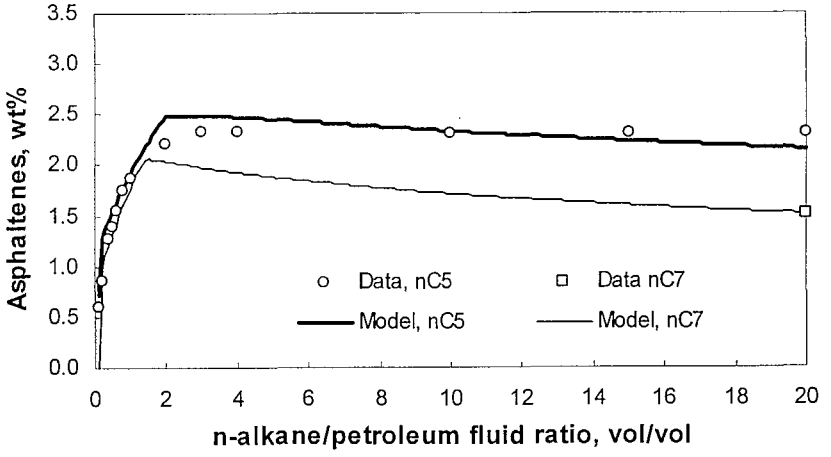


Fig. 6.13 – Effect of n-alkanes on asphaltene precipitation from petroleum fluid C.

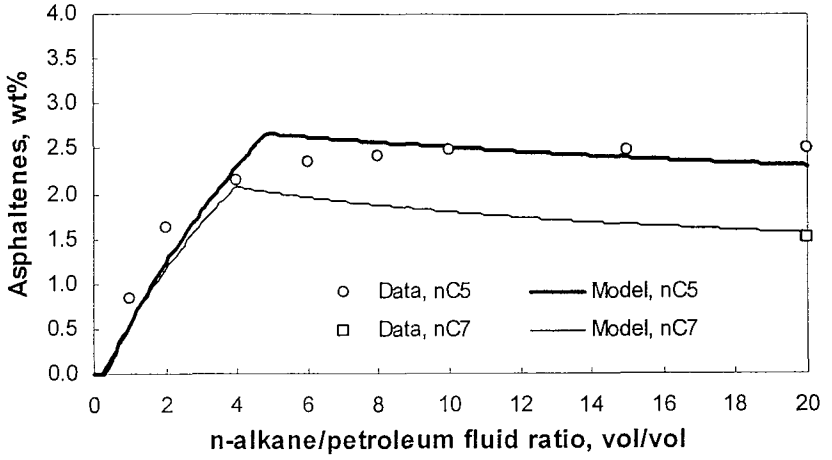


Fig. 6.14 – Effect of n-alkanes on asphaltene precipitation from petroleum fluid U.

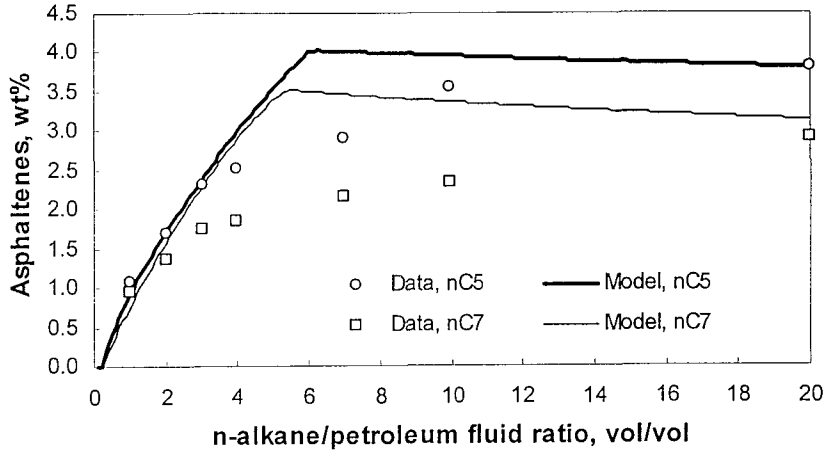


Fig. 6.15 – Effect of n-alkanes on asphaltene precipitation from petroleum fluid Mex-C.

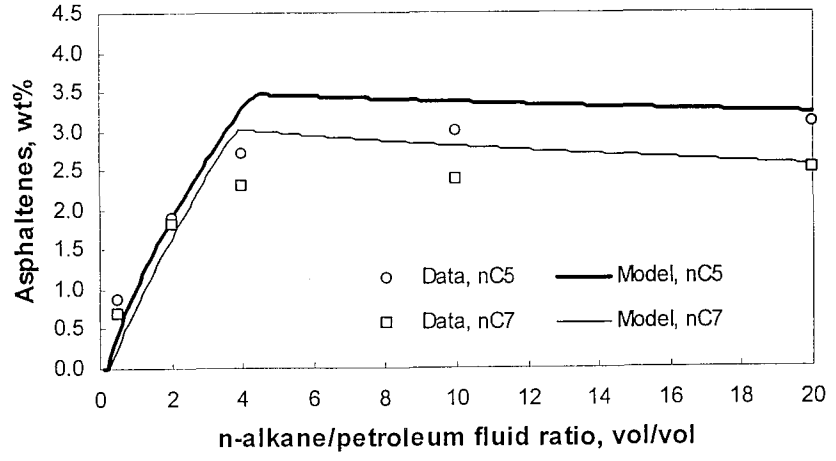


Fig. 6.16 – Effect of n-alkanes on asphaltene precipitation from petroleum fluid Mex-Y3.

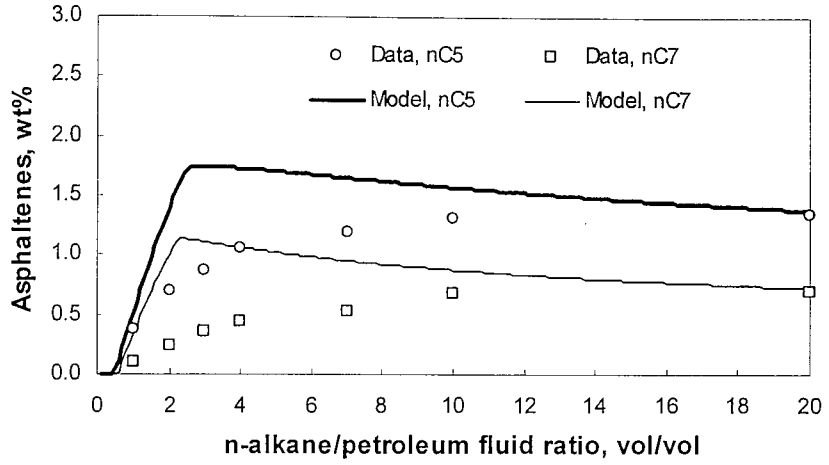


Fig. 6.17 – Effect of n-alkanes on asphaltene precipitation from petroleum fluid Mex-P.

Figs. 6.18–6.20 present the effect of the two n-alkanes on the micellar size and number as well as the number of asphaltene and resin molecules in micelles and bulk liquid, for one mole of stock tank petroleum fluid. It appears from Fig 6.18, that dilution with nC_7 results in smaller micelles and in a larger number than dilution with nC_5 does. As a consequence, less asphaltene and resin molecules are present in micelles (see Fig. 6.19) and more asphaltene and resin monomers are kept in the bulk phase with nC_7 as compared to nC_5 (see Fig. 6.20).

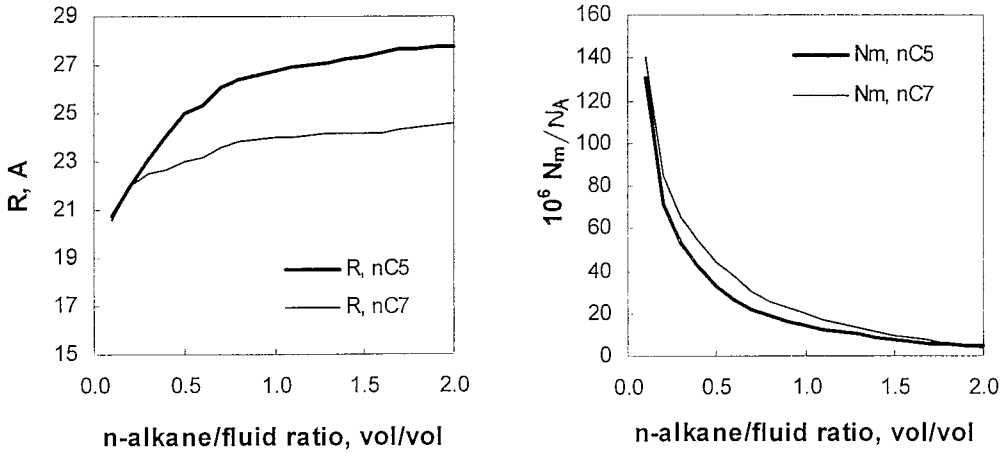


Fig. 6.18 – Effect of n-alkanes on the core radius and number of micelles in petroleum fluid TK

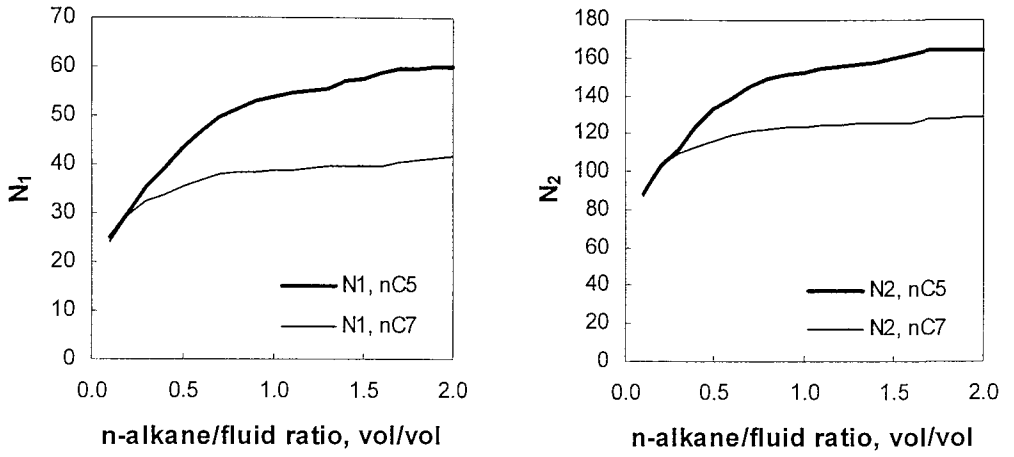


Fig. 6.19 – Effect of n-alkanes on the number of asphaltene and resin molecules in the micelles of petroleum fluid TK.

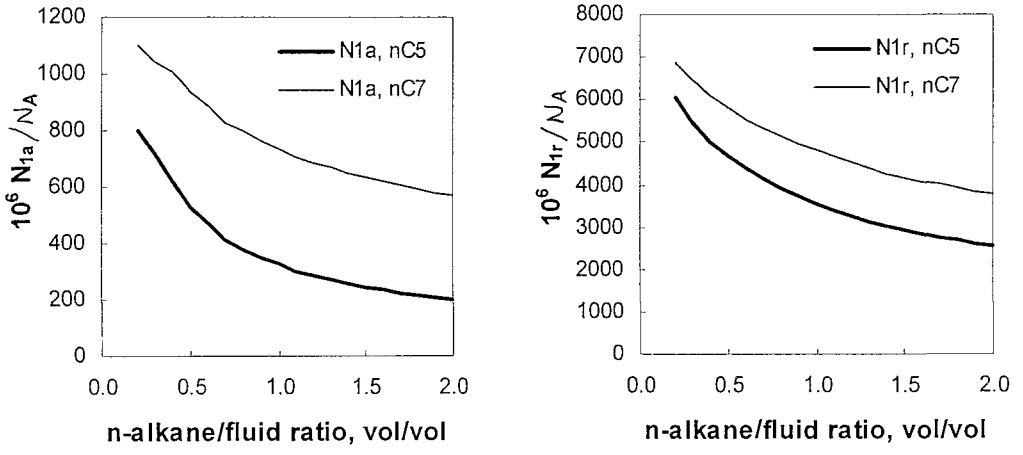


Fig. 6.20 – Effect of n-alkanes on the number of asphaltene and resin monomers in petroleum fluid TK

6.3.1.2 Effect of petroleum resins

Addition of resins to a petroleum fluid affects the dielectric constant of the fluid medium. Proper representation of the dielectric constant variation with resin concentration is important in modelling the effect of resins on precipitation. The calculation of the average dielectric constant ε of the medium upon resin addition using the Clausius-Mosotti mixing rule (see Eq. (6.79)) suggests that ε increases with resin concentration (see Fig. 6.21). Consequently, the induction energy given by Eq. (6.9) increases.

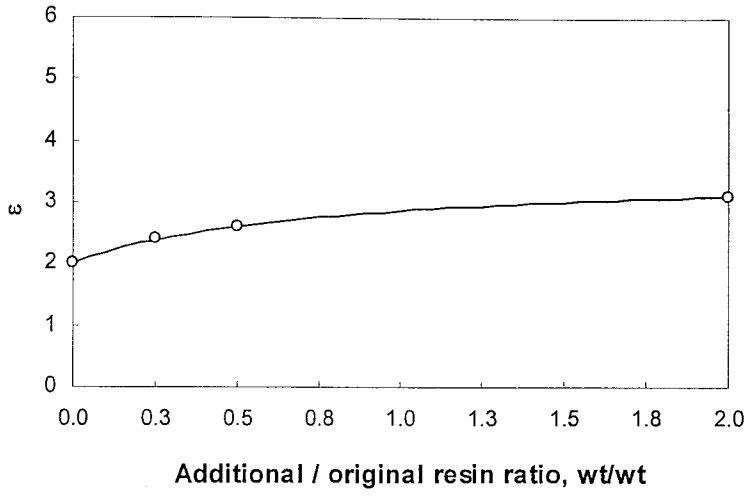


Fig. 6.21 – Effect of resins on the dielectric constant of the medium.

The effect of resin concentration increase in the petroleum fluids TK, C and U is modelled. The concentration of resins is first increased from the original amount by a factor of two, by mixing the petroleum fluids with additional resins (see Table 6.9). Because there is a limit to the solubility of resins in petroleum fluids and nC_5, the precipitate contains both asphaltenes and resins. At a zero dilution ratio, the amount of resin precipitation from the petroleum fluids is calculated from solubility curves established in chapter 5. Similarly, an additional amount of resin precipitation in nC_5 is considered from an excess dilution ratio of say 2 vol/vol (see Chapter 5). A linear increase in resin precipitation between the two limiting dilution ratios (0 and 2 vol/vol) is used and the total amount of resin precipitation in the petroleum fluids TK, C and U is presented in Table 6.9. Figs. 22–24 show the amounts of asphaltene and resin precipitation in the three petroleum fluids. The predicted amounts are in good agreement with the data for petroleum fluid C but slightly underestimated for petroleum fluids TK and U.

Table 6.9 – Precipitation of additional resins from petroleum fluids and nC_5

	Petroleum fluid		
	TK	C	U
Original resins, wt%	7.5	6.5	8.6
Additional resins, wt%	13.0	11.5	14.7
Resin precipitate (wt%) from			
Petroleum fluid (at 0 vol/vol)	0.52	0.11	0.59
nC_5 (at 2 vol/vol)	0.13	0.11	0.15
Total (after 2 vol/vol)	0.65	0.22	0.74

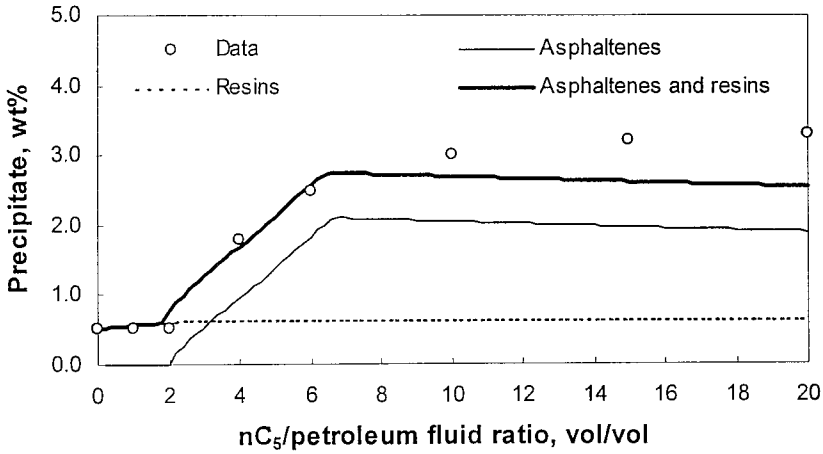


Fig. 6.22 – Effect of additional resins from petroleum fluid TK on precipitation from the same petroleum fluid (Resins = 19.9 wt%).

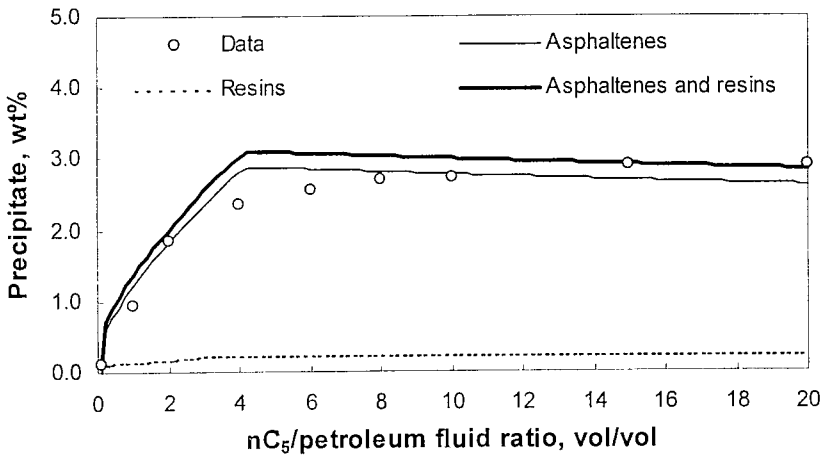


Fig. 6.23 – Effect of additional resins from petroleum fluid C on precipitation from the same petroleum fluid (Resins = 17.8 wt%).

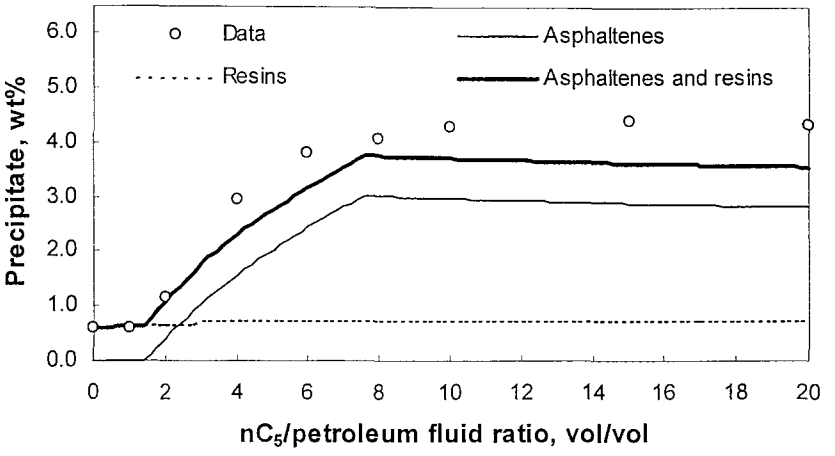


Fig. 6.24 – Effect of additional resins from petroleum fluid U on precipitation from the same petroleum fluid (Resins = 22.6 wt%).

Figs 6.25–6.27 present the effect of resins on precipitation for four concentrations in the petroleum fluids TK, C and U, respectively. Resins at the first three concentrations are completely soluble in the petroleum fluids, and therefore do not precipitate. Note that the results with the last resin concentration, which is the highest, have been presented above. For all resin concentrations, the model successfully describes the effect on the precipitation onset point and the amount of precipitation for the three petroleum fluids. The increase in the induction energy results in a higher amount of precipitation whereas the decrease in the standard Gibbs free energy of micelle formation results in a higher onset point of precipitation. The decrease of the free energy of micellization is the result of two reverse effects. The first one and probably the most important is the negative energy of adsorption, which decreases the free energy of micellization. The second one is the positive interfacial and steric energy, which increases the free energy of micellization.

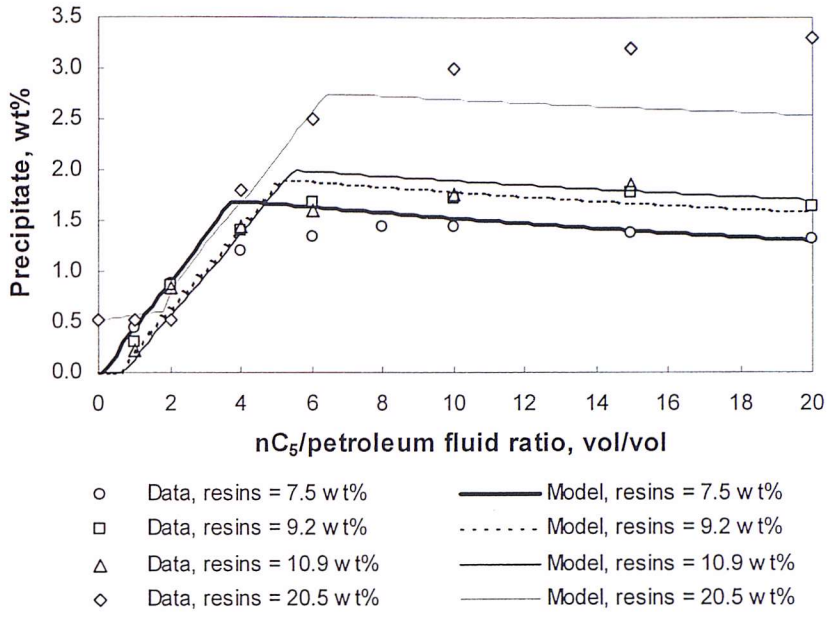


Fig. 6.25 – Effect of resin concentration on asphaltene precipitation from petroleum fluid TK.

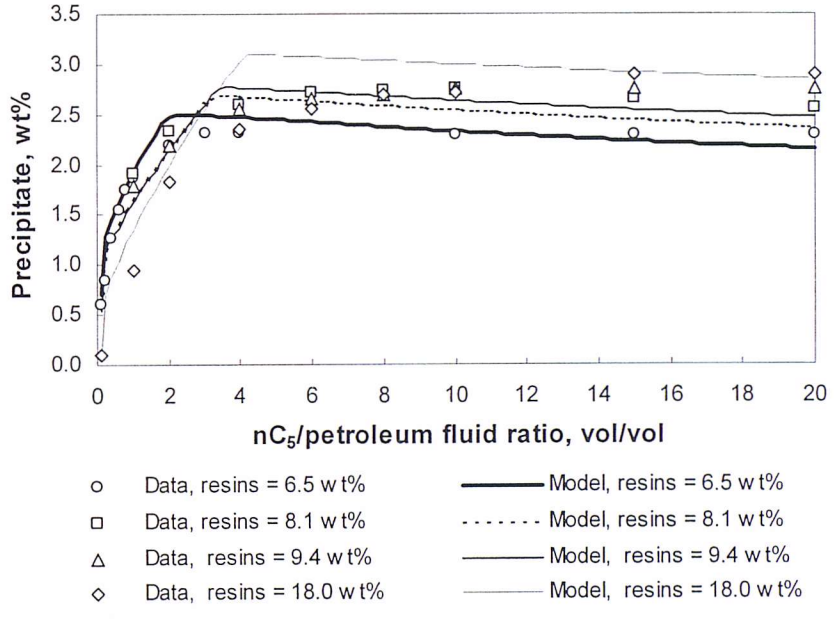


Fig. 6.26 – Effect of resin concentration on asphaltene precipitation from petroleum fluid C.

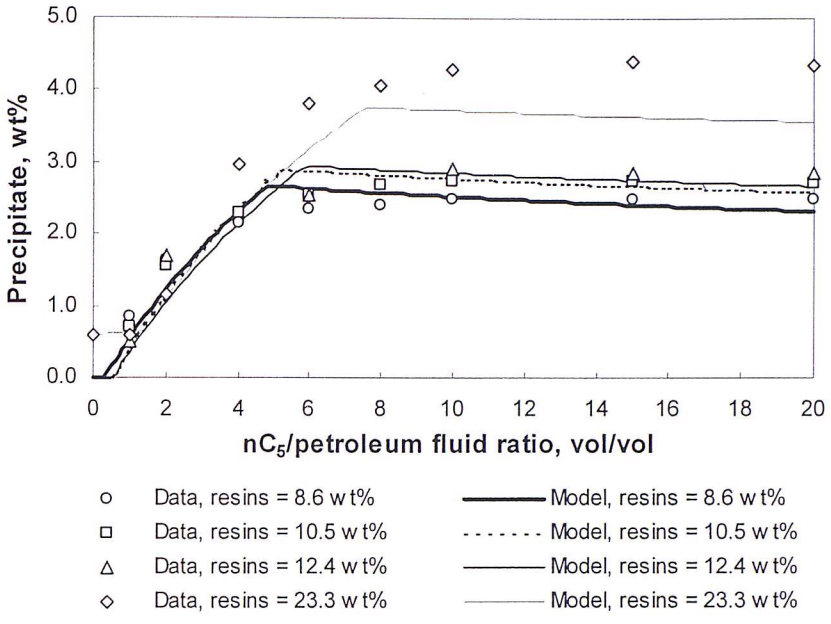


Fig. 6.27 – Effect of resin concentration on asphaltene precipitation from petroleum fluid U.

The effect of resins on the molecular distribution of asphaltenes and resins in the bulk liquid and in micelles is presented in Figs. 6.28–6.30, for one mole of petroleum fluid TK. The figures suggests that addition of resins to a petroleum fluid enhances the formation of larger micelles and in a higher number than in the original fluid (see Fig. 6.28). As a result, micelles contain more asphaltene and resin molecules (see Fig. 6.29), and the number of asphaltene monomers in the bulk liquid phase decreases whereas the number of resin monomers increases (see Fig. 6.30).

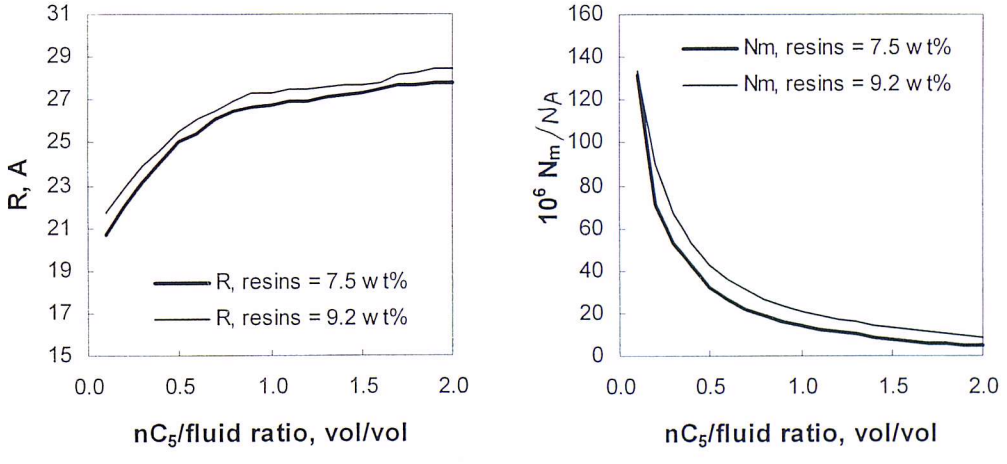


Fig. 6.28 – Effect of resins from petroleum fluid TK on the core radius and number of micelles in the same petroleum fluid.

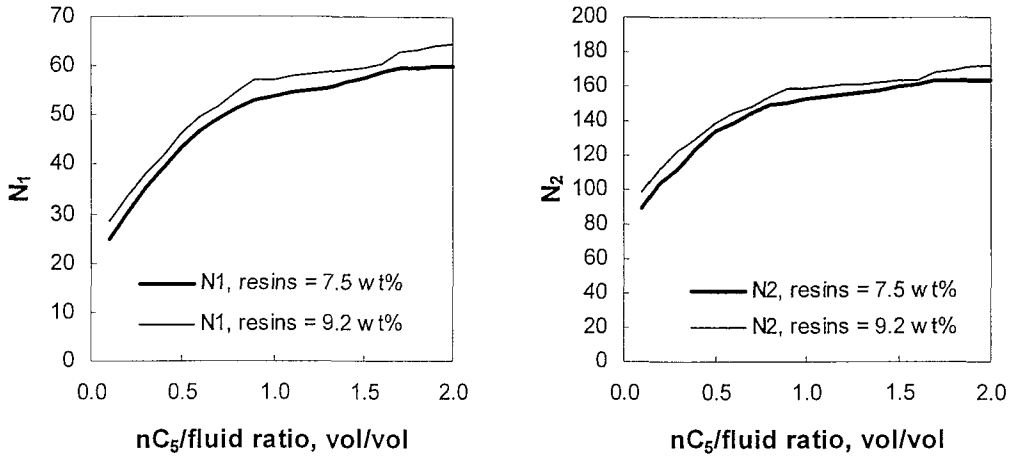


Fig. 6.29 – Effect of resins from petroleum fluid TK on the number of asphaltene and resin molecules in the micelles of the same petroleum fluid.

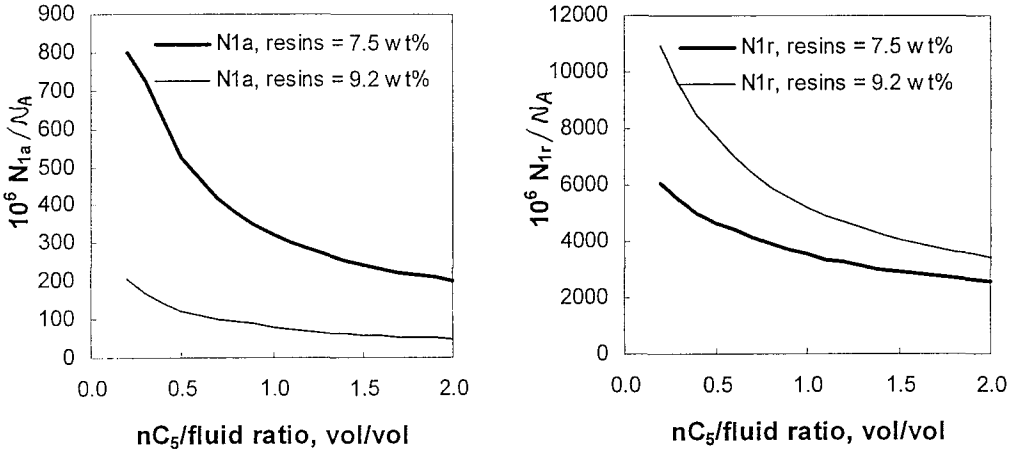


Fig. 6.30 – Effect of resins from petroleum fluid TK on the number of asphaltene and resin monomers in the same petroleum fluid.

6.3.2 Precipitation from reservoir fluids

The revised model is used to predict precipitation in three reservoir fluids: Weyburn, North Sea and Hirshberg fluids (Firoozabadi, 1999). The saturation pressure of each fluid is first computed to allow for flash calculations at pressures below the bubble point pressure. Because the model at reservoir conditions is more sensitive to the interaction coefficients between asphaltenes and other hydrocarbons and non-hydrocarbons than at stock tank conditions, it is sometimes necessary to adjust once these coefficients in order to match the saturation pressure. Yet, the sensitivity of the model to the interaction coefficients is less pronounced with the revised formulation

than the original model due to the WS mixing rule. The amount of precipitation is then calculated at various pressures. From experience, it is preferable to start the modelling at high pressures then decrease the pressure gradually. The input variables of each run are the output variables of the previous run.

Figs. 6.31–6.34 present in the precipitation from the three fluids. Fig. 6.31 shows the effect of dilution with CO_2 on asphaltene precipitation from the Weyburn fluid. By setting the interaction coefficient between asphaltenes and CO_2 to 0.2, the predicted precipitation is in good agreement with experimental data. Moreover, the predictions are improved with the revised formulation. Fig. 6.32 depicts the amount of asphaltene and resin precipitation from the Hirshberg reservoir fluid and propane mixture (at a weigh ratio of 1 to 7) when the pressure is reduced from 1400 bara to atmospheric pressure. As expected, the maximum amount of precipitation occurs around the bubble point pressure. Again, the predictions with the revised model are more in line with the data than the predictions with the original model. Fig. 6.32 also shows that because of the high concentration of propane in the fluid, the amount of precipitated resins is higher than that of asphaltenes. Figs. 6.33 and 6.34 present the results of precipitation from the North Sea fluid by a separator gas. The interaction coefficients are adjusted to match the saturation pressure and the pressure at the onset of precipitation at two temperatures 333 K and 365 K (see Fig. 6.33). The precipitation results are presented in Fig. 6.34. The model slightly underestimates the amounts of asphaltenes and resins however, the onset of precipitation is well predicted.

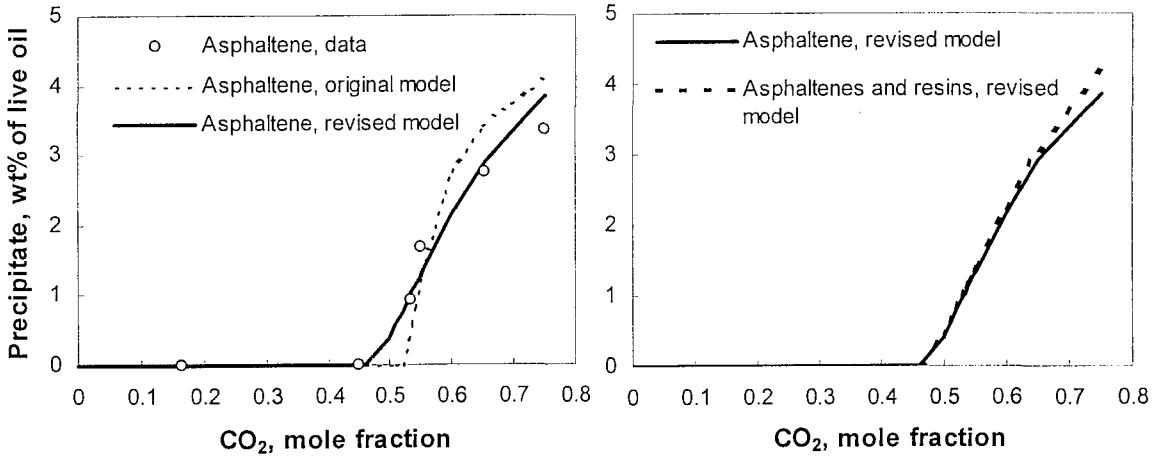


Fig. 6.31 – Asphaltene and resin precipitation from the Weyburn petroleum fluid

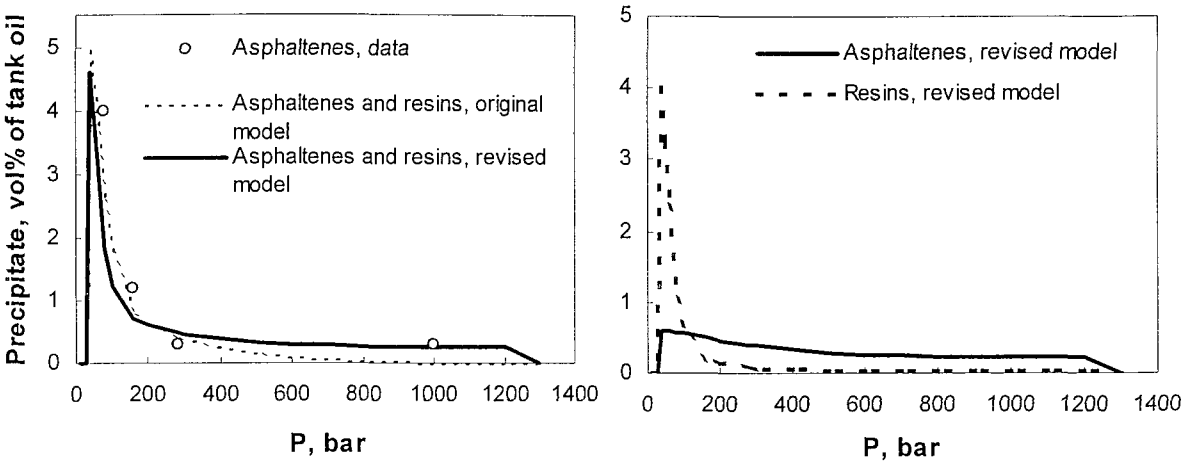


Fig. 6.32 – Asphaltene and resin precipitation from the Hirshberg petroleum fluid

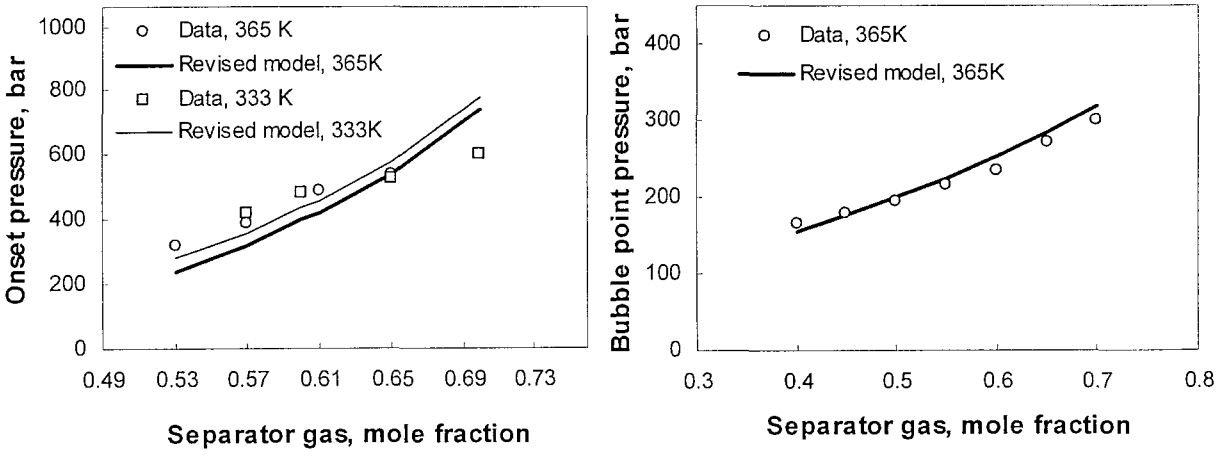


Fig. 6.33 – Pressure at the onset of precipitation and bubble point pressure of the North Sea petroleum fluid

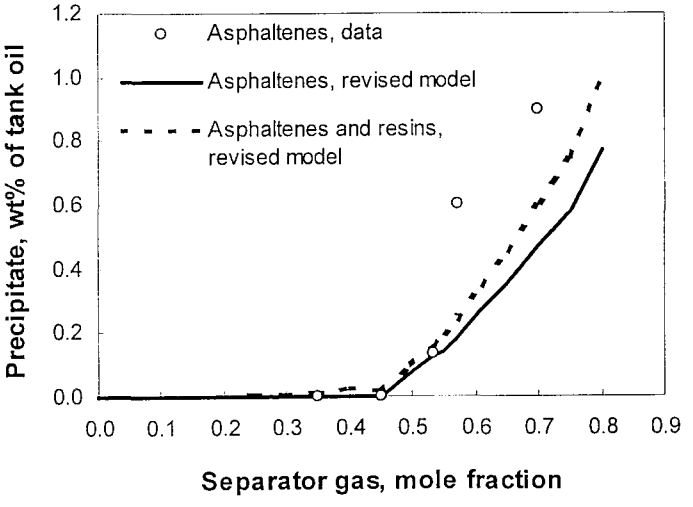


Fig. 6.34 – Asphaltene and resin precipitation from the North Sea petroleum fluid

6.4 Conclusions

The thermodynamic micellization framework proposed by Pan and Firoozabadi is modified to improve the prediction of asphaltene aggregation and precipitation from petroleum fluids at ambient and reservoir conditions. The revised formulation predicts properly the effect of n-alkanes on precipitation from stock tank petroleum fluids and can capture the effect of petroleum resins on precipitation. The same model can be applied to stock tank and live petroleum fluids. The main novelties are summarized in the following points:

1) The amount of precipitation is directly related to the interactions between asphaltenes and the other hydrocarbons. To improve the interaction parameter calculation in PR-EOS, the WS mixing rule is used. As a result, more asphaltene monomers are kept in the bulk liquid phase. However, it is mainly the induction energy between asphaltene monomers and the solvent that affects the amount of precipitation as a large number of monomers are maintained in the solution. The induction energy represents an important component of the interaction energy and is not described by the mean-field approximation. The effect of the induction energy is mainly observed at stock tank conditions because of large composition variations. This effect may not contribute much at reservoir conditions. Moreover, the WS mixing rule reduces the sensitivity of the model to interaction coefficients at reservoir conditions.

2) The interfacial tension between the liquid in the shell and the asphaltene core affects the onset point of precipitation and the slope of the precipitation curve. The effect of composition described by Helfand and Tagami is modified and the effect of curvature is included. The new equation for the interfacial tension improves the profile of the precipitation curve.

3) The effect of resins on the amount of precipitation is modeled through the effect of the dielectric properties of the medium on the induction energy between the asphaltene monomers and the solvent. As resins are added to the petroleum fluid, the dielectric constant of the medium increases and as a result, the induction interactions are less favored and more asphaltenes precipitate.

6.5 References

Andersen, S. I., and J. G. Speight, "Thermodynamic Models for Asphaltene Solubility and Precipitation", *J. of Petrol. Sci. and Eng.*, **22**, 53 (1999).

Böttcher, C. J. F., *Theory of Electric Polarization*, Elsevier, Amsterdam (1952).

Buenrostro-Gonzalez, E., A. Gil-Villegas, J. Wu, and C. Lira-Galeana, "Modelling of Asphaltene Precipitation using the SAFT-VR EOS Approach", *International Conference of Heavy Organic Depositions*, Puerto-Vallarta, Jalisco, Mexico, Nov. 17-21 (2002).

Burke, N. E., R. E. Hobbs, and S. F. Kashou, "Measurement and Modelling of Asphaltene Precipitation", *J. of Petrol. Technol.*, **42**, 1440 (1990).

Chapman, W. G., G. Jackson, and K. E. Gubbins, "Phase Equilibria of Associating Fluids, Chain Molecules with Multiple Bonding Sites", *Mol. Phys.*, **65**, 1057 (1988).

Chapman, W. G., K. E. Gubbins, G. Jackson, and M. Radosz, "New Reference Equation of State for Associating Liquids", *Ind. Eng. Chem. Res.*, 29, 1790 (1990).

Chung, T-H, "Thermodynamic Modelling for Organic Solid Precipitation", *SPE* paper # 24851 (1992).

Cimino, R., S. Correra, P. A. Sacomani, and C. Carniani, "Thermodynamic Modelling for Prediction of Asphaltene Deposition in Live Oils", *SPE* paper # 24851 (1992).

Duda, Y., and C. Lira-Galeana, "Modelling Asphaltene Precipitation using Integral Equations. An Analytical Solution to the Associative Ornstein-Zernike Integral Equation", *International Conference of Heavy Organic Depositions*, Puerto-Vallarta, Jalisco, Mexico, Nov. 17-21 (2002).

Firoozabadi, A., *Thermodynamics of Hydrocarbon Reservoirs*, McGraw-Hill, New York (1999).

Galindo, A., A. Gil-Villegas, and G. Jackson, "The Thermodynamics of Mixtures and the Corresponding Mixing Rules in the SAFT-VR Approach for Potentials of Variable Range", *Molecular Physics*, **93**, 1, 241 (1998).

Ghonasgi, D., and W. G. Chapman, "Theory and Simulation for Associating Hard Chain Fluids", *Mol. Phys.*, **83**, 145 (1994).

Gibbs, J. W., *The Scientific Papers of J. Willard Gibbs*, Dover, New York (1961).

Gil-Villegas, A., A. Galindo, P. J. Whitehead, S. J. Mills, G. Jackson, and A. N. Burgess, "Statistical Associating Fluid Theory for Chain Molecules with Attractive Potentials of Variable Range", *The J. of Chem. Phys.*, 106, 10, 4168 (1997).

Gupta, A. K., *A Model for Asphaltene Flocculation using an Equation of State*, MSc Thesis, Department of Chemical and Petroleum Engineering, University of Calgary (1986).

Helfand, E., and Y. Tagami, "Theory of the Interface between Immiscible Polymers", *J. Polymer Letters*, **9**, 741 (1971).

Hildebrand, J. H., and R. L. Scott, Regular Solutions, Prentice-Hall, Englewood Cliffs, New Jersey (1962).

Hirschberg, A., L. N. J. de Jong, B. A. Schipper, and J. G. Meijer, "Influence of Temperature and Pressure on Asphaltenes Flocculation", *SPE* paper # 11202 (1984).

Huron, M. J., and J. Vidal, "New Mixing Rules in Simple Equations of State for Representing Vapor-Liquid Equilibria of Strongly Non-Ideal Mixtures", *Fluid Phase Equilibria*, **3**, 255 (1977).

Israelachvili, J. N., *Intermolecular and Surface Forces*, Academic Press, San Diego (1991).

Jhaveri, B. S., and G. K. Youngren, "Three-Parameter Modification of the Peng Robinson Equation of State to Improve Volumetric Predictions", *SPE* paper # 13118 (1988).

Kokal, S. L., J. Najman, S. G. Sayegh, and A. E. George, "Measurement and Correlation of Asphaltene Precipitation from Heavy Oils by Gas Injection", *J. of Can. Petrol. Technol.*, **31**, 24 (1992).

Lee, L. L., *Molecular Thermodynamics of Nonideal Fluids*, Butterworth, Boston (1988).

Leontaritis, K. J., and G. A. Mansoori, "Asphaltene Flocculation during Production and Processing: A Thermodynamic-Colloidal Model", *SPE* paper # 16258 (1987).

MacMillan, D. J., J. E. Tackett, M. A. Jessee, and T. G. Monge-McClure, " A Unified Approach to Asphaltene Precipitation: Laboratory Measurement and Modelling", *J. of Petro. Technol.*, **47**, 788 (1995).

Maitland, G. C., M. Rigby, E. B. Smith, and W. A. Wakeham, *Intermolecular Forces: Their Origin and Determination*, Clarendon Press, Oxford (1981).

Monteagudo, J. E. P., P. L. C. Lage, and K. Rajakopal, "Towards a Polydisperse Thermodynamic Model for Asphaltene Precipitation in Live Oil", *Fluid Phase Equilibria*, **187**, 443 (2001).

Nagarajan, R., and E. Ruckenstein, "Theory of Surfactant Self-Assembly. A Predictive Molecular Thermodynamic Approach", *Langmuir*, **7**, 12, 2934 (1991).

Nghiem, L. X., M. S. Hassam, R. Nutakki, and A. E. D. George, "Efficient Modelling of Asphaltene Precipitation", *SPE* paper # 26642 (1993).

Nghiem, L. X., B. F. Kohse, S. M. F. Ali, and Q. Doan, "Asphaltene Precipitation: Phase Behaviour Modelling and Compositional Simulation", *SPE* paper # 59432 (2000).

Ono, S., and S. Kondo, "Molecular Theory of Surface Tension in Liquids", *Encyclopedia of Physics*, vol. 10, edited by S. Flugge, Springer (1960).

Orbey, H., and S. I. Sandler, "Reformulation of Wong-Sandler Mixing Rule for Cubic Equations of State", *AIChE J.*, **41**, 3 (1995).

Pan, H., and A., Firoozabadi, "Thermodynamic Micellization Model for Asphaltene Aggregation and Precipitation in Petroleum Fluids", *SPE Prod. & Facilities J.*, 118 (May 1998).

Pan, H., and A., Firoozabadi, "Thermodynamic Micellization Model for Asphaltene Precipitation from Reservoir Crudes at High Pressures and Temperatures", *SPE Prod. & Facilities*, **15**, 1, 58 (2000).

Park, S. J., and A. Mansoori, "Aggregation and Deposition of Heavy Organics in Petroleum Crudes", *Energy Resources*, **10**, 109 (1988).

Park, S. J., *A Thermodynamic Polydisperse Polymer Model: Asphaltene Flocculation, Aggregation, and Deposition*, Ph.D. dissertation, University of Illinois, Chicago (1989).

Peneloux, A., E. Rauzy, and R. Freze, "A Consistent Correction for Redlich-Kwong-Soave Volumes", *Fluid Phase Equilibria*, **8**, 7 (1982).

Poling, B. E., J. Prausnitz, and J. O'Connell, *The properties of Gases and Liquids*, 5th ed. McGraw-Hill, New York (2001).

Prausnitz, J. M., R. N. Lichtenthaler, and E. G. de Azevedo, *Molecular Thermodynamics of Fluid-Phase Equilibria*, Prentice-Hall, New Jersey (1999).

Prigogine, I., A. Bellmans, and V. Mathot, *The Molecular Theory of Solutions*, Amsterdam, Holland (1957).

Puvvada, S., and D. Blankenstein, "Theoretical and Experimental Investigations of Micellar Properties of Aqueous Solutions containing Binary Mixtures of Nonionic Surfactants", *J. Phys. Chem.*, **96**, 5579 (1992).

Sandler, S. I., *Chemical and Engineering Thermodynamics*, John Wiley & Sons, New York (1999).

Sheu, E. Y. L., and O. C. Mullins, *Asphaltenes: Fundamentals and Applications*, Plenum Press, New York (1995).

Sihvola, A., Electromagnetic Mixing Formulas and Applications, IEE Electromagnetic Wave Series (1999).

Sorensen, T. S., in *Surfactants in Solution*, K. L., Mittal and B., Lindman, vol. 2, Plenum Press (1982).

Storm D. A., and E. Y. Sheu, "Characterization of Asphaltenic Colloidal Particle in Heavy Oil", *Fuel*, **74**, 8, 1140 (1995).

Thomas, E. R., and C. A. Eckert, "Prediction of Limiting Activity Coefficients by a Modified Separation of Cohesive Energy Density Model and UNIFAC", *Ind. Eng. Chem. Process Des. Dev.*, **23**, 194 (1984).

Thomas, F. B., D. B. Bennion, D. W. Bennion, and B. E. Hunter, "Experimental and Theoretical Studies of Solids Precipitation from Reservoir Fluid", *J. Can. Petrol. Technol.*, **31**, 1, 22 (1992).

Tolman, R. C., "The Effect of Droplet Size on Surface Tension", *J. Chem. Phys.*, **17**, 119, 333 (1949).

Vakarin, F., M. F. Holovko, and Y. Duda, "Integral Equation Theory for the Four Bonding Sites Model for Associating Fluids. 2. Density Profiles and Adsorption onto a Solid Surface", *Molecular Physics*, **91**, 2, 203 (1997).

Whitson, C. H., "Characterizing Hydroacarbon Plus Fractions", *SPE* paper # 12233 (1983).

Wong, D. S. H., and S. I. Sandler, "A Theoretically Correct Mixing Rule for Cubic Equations of State", *AIChE J.*, **38**, 5 (1992).

Wu, J., J. M. Prausnitz, and A. Firoozabadi, "Molecular-Thermodynamic Framework for Asphaltene-Oil Equilibria", *AIChE J.*, **44**, 5, 1188 (1998).

Wu, J., J. M. Prausnitz, and A. Firoozabadi, "Molecular Thermodynamics of Asphaltene Precipitation in Reservoir Fluids", *AIChE J.*, **46**, 1, 197 (2000).

Zhou, J. L., A. L. Tits, and C. T. Lawrence, *User's Guide for FFSQP Version 3.7: A Fortran Code for Solving Optimization Programs, Possibly Minimax, with General Inequality Constraints and Linear Equality Constraints, Generating Feasible Iterates*, Institute for Systems Research, University of Maryland, Technical Report SRC-TR-92-107r5, College Park, MD 20742 (1997).

Chapter 7

Conclusions and recommendations

7.1 Introduction

A comprehensive experimental and modelling work has been conducted to study the precipitation of asphaltenes from petroleum fluids and the effect of resins and amphiphiles. The major contribution of this thesis is in the quantification of the polarity of asphaltenes and resins and its effect on the precipitation. The experimental investigations provide valuable data for the revision of the thermodynamic micellization model by Pan and Firoozabadi (1998, 2000). The measurement of resin dipole moment, and the effect of resins and DBSA amphiphile on the amount of precipitation add new data for the first time to the literature. This chapter summarises the key findings of the thesis. We present in separate sections the conclusions drawn from the experimental and modelling work and provide some suggestions for future study.

7.2 Conclusions from the experimental work

An improved method for the measurement of resins in petroleum fluids is devised based on the dipole moment of molecules. It is found that the propane precipitation separates only part of the resins, the most polar fraction. The modified ASTM D-2007 adsorption method on the other hand, gives the total amount of resins provided no aromatic solvent is used to elute the oils. In the previous investigations, emphasis has

been placed on the choice of the adsorbent and the solvents for resin desorption from the adsorbent. This study shows that the choice of the solvent to elute the oils is very important. The introduction of toluene even at small proportions may elute some resin molecules with nitrogen functions that are weakly bound to the clay.

The molecular size of asphaltenes and resins is similar to the literature and confirms that the molecules are relatively small compared to the previous reports. The radius of asphaltene molecules by time-dependent fluorescence emission spectroscopy is found to vary between 2.5 to 5.9 Å depending on the nature of the petroleum fluid. The comparison of the population size distribution of different asphaltenes and resins by steady-state fluorescence emission spectroscopy suggests that resins precipitated by propane contain the largest and most polar molecules. The observations confirm that petroleum fluid is indeed a continuum. The heaviest fractions of asphaltenes and resins, composed of the largest molecules, are the most polar.

The dipole moment of asphaltenes and resins is calculated in order to model the interactions involving these molecules in the petroleum fluid. It is demonstrated that the Onsager formulation provides the most accurate data of dipole moments. The dipole moments are in the range of 3.3–7.0 D for nC_5 asphaltenes, 2.4–3.2 D for resins, and 0.0–0.9 D for oils. Thus, asphaltenes and to a lesser degree resins are highly polar molecules. Oils may be slightly polar due to high electronic and atomic polarizations of heavy aromatic hydrocarbons. Asphaltenes precipitated by heavy normal alkanes are more polar than asphaltenes precipitated by light normal alkanes. This observation confirms that petroleum fluid is a continuum in size and polarity. In this work, the dipole moment of resins is measured for the first time. Results reveal that for a given petroleum fluid, asphaltenes have a higher dipole moment than resins. However, resins from one petroleum fluid can have a higher dipole moment than asphaltenes from another petroleum fluid.

The study of the effect of resins and amphiphiles on precipitation shows that the molecular interactions depend strongly on the medium. The previous investigations have examined mainly the effect on the onset point of precipitation, very few provide the amount, which is limited in scope and is not in agreement with our extensive measurements. The new results on the effect of resins on the amount of precipitation

show that asphaltenes and resins interact differently when they are in the petroleum fluid and when they are in aromatic solvents. Also, the resins are partially soluble in nC_5, although resins in the nC_5-deasphaltened fluid are completely soluble in nC_5. There are two novelties in the study of the effect of resins on precipitation. First, resins increase the amount of precipitation and hence may not be good inhibitors for asphaltene precipitation. Second, resins with a large dipole moment increase less the amount of precipitation than resins with a small dipole moment, implying that electrostatic interactions between asphaltenes and resins may not be negligible. The study on the effect of DBSA amphiphile on the amount of precipitation is also new and has not been reported by others. The retrograde precipitation with increasing concentration of the amphiphile suggests that before a certain concentration, the amphiphile is not effective. The results show that the mechanisms by which resins and DBSA stabilize asphaltenes are different and provide a basis for successful field applications.

7.3 Conclusions from the modeling work

The results of the modelling work show that the limitations of the previous formulation are mainly due to a misrepresentation of the molecular interactions between the polar and nonpolar molecules. The introduction of inductive interactions between asphaltenes and the medium allows the model to capture the effect of the medium on the precipitation, specifically the effect of density and dielectric constant (that is, the effect of n-alkanes and resins, respectively). The Wong and Sandler mixing rule in PR-EOS provides a better description of the non-ideal mixing of asphaltenes and resins, mainly due to differences in molecular size. In this mixing rule, the modified NRTL model is used to calculate the excess Gibbs free energy of mixing, and the MOSCED model to estimate the activity coefficient at infinite dilution of asphaltenes and resins. The modification of the interfacial tension expression between asphaltene core and surrounding liquid improves the prediction at low dilution ratio. With the above modifications, the model can predict properly the precipitation from stock tank and reservoir petroleum fluids. The results from the same model on the effect of resins on precipitation are also in good agreement with the experimental data.

7.4 Recommendations

This study has shown that asphaltene precipitation results from different interactions between species in the petroleum fluid. Further research should be directed towards the understanding of such interactions including electrostatic and induction interactions. The following areas are recommended for future study:

a. Allow for resin precipitation from stock tank petroleum fluids by considering other minimisation algorithms that can perform with a higher number of independent variables.

b. Include the electrostatic and induction interactions between polar molecules in the revised model in order to reproduce the effect of various resins on the precipitation. These interactions, which constitute approximately 20% of the total van der Waals interactions (see Chapter 5), may not be included in G^{int} because of the mean field approximation used.

c. Investigate the mechanism by which asphaltenes associate in order to predict their Gibbs free energy of association (currently a fitting parameter of the model).

d. Validate the high dipole moments of asphaltenes from quantum mechanics calculations. Also, investigate the effect of water on the dipole moment and the electrostatic interactions in the petroleum fluid.

e. Include the effect of higher moments (such as quadrupoles) in the interactions, which may be important because of the high aromaticity of asphaltene molecules.

f. Investigate other methods to quantify polarity.

g. Model the effect of DBSA amphiphile on the precipitation. The experimental data gathered in this thesis provide a challenge for the prediction of the retrograde effect measured.

h. Extend the application of the model to other amphiphiles.

i. Perform experiments on the effect of resins and DBSA amphiphile at various concentrations on precipitation at reservoir conditions.

Appendix A

Characterization of the plus fraction

The characterization of the heavy fraction in a petroleum fluid is obtained by using the three-parameter Γ distribution function to generate the molar distribution of the deasphalted plus fraction (Whitson, 1983). The input parameters are: 1) the carbon number CN of the plus fraction, here equal to 8, 2) the mole fraction z_{CN+} and molecular weight M_{CN+} of the C_{8+} fraction, 3) the molecular weight of the petroleum fluid, 4) the weight fraction and molecular weight of asphaltene and resin fractions, and 5) the number of pseudo-components. The procedure consists first of calculating the mole fraction and molecular weight of the deasphalted C_{8+} fraction. The probability function that describes the relation between mole fraction z_i and molecular weight M_i of the deasphalted C_{8+} sub-fractions is then computed from,

$$p(M) = \frac{(M - LM)^{A-1} e^{[(M-LM)/B]}}{B^A \Gamma(A)} \tag{A.1}$$

where A, B, and LM are parameters defining the distribution. A gives a measure of the shape of the distribution and is calculated from an empirical correlation (Whitson, 1983). LM is the lowest molecular weight in the plus fraction given by $LM = 14CN - 7$, and B is calculated from $B = \left(M_{CN^+} - LM\right)/A$. The cumulative distribution function is the integral of the probability function $p(x,\alpha)$ from LM to x.

$$p(x,A) = \int_{LM}^{x} p(x)dx = e^{-[(x-A)/B]} \sum_{j=0}^{\infty} \frac{y^{A+1}}{\Gamma(A+j+1)} \tag{A.2}$$

Therefore the mole fraction and the molecular weight are,

$$z_i = p(M_i, A) - p(M_{i-1}, A) \tag{A.3}$$

$$M_i = LM + \frac{AB}{z_i}\left[p(M_i, A+1) - p(M_{i-1}, A+1)\right] \tag{A.4}$$

The split sub-fractions are then lumped into several pseudo-components of approximately equal weight. Since the number of pseudo-components is set initially, the composition and the molecular weight of the grouped fractions are readily determined.

Appendix B

Standard Gibbs free energy of micellization

Pan and Firoozabadi (1998) devised a four-step hypothetical path to describe the formation of micelles in a petroleum fluid (see Fig. B.1). In the following, the superscripts Θ and 0 represent the standard state (infinite dilution) and the pure state, respectively.

Step # 1

Asphaltene molecules first transfer from the infinite-dilution solution to the aggregated state, assumed as an ideal liquid solution, then deform inside the micellar core. The Gibbs free energy of asphaltene transfer is negative and is given by,

$$\Delta g_{a,i}^{tr} = \mu_{a,i}^{m} - \mu_{1a,i}^{\Theta} \tag{B.1}$$

$\mu_{a,i}^{m}$ is the liquid chemical potential of asphaltene i in the micellar core given by,

$$\mu_{a,i}^{m} = \Delta g_{a,i}^{as} + \mu_{a,i}^{0} + kT \ln z_{a,i}^{m} \tag{B.2}$$

where $\Delta g_{a,i}^{as}$ is the Gibbs free energy of asphaltene association.

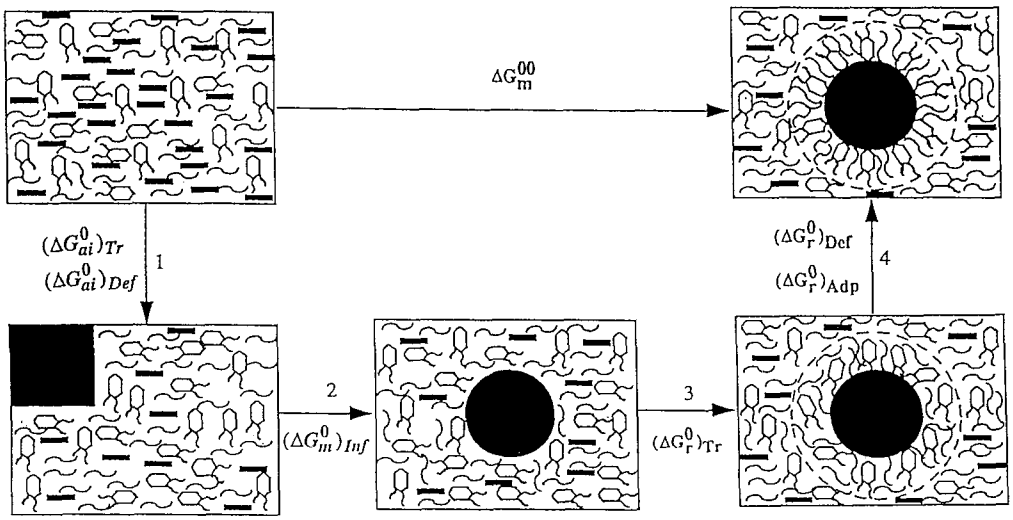


Fig. B.1 – Schematic representation of micelle formation. (Pan and Firoozabadi, 1998)

From $\mu_{1a,i} = \mu_{a,i}^0 + kT\,ln\,z_{a,i}\gamma_{1a,i}^{\infty} = \mu_{a,i}^{\Theta} + kT\,ln\,z_{a,i}$, where $\gamma_{1a,i}^{\infty}$ is the activity coefficient of asphaltene at infinite dilution with the pure liquid as the standard state,

$$\mu_{1a,i}^{\Theta} = \mu_{a,i}^0 + kT\,ln\,\gamma_{1a,i}^{\infty} \tag{B.3}$$

and from $\gamma_{1a,i}^{\infty} = P^{\infty}\varphi_{a,i}^{\infty} / f_{a,i}^0$ and $1 = P^{\infty}\varphi_{a,i}^{L} / f_{a,i}^0$ one can write,

$$\gamma_{1a,i}^{\infty} = \frac{\varphi_{a,i}^{\infty}}{\varphi_{a,i}^{L}} \tag{B.4}$$

Thus,

$$\Delta g_{a,i}^{tr} = \Delta g_{a,i}^{as} + kT\,ln\frac{\varphi_{a,i}^{L} z_{a,i}^{m}}{\varphi_{a,i}^{\infty}} \tag{B.5}$$

The Gibbs free energy of asphaltene deformation in the micellar core is positive, which prevents asphaltenes from infinite growth. According to Nagarajan and Ruckenstein (1991), it is approximately equal to,

$$\Delta g_{a,i}^{def} = \frac{kT}{2}\left[\frac{R^2}{m_{a,i}L_{oil}^2} + \frac{2m_{a,i}^{1/2}L_{oil}}{R} - 3\right] \tag{B.6}$$

where $m_{a,i}$ is the ratio of the molecular volumes of asphaltenes and asphalt-free oil species, and L_{oil} is the characteristic length of the asphalt-free oil (equal to $\sqrt[3]{v_{oil}}$).

Step # 2

An interface between asphaltene core and liquid is formed and the contribution of the interfacial free energy is positive and given by,

$$\Delta g_{a,i}^{int} = \sigma \; a \tag{B.7}$$

where a is the core area divided by the number of resin molecules in the shell, and σ is the interfacial tension described in a previous section.

Step # 3

Resin molecules transfer from the infinitely diluted solution to the shell region, then adsorb onto asphaltene core and deform inside the micellar shell. The Gibbs free energy of resin transfer is negative and is given by,

$$\Delta g_{r,j}^{tr} = \mu_{r,j}^{m} - \mu_{1r,j}^{\Theta} \tag{B.8}$$

$\mu_{r,j}^{m}$ is the liquid chemical potential of asphaltene j in the micellar shell given by,

$$\mu_{r,j}^{m} = \mu_{r,j}^{0} + kT\, ln\, z_{r,j}^{m} + kT\, ln\, \gamma_{1r,j}^{m} \tag{B.9}$$

Similar to previously, the chemical potential of liquid resin molecules at infinite dilution is,

$$\mu_{1r,j}^{\Theta} = \mu_{r,j}^{0} + kT\, ln\, \gamma_{1r,j}^{\infty} \tag{B.10}$$

and from $\gamma_{1r,j}^{\infty} = \varphi_{r,j}^{\infty} / \varphi_{r,j}^{L}$ and $\gamma_{1r,j}^{m} = \varphi_{r,j}^{m} / \varphi_{r,j}^{L}$ one can write,

$$\Delta g_{r,j}^{tr} = kT\, ln \frac{\varphi_{r,j}^{m} z_{r,j}^{m}}{\varphi_{r,j}^{\infty}} \tag{B.11}$$

Step # 4

Resins adsorb onto the asphaltene core, rearrange in the shell by deformation and steric repulsions. The Gibbs free energy change due to resin adsorption onto the core surface is negative and can be expressed as,

$$\Delta g_{r,j}^{ads} = \Delta h_{r,j}^{ads} - kT\,ln\left(1-\frac{a_{p,j}}{a}\right) - \sigma\, a_{o,j} \tag{B.12}$$

where $\Delta h_{r,j}^{ads}$ is the adsorption enthalpy of resins onto asphaltene core. The second term in the right-hand side is the adsorption entropy and the third term is the interfacial screening energy.

The Gibbs free energy of resin deformation in the micellar shell is positive and its expression is similar to that of asphaltenes Nagarajan and Ruckenstein (1991),

$$\Delta g_{r,j}^{def} = \frac{kT}{2}\left[\frac{D^2}{m_{r,j}L_{oil}^2} + \frac{2m_{r,j}^{1/2}L_{oil}}{D} - 3\right] \tag{B.13}$$

where $m_{r,j}$ is the ratio of the molecular volumes of resins and resin-free oil species.

In addition, a positive steric energy between additional resins is introduced for a better prediction of the onset of precipitation. The steric interaction may be due to the unfavorable entropy associated with compressing the additional resin chains between shell layer surfaces. In the limit of low surface coverage and assuming the average distance between micelles is approximately twice the micellar radius, the steric or overlap repulsion energy per molecule is expressed as $\Delta g_{r,2}^{ste} \approx 36kTe^{-2} \approx 4kT$ (Israelachvili, 1991). It is important to consider the steric energy between additional resins as it affects notably the onset of precipitation. Without the steric energy, the effect of additional resins on the onset of precipitation is overestimated.

Bibliography

Al-Sahhaf, T. A., A. F. Mohammed, and A. S. Elkilani, "Retardation of Asphaltene Precipitation by Addition of Toluene, Resins, Deasphalted Oil and Surfactants", *Fluid Phase Equilibria*, **194**, 1045 (2002).

Andersen, S. I., and J. G. Speight, "Thermodynamic Models for Asphaltene Solubility and Precipitation", *J. of Petrol. Sci. and Eng.*, **22**, 53 (1999).

Andersen, S. I., and J. G. Speight, "Petroleum Resins: Separation, and Role in Pertoleum", *Petroleum Science and Technology*, **19** (1&2), 1-34 (2001).

Annual Book of ASTM Standards, ASTM D2006, D3279, D893, D2007, D4124, *American Society for Testing and Material* (1970, 1978, 1980, 1991, 1991).

Atkins, P. W., *Physical Chemistry*, Oxford University Press, Oxford (1978).

Bardon, Ch.; L. Barre, D. Espinat, V. Guille, M. H. Li, J. Lambard, J. C. Ravey, E. Rosenberg, and T. Zemb, "The Colloidal Structure of Crude Oils and Suspensions of Asphaltenes and Resins", *Fuel Science & Technology International*, **14**, 1-2, 203 (1996).

Becker, H. L., "Asphaltene: To Treat or Not", SPE paper # 59703 presented at the 2000 SPE Permian Basin Oil and Gas Recovery Conference, Midland, TX, 21-23 March (2000).

Bitter, F., *Currents, Fields and Particles*, The Technology Press of Massachusetts Institute of Technology and John Wiley & Sons, Inc., NY (1956).

Boduszynski, M. M., "Composition of Heavy Petroleums. 2. Molecular Characterization", *Energy & Fuels*, **2**, 597 (1988).

Boduszynski, M. M., Private Communication, Chevron Technology Company, Richmond, CA (2000).

Born, M., and E. Wolf, *Principles of Optics*, Pergamon Press (1980).

Böttcher, C. J. F., *Theory of Electric Polarization*, Elsevier, Amsterdam (1952).

Buckley, J. S., G. J. Hirasaki, Y. Liu, S. Von Drasek, J-X. Wang, and B. S. Gill, "Asphaltene Precipitation and Solvent Properties on Crude Oils", *Petroleum Science and Technology Int.*, **16**, 3-4, 251 (1998).

Buenrostro-Gonzalez, E., H. Groenzin, C. Lira-Galeana, O. C. Mullins, "The Overriding Chemical Principles that Define Asphaltenes", *Energy and Fuels*, **15**, 4, 972 (2001).

Buenrostro-Gonzalez, E., A. Gil-Villegas, J. Wu, and C. Lira-Galeana, "Modelling of Asphaltene Precipitation using the SAFT-VR EOS Approach", *International Conference of Heavy Organic Depositions*, Puerto-Vallarta, Jalisco, Mexico, Nov. 17-21 (2002).

Burke, N. E., R. E. Hobbs, and S. F. Kashou, "Measurement and Modelling of Asphaltene Precipitation", *J. of Petrol. Technol.*, **42**, 1440 (1990).

Callen, R. B., J. G. Bendoraitis, C. A. Simpson, and S. E. Voltz, "Upgrading Coal Liquids to Gas Turbine Fuels 1. Analytical Characterization of Coal Liquids", *Ind. Eng. Chem. Prod. Res. Dev.*, **15**, 4, 223 (1976).

Carbognani, L., and Y. Espidel, "Characterization of Solid Deposits from Production Facilities- Identification of Possible Causes of Deposits Formation", Vision Tecnologica, 3, 1, 35 (1995).

Carbognani, L., M. Orea, and M. Fonseca, "Complex Nature of Separated Solid Phases from Crude Oils", *Energy and Fuels*, **13**, 351 (1999).

Carnahan, N. F.; J. L. Salager, R. Anton, and A. Davila, "Properties of Resins Extracted from Boscan Crude Oil and their Effect on the Stability of Asphaltenes in Boscan and Hamaca Crude Oils", *Energy & Fuels*, **13**, 2, 309 (1999).

Chang, C., and H. S. Fogler, "Stabilization of Asphaltenes in Aliphatic Solvents using Alkylbenzene-derived Amphiphiles. 1. Effect of the Chemical Structure of Amphiphiles on Asphaltene Stabilization", *Langmuir*, **10**, 6, 1753 (1994).

Chapman, W. G., G. Jackson, and K. E. Gubbins, "Phase Equilibria of Associating Fluids, Chain Molecules with Multiple Bonding Sites", *Mol. Phys.*, **65**, 1057 (1988).

Chapman, W. G., K. E. Gubbins, G. Jackson, and M. Radosz, "New Reference Equation of State for Associating Liquids", *Ind. Eng. Chem. Res.*, 29, 1790 (1990).

Chuang, T., and K. Eisenthal, "Theory of Fluorescence Depolarization by Anisotropic Rotational Diffusion", *J. of Chem. Physics*, **57**, 5094 (1972).

Chung, T-H, "Thermodynamic Modelling for Organic Solid Precipitation", *SPE* paper # 24851 (1992).

Cimino, R., S. Correra, P. A. Sacomani, and C. Carniani, "Thermodynamic Modelling for Prediction of Asphaltene Deposition in Live Oils", *SPE* paper # 24851 (1992).

Clarke, P. F., and B. B. Pruden, "Asphaltene Precipitation from Cold Lake and Athabasca Bitumens", *Petroleum Science and Technology*, **16**, 3-4, 287 (1998).

Debye, P., *Polar Molecules*, Dover Publications Inc., NY (1929).

De Hemptinne, J-C., A. Aubertin-Couvreur, I. Fondio, and D. Broseta, "Viscosity Prediction of Heavy Crudes in Hydrotreatment Conditions", Paper presented at the International Conference on Petroleum Phase Behavior and Fouling, Houston, March 14-18 (1999).

Dolphin, D., *The Porphyrins*, vol. 3, Academic Press, NY (1978).

Duda, Y., and C. Lira-Galeana, "Modelling Asphaltene Precipitation using Integral Equations. An Analytical Solution to the Associative Ornstein-Zernike Integral

Equation", *International Conference of Heavy Organic Depositions*, Puerto-Vallarta, Jalisco, Mexico, Nov. 17-21 (2002).

Durandeau, M., Private Communication, Total Elf Fina Research Center, Pau, France (1999).

Einstein, A., "Zur Theorie der Brownschen Bewegung", *Annalen der Physik*, **19**, 371 (1906).

Ese, M. -H., X. Yang, and J. Sjoblom, "Film Forming Properties of Asphaltenes and Resins. A Comparative Langmuir-Blodgett Study of Crude Oils from North Sea, European Continent and Venezuela", *Colloid Polymer Science*, **276**, 800 (1998).

Farcasiu, M., "Fractionation and Structural Characterization of Coal Liquids", *Fuel*, **56**, 9 (1977).

Feynman, R. P., R. B. Leighton, and M. Sands, *The Feynman Lectures on Physics*, Vol. 2, Addison-Wesley Publishing Company, Redwood City, CA (1964).

Firoozabadi, A., *Thermodynamics of Hydrocarbon Reservoirs*, McGraw-Hill, New York (1999).

Galindo, A., A. Gil-Villegas, and G. Jackson, "The Thermodynamics of Mixtures and the Corresponding Mixing Rules in the SAFT-VR Approach for Potentials of Variable Range", *Molecular Physics*, **93**, 1, 241 (1998).

Ghonasgi, D., and W. G. Chapman, "Theory and Simulation for Associating Hard Chain Fluids", *Mol. Phys.*, **83**, 145 (1994).

Gibbs, J. W., *The Scientific Papers of J. Willard Gibbs*, Dover, New York (1961).

Gil-Villegas, A., A. Galindo, P. J. Whitehead, S. J. Mills, G. Jackson, and A. N. Burgess, "Statistical Associating Fluid Theory for Chain Molecules with Attractive Potentials of Variable Range", *The J. of Chem. Phys.*, 106, 10, 4168 (1997).

Groenzin, H, *Resonant Fluorescence Quenching by CS_2 and Asphaltene Molecular Size and Structure Analysis by Fluorescence Anisotropy*, MSc. Thesis, Applied Optics, Rose- Hulman Institute of Technology, Boston (1999).

Groenzin, H., and O. C. Mullins, "Asphaltene Molecular Size and Structure", *J. Phys. Chem. A,* **103**, 11237 (1999).

Groenzin, H., and O. C. Mullins, "Molecular Size and Structure of Asphaltenes from Various Sources", *Energy and Fuels*, **14**, 677 (2000).

Guggenheim E. A., "The Computation of Electric Dipole Moments", *Trans. Faraday Soc.*, **47**, 573 (1951).

Gupta, A. K., *A Model for Asphaltene Flocculation using an Equation of State*, MSc Thesis, Department of Chemical and Petroleum Engineering, University of Calgary (1986).

Halverstadt, I. F., and W. D. Kumler, "Solvent Polarization Error and its Elimination in Calculating Dipole Moments', *J. Am. Chem. Soc.*, **64**, 2988 (1942).

Halvorsen, K., *Dipole Moments and Molecular Weights for Alkane Precipitated Solid Fractions for Some North-Sea Oils*, MSc Thesis, University of Bergen, Institute of Chemistry, Norway (1997).

Hammami, A., K. A. Ferworn, J. A. Nighswander, S. Overa, and E. Stange, "Asphaltenic Petroleum fluid Oil Characterization: An Experimental Investigation of the Effect of Resins on the Stability of Asphaltenes", *Petroleum Science and Technology*, **16**, 3-4, 227 (1998).

Helfand, E., and Y. Tagami, "Theory of the Interface between Immiscible Polymers", *J. Polymer Letters*, **9**, 741 (1971).

Hewlett Packard, *The Impedance Measurement Handbook: A guide to Measurement, Technology and Techniques*, Hewlett Packard, Hyogo- Japan (1999).

Hiemenz, P. C., *Principles of Colloid and Surface Chemistry*, Marcel Dekker Inc., New York (1986).

Hildebrand, J. H., and R. L. Scott, Regular Solutions, Prentice-Hall, Englewood Cliffs, New Jersey (1962).

Hirschberg, A., L. N. J. de Jong, B. A. Schipper, and J. G. Meijer, "Influence of Temperature and Pressure on Asphaltenes Flocculation", *SPE* paper # 11202 (1984).

Huron, M. J., and J. Vidal, "New Mixing Rules in Simple Equations of State for Representing Vapor-Liquid Equilibria of Strongly Non-Ideal Mixtures", *Fluid Phase Equilibria*, **3**, 255 (1977).

Huyskens, P. L., W. A. P. Luck, and T. Zeegers-Huyskens, *Intermolecular Forces: An Introduction to Modern Methods and Results*, Springer-Verlag, Berlin (1991).

Israelachvili, J. N., *Intermolecular and Surface Forces*, Academic Press, San Diego (1991).

Jhaveri, B. S., and G. K. Youngren, "Three-Parameter Modification of the Peng Robinson Equation of State to Improve Volumetric Predictions", *SPE* paper # 13118 (1988).

Kaminski, T. J., H. S. Fogler, and A. Mairal, "Classification of Asphaltenes via Fractionation and the Effect of Heteroatom Content on Dissolution Kinetics", Paper presented at the International Conference on Petroleum Phase Behavior and Fouling, Houston, March 14-18 (1999).

Kokal, S. L., J. Najman, S. G. Sayegh, and A. E. George, "Measurement and Correlation of Asphaltene Precipitation from Heavy Oils by Gas Injection", *J. of Can. Petrol. Technol.*, **31**, 24 (1992).

Kumler, W. D., "The Dipole Moment of ms-Tetraphenylporphirine", *J. Am. Chem. Soc.*, **64**, 2993 (1942).

Lee, L. L., *Molecular Thermodynamics of Nonideal Fluids*, Butterworth, Boston (1988).

LeFèvre, R. J. W., *Dipole Moments*, 2nd Edition, London (1948).

Leontaritis, K. J., and G. A. Mansoori, "Asphaltene Flocculation during Production and Processing: A Thermodynamic-Colloidal Model", *SPE* paper # 16258 (1987).

Leontaritis, K. J., A. G. Mansoori, "Asphaltene Deposition: A Survey of Field Experience and Research Approaches", *Journal of Petroleum Science & Engineering*, **1**, 229 (1988).

Li, S., C. Liu, G. Que, W. Liang, and Y. Zhu, "A Study of the Interactions Responsible for Colloidal Structures in Petroleum Residua", *Fuel*, **76**, 14/15, 1459 (1997).

Lian, H., J. R. Lin, and T. F. Yen, "Peptization Studies of Asphaltene and Solubility Parameter Spectra," *Fuel,* **73**, 423 (1994).

Liang, W., G. Que, Y. Chen, and C. Liu, "Chemical Composition and Characteristics of Residues of Chinese Crude Oils", in *Asphaltenes and Asphalts*, 2. Developments in Petroleum Science, 40B, Chapter 10, Edited by T. F. Yen, and G. V. Chilingarian, Elsevier (2000).

Lide, D. R., and H. P. R. Frederikse, *Handbook of Chemistry and Physics*, 81st Edition 2000-2001, CRC Press, Boca Raton, FL (2000).

MacMillan, D. J., J. E. Tackett, M. A. Jessee, and T. G. Monge-McClure, " A Unified Approach to Asphaltene Precipitation: Laboratory Measurement and Modelling", *J. of Petro. Technol.*, **47**, 788 (1995).

Maitland, G. C., M. Rigby, E. B. Smith, and W. A. Wakeham, *Intermolecular Forces: Their Origin and Determination*, Clarendon Press, Oxford (1981).

Maruska, H. P., and B. M. L Rao, "The Role of Polar Species in the Aggregation of Asphaltenes", *Fuel Science & Technology Int'L*, **5**, 2, 119 (1987).

Maxwell, J. C., *A Treatise on Electricity and Magnetism*, Oxford University Press, Vol. 2, Third edition, Dover Publications, New York (1954).

McClellan, A. L., *Tables of Experimental Dipole Moments*, Vol. 1, W.H Freeman and Company, San Francisco (1963).

McLean, J. D., and P. K. Kilpatrick, "Comparison of Precipitation and Extrography in the Fractionation of Crude Oil Residua", *Energy and Fuels*, **11**, 570 (1997).

Mitra-Kirtley, S., O. C. Mullins, J. Van Elp, S. J. George, J. Chen, and S. P. Cramer, "Determination of the Nitrogen Chemical Structures in Petroleum Asphaltenes using XANES Spectroscopy", *J. Am. Chem. Soc.*, **115**, 1, 252 (1993).

Moinelo, S. R., R. M. Menendez, and J. Bermejo, "Fractionation of Coal-derived Liquids by Extrography", *Fuel,* **67**, 682 (1988).

Monteagudo, J. E. P., P. L. C. Lage, and K. Rajakopal, "Towards a Polydisperse Thermodynamic Model for Asphaltene Precipitation in Live Oil", *Fluid Phase Equilibria*, **187**, 443 (2001).

Moschopedis, S. E., and J. G. Speight, "Investigation of Hydrogen Bonding by Oxygen Functions in Athabasca Bitumen", *Fuel*, **55**, 3, 187 (1976).

Murgich, J., "Intermolecular Forces in Aggregates of Asphaltenes and Resins", *Petroleum Science and Technology*, **20**, 9-10, 983 (2002).

Murzakov, R. M., S. A. Sabanenkov, and Z. I. Syunyaev, "Influence of Petroleum Resins on Colloidal Stability of Asphaltene-containing Disperse Systems", *Khim. Tekhnol. Topl. Masel.*, **10**, 40 (1981).

Nagarajan, R., and E. Ruckenstein, "Theory of Surfactant Self-Assembly. A Predictive Molecular Thermodynamic Approach", *Langmuir*, **7**, 12, 2934 (1991).

Nalwaya, V., V. Tangtayakom, P. Piumsomboon, and S. Fogler, "Studies on Asphaltenes through Analysis of Polar Fractions", *Ind. Eng. Chem. Res.*, **38**, 964 (1999).

Newberry, M. E., and K. M. Barker, "Organic Formation Damage Control and Remediation", SPE paper # 58723 presented at the 2000 SPE International Symposium on Formation Damage Control, Lafayette, Louisiana, 23-24 Feb (2000).

Nghiem, L. X., M. S. Hassam, R. Nutakki, and A. E. D. George, "Efficient Modelling of Asphaltene Precipitation", *SPE* paper # 26642 (1993).

Nghiem, L. X., B. F. Kohse, S. M. F. Ali, and Q. Doan, "Asphaltene Precipitation: Phase Behaviour Modelling and Compositional Simulation", *SPE* paper # 59432 (2000).

Nighswander, J. A., H. Kaira, and A. Majeed, "Effect of Low Molecular Weight Hydrocarbons on the Onset Concentration and Bulk Properties of Asphaltenes at in-Situ Temperature and Pressure Conditions", presented at the AIChE Spring National Meeting, March 28- April 1 (1993).

Ono, S., and S. Kondo, "Molecular Theory of Surface Tension in Liquids", *Encyclopedia of Physics*, vol. 10, edited by S. Flugge, Springer (1960).

Onsager, L., "Electric Moments of Molecules in Liquids", *J. Am. Chem. Soc.*, **58**, 1486 (1936).

Orbey, H., and S. I. Sandler, "Reformulation of Wong-Sandler Mixing Rule for Cubic Equations of State", *AIChE J.*, **41**, 3 (1995).

Oudin, J. L., "Analyse Géochimique de la Matière Organique Extraite des Roches Sédimentaires I. Composés Extractibles au Chloroforme", *Revue de l'Institut Français du Pétrole*, **25**, 1, 4 (1970).

Pan, H., and A., Firoozabadi, "Thermodynamic Micellization Model for Asphaltene Aggregation and Precipitation in Petroleum Fluids", *SPE Prod. & Facilities J.*, 118 (May 1998).

Pan, H., and A., Firoozabadi, "Thermodynamic Micellization Model for Asphaltene Precipitation from Reservoir Crudes at High Pressures and Temperatures", *SPE Prod. & Facilities*, **15**, 1, 58 (2000).

Park, S. J., and A. Mansoori, "Aggregation and Deposition of Heavy Organics in Petroleum Crudes", *Energy Resources*, **10**, 109 (1988).

Park, S. J., *A Thermodynamic Polydisperse Polymer Model: Asphaltene Flocculation, Aggregation, and Deposition*, Ph.D. dissertation, University of Illinois, Chicago (1989).

Pedersen, C., and S. I. Andersen, "Dielectric Properties of Asphaltenes and Oils", presented at the AIChE Spring National Meeting, Houson, TX, March 14-18 (1999).

Peneloux, A., E. Rauzy, and R. Freze, "A Consistent Correction for Redlich-Kwong-Soave Volumes", *Fluid Phase Equilibria*, **8**, 7 (1982).

Permsukarome, P., C. Chang, and H. S. Fogler, "Kinetic Study of Asphaltene Dissolution in Amphiphile/Alkane Solutions", *Industrial & Engineering Chemistry Research*, **36**, 9, 3960 (1997).

Perrin, F., "Polarisation de la Lumière de Fluorescence. Vie Moyenne des Molecules dans l'Etat Excite", *J. de Physique et le Radium*, **5**, 497 (1926).

Pfeiffer, J. Ph., and R. N. J. Saal, "Asphaltic bitumen as colloid system", *Journal of Physical Chemistry*, **44**, 139 (1940).

Poling, B. E., J. Prausnitz, and J. O'Connell, *The properties of Gases and Liquids*, 5th ed. McGraw-Hill, New York (2001).

Prausnitz, J. M., R. N. Lichtenthaler, and E. G. de Azevedo, *Molecular Thermodynamics of Fluid-Phase Equilibria*, Prentice-Hall, New Jersey (1999).

Prigogine, I., A. Bellmans, and V. Mathot, *The Molecular Theory of Solutions*, Amsterdam, Holland (1957).

Puvvada, S., and D. Blankenstein, "Theoretical and Experimental Investigations of Micellar Properties of Aqueous Solutions containing Binary Mixtures of Nonionic Surfactants", *J. Phys. Chem.*, **96**, 5579 (1992).

Ratajczak. H., and W. J. Orville-Thomas, *Molecular Interactions*, Vol. 1, John Wiley & Sons, Bath, UK (1980).

Riazi, M. R., and T. E. Daubert, "Improved Characterization of Wide Boiling Range Undefined Petroleum Fractions", *Ind.& Eng. Chem. Res.*, **26**, 3, 629 (1987).

Rogel, E., "Simulation of Interactions in Asphaltene Aggregates", *Energy & Fuels*, **14**, 566 (2000).

Rogel, E., O. Leon, J. Espidel, and Y. Gonzales, "Asphaltene Stability in Crude Oils", SPE paper 72050 presented at the SPE Production & Facilities Conference (2001).

Sandler, S. I., *Chemical and Engineering Thermodynamics*, John Wiley & Sons, New York (1999).

Schabron, J. F., and J. G. Speight, "Solubility and Three-Dimensional Structure of Asphaltenes", *Petroleum Science and Technology*, **16**, 3-4, 361 (1998).

Schwager, I., and T. F. Yen, "Coal Liquefaction Products from Major Demonstration Processes 1. Separation and Analysis", *Fuel,* **57**, 100 (1978).

Sen, A. D., V. G. Anicich, and T. Arakelian, "Dielectric Constant of Liquid Alkanes and Hydrocarbon Mixtures", *Journal of Physics D: Applied Physics*, **25**, 3, 516 (1992).

Sheu, E. Y. L., and O. C. Mullins, *Asphaltenes: Fundamentals and Applications*, Plenum Press, New York (1995).

Sihvola, A., Electromagnetic Mixing Formulas and Applications, IEE Electromagnetic Wave Series (1999).

Smyth, J.W., "Some Developments of Guggenheim's Simplified Procedure for Computing Electric Dipole Moments", *Trans. Faraday Soc.*, **46**, 394 (1950).

Smyth, C. P., *Dielectric Behavior and Structure*, McGraw-Hill, Amsterdam (1955).

Sorensen, T. S., in *Surfactants in Solution*, K. L., Mittal and B., Lindman, vol. 2, Plenum Press (1982).

Speight J. G., R. B. Long, and T. D. Trowbridge, "Factors Infiuencing the Separation of Asphaltenes from Heavy Petroleum Feedstocks", *Fuel,* **63**, 616 (1984).

Speight J. G., *The chemistry and Technology of Petroleum*, Marcel Dekker, New York (1999).

Standards for Petroleum and its Products, "IP 143: Asphaltenes Precipitation with Normal Heptane", *Institute of Petroleum*, London (1957).

Storm, D. A., S. J. DeCanio, M. M. DeTar, and V. P. Nero, "Upper Bound on Number Average Molecular Weight of Asphaltenes", *Fuel*, **69**, 735 (1990).

Storm D. A., and E. Y. Sheu, "Characterization of Asphaltenic Colloidal Particle in Heavy Oil", *Fuel*, **74**, 8, 1140 (1995).

Swanson, J. M., "A contribution to the Physical Chemistry of the Asphalts", *Journal of Physical Chemistry*, **46**, 141 (1942).

Syncrude Analytical Method for Oil Sand and Bitumen Processing, Edmonton, Syncrude Canada Ltd (1979).

Tao, T., "Time-dependent Fluorescence Depolarization and Brownian Rotational Diffusion Coefficients of Macromolecules". *Biopolymers*, **8**, 609 (1969).

Thomas, E. R., and C. A. Eckert, "Prediction of Limiting Activity Coefficients by a Modified Separation of Cohesive Energy Density Model and UNIFAC", *Ind. Eng. Chem. Process Des. Dev.*, **23**, 194 (1984).

Thomas, F. B., D. B. Bennion, D. W. Bennion, and B. E. Hunter, "Experimental and Theoretical Studies of Solids Precipitation from Reservoir Fluid", *J. Can. Petrol. Technol.*, **31**, 1, 22 (1992).

Tolman, R. C., "The Effect of Droplet Size on Surface Tension", *J. Chem. Phys.*, **17**, 119, 333 (1949).

Vakarin, F., M. F. Holovko, and Y. Duda, "Integral Equation Theory for the Four Bonding Sites Model for Associating Fluids. 2. Density Profiles and Adsorption onto a Solid Surface", *Molecular Physics*, **91**, 2, 203 (1997).

Waldo, G. S., O. C. Mullins, J. E. Penner-Hahn, and S. P. Cramer, "Determination of the Chemical Environment of Sulphur in Petroleum Asphaltenes by X-ray Absorption Spetroscopy", *Fuel*, 71, 53 (1992).

Wallace D., D. Henry, K. Pongar, and D. Zimmerman, "Evaluation of Some Open Column Chromatographic Methods for Separation of Bitumen Components", *Fuel,* **66**, 44 (1987).

Whitson, C. H., "Characterizing Hydroacarbon Plus Fractions", *SPE* paper # 12233 (1983).

Wong, D. S. H., and S. I. Sandler, "A Theoretically Correct Mixing Rule for Cubic Equations of State", *AIChE J.*, **38**, 5 (1992).

Wu, J., J. M. Prausnitz, and A. Firoozabadi, "Molecular-Thermodynamic Framework for Asphaltene-Oil Equilibria", *AIChE J.*, **44**, 5, 1188 (1998).

Wu, J., J. M. Prausnitz, and A. Firoozabadi, "Molecular Thermodynamics of Asphaltene Precipitation in Reservoir Fluids", *AIChE J.*, **46**, 1, 197 (2000).

Zajac, G. W., N. K. Sethi, and J. T. Joseph, "Molecular imaging of Petroleum Asphaltenes by Scanning-Tunneling-Microscopy- Verification of Structure from C13 and Proton Nuclear-Magnetic-Resonance Data", *Scanning Microscopy*, **8**, 3, 463 (1994).

Zhou, J. L., A. L. Tits, and C. T. Lawrence, User's Guide for FFSQP Version 3.7: A Fortran Code for Solving Optimization Programs, Possibly Minimax, with General Inequality Constraints and Linear Equality Constraints, Generating Feasible Iterates, Institute for Systems Research, University of Maryland, Technical Report SRC-TR-92-107r5, College Park, MD 20742 (1997).

Measuring Asphaltenes and Resins, and Dipole Moment in Petroleum Fluids

Lamia Goual
Earth Science and Engineering, Imperial College, London SW7 2BP, UK

Abbas Firoozabadi
Reservoir Engineering Research Institute, Palo Alto, CA 94306

A petroleum fluid can be divided into three types of species: asphaltenes, resins, and oils. Asphaltenes and resins are polar, while the rest of the so-called oils are either nonpolar or mildly polar. The interaction among these species strongly affect asphaltene precipitation from petroleum fluids. Different measuring methods for asphaltenes in a petroleum fluid give similar results, but different results for the resin content of a petroleum fluid. In addition to the amount affecting precipitation, the polarity of asphaltenes and resins affects precipitation strongly. The Onsager formulation of dipolar moments was used to measure the dipole moment of asphaltenes, resins and the oil species from eight different petroleum fluids from various parts of the world. The dipole moment, a measure of polarity, for resins was measured in this work for the first time. Results showed that resin separated from a petroleum fluid by propane is part of the total resin. Adsorption methods, however, give the total amount of resins. For a given petroleum fluid, asphaltenes had a higher dipole moment than resins. However, resins from one petroleum fluid can have a higher dipole moment than asphaltenes from another petroleum fluid.

Introduction

A large number of subsurface petroleum reservoirs from various parts of the world experience asphaltene precipitation in the subsurface formation, in the wellbore, in the well, and in the surface facilities and pipelines. Asphaltene precipitation is undesirable because it reduces well productivity and limits fluid flow. In some cases, asphaltene precipitation can result in complete plugging of flow lines. Paradoxically, the asphaltene precipitation is often observed in petroleum fluids that contain very low asphaltene content. A heavy petroleum fluid with an asphaltene content of say 20 wt % may not have precipitation problems. On the other hand, a light petroleum fluid with an asphaltene content of less than 0.2 wt % may precipitate asphaltene. Examples are the light petroleum fluid from the Hassi-Messaoud field in Algeria (44 API gravity) with an asphaltene content of 0.1 wt % that precipitates a considerable amount of deposit in tubings and surface facilities (Leontaritis and Mansoori, 1988). On the other hand, the heavy crude from Boscan in Venezuela (10 API gravity) containing approximately 17 wt % asphaltenes does not encounter asphaltene deposition (Leontaritis and Mansoori, 1988).

A petroleum fluid at atmospheric pressure and ambient temperature has three main constituents: (1) oils (that is, saturates and aromatics), (2) resins, and (3) asphaltenes. Oils are often nonpolar or are mildly polar (as we will see in this work). Asphaltenes and resins are polar and may associate to form micelles. In a petroleum fluid, asphaltenes and resins exist in the form of monomers, as well as in micelles (Pfeiffer and Saal, 1940; Swanson, 1942). In a micelle, the micellar core is formed from the self-association of asphaltene molecules, and resins adsorb onto the core surface to form the shell that also contains the oils (Firoozabadi, 1999). The properties and the amount of asphaltenes and resins affect the formation of micelles. One purpose of this work is to measure the properties that are believed to influence the micellar formation and precipitation. Another main objective is to find how to measure the amount of resins in a petroleum

Correspondence concerning this article should be addressed to A. Firoozabadi.

fluid. A petroleum fluid is a continuum of several thousands of molecules, and it is very difficult to define a cutoff between the asphaltene, the resin, and the oil fractions. Nevertheless, asphaltene molecules are believed to contain one or two aromatic chromophores (containing on average seven rings) with short aliphatic side-chains (Groenzin and Mullins, 2000). Resin molecules have a similar structure but smaller chromophores and relatively longer aliphatic side-chains, which increase their solubility in aliphatic solvents (Speight, 1999; Firoozabadi, 1999).

There is a wide range of methods for the measurement of the amount of asphaltenes and resins in petroleum fluids. The diversity of the methods is related to the operational definition of these fractions. Indeed, asphaltenes are defined as those hydrocarbons insoluble in an excess of *n*-pentane (or *n*-heptane). Resins remain soluble when petroleum fluid is mixed with *n*-pentane (or *n*-heptane) but can adsorb on surface-active materials such as fuller's earths, attapulgus clay, alumina, or silica gel (Speight, 1999). In addition, resins are insoluble in an excess of liquid propane, butane(s), and some other chemicals (such as acids, acetates, alcohols). Both asphaltenes and resins are represented by average properties such as average molecular weight and average dipole moment. In recent years, it has been demonstrated that the average molecular weight of asphaltenes and resins is less than 1,000 g/mol (Lian et al., 1994; Storm and Sheu, 1995; Groenzin and Mullins, 2000). There has been very little work on the measurement of asphaltenes and resins' dipole moment, despite their polar character. To the best of our knowledge, the dipole moment of resins has not yet been reported in the literature. The dipole moment depends on the structure and size of the molecule, and is a guide to the polarity generated by functional groups and metallic elements. The polarity of asphaltenes has often been related to heteroatom or metal content (Nalwaya et al., 1999; Kaminski et al., 1999). Swanson (1942) studied qualitatively the polarity of asphaltenes, resins, and oils by dielectric constant measurements in benzene solution at different frequencies. Asphaltenes were found to be highly polar while resins had intermediate polarity between asphaltenes and oils. Conversely, Ese et al. (1998) analyzed the adsorptive properties of asphaltenes and resins and concluded that resins were more polar than asphaltenes. Maruska and Rao (1987) investigated the dipole moment of asphaltenes and reported a value of 5.3 D (the symbol for debye) for a vacuum residue of a heavy crude. They used the Onsager theory (1936) to correlate the dipole moment of asphaltenes to the dielectric constant and refractive index. Because asphaltenes are solid, it was not possible to determine directly the dielectric constant by dielectric spectroscopy; instead, Maruska and Rao dissolved asphaltenes in dilute toluene solutions. At low asphaltene concentrations (< 10 wt %), the dielectric constant and refractive index were found to vary linearly with concentration. The linear variations were then extrapolated to 100 wt % concentration to estimate the properties of pure asphaltenes. Halvorsen (1997) measured the dipole moment of asphaltenes from several North Sea crudes precipitated by *n*-pentane. Dielectric constants were determined by dielectric spectroscopy (100 Hz to 15 MHz), and a loop system allowed the circulation of *p*-xylene solutions from the dielectric cell to the impedance meter. Halvorsen used the Debye theory (1929) to relate the dielectric constant to the dipole moment of asphaltenes and reported values ranging from 4 to 17 D. In this work, it will be demonstrated that the Debye theory may not provide reliable results. A study of the dielectric behavior of hydrocarbon mixtures by Sen et al. (1992) revealed that the Debye theory can be used for mixtures of nonpolar liquids (such as *n*-octane in *n*-hexane), while the Onsager theory can be used for mixtures of polar and nonpolar liquids (such as acetone in *n*-hexane).

The standard procedures for asphaltene measurement are similar and generate comparable results. The methods consist mainly of precipitation by *n*-alkanes (*n*-pentane or *n*-heptane). Although acids and heavy paraffins may coprecipitate with asphaltenes (Becker, 2000; Newberry and Barker, 2000), precipitation with *n*-alkanes is the main separation method of asphaltenes from petroleum fluids. In Institute of Petroleum Standard IP 143 (1957), asphaltenes are separated from petroleum fluids with *n*-heptane; the precipitated phase is then washed for one hour with a reflux of hot heptane to remove waxy constituents. In the ASTM D-3279 method (1978), asphaltenes from petroleum residues are precipitated with *n*-heptane and filtered after 30 min of heating and stirring with a reflux system. In the ASTM D-893 method (1980), asphaltenes are precipitated from lubricating oils by centrifugation in *n*-heptane. Finally, in the Syncrude analytical method (1979), crudes are mixed with benzene prior to asphaltene precipitation with *n*-pentane. After 2-h settling in the dark, they are filtered and washed.

There are two main methods for separation of resins from petroleum fluids: (1) precipitation, and (2) adsorption. The precipitation by liquid propane is inspired from refinery processes and has found application in the laboratory by Schwager and Yen (1978), Murzakov et al. (1981), and others. Other precipitation methods using chemicals have also been proposed. In the standard ASTM D-2006 procedure (1970), resins are separated from rubber extender and processing oils by precipitation in sulfuric acid. A method prevalent in Germany applied by the German Petroleum Institute advocates the precipitation of asphalt (that is, asphaltenes and resins) from petroleum fluids with ethyl acetate and solubilization of resins from the precipitate with *n*-pentane (Andersen and Speight, 2001). The adsorption methods have been extensively used and consist of adsorbing resins on surface-active materials. The oils are eluted (that is, washed away from the column) with a nonpolar solvent, and the resins remain on the adsorbent until desorbed by a polar solvent. Following this separation scheme, a series of standard procedures have been established. The Syncrude analytical method (1979) separates resins by adsorption on attapulgus clay; oils are eluted with *n*-pentane and resins are desorbed by successive elution with methyl-ethyl-ketone and tetrahydrofuran/water (95/5 vol/vol). ASTM D-2007 (1991a) uses the same adsorbent and eluting solvent for oils, but a mixture of toluene and acetone (50/50 vol/vol) to desorb resins. In ASTM D-4124 (1991b), resins are adsorbed on activated alumina, and oils are eluted with *n*-heptane and toluene (33/67 vol/vol); a mixture of toluene–methanol–trichloroethylene (17/17/66 vol/vol/vol) recovers resins. In all the preceding methods, oils are eluted by the *n*-alkane used to precipitate asphaltenes. The separation is time-consuming and it is sometimes found that heavy aromatics are eluted with resins due

to a high retention time in the column. This has oriented some to introduce a certain amount of aromatic solvent with n-alkanes to elute the oils. Callen et al. (1976) used 6 vol % dichloromethane in n-hexane, Farcasiu (1979) used 15 vol % toluene in n-heptane, Moinelo et al. (1988) used 36 vol % benzene in n-hexane, and more recently, McLean and Kilpatrick (1997) used 32 vol % toluene in n-heptane.

Resins recovered by precipitation or adsorption show marked differences in the amount and chemical composition. Even within adsorption methods, discrepancies can be found if adsorbents are different or elution time is varied (Wallace et al., 1987). Currently, resins are defined according to the solvents used for their separation. Considerable effort has been dedicated to the selection of appropriate polar solvents to desorb resins from surface-active materials, with less effort to the choice of nonpolar solvents to elute oils. The principle of resin separation by adsorption assumes that the nonpolar solvent should not dissolve any resin. Yet, aromatic solvents such as toluene or benzene are very good solvents for resins and their use may cause unreliablity for resin separation.

In this work, resins are separated by both precipitation and adsorption. In the adsorption method, different n-C_5/toluene volume ratios are used to recover oils in order to accelerate the separation and to ensure that heavy aromatics are washed from the column with oils. Because toluene can elute some resin constituents with oils, we would study the n-C_5/toluene volume ratio that separates oils by preserving all the constituents of resins in the resin fraction. This is possible by measuring the dipole moment of resins recovered in each test.

With the preceding background, the main objectives of this work are: (1) to devise a simple method for proper measurement and separation of resins in crudes, and (2) to determine the dipole moment of asphaltenes and resins. In the first part, we measure the resin content using a precipitation method with liquid propane and an adsorption method according to the modified ASTM D-2007 (1991a) procedure with different mixtures of n-pentane/toluene to elute the oils. Simplicity, scale, and practicality are considered when choosing the methods. In the second part, the theory of dipole moment is briefly reviewed and various methods are compared using chemicals with a known dipole moment. The appropriate method is selected and applied for measuring the dipole moment of asphaltenes and resins. The determination of asphaltene and resin dipole moments is important in that it allows the selection of a definitive procedure for resin measurement in crudes and provides a valuable database for studying the effect of resins on precipitation and the modeling of asphaltene–asphaltene and asphaltene–resin interactions. In a future publication, the effect of resins with different dipole moments and surfactants on asphaltene precipitation will be presented for different petroleum fluids.

Experimental

We use eight different petroleum fluids with API gravities in the range of 10 to 56 (see Table 1). Two of the petroleum fluids are from two different wells in the Hamaca field in Venezuela. The other petroleum fluids are from various parts of the world. Detailed composition of three crudes at ambient conditions is available in Table 2. In this work, asphaltenes are first precipitated from the petroleum fluids using n-C_5, n-C_7, and n-C_{10}, then resins are separated from the n-C_5 deasphaltened crude by: (1) precipitation with liquid propane, and (2) modified ASTM D-2007 (1991a) adsorption procedure. In the adsorption method, the oils are eluted with five different n-C_5/toluene volume ratios.

Table 1. Crude Data

Crude	Density at 20°C (g/cm^3)	API Gravity at 20°C	Refractive Index at 20°C	Description
H	1.0089	9	—	Very heavy
TE	0.9990	10	—	Very heavy
C	0.8588	33	1.487	Medium
TA	0.8372	37	1.479	Medium
TK	0.8520	35	1.488	Medium
S	0.8627	32	1.472	Medium
U	0.8550	34	1.491	Medium
B	0.7554	56	1.431	Very light

— ≡ not measured.

The dipole moment determination is made by measuring the dielectric constant, refractive index, and density of dilute solutions of asphaltenes, resins, and oils in toluene. The procedure is similar to Maruska and Rao's (1987); however, we use lower concentrations of polar solutes to allow a visual reading of the refractive index and to reduce the effect of association.

There has been a debate if n-C_5 asphaltenes are less polar than n-C_7 asphaltenes or vice versa (Speight, 1999). We separate the asphaltenes with both n-alkanes to clarify the issue of polarity by measuring the dipole moment. Furthermore, in the adsorption method, we opt to work with n-C_5 deasphaltened crudes instead of n-C_7 deasphaltened crudes, because

Table 2. Composition of Selected Crudes at Ambient Conditions

	Crude					
	C		TK		U	
Fraction	Comp. mol %	M g/mol	Comp. mol %	M g/mol	Comp. mol %	M g/mol
C_1	0.00	0.00	0.00	0.00	0.00	0.00
C_2	0.00	0.00	0.01	30.1	0.04	30.1
C_3	0.00	0.00	0.15	44.1	0.73	44.1
C_4	0.82	58.1	0.85	58.1	4.15	58.1
C_5	2.12	72.1	2.48	72.1	6.00	72.1
C_6	3.84	86.2	4.91	85.8	8.33	85.8
C_7	5.18	100.2	8.39	95.8	80.75*	—
C_8	7.32	114.2	11.14	108.5		
C_9	6.58	128.3	10.29	123.2		
C_{10}	6.11	142.3	7.83	137.8		
C_{11}	5.77	156.3	5.67	148.3		
C_{12}	4.99	170.3	4.38	154.4		
C_{13}	5.17	184.4	4.46	172.4		
C_{14}	4.81	198.4	3.79	187.9		
C_{15}	4.61	212.4	3.59	197.2		
C_{16}	3.72	226.4	3.02	210.1		
C_{17}	3.63	240.5	2.69	227.1		
C_{18}	3.48	254.5	2.62	240.9		
C_{19}	2.72	268.5	2.42	254.2		
C_{20+}	29.13	433.6	21.31	441.2		
Total	100.00	242.0	100.00	206.1	100.00	—

* ≡ C_{7+}
— ≡ not available

the latter would leave the C_5–C_7 fraction of asphaltenes soluble with resins.

All chemicals are reagent grade except propane (commercial grade). Once fractions are recovered, the solvent is evaporated under low vacuum. The fractions are then dried and weighed (within 0.01 g accuracy) using an analytical balance.

Asphaltene precipitation

From the examination of the various asphaltene precipitation methods and the identification of optimum separation conditions (Speight et al., 1984), we select the Syncrude analytical method (1979) with some modifications. The precipitation sequence includes mixing the crude with toluene (10 mL/g asphaltene in the crude) followed by an addition of n-C_5 (50 mL/mL toluene). The settling time is set to 12 h to allow complete precipitation. Asphaltenes are filtered under a vacuum using a Whatman glass microfibre filter paper (7 mm diameter and 1.5 μm pore size). The sequence is repeated several times to remove resins adsorbed onto asphaltenes until the liquid filtrate is colorless.

Apparatus. The experimental setup consists of a filtration flask and funnel connected to a vacuum pump through rubber tubings. To avoid solvent infiltration into the pump, a trap is used at a temperature of -60°C to liquefy pentane from vapor.

Resin adsorption. Once asphaltenes are removed, resins are separated from the deasphaltened oil using the ASTM D-2007 (1991a) method with some modifications. The deasphaltened crude is charged into an adsorption column containing attapulgus clay immersed in n-pentane. We use the following n-C_5/toluene volume ratios: 100/0, 85/15, 70/13, 50/50, and 0/100 to elute the oils. The elution continues until the yellow coloration of the liquid leaving the column reduces appreciably (the yellow coloration is attributed to aromatic hydrocarbons in oils). The column is then drained from solvent and resins are desorbed using a 40/40/20 volume mixture of toluene–acetone–methylene chloride.

Apparatus. The adsorption column (300 mm height × 44 mm diameter) is made of glass and contains attapulgus clay (250–500 μm pore size) with a sample/clay ratio of approximately 1/20 (wt/wt). The high quality of the clay (azobenzene equivalence value of 30–35) assures good selectivity and reproducibility of the tests.

Resin precipitation

We use a high-pressure cylinder with a piston connected to a high-pressure filter holder at one side, and a water pump at the other side. The filter holder contains a Whatman glass microfibre (4.7 mm diameter and 0.8 μm pore size) filter paper. Liquid propane from a 1-gal high-pressure bottle is charged at a low temperature (-5 to 0°C) into the cylinder containing the deasphaltened oil sample, with a sample propane ratio of 1/20 (wt/wt). The pressure in the cylinder is increased to 1400 psi and the mixture is left for 4–6 h at room temperature. A piston is then used to push the mixture through the filter. The resins are recovered from the filter as well as the cylinder walls by washing with toluene.

Apparatus. The cylinder used is made of stainless steel (400 mm long × 20 mm ID) and can stand a maximum pressure of 680 atm. Stainless steal tubings (1/16-in. ID) are used for connections to the water pump (max pressure 272 atm) and to the high-pressure filter holder. Ball valves (max pressure 136 atm) and needle valves (max pressure 408 atm) control the flow rate. The pressure of water pumped into the cylinder is read from a pressure gauge (max pressure 272 atm). The filter holder (stainless steel, 47 mm size) is designed to stand pressures up to 95 atm.

Dielectric constant

In a class of substances called insulators or dielectrics, the electrons move a very small distance from the nucleus when the substance is subjected to an electric field. The dielectric constant of a dielectric substance is a measure of chemical composition and density (Feynman, 1964). When a condenser containing a dielectric substance is subjected to an electric field, the dielectric constant is given by $\epsilon_r = C/C_0$, where C and C_0 are the capacitance of the condenser filled with the dielectric and air, respectively. In this work, a liquid test fixture is used as a condenser. The determination of capacitance is performed through impedance measurements (Hewlett-Packard, 1999). The electronic circuit makes up the liquid fixture connected to an *LCR* meter that measures the inductance L, the capacitance C, and the resistance R of the circuit. The choice of the equipment is driven by the frequency coverage, measurement range, accuracy, and ease of operation.

Apparatus. We use a precision *LCR* meter (HP 4284A) (20 Hz to 1 MHz frequency range) connected to a liquid test fixture (HP16452A) through 1-m long test leads (HP 16048A). The capacity of the liquid test fixture is 3.4 mL. For accurate reading of capacitance, the equipment is calibrated to account for lead capacitance. Measurements are performed at a frequency of 800 Hz and a voltage level of 1 V.

Refractive index

For a nonabsorbing medium, the refractive index is the ratio of the velocity of light in the vacuum to the velocity of light in the medium (Bitter, 1956). In the visible range of frequencies, measurements of the refractive index of the sodium D-line of light are possible using a refractometer. The effective speed of light is different in different materials, and on this basis, the refractive index depends on the nature of the material (Feynman, 1964).

Apparatus. We used an Abbe C-10 refractometer to measure the refractive index of liquid mixtures to be described later. A built-in thermometer allows the reading of the temperature. The refractive index range covered is 1.300 to 1.700, with an accuracy of 0.0003. Calibration is performed with naphthalene bromide, which has a refractive index of 1.656 at 25°C.

Density

The density of a substance is its mass per unit volume. The density is usually measured using pycnometers; however, digital density-meters, when available, provide more accurate data. In this work, density is measured using two types of pycnometers with a fixed volume. Density and refractive index are temperature-dependant. Density at a given tempera-

ture can be estimated from measurements at another temperature using the correlations of Van Ness and Van Westen (1951).

Apparatus. The density is measured using a weld-type pycnometer devised for the specific gravity of volatile liquids with an accuracy of 0.001 g/cm^3. The pycnometer made of borosilicate glass, has a capacity of 25 mL and is equipped with a glass stopper and a cap to reduce evaporation of the sample. The density of oils is measured with a Moore-Van Slyke specific-gravity bottle with ground-in stopper. The bottles made of borosilicate glass have a capacity of 2 mL.

Theory of Dipole Moment of Molecules

In a dipolar molecule, the center of negative charges (say electrons) and the center of positive charges (say protons) do not coincide. In such molecules, the charge multiplied by the separation between the centers is called dipole moment (Feynman, 1964). Large molecules containing heteroatoms such as *ms*-tetraphenylporphine do not necessarily possess a dipole moment when they have a symmetrical structure (Kumler, 1942). For nonsymmetrical molecules, the dipole moment is the vector (directed from the negative to the positive charge) that tends to orient a molecule in a polarized dielectric. The dipole moment is generally given in debye (1 D = 3.338×10^{-30} C·m); it is given by

$$\mu = \sum_i e_i r_i \tag{1}$$

where i refers to the number of atoms in the molecules, e_i is the charge of an atom in the molecule, and r_i is the distance vector between charges. The charge distribution creates an electric field that tends to line up the individual dipoles to produce a net moment per unit volume called electric polarization. The electric polarization, P, is given by

$$P = N\mu \tag{2}$$

where N is the number of molecules per unit volume.

One can study the behavior of dielectrics in a condenser to estimate the electric properties. Dielectrics, such as crude oils are insulators; such materials do not conduct electricity, but when placed in a small electric field, molecules become polarized. When an electric field is applied, the charges that build on the plates of the condenser are two types: free charges, and polarization charges (of the opposite sign) due to polarization; the net charge on the plates will be the difference between the two. The charge density due to polarization is equal to the electric polarization inside the dielectric (Feynman, 1964). The dielectric constant is a characteristic of the dielectric, and is given by

$$\epsilon_r = \frac{\epsilon}{\epsilon_0} \tag{3}$$

where ϵ is the permittivity of the dielectric and ϵ_0 is the permittivity of the vacuum (equals 854×10^{-12} C^2/J/m or $1.11\times10^{-10}/4\pi$, F/m). The dielectric constant depends on

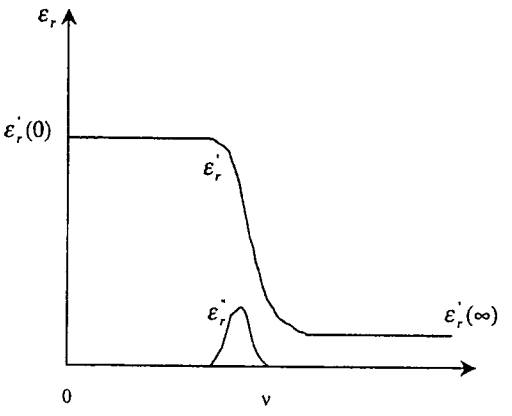


Figure 1. Dielectric constant vs. frequency.

the frequency ν and is written in the complex space as

$$\epsilon_r(\nu) = \epsilon_r'(\nu) - i\epsilon_r''(\nu) \tag{4a}$$

$$\epsilon_r(\nu) = \begin{cases} \epsilon_r'(0) & \text{at radio } \nu \quad (4b) \\ \epsilon_r'(\infty) = n^2 & \text{at visible } \nu \quad (4c) \end{cases}$$

where ϵ_r' and ϵ_r'' are the dielectric storage and loss, respectively (see Figure 1). The dielectric storage is the amount of polarization created at a given frequency and helps to determine the nature of the constituent material. The dielectric loss represents the energy of molecules dissipated or lost as heat; it is used to estimate the penetration of the sensing wave into the material (Sen et al., 1992; Pedersen et al., 1999). At radio frequency, the dielectric constant equals the dielectric storage at zero frequency; it is also called static dielectric constant $\epsilon_r'(0)$. At visible frequency, the dielectric constant is approximated by the dielectric storage at infinite frequency $\epsilon_r'(\infty)$; it is equal to the square root of the refractive index n of the sodium D-line of light (Maxwell, 1954).

Using fundamental electrostatic equations, one can readily derive the following expression that relates electric polarization to electric field E

$$P = \frac{(\epsilon_r - 1)}{4\pi} E \tag{5}$$

The dipole moment cannot be measured directly. Several theories exist to relate the dipole moment to macroscopic measurable quantities, such as dielectric constant, refractive index, and density. The first theory from Clausius and Mosotti (Böttcher, 1952) is applicable to nonpolar molecules. Debye (1929) extended the formulation of Clausius and Mosotti to polar gases and liquid solutions. Later, Onsager (1936) advanced the original Clausius and Mosotti theory for polar molecules and proposed a new formulation. In the following, we present a brief review of these theories.

Clausius and Mosotti theory

Clausius and Mosotti used the notion of an internal field to relate the dielectric constant of a nonpolar spherical molecule to the density (Böttcher, 1952; Born and Wolf,

1980). While the electric field is the mean field obtained by averaging over a region that contains a large number of molecules, the internal (or effective) field acts on the molecule itself. The difference between the two fields is due to the gaps between molecules (Born and Wolf, 1980). To estimate the internal field, each molecule is considered to be surrounded by a small sphere. For nonpolar molecules, molecules inside the sphere do not produce any resulting field at the central molecule, and one can regard the molecule as being situated in a spherical region, inside which there is a vacuum and outside there is a homogeneously polarized medium. The internal field is derived by assuming that the field at the spherical hole is equal to the difference between the field at any point in the dielectric and the field due to a spherical plug. The expression for the internal field F is given by

$$F = E + \frac{4\pi}{3}P \tag{6}$$

In vacuum, the internal field equals the electric field, but in other materials, it is higher. Clausius and Mosotti assumed that the electric dipole moment induced in a molecule is proportional to the internal field

$$\mu_{\text{ind}} = \alpha F \tag{7}$$

where α is the polarizability of the molecule, a macroscopic quantity that has the unit of volume (Smyth, 1955). The polarizability is a measure of the strength with which protons in the nucleus attract the electrons and prevent their distortion by the applied field. This parameter increases with increasing the atomic number, atomic size, and the ease of excitation of atoms in the molecules (Atkins, 1978). When N molecules are contained in a unit volume, one can write

$$\frac{4\pi a^3}{3}N = 1 \tag{8}$$

where a is the radius of the spherical molecules. Combining Eqs. 2, 5, 6 and 7

$$\frac{\epsilon_r - 1}{\epsilon_r + 2} = \frac{4\pi}{3}N\alpha \tag{9}$$

Equation 9 is the general expression of Clausius and Mosotti. Combining Eqs. 4c, 8 and 9

$$\alpha = \frac{n^2 - 1}{n^2 + 2}a^3 \tag{10}$$

The polarizability (also dipole moment) can have two contributions, depending on the nature of the molecule and the frequency of excitation: (1) permanent (orientation), and (2) induced. Polar molecules experience both contributions at very low frequencies (such as radio frequencies), while nonpolar molecules experience only the induced one. The induced contribution is the result of two parts: (1) atomic (or distortion), and (2) electronic effects. The former is associated with the molecular vibrations and the latter results from the displacement of the electron cloud by the field in the visible–ultraviolet frequency domain. The atomic polarizability is not readily determined and can be neglected on the grounds that it is small or is partially compensated by the use of the refractive index of the sodium D-line of light to estimate the electronic polarizability (or dipole moment).

Limitations. The Clausius and Mosotti equation applies to gases at moderate pressures, but deviations may occur at high pressures when the polarizability of molecules is large. There may also be some deviations for liquids, especially for mixtures (Böttcher, 1952).

Debye theory

Debye (1929) borrowed the oldest model of conductive spheres proposed by Clausius and Mosotti. He made the implicit assumption that the average permanent dipole moment of a molecule is proportional to the internal field. In the absence of external forces, the moments of a number of molecules will, on average, be distributed with the same probability over all directions in space. Therefore, when we consider a small solid angle at a given orientation, the average dipole moment is, according to Debye, equal to the total dipole moment divided by the number of molecules in the direction confined within the solid angle. Debye used the Boltzmann–Maxwell distribution law to calculate the small variations of the number of molecules confined within the solid angle. The final expression of the average dipole moment found is

$$\mu = \left(\alpha + \frac{\mu^2}{3kT}\right)F \tag{11}$$

where F is the magnitude of the internal field vector. Combining Eqs. 2, 5, 6, 8, 10 and 11 gives the Debye equation

$$\frac{\epsilon_r - 1}{\epsilon_r + 2} = \frac{n^2 - 1}{n^2 + 2} + \frac{4\pi N}{9kT}\mu^2 \tag{12}$$

It is more convenient to work with molar polarization P_M because of its additivity in mixtures (Debye, 1929; Böttcher, 1952; and Smyth, 1955). The molar polarization is defined by

$$P_M = \frac{\epsilon_r - 1}{\epsilon_r + 2}\frac{M}{\rho} \tag{13}$$

From the expression of the number of molecules per unit volume

$$N = \frac{N_A \rho}{M} \tag{14}$$

Combining Eqs. 12, 13 and 14, one can write

$$P_M = \frac{n^2 - 1}{n^2 + 2}\frac{M}{\rho} + \frac{4\pi N_A}{9kT}\mu^2 \tag{15}$$

The first term on the righthand side of Eq. 15 is the induced molar polarization, and the second term is the orientation molar polarization. Therefore

$$P_M = P_{\text{ind}} + P_\mu \tag{16}$$

Limitations. At moderate pressures, the dielectric constant of a gas conforms accurately to the Debye equation. The dipole moment is generally determined from temperature variation. The procedure consists of plotting the molar polarization against $1/T$ and deducing the dipole moment from the slope of the straight line. For polar liquids, the dipole moment is usually overestimated and the theory does not hold. Several authors claimed that the limitations of the Debye equation are due to association between polar molecules (Böttcher, 1952). To overcome this deficiency, it was suggested one work with a very dilute solution of polar solutes in a nonpolar solvent. A series of differentiation techniques was proposed to measure the dipole moment of polar liquid solutions.

Differentiation Methods. The Debye theory was recast according to the modifications introduced by various authors. We retain only the methods in which the electronic molar polarization of the polar molecule is not required. The selected methods are those proposed by Cohen-Henriquez (Böttcher, 1952), LeFèvre (1948), Smyth (1950), and Guggenheim (1951). Measurements are performed with dilute solutions of a polar solute (species 1) in a nonpolar solvent (species 2). The methods consider the additivity of molar polarization and molecular weight, and assume linear variations of the dielectric constant, refractive index (and density in some cases) with the mole or weight fraction of the solute, as shown in Table 3. The authors listed in Table 3 expressed the difference between the molar polarization at a low frequency and at visible frequency in order to eliminate the solvent and the electronic polarization of the solute. The expression obtained is then differentiated with respect to mole (or weight) fraction of the solute at very low concentrations; the expressions of the orientation molar polarization of the solute are obtained (see Table 3). The equation of Smyth is similar to the one by LeFèvre, except that the density term is neglected. Guggenheim further simplified Smyth's equation by assuming that the dielectric constant of the solvent is approximately equal to the square of its refractive index. Böttcher found that the last three methods give similar results (1951). We select the Guggenheim version for its simplicity. We also select the Cohen-Henriquez equation and compare it with the one by Guggenheim.

Onsager theory

Because the internal field depends on the orientation, Onsager (1936) proposed to compute the orienting force-couple for each individual direction of the dipole. Onsager considered the original Clausius and Mosotti theory of the internal field not applicable to permanent dipoles. In his work, the total dipole moment is the vector sum of the permanent and the induced dipole moments

$$\boldsymbol{m} = \mu \boldsymbol{u} + \alpha \boldsymbol{F} \tag{17}$$

where μ is the permanent dipole moment in vacuum (which rotates around a mean orientation) and $\boldsymbol{u}$ is the unit vector in the direction of the dipole axis. In addition, the internal field is the sum of a cavity field and a reaction field

$$\boldsymbol{F} = \boldsymbol{G} + \boldsymbol{R} \tag{18}$$

where $\boldsymbol{G}$ is the cavity field and $\boldsymbol{R}$ is the reaction field. The reaction field is parallel to the average dipole moment and it is only the cavity field that contributes to the orientation of the polar molecule. Onsager solved the electrostatic problem by combining the results of a dipolar molecule in a nonpolarized dielectric with those of a spherical cavity in a polarized dielectric. The internal field is then expressed as [detailed derivations are provided by Onsager (1936)]

$$\boldsymbol{F} = \left(1 + \frac{n^2(\epsilon_r - 1)}{2\epsilon_r + n^2}\right)\boldsymbol{E} + \frac{\mu}{a^3}\frac{2(\epsilon_r - 1)}{2\epsilon_r + 1}\frac{(n^2+2)(2\epsilon_r+1)}{3(2\epsilon_r + n^2)}\boldsymbol{u} \tag{19}$$

Table 3. Differentiation Methods of Debye Equation for Binary Mixtures of Polar Solute (species 2) in Nonpolar Solvent (species 1)

Author	Assumptions	Orientation Molar Polarization	Eq.
Cohen-Henriquez	$\epsilon_r = ax_2 + \epsilon_{r_1}$	$P_{\mu_2} = \dfrac{3M_1}{\rho_1(n_1^2+2)^2}(a - 2n_1c)$ $n = cx_2 + n_1$	(T1)
LeFèvre	$\epsilon_r = \epsilon_{r_1}(aw_2 + 1)$	$P_{\mu_2} = \dfrac{3M_2}{\rho_1}\left(\dfrac{(1-b)(\epsilon_{r_1} - n_1^2)}{(\epsilon_{r_1}+2)(n_1^2+2)} + \dfrac{a\epsilon_{r_1}}{(\epsilon_{r_1}+2)^2} - \dfrac{cn_1^2}{(n_1^2+2)^2}\right)$ $\rho = \rho_1(bw_2 + 1)$ $n^2 = n_1^2(cw_2 + 1)$	(T2)
Smyth	$\epsilon_r = \epsilon_{r_1}(aw_2 + 1)$	$P_{\mu_2} = \dfrac{3M_2}{\rho_1}\left(\dfrac{a\epsilon_{r_1}}{(\epsilon_{r_1}+2)^2} - \dfrac{cn_1^2}{(n_1^2+2)^2}\right)$ $n^2 = n_1^2(cw_2 + 1)$	(T3)
Guggenheim	$\epsilon_{r_1} \approx n_1^2$	$P_{\mu_2} = \dfrac{3M_2}{\rho_1}\dfrac{\epsilon_{r_1}}{(\epsilon_{r_1}+2)^2}(a - c)$ $\epsilon_r = \epsilon_{r_1}(aw_2 + 1)$	(T4)

Table 4. Asphaltenes Precipitated by n-C_5, n-C_7, and n-C_{10} from Crudes

Precipitant	Crude (wt %)							
	H	TE	C	TA	TK	S	U	B
n-C_5	17.7	14.8	2.3	0.18	1.33	1.1	2.5	0.05
n-C_7	13.5	11.9	1.52	0.10	0.46	0.77	—	0.04
n-C_{10}	13.0	11.2	1.42	0.05	0.26	0.63	—	0.03

— ≡ not measured.

Equations 6 and 19 are identical for nonpolar molecules (for which $\mu = 0$ and $\epsilon_r = n^2$). Unlike the induced dipole moment, the permanent dipole moment depends on the orientation of the molecule and its average value is equal to the actual dipole moment times the mean orientation of the molecule. The mean orientation is determined from the Boltzmann–Maxwell formula using the work of orientation. The expression derived by Onsager is then introduced into Eqs. 17–19 to give the Onsager equation

$$\frac{\epsilon_r - 1}{\epsilon_r + 2} = \frac{n^2 - 1}{n^2 + 2} + \frac{4\pi N}{9kT}\left(\frac{3\epsilon_r(n^2+2)}{(2\epsilon_r + n^2)(\epsilon_r + 2)}\mu^2\right) \quad (20)$$

Equations 12 and 20 are identical for $\epsilon_r = n^2$. Therefore, the Onsager and Debye equations give similar results for nonpolar molecules. However, for polar molecules ($\epsilon_r > n^2$), the dipole moments calculated from Debye and Onsager equations are different.

Limitations. The formulation of Onsager is limited to spherical molecules in liquid systems. In addition, the neighborhood of a molecule is considered to be a continuum.

Results

The results are presented in three different parts. In the first part, the amount of asphaltenes precipitated with n-alkanes (n-C_5, n-C_7, and n-C_{10}) and resins separated by propane precipitation and the ASTM D2007 (1991a) adsorption method with different solvents are presented. In the second part, we provide the results of the dipole moment calculation from the Debye and Onsager methods for several chemicals with known dipole moments from the literature. We select the Onsager method and in the third part present the dipole moment of the asphaltenes, resins, and oils.

Asphaltene and resin amounts

Table 4 provides the results of asphaltene precipitation with n-C_5, n-C_7, and n-C_{10} from the eight petroleum fluids (from here on, we refer to petroleum fluids as crudes). The amount of n-C_5 asphaltenes varies from 0.05 wt % in crude B to 17.7 wt % in crude H and decreases with the carbon number of the precipitating n-alkane. In Table 5 we present the results of asphaltene and resin (that is, asphalt) precipitation by propane. When propane is mixed with the crude, C_3 asphaltenes and C_3 resins precipitate. However, when propane is mixed with the n-C_5 deasphaltened crude, C_3–C_5 asphaltenes and C_3 resins precipitate. Thus, the difference between the two amounts provides the n-C_5 asphaltenes in the crude (see Table 5). The difference compares well with the amounts of n-C_5 asphaltenes reported in Table 4. The disparity is due to some loss during the separation. Results of resin separation by the modified ASTM D2007 adsorption method (1991a) using different solvents are provided in Tables 6 and 7. Table 6 shows the amount of resins recovered after elution of oils with n-C_5, n-C_7, and n-C_{10}. The amount of resins slightly increases with the carbon number of n-alkane used to elute oils. For all the crudes, the amount of resins by adsorption are higher than those by propane precipitation. It is also observed that crudes with high asphaltene content contain substantial amounts of resins. Material balance calculation on the very heavy crudes reveals minor losses [that is, irreversible adsorption of polar compounds on the clay (< 1 wt %)]. Table 7 provides the amount of resins recovered from the n-C_5 deasphaltened crudes after elution of oils with different n-C_5/toluene volume ratios of 85/15, 70/30, 50/50, and 0/100 (vol/vol). It is found that the amount of resins decreases with the volume of toluene in n-C_5/toluene mixtures. When using only n-C_5 to elute oils, we obtain almost two times more resins than when using only toluene. In order to compare our results with other separation techniques, the resin content of crude E has been determined in two different laboratories (Durandeau, 1999; Boduszynski, 2000). Durandeau used thin-layer chromatography (TLC) and reported a value of 14 wt %, while Boduszynski used high-performance liquid chromatography (HPLC) and

Table 5. Asphalt (asphaltenes and resins) Precipitated by Propane from Crudes and n-C_5 Deasphaltened Crudes

Precipitation from	Crude (wt %)							
	H	TE	C	TA	TK	S	U	B
Crudes	38.6	36.3	6.2	3.9	5.7	—	—	—
n-C_5 deasphaltened crudes	19.8	20.0	3.3	3.6	4.2	1.5	—	0.3
Difference	18.8	16.3	2.9	0.2	1.5	—	—	—

— ≡ not measured.

Table 6. Resins Adsorbed on Clay after Elution of Oils With n-C_5, n-C_7, and n-C_{10}

Elution of Oils with	Crude (wt %)							
	H	TE	C	TA	TK	S	U	B
n-C_5	30.3	28.6	6.5	6.0	7.5	3.5	8.6	0.56
n-C_7	31.1	28.7	7.4	6.2	7.6	3.8	—	0.65
n-C_{10}	32.0	30.0	7.8	6.5	7.9	4.0	—	0.68

— ≡ not measured.

Table 7. Resins Adsorbed on Clay after Elution of Oils With Various n-C_5/Toluene Mixtures

Elution of Oils with n-C_5/Toluene	Crude (wt %)							
	H	TE	C	TA	TK	S	U	B
100/0 (vol/vol)	30.3	28.6	6.5	6.0	7.5	3.5	8.6	0.56
85/15 (vol/vol)	26.4	24.0	5.9	4.8	5.9	2.7	—	0.45
70/30 (vol/vol)	21.8	19.9	4.9	3.9	5.2	2.2	—	0.37
50/50 (vol/vol)	20.0	18.0	4.2	3.6	4.2	1.5	—	0.30
0/100 (vol/vol)	14.0	13.3	2.9	2.8	2.9	1.1	—	0.25

— ≡ not measured.

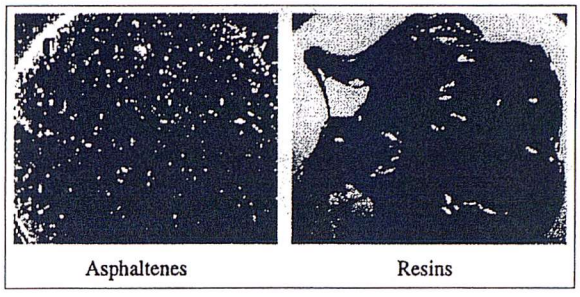


Figure 2. Asphaltenes and resins separated from crude H.

reported a resin content of 25 wt. %. In TLC, saturates are eluted with *n*-hexane and aromatics with toluene, while in HPLC, *n*-hexane is used to elute oils. The solvents used in the two techniques correspond to the extreme proportion of n-C_5/toluene volume ratios. The results from HPLC correspond to 100% n-C_5 (0% toluene) and the results from TLC correspond to 100% toluene (0% n-C_5) when compared with our adsorption method. It is interesting to see that the results from HPLC and TLC for resins, which are, respectively, 25 and 14 wt % for crude TE, are in line with our measurements of 28.6 wt % and 13.3 wt %, respectively. Later we comment on the true resin content of various crudes once the dipole moment of separated resins are presented.

Figure 2 shows the separated asphaltenes and resins from crude H. The resins are those separated by adsorption after elution of oils with n-C_5. We observe that asphaltenes and resins have very different appearances. Indeed, asphaltenes from all the crudes are black, shiny, and friable solids, while resins are dark brown, shiny, and gummy. Oils are orange/brown liquids with a density that varies from one crude to another. The color of oils changes from orange/brown to red/brown when we increase the proportion of toluene in the n-C_5/toluene mixtures. This change in coloration may suggest the presence of polar species in the oils (Becker, 2000).

Dipole moment verification

The methods presented for the estimation of the dipole moment of molecules are applied to 12 chemicals with known dipole moments from the literature (Lide and Frederikse, 2000; McClellan, 1963); see Table 8. The objective is to verify the validity of the methods; the most accurate method will be used to determine the dipole moment of asphaltenes, resins, and oils. In the selection of the chemicals, we aim to cover a wide range of dipole moments (0 to 4 D) as well as a variety of chemical functions (ketones, alcohols, amines, and so on).

The dipole moment of toluene, dibutylamine, anisole, ethanol, ethyl acetate, ethyl benzoate, and acetone were measured in the vapor phase by the temperature variation procedure in the microwave-frequency region, using the Debye equation (Lide and Frederikse, 2000; McClellan, 1963). The dipole moments of the remaining substances were measured in liquid solutions, with benzene at 20°C. For instance, the dielectric constant of 2-butanone solutions in benzene was

Table 8. Substances with Known Dipole Moments

Substance	Formula	M g/mol	$\rho^{20°C}$ g/cm^3	μ D
Toluene	C_7H_8	100.2	0.940	0.37
Dibutylamine	$C_8H_{19}N$	129.2	0.760	1.18
Anisole	C_7H_8O	108.1	1.000	1.36
Ethanol	C_2H_6O	46.1	0.790	1.69
Ethyl acetate	$C_4H_8O_2$	88.1	0.894	1.78
Ethyl benzoate	$C_9H_{10}O_2$	150.2	1.051	1.95
2-Butanone	C_4H_8O	72.1	0.800	2.78
Acetone	C_3H_6O	58.1	0.790	2.88
N,*N*-Dimethylformamide	C_3H_7NO	73.1	0.944	3.82
Dimethylsulfoxide	C_2H_6OS	78.1	1.096	3.96
3-Methyl-2-Cyclopenten-1-one	C_6H_8O	96.1	0.980	4.33

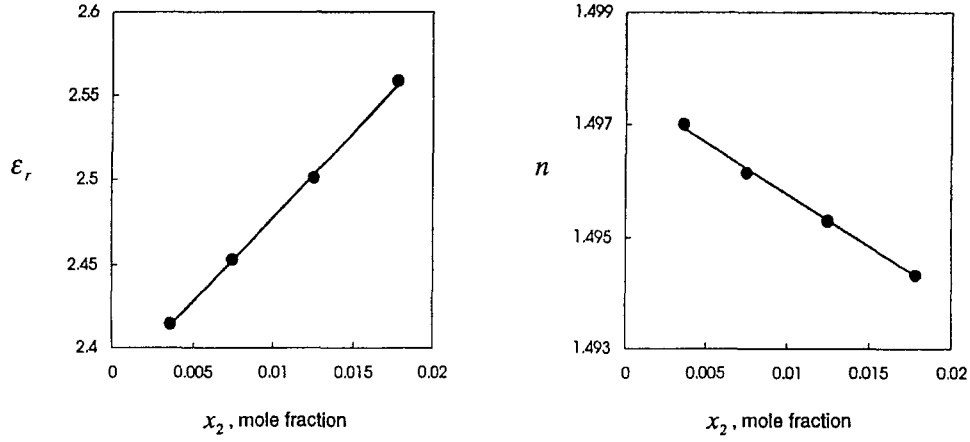
Source: Lide and Frederikse (2000); McClellan, (1963).

measured by a bridge method and the dipole moment calculated from the LeFèvre (1948) equation. For dimethylsulfoxide, the dielectric constant was measured by a resonance method and the dipole moment was calculated from the Halverstadt–Kumler (1942) equation. Usually, the dipole moment measurements in the gas phase are the most reliable (McClellan, 1963).

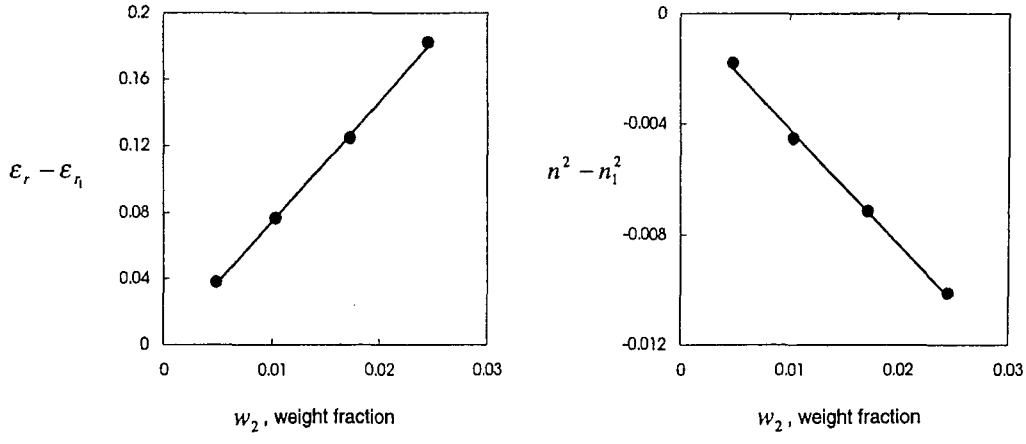
In our measurements, toluene is selected as a solvent, although it has a small dipole moment ($\mu = 0.4$ D). We found that the results did not differ significantly when using *p*-xylene ($\mu = 0$ D). Toluene is preferred because of the high solubility of asphaltenes, resins, and oils in this solvent. While preparing the solutions, we make sure that all the chemicals are dissolved in toluene. The dipole moment of the substances in Table 8 is calculated from various methods, using Eqs. T1 (Cohen-Henriquez) and T4 (Guggenheim) from Table 3, and Eq. 20 (Onsager). The atomic polarization is neglected in our calculations. Figure 3 presents results for the ethanol solution in toluene. The variation of the dielectric constant and refractive index of the solution with the mole fraction of ethanol in toluene is determined by the Cohen-Henriquez method. The Guggenheim method requires the determination of $\epsilon_r - \epsilon_{r_1}$ and $n^2 - n_1^2$ vs. the weight fraction of ethanol in toluene (ϵ_{r_1} and n_1 are the dielectric constant and refractive index of toluene, respectively). For the Onsager method, we present the variation of the dielectric constant and refractive index of ethanol solutions as a function of the weight percent of ethanol in toluene. In the Cohen-Henriquez and Guggenheim methods, the slope of the straight lines is substituted in the corresponding equations. For the Onsager method, the variations are extrapolated to $w_2 = 100$ wt % to determine the dielectric constant and refractive index of ethanol. The same procedure is applied to all substances, and the results are summarized in Table 8. For each method, we report the absolute relative error (%) of the dipole moment and the data from the literature.

Examination of the results in Table 9 reveals that the Cohen-Henriquez and Guggenheim methods overestimate the dipole moment of the substances in Table 8. The differences with data in the literature are very high, and can be as high as 80%. The error in estimation becomes large for substances with a high dipole moment. On the other hand, the Onsager equation underestimates the dipole moment. Deviations may arise from the extrapolation technique used, which produces

(a) Cohen-Henriquez



(b) Guggenheim



(c) Onsager

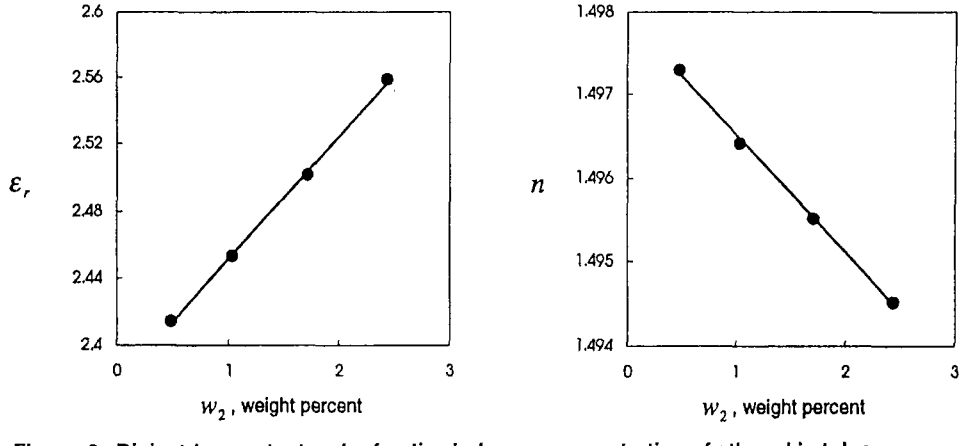


Figure 3. Dielectric constant and refractive index vs. concentration of ethanol in toluene.

Table 9. Dipole Moment of Substances Using Different Methods

Substance	Calculated μ, D					
	CH	Relative Error, %	G	Relative error, %	O	Relative Error, %
Toluene	0.35	−7	0.53	40	0.36	−3
Dibutylamine	0.86	−27	1.57	33	1.14	3
Anisole	1.57	14	1.93	40	1.13	−16
Ethanol	3.01	78	2.68	58	1.82	8
Ethyl acetate	2.23	25	2.76	55	1.75	−2
Ethyl benzoate	2.45	25	3.01	54	1.67	−14
2-Butanone	3.39	22	4.12	48	2.66	−4
Acetone	3.68	28	4.16	44	2.78	−4
N,*N*-Dimethylformamide	5.13	34	6.31	65	3.49	−7
Dimethylsulfoxide	5.76	45	7.11	79	3.49	−12
3-Methyl-2-cyclopenten-1-one	6.90	59	7.62	76	4.10	−5

Note: CH: Cohen-Henriquez; G: Guggenheim; O: Onsager.

some uncertainties in the results, especially for refractive indices. Nevertheless, the overall deviation with the Onsager method is small. We select this method for the determination of the dipole moment of asphaltenes, resins, and oils.

Dipole moment of asphaltenes, resins, and oils

Following the preceding procedure, four different solutions with an increasing concentration of solute (that is, asphaltenes, resins, or oils) in toluene are prepared. The oils considered comprise only the hydrocarbons that are nonvolatile at atmospheric conditions; the light hydrocarbons were removed by evaporation. We use a small concentration of solutes (< 5 wt %) in order to allow a complete dissolution of asphaltenes and resins in toluene and for an accurate reading of refractive indices. For each sample, the tests are repeated two to four times to assure reproducibility of the results.

Among the parameters required in the dipole moment calculation are the molecular weight and density of asphaltenes and resins. The molecular weight of asphaltenes and resins is estimated by fluorescence depolarization spectroscopy according to the procedure described by Groenzin and Mullins (2000). The average molecular weights are approximately 900 for asphaltenes and 700 amu for resins. The density is assumed to be 1.2 g/cc for asphaltenes (Schabron and Speight, 1998; De Hemptinne et al., 1999) and 1.0 g/cc for resins (Wu et al., 2000). For oils, the density and refractive index are measured at 20°C and the molecular weight is calculated using the Riazi and Daubert (1987) correlation.

Figures 4 and 5 illustrate the variation of the dielectric constant and refractive index of n-C_5 asphaltenes, resins, and oils for the very heavy crude H and the very light crude B, respectively. The linear variations are extrapolated to w_2 (weight fraction in toluene) of 100 wt % to estimate the dielectric constant and refractive index of asphaltenes, resins, and oils. The small range of variation of w_2, especially for asphaltenes, increases the uncertainty in the extrapolation results. The dielectric constant of asphaltenes, resins, and oils are calculated with a maximum error of 2%. The error on the estimation of refractive index of asphaltenes and resins increases because of the extrapolation; however, it does not exceed 1%. Oils are viscous translucent liquids and their refractive index can be measured directly with an error of about 0.1%. The data obtained by direct measurement and extrapolation from oils in toluene solutions compare very well. The dielectric constant and refractive index of asphaltenes, resins and oils are reported in Table 10 along with the density and molecular weight. The dielectric constants of asphaltenes, resins, and oils are in the ranges of 5.5–18.4, 3.8–5.1, and 2.1–2.6, respectively. The range of variation of the refractive index is 1.638–1.707 for asphaltenes, 1.576–1.608 for resins, and 1.472–1.527 for oils. The refractive indices of asphaltenes are in line with those reported in the literature (see Table 11). However, some measured dielectric constants of asphaltenes (crudes H, TE, C, and TK) are high compared to 6–7 range in the literature in Table 11. Oudin (1970) measured the dielectric constant of asphaltenes in chloroform at a concentration of 20 g/L and reported a value of 6.2 for asphaltenes soluble in CCl_4 and 6.9 for asphaltenes insoluble in CCl_4. Maruska et al. (1987) measured the dielectric constant of asphaltenes in toluene at a concentration of 1–100 g/L and reported a value of 6.8. We measured the dielectric constant of asphaltenes in toluene at a concentration of 1–8 g/L and obtained dielectric constants in the range of 5.5–18.4. In this work, the asphaltene concentrations in toluene are low compared to those used by Maruska et al. and Oudin. This suggests that the high dielectric constants measured in our work may not be due to an association between molecules.

Table 12 provides the dipole moment of asphaltenes, resins, and oils calculated with the Onsager equation. The dipole moments are in the 3.3–7.0 D range for n-C_5 asphaltenes. It is found that the dipole moment of asphaltenes increases with the carbon number of the precipitating n-alkane. The results show that n-C_7 asphaltenes are more polar than n-C_5 asphaltenes (note that we have used the same molecular weight for both n-C_5 and n-C_7 asphaltenes). Previous studies by Nighswander et al. (1993), Speight (1999), and Nalwaya et al. (1999) suggest that the molecular weight and the metal content of asphaltenes increases with the carbon number of the precipitating n-alkane, which is consistent with our dipole moment data. Table 12 provides the dipole moment of resins by precipitation and adsorption methods. Resins precipitated by propane are more polar than resins separated by adsorption. This reveals that propane precipitates only part of the resin fraction containing the most polar molecules. In the adsorption method, n-C_7 resins are more polar than n-C_5 resins, because they contain the C_5–C_7 fraction of as-

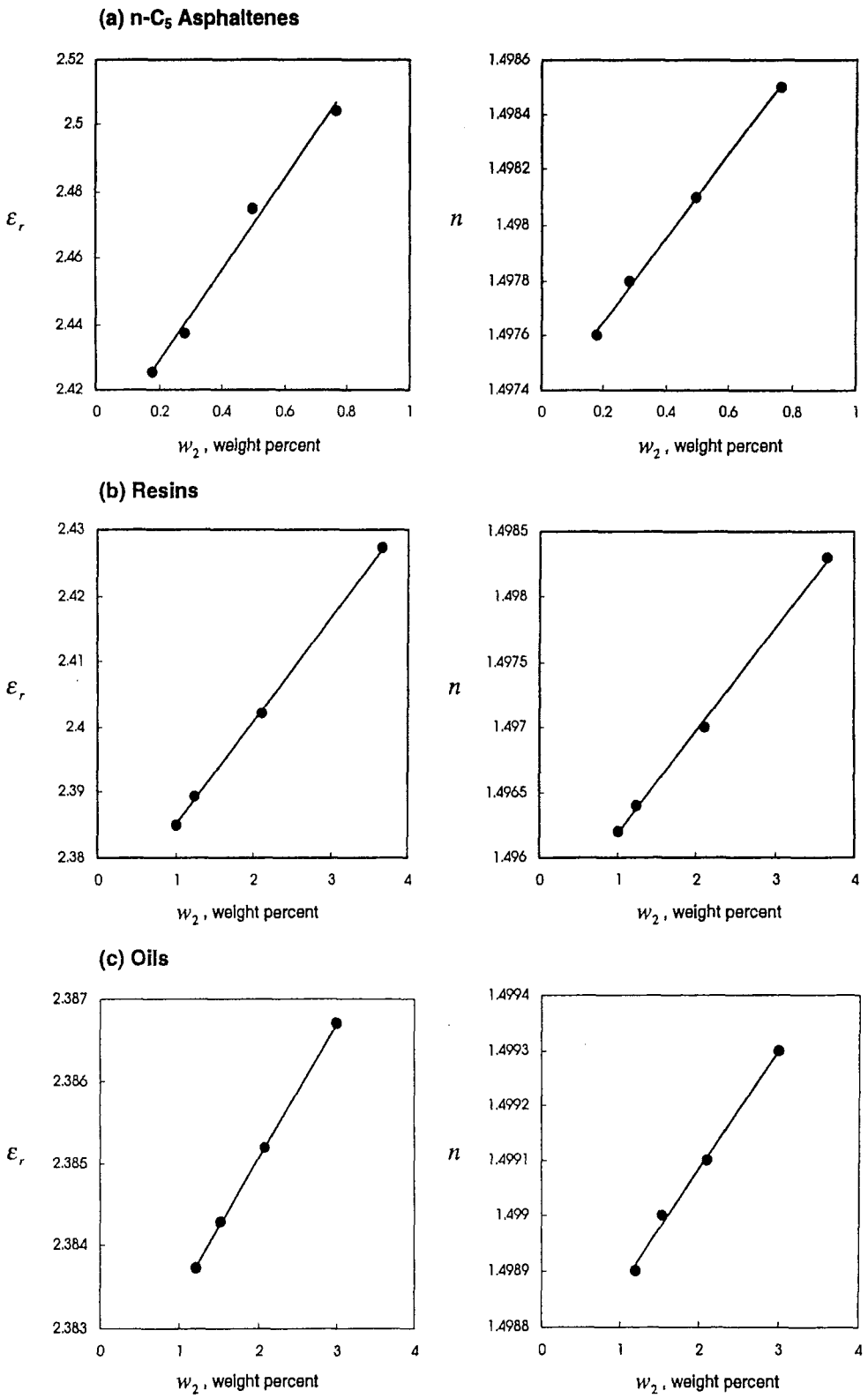


Figure 4. Dielectric constant and refractive index vs. concentration of n-C_5 asphaltenes, resins, and oils (eluted with n-C_5) in toluene for crude H.

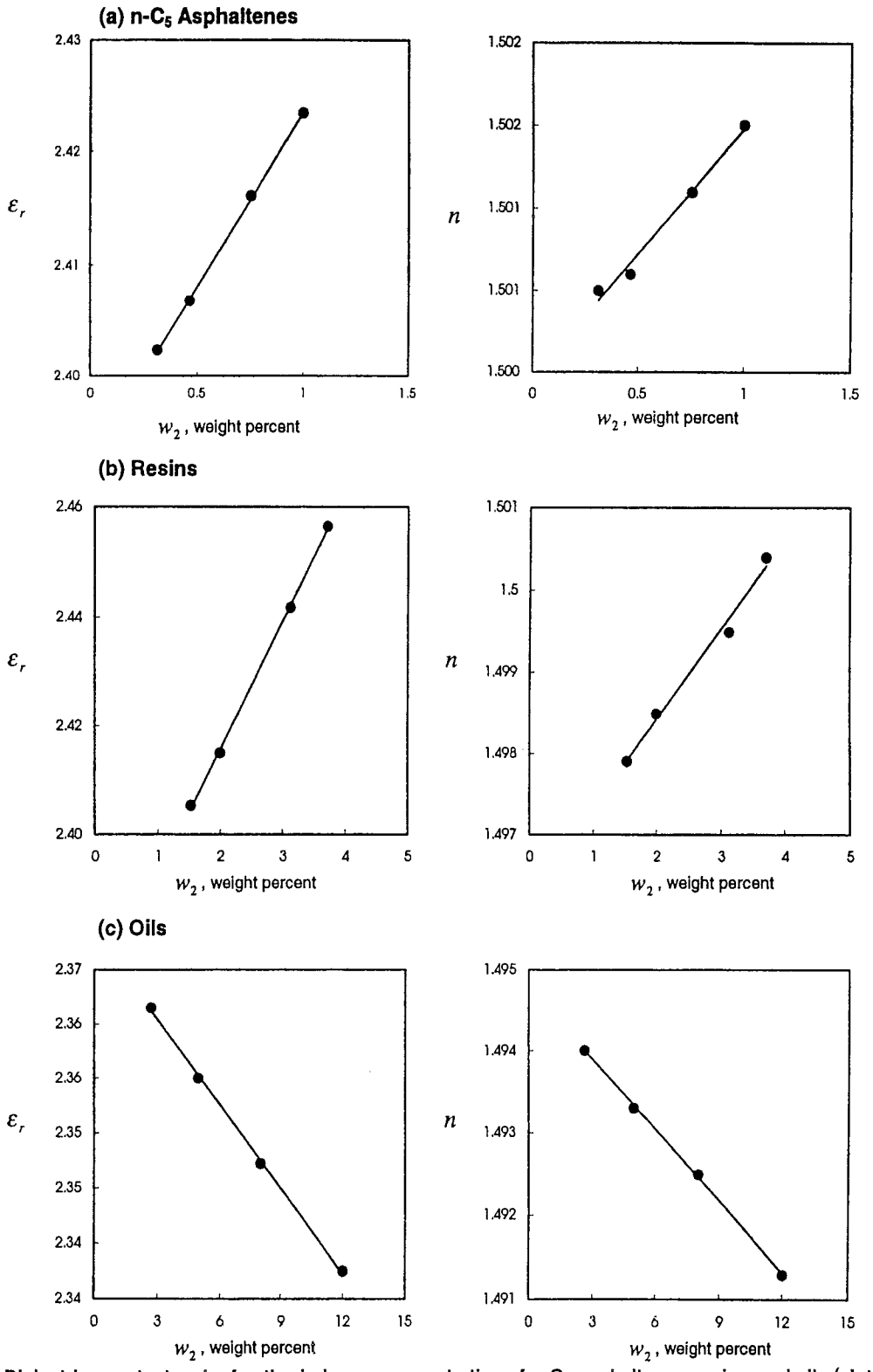


Figure 5. Dielectric constant and refractive index vs. concentration of n-C_5 asphaltenes, resins, and oils (eluted with n-C_5) in toluene for crude B.

Table 10. Dielectric Constant, Refractive Index, Density, and Molecular Weight of n-C_5 Asphaltenes, Resins, and Oils

	H	TE	C	TA	TK	S	U	B
				n-C_5 Asphaltenes				
$n^{20°C}$	1.647	1.707	1.638	1.676	1.706	1.668	1.685	1.650
ϵ_r	16.2	18.4	15.2	9.2	10.9	10.1	8.2	5.5
$\rho^{20°C}$, g/cm^3	1.2	1.2	1.2	1.2	1.2	1.2	1.2	1.2
M, g/mol	900	900	900	900	900	900	900	900
				Resins				
$n^{20°C}$	1.576	1.587	1.606	1.585	1.608	1.608	1.595	1.606
ϵ_r	3.9	3.8	5.1	4.8	4.5	3.9	3.8	4.7
$\rho^{20°C}$, g/cm^3	1.0	1.0	1.0	1.0	1.0	1.0	1.0	1.0
M, g/mol	700	700	700	700	700	700	700	700
				Oils				
$n^{20°C}$	1.527	1.522	1.487	1.497	1.496	1.498	1.496	1.472
ϵ_r	2.6	2.5	2.2	2.3	2.4	2.4	2.4	2.1
$\rho^{20°C}$, g/cm^3	0.935	0.935	0.875	0.876	0.876	0.870	0.881	0.830
M, g/mol	371	389	269	287	300	290	320	196

Table 11. Dielectric Constant and Refractive Index of Asphaltenes and Resins

Source	Sample	ϵ_r	$n^{20°C}$
Oudin (1970)	n-C_5 Asphaltenes soluble in CCl_4	6.16	—
	n-C_5 Asphaltenes insoluble in CCl_4	6.92	—
	Resins	5.32	—
Maruska and Rao (1987)	n-C_5 Asphaltenes	6.8	1.682
Buckley et al. (1998)	n-C_6 Asphaltenes	—	1.720

— ≡ not reported.

phaltenes (that is, the fraction of asphaltenes soluble in n-C_7 but insoluble in n-C_5). When toluene is introduced into the eluting solvent of oils, even at small concentrations, the dielectric constant of resins increases linearly with the amount of toluene in the solvent as shown in Figure 6. The dipole moment of resins separated after elution of oils with various n-C_5/toluene volume ratios is given in Table 12. A gradual increase in the dipole moment is observed with the increasing volume of toluene. These results imply that toluene does elute some resins with oils, probably those weakly bound to the clay. A nitrogen analysis of the oils of crudes H and C shows that the resins eluted by toluene are those containing nitrogen functions (see Table 13). Therefore, it is recommended that toluene not be used with n-C_5 to separate oils from resins. In fact, the oils eluted by pure n-C_5 possess a small dipole moment that does not exceed 1 D (see Table 12). In order to elucidate the origin of this dipole moment, we used distillation cuts from two different crudes (an asphaltic crude and a waxy crude). The asphaltic crude is heavy and viscous with high sulfur, asphaltene, resin and aromatic content (> 50 wt %). The waxy crude contains large amount of paraffins and small amount of aromatics. The asphaltene

Table 12. Dipole Moment (in debye) of Asphaltenes, Resins and Oils

	Crude							
	H	TE	C	TA	TK	S	U	B
				Asphaltenes				
Precipitated by								
n-C_5	6.9	7.0	6.7	4.8	5.2	5.1	4.4	3.3
n-C_7	7.2	7.7	7.2	5.8	6.5	6.4	—	4.0
				Resins				
Precipitated by								
C_3	4.0	3.8	4.4	3.5	4.0	4.2	—	3.7
Adsorbed after elution of oils with								
n-C_5	2.5	2.4	3.2	3.1	2.8	2.4	2.4	3.0
n-C_5/toluene, 85/15 vol/vol	2.6	2.5	3.3	3.1	3.0	2.5	—	3.1
70/30 vol/vol	2.7	2.6	3.5	3.2	3.1	2.6	—	3.2
50/50 vol/vol	2.9	2.8	3.6	3.3	3.2	2.7	—	3.4
0/100 vol/vol	3.1	2.9	3.7	3.3	3.4	2.8	—	3.5
n-C_7	3.5	3.6	3.9	3.4	3.6	3.9	—	3.7
				Oils				
Eluted by								
n-C_5	0.9	0.8	0.0	0.4	0.6	0.7	0.7	0.0

— ≡ not measured.

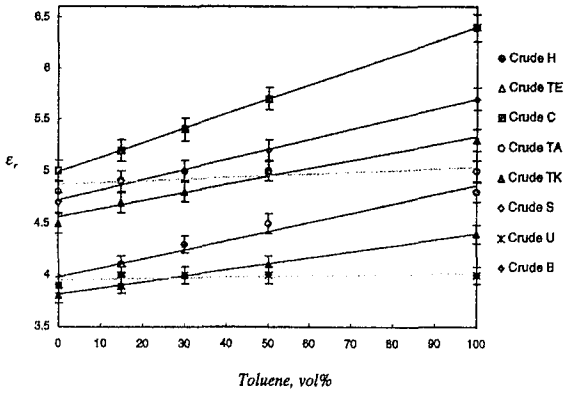


Figure 6. Increase of the dielectric constant of resins with the amount of toluene in the eluting solvent of oils.

Table 13. Nitrogen Cotent of Oils from Crude H and C Eluted with Various n-C_5/Toluene Mixtures

n-C_5/Toluene (Vol/vol)	Crude (ppm)	
	H	C
100/0	213	250
85/15	655	300
70/30	1,100	356
50/50	1,700	415

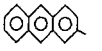
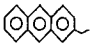
and resin content in waxy crudes is low (< 10 wt %) (Whauquier, 1995). The dipole moment of the distillation cuts is determined and presented in Table 14. The cuts from the waxy crude are completely apolar, while the cuts from the asphaltic crude have dipole moments in the same range as the oils listed in Table 12. Moreover, it is unlikely that the distillation cuts up to 550°F contain traces of asphaltenes or resins. Asphaltic crudes are characterized by a high amount of aromatic hydrocarbons (Whauquier, 1995), and this may be the precursor of the small polarity measured. Although still a subject of controversy, we consider that slightly polar resins are distinguished from slightly polar aromatics in that the polarity of resins stems from the presence of heteroatoms in the molecule. Swanson (1942) reported the small polarity of oils and attributed it to the high electronic and atomic polarizations of heavy aromatic hydrocarbons.

The results just presented for different crudes show that the dipole moment is in the 3.3–7.0 D range for n-C_5 asphaltenes, 2.4–3.2 D for resins, and 0–0.9 D for oils. Water is a polar substance and its dipole moment is 1.87 D. Our dipole

Table 14. Dipole Moment (in debye) of Distillation Cuts from Asphaltic Crude and Waxy Crude

Cut, °C	Asphaltic Crude	Waxy Crude
177–132	0.3	0.0
232–288	0.6	0.0
288–343	0.7	0.0
343–454	0.9	0.0

Table 15. Effect of Charge Separation on Dipole Moment

Molecule	Formula	μ, D
Toluene		0.4
Ethyl benzene		0.6
2-Methyl naphthalene		0.4
2-Ethyl naphthalene		0.6
2-Methyl anthracene		0.5
2-Ethyl anthracene		0.6

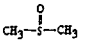
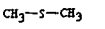
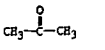
Source: Lide and Frederikse, 2000; McClellan, 1963.

moment measurements show that in these crudes, asphaltenes, and to a lesser degree resins are highly polar molecules. Asphaltenes are more polar than resins in the same crude, although resins of one crude can be more polar than asphaltenes of another crude.

Tables 15 and 16 show the effect of charge separation and the presence of heteroatoms on the dipole moment of several substances, respectively. The dipole moment slightly increases from toluene to ethyl anthracene (see Table 15), suggesting that charge separation does not contribute significantly to the dipole moment of asphaltenes. Table 16 provides the dipole moment of some chemicals that have been reported to be part of the asphaltenes (Waldo et al., 1992; Mitra-Kirtley et al., 1993). The presence of certain groups (such as sulfoxide) in a molecule has a significant effect on the dipole moment.

Figure 7 illustrates the variation of the dielectric constant and refractive index of n-C_5 asphaltenes and resins from adsorption vs. the dipole moment. There is a linear relationship

Table 16. Effect of Heteroatoms on Dipole Moment

Molecule	Formula	μ, D
1.H-Pyrrole		1.7
Pyridine		2.2
Dimethyl sulfoxide		4.0
Thiophene		0.6
Dimethyl sulfide		1.6
Phenol		1.2
Acetone		2.9

Source: Lide and Frederikse, 2000; McClellan, 1963.

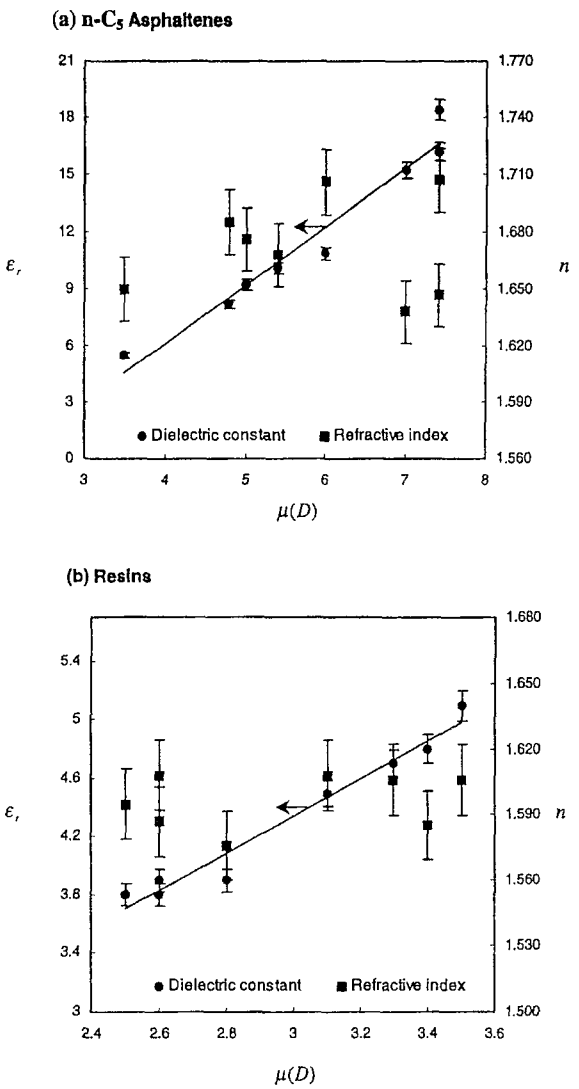


Figure 7. Dielectric constant and refractive index vs. dipole moment of n-C_5 asphaltenes and resins.

between the dielectric constant and dipole moment for both asphaltenes and resins. However, no correlation is observed between the refractive index and the dipole moment of these fractions. A close examination of Figure 7 shows that the refractive index is around 1.68 for asphaltenes and 1.60 for resins. The refractive index has been previously used to determine the onset of asphaltene precipitation from crudes (Buckley, et al., 1998), and it was concluded that asphaltene precipitation is dominated by London dispersion interactions. In a separate study on the effect of resins/surfactants on asphaltene precipitation (work to be published in the near future), we demonstrate that the effect of resins on asphaltene precipitation is a function of their dipole moment. In the same work, the onset of asphaltene precipitation is found to increase when resins or surfactants are added to the crude; the magnitude of the increase as well as the amount of precipitation depend on the dipole moment of the added resin/surfactant. These measurements suggest that dipole–dipole interactions should be included in the study of asphaltene precipitation from crudes.

Conclusions

Based on extensive work on the separation of asphaltenes and resins from petroleum fluids and the measurement of the dipole moment of asphaltenes, resins, and oils, we draw the following conclusions.

1. Asphaltenes precipitated by heavy normal alkanes are more polar than asphaltenes precipitated by light normal alkanes; n-C_{10} asphaltenes are more polar than n-C_7 asphaltenes, and n-C_7 asphaltenes are more polar than n-C_5 asphaltenes.

2. The propane precipitation method separates only part of the resins. This part is the most polar fraction of the resins.

3. The total resins can be precipitated by adsorption using n-C_5 deasphaltened crude. Use of an aromatic solvent such as toluene with n-C_5, even a small quantity, may reduce the amount of the separated resins.

4. For a variety of crudes used in this study, the dipole moment of resins and asphaltenes are in the ranges of 2–3 D and 3–7 D, respectively.

5. For all the crudes used in this study, the asphaltenes are more polar than the resins in the same crude. However, resins from one crude could be more polar than the asphaltenes in another crude.

6. The oil fraction (that is, the atmospheric crude minus the asphaltenes and resins and volatiles) can be slightly polar with a dipole moment of less than 1 D.

Acknowledgments

This work was supported by the member companies of the Reservoir Engineering Research Institute (RERI). We thank Dr. O. Mullins and H. Groenzin (Schlumberger-Doll Research Center, CT), Dr. M. Boduszynski and B. Mossberger (Chevron Technology Company, CA), and P. Fotland (Norsk Hydro SA, Bergen) for their help and valuable comments during the course of this work.

Notation

a = molecular radius, m
C = capacitance, $J^{-1}\cdot C^2$
E = electric field, $J\cdot m^{-1}\cdot C^{-1}$
F = internal field, $J\cdot m^{-1}\cdot C^{-1}$
G = cavity field, $J\cdot m^{-1}\cdot C^{-1}$
k = Boltzmann constant, $J\cdot K^{-1}$ ($k = 1.381\times10^{-23}$ $J\cdot K^{-1}$)
L = inductance, H
m = total dipole moment, $C\cdot m$
M = molecular weight, $kg\cdot mol^{-1}$
n = refractive index
N = number of molecules per unit volume, $mol\cdot m^{-3}$
N_A = Avogadro number, mol^{-1} ($N_A = 6.022\times10^{23}$ mol^{-1})
P = polarization, $C\cdot m^{-2}$
e = electric charge, C
r = distance between charges, m
R = reaction field, $J\cdot m^{-1}\cdot C^{-1}$
R = resistance, Ω
T = temperature, K
u = unit dipole moment
v = volume fraction
w = weight fraction
x = mole fraction

Greek letters

α = polarizability, m^3
ϵ = permittivity, $J^{-1} \cdot C^2 \cdot m^{-1}$ ($\epsilon_0 = 8.854 \times 10^{-12}$ $J^{-1} \cdot C^2 \cdot m^{-1}$)
ϵ_r = dielectric constant
ϵ_r' = dielectric storage
ϵ_r'' = dielectric loss
μ = dipole moment, $C \cdot m$
ν = frequency, Hz
ρ = mass density, $kg \cdot m^{-3}$

Subscripts

0 = air/vacuum
1 = nonpolar solvent
2 = polar solute
a = actual
i = component index
ind = induced
M = molar
μ = orientation (or permanent)

Literature Cited

American Society for Testing and Material, Annual Book of ASTM Standards, ASTM D2006, D3279, D893, D2007, D4124, ASTM, Philadelphia, PA (1970, 1978, 1980, 1991a, 1991b).

Andersen, S. I., and J. G. Speight, "Petroleum Resins: Separation, and Role in Petroleum," *Pet. Sci. Technol.*, **19** (1&2) 1 (2001).

Atkins, P. W., *Physical Chemistry*, Oxford University Press, Oxford (1978).

Becker, H. L., "Asphaltene: To Treat or Not," 2000 SPE Permian Basin Oil and Gas Recovery Conf., Midland, TX (2000).

Bitter, F., *Currents, Fields and Particles*, The Technology Press of Massachusetts Institute of Technology and Wiley, New York (1956).

Boduszynski, M., Private Communication, Chevron Technology Company, Richmond, CA (2000).

Born, M., and E. Wolf, *Principles of Optics*, Pergamon Press, New York (1980).

Böttcher, C. J. F., *Theory of Electric Polarization*, Elsevier, Amsterdam (1952).

Buckley, J. S., G. J. Hirasaki, Y. Liu, S. Von Drasek, J.-X. Wang, and B. S. Gill, "Asphaltene Precipitation and Solvent Properties on Crude Oils," *Petroleum Sci. and Technol. Int.*, **16** (3-4), 251 (1998).

Callen, R. B., J. G. Bendoraitis, C. A. Simpson, and S. E. Voltz, "Upgrading Coal Liquids to Gas Turbine Fuels 1. Analytical Characterization of Coal Liquids," *Ind. Eng. Chem. Prod. Res. Dev.*, **15** (4), 223 (1976).

Debye, P., *Polar Molecules*, Dover, New York (1929).

De Hemptinne, J-C., A. Aubertin-Couvreur, I. Fondio, and D. Broseta, "Viscosity Prediction of Heavy Crudes in Hydrotreatment Conditions," Int. Conf. Petroleum Phase Behavior and Fouling, Houston, TX (1999).

Durandeau, M., Private Communication, Total Elf Fina Research Center, Pau, France (1999).

Ese, M.-H., X. Yang, and J. Sjoblom, "Film Forming Properties of Asphaltenes and Resins. A Comparative Langmuir-Blodgett Study of Crude Oils from North Sea, European Continent and Venezuela," *Colloid Polym. Sci.*, **276**, 800 (1998).

Farcasiu, M., "Fractionation and Structural Characterization of Coal Liquids," *Fuel*, **56**, 9 (1977).

Feynman, R. P., R. B. Leighton, and M. Sands, *The Feynman Lectures on Physics*, Vol. 2, Addison-Wesley, Redwood City, CA (1964).

Firoozabadi, A., *Thermodynamics of Hydrocarbon Reservoirs*, McGraw-Hill, New York (1999).

Groenzin, H., and O. C. Mullins, "Molecular Size and Structure of Asphaltene from Various Sources," *Energy Fuels*, **14** (3), 677 (2000).

Guggenheim, E. A., "The Computation of Electric Dipole Moments," *Trans. Faraday Soc.*, **47**, 573 (1951).

Halverstadt, I. F., and W. D. Kumler, "Solvent Polarization Error and its Elimination in Calculating Dipole Moments," *J. Amer. Chem. Soc.*, **64**, 2988 (1942).

Halvorsen, K., *Dipole Moments and Molecular Weights for Alkane Precipitated Solid Fractions for Some North-Sea Oils*, MSc Thesis, Univ. of Bergen, Institute of Chemistry, Bergen, Norway (1997).

Hewlett-Packard, *The Impedance Measurement Handbook: A Guide to Measurement, Technology and Techniques*, Hewlett-Packard, Hyogo, Japan (1999).

Kaminski, T. J., H. S. Fogler, and A. Mairal, "Classification of Asphaltenes via Fractionation and the Effect of Heteroatom Content on Dissolution Kinetics," Int. Conf. on Petroleum Phase Behavior and Fouling, Houston, TX (1999).

Kumler, W. D., "The Dipole Moment of ms-Tetraphenylporphirine," *J. Amer. Chem. Soc.*, **64**, 2993 (1942).

LeFèvre, R. J. W., *Dipole Moments*, 2nd ed., London (1948).

Leontaritis, K. J., and A. G. Mansoori, "Asphaltene Deposition: A Survey of Field Experience and Research Approaches," *J. Pet. Sci. Eng.*, **1**, 229 (1988).

Lian, H., J. R. Lin, and T. F. Yen, "Peptization Studies of Asphaltene and Solubility Parameter Spectra, *Fuel*, **73**, 423 (1994).

Lide, D. R., and H. P. R. Frederikse, *Handbook of Chemistry and Physics*, 81st ed., CRC Press, Boca Raton, FL (2000).

Maruska, H. P., and B. M. L. Rao, "The Role of Polar Species in the Aggregation of Asphaltenes," *Fuel Sci. Technol. Int.*, **5**(2), 119 (1987).

Maxwell, J. C., *A Treatise on Electricity and Magnetism*, Vol. 2, 3rd ed., Dover, New York (1954).

McClellan, A. L., *Tables of Experimental Dipole Moments*, Vol. 1, Freeman, San Francisco (1963).

McLean, J. D., and P. K. Kilpatrick, "Comparison of Precipitation and Extrography in the Fractionation of Crude Oil Residua," *Energy Fuels*, **11**, 570 (1997).

Mitra-Kirtley, S., O. C. Mullins, J. Van Elp, S. J. George, J. Chen, and S. P. Cramer, "Determination of the Nitrogen Chemical Structures in Petroleum Asphaltenes using XANES Spectroscopy," *J. Amer. Chem. Soc.*, **115**(1), 252 (1993).

Moinelo, S. R., R. M. Menendez, and J. Bermejo, "Fractionation of Coal-Derived Liquids by Extrography," *Fuel*, **67**, 682 (1988).

Murzakov, R. M., S. A. Sabanenkov, and Z. I. Syunyaev, "Influence of Petroleum Resins on Colloidal Stability of Asphaltene-Containing Disperse Systems," *Khim. Tekhnol. Topl. Masel.*, **10**, 40 (1981).

Nalwaya, V., V. Tangtayakom, P. Piumsomboon, and S. Fogler, "Studies on Asphaltenes Through Analysis of Polar Fractions," *Ind. Eng. Chem. Res.*, **38**, 964 (1999).

Newberry, M. E., and K. M. Barker, "Organic Formation Damage Control and Remediation," 2000 SPE Int. Symp. on Formation Damage Control, Lafayette, LA (2000).

Nighswander, J. A., H. Kaira, and A. Majeed, "Effect of Low Molecular Weight Hydrocarbons on the Onset Concentration and Bulk Properties of Asphaltenes at In-Situ Temperature and Pressure Conditions," AIChE Meeting, Houston (1993).

Onsager, L., "Electric Moments of Molecules in Liquids," *J. Amer. Chem. Soc.*, **58**, 1486 (1936).

Oudin, J. L., "Analyse Géochimique de la Matière Organique Extraite des Roches Sédimentaires I. Composés Extractibles au Chloroforme," *Rev. Ins. Fr. Pét.*, **25** (1), 4 (1970).

Pedersen, C., and S. I. Andersen, "Dielectric Properties of Asphaltenes and Oils," AIChE Meeting, Houson, TX (1999).

Pfeiffer, J. Ph., and R. N. J. Saal, "Asphaltic Bitumen as Colloid System," *J. Phys. Chem.*, **44**, 139 (1940).

Riazi, M. R., and T. E. Daubert, "Improved Characterization of Wide Boiling Range Undefined Petroleum Fractions," *Ind. Eng. Chem. Res.*, **26**(3), 629 (1987).

Schabron, J. F., and J. G. Speight, "Solubility and Three-Dimensional Structure of Asphaltenes," *Pet. Sci. Technol.*, **16**(3/4), 361 (1998).

Schwager, I., and T. F. Yen, "Coal Liquefaction Products from Major Demonstration Processes 1. Separation and Analysis," *Fuel*, **57**, 100 (1978).

Sen, A. D., V. G. Anicich, and T. Arakelian, "Dielectric Constant of Liquid Alkanes and Hydrocarbon Mixtures," *J. Phys. D: Appl. Phys.*, **25** (3), 516 (1992).

Smyth, J. W., "Some Developments of Guggenheim's Simplified Procedure for Computing Electric Dipole Moments," *Trans. Faraday Soc.*, **46**, 394 (1950).

Smyth, C. P., *Dielectric Behavior and Structure*, McGraw-Hill, Amsterdam (1955).

Speight, J. G., R. B. Long, and T. D. Trowbridge, "Factors Influencing the Separation of Asphaltenes from Heavy Petroleum Feedstocks," *Fuel*, **63**, 616 (1984).
Speight, J. G., *The Chemistry and Technology of Petroleum*, Marcel Dekker, New York (1999).
Institute of Petroleum, *Standards for Petroleum and its Products*, "IP 143: Asphaltenes Precipitation with Normal Heptane," Institute of Petroleum, London (1957).
Storm, D. A., and E. Y. Sheu, "Characterization of the Asphaltenic Colloidal Particle in Heavy Oil," *Fuel*, **74** (8), 1140 (1995).
Swanson, J. M., "A Contribution to the Physical Chemistry of the Asphalts," *J. Phys. Chem.*, **46**, 141 (1942).
Syncrude, *Syncrude Analytical Method for Oil Sand and Bitumen Processing*, Syncrude Canada Ltd., Edmonton, Alta., Canada (1979).
Van Ness, K., and H. A. Van Westen, *Aspects of the Constitution of Mineral Oils*, Elsevier, Amsterdam (1951).
Waldo, G. S., O. C. Mullins, J. E. Penner-Hahn, and S. P. Cramer, "Determination of the Chemical Environment of Sulphur in Petroleum Asphaltenes by X-ray Absorption Spetroscopy," *Fuel*, **71**, 53 (1992).
Wallace, D., D. Henry, K. Pongar, and D. Zimmerman, "Evaluation of Some Open Column Chromatographic Methods for Separation of Bitumen Components," *Fuel*, **66**, 44 (1987).
Whauquier, J. P., *Crude Oil Petroleum Products Process Flowsheets*, Vol. 1, Technip, Paris (1995).
Wu, J., J. M. Prausnitz, and A. Firoozabadi, "Molecular Thermodynamics of Asphaltene Precipitation in Reservoir Fluids, *AIChE J.*, **46**, 1 (2000).

Manuscript received Dec. 5, 2001, and revision received Mar. 25, 2002.

MIAMI UNIVERSITY
OXFORD OHIO

Assistant/Associate Professor
Paper Science & Engineering

We are seeking an Assistant or Associate Professor to teach undergraduate and graduate courses; develop curriculum enhancements; initiate and maintain active program of scholarship; supervise undergraduate senior design projects and graduate thesis research; and participate in departmental and professional service activities.

Requires a Ph.D. by time of appointment in Paper Science, Chemical Engineering or a closely related field. Desired is professional experience in the Paper or Chemical industry and undergraduate or graduate teaching experience. Persons with expertise in any area of Paper Science, Chemical Engineering or Environmental Engineering will be considered for this position. Strength in papermaking, wet-end chemistry and/or coating is especially desired.

Send resume, description of teaching philosophy and research experience, descriptions of other appropriate experiences and three letters of reference to: **Michael Waller, 229 Gaskill Hall, 9-2205, Miami University, Oxford, OH 45056, E-mail: wallermh@muohio.edu**

Screening of applications begins December 1, 2002 and will continue until the position is filled.

EQUAL OPPORTUNITY IN EDUCATION AND EMPLOYMENT.

Miami University's report, Campus Crime and Safety, is available at www.muohio.edu/righttoknow. A hard copy may be obtained by contacting the Personnel Office.

Visit our Web site at:
www.MUOhio.edu

It's Not Your Eyes...
It's Your Information Sources



Regulations get tougher to understand all the time. AIChE publishes more than 150 ESH titles that can make compliance—with OSHA, EPA, and all the rest of the regulatory alphabet—much, much clearer, including:

Environmental Progress and Process Safety Progress—Subscribe to both periodicals so no critical information is lost in the overlapping boundaries of environmental and process safety management.

Supplement your ESH knowledge with book titles like:
Pollution Prevention: Methodology, Technologies and Practices
Practical Solutions for Reducing Volatile Organic Compounds and Hazardous Air Pollutants

For more information, contact us at 1-800-242-4363, or on the Web at www.aiche.org/pubcat

AIChE

© 2002 American Institute of Chemical Engineers

Effect of Resins and DBSA on Asphaltene Precipitation from Petroleum Fluids

Lamia Goual
Earth Science and Engineering, Imperial College London, SW7 2BP, UK

Abbas Firoozabadi
Reservoir Engineering Research Institute, Palo Alto, CA 94306

This work examines the effect of various resins and dodecyl benzene sulfonic acid (DBSA) amphiphile on asphaltene precipitation from different petroleum fluids. Various resins are added to three different petroleum fluids to measure precipitation with n-pentane. Results show that the dipole moment of resins (which is a measure of polarity) has a strong effect on precipitation. Resins with a high dipole moment are more effective than resins with a low dipole moment. The effectiveness is defined in terms of the increase in the onset point of precipitation. However, addition of resins to a petroleum fluid increases the amount of precipitated asphaltenes. This is the first report of such a behavior in the literature; the increase is less pronounced with the most polar resins. Addition of asphaltenes to a petroleum fluid results in a high amount of precipitation. As expected, the onset point of precipitation from asphaltene addition to a petroleum fluid is different from that of resins. When the DBSA amphiphile is mixed with the petroleum fluid at different concentrations, we observe a retrograde phenomenon. The amount of precipitated asphaltene increases first with increasing DBSA concentration. Beyond a certain concentration, there is a decrease in precipitation. At higher concentrations, DBSA proves to be very effective to move the onset point of precipitation. The data show the complex interactions between various species in petroleum fluids.

Introduction

A molecule where the center of negative charges and the The description of the structure and properties of asphaltenes has been a challenge over the past several decades. More recently, a growing interest has developed towards the study of resins with the recognition of their effect on the stability of asphaltenes in petroleum fluids. The stabilizing effect is understood to be related to the association of resins with asphaltenes to form micelles (Swanson, 1942). It is believed that in a micelle, asphaltenes self-associate into an aggregate to form the core and resins adsorb onto the core to form a steric shell (Firoozabadi, 1999).

A petroleum fluid can be divided into three parts: 1) oils (that is, saturates and aromatics), 2) resins, and 3) asphaltenes. This partition is very broad; every part of the petroleum fluid also consists of a wide range of molecules with varying structures and properties. Asphaltenes and resins are polar molecules while the oils are either non- or mildly polar. In a previous work (Goual and Firoozabadi, 2002), the dipole moment (a measure of polarity) of asphaltenes, resins and oils was investigated for eight petroleum fluids. The dipole moment was found to increase sharply from oils (0–1 D) to resins (2.4–3.2 D) to asphaltenes (3.3–6.9 D). Polar species with a high dipole moment (greater than 2 D) affect molecular interactions in the petroleum fluid and result in the formation of micelles. Therefore, resins act as natural dispersants of asphaltenes because of their polar character. A viable option for the inhibition of asphaltene precipitation is the mixing of resins or some dispersants with the petroleum fluid in a batch process. Yet, field data show that in some cases the resins and dispersants not only do not inhibit precipitation; they may also promote it. The study of the effect of resins and chemical dispersants on precipitation contributes significantly into the understanding of molecular interactions in petroleum fluids. Such interactions are believed to be key elements for proper modeling of asphaltene precipitation. Presently, most models fail to predict precipitation because they do not take into account the interactions involving polar molecules.

Generally, molecular interactions are classified into two types:

To appear in AIChE Journal in 2003

1) short-range, and 2) long-range interactions. Hydrogen bonding, charge transfer, and repulsion are short-range interactions while van der Waals interactions are long-range (Ratajczak and Orville-Thomas, 1980). The difference between short- and long-range interactions is mainly in the bond distance between interacting molecules. Short-range interactions occur when the bond distance between molecules is smaller than the sum of the van der Waals radii, resulting in an overlap between the electron clouds and the formation of molecular complexes (Ratajczak and Orville-Thomas, 1980). Hydrogen bonding consists of the sharing of a proton between the proton acceptor of a molecule and the anion derived from the proton donor of another molecule; charge transfer consists of the transfer of electrons between an electron donor and electron acceptor of two molecules (Huyskens *et al.*, 1991). The repulsion interaction is orientation-dependent and occurs when the electronic orbital of two approaching molecules begin to overlap noticeably (Israelachvili, 1991). The main contributions to the van der Waals interactions are: 1) electrostatic (orientation or dipole-dipole), 2) induction (Debye or dipole-induced dipole), and 3) dispersion (London or induced dipole-induced dipole) interactions (Maitland *et al.*, 1981). In electrostatic interactions, the rotating dipoles of two polar molecules interact by aligning into a favorable arrangement. Hydrogen bonding is no more than a particularly strong type of directional dipole-dipole interaction (Israelachvili, 1991). In induction interactions, the permanent dipole of a polar molecule distorts the electron charge distribution of a non-polar molecule and an induced dipole moment is created. In dispersion interactions, the instantaneous positions of the electrons around the nucleus protons of a molecule create a finite dipole moment, which in turn generates an electric field that polarizes a nearby molecule, inducing a dipole moment in it (Israelachvili, 1991).

It is believed that dispersion interactions affect asphaltene flocculation (Buckley *et al.*, 1998; Rogel, 2000). Electrostatic and induction interactions, on the other hand, help stabilize the asphaltenes in the petroleum fluid (Moschopedis and Speight, 1976; Bardon *et al.*, 1996; Li *et al.*, 1997). Murgich (2002) presented a comprehensive analysis on the intermolecular forces in aggregates of asphaltenes and resins and stated that the main contributions involved are the electrostatic, repulsion, and dispersion interactions. In this work, we will demonstrate that electrostatic interactions between asphaltenes and resins affect the precipitation. In order to understand the mechanism of asphaltene precipitation, it is primordial to analyze the effect of resins on asphaltenes and to define the main interactions involved.

Very few studies have delved into the effect of resins on asphaltene precipitation. The limited studies center around the effect of resins on the onset point of precipitation. In addition, the effect of resins on asphaltene precipitation is usually assessed after asphaltenes have been precipitated from petroleum fluids and solubilized in aromatic solvents. Murzakov *et al.* (1981) investigated the micellar stability of asphaltenes in benzene solutions by means of gravimetric sedimentation analysis and found that the addition of resins (2-8 wt%) to the solution decreased the amount of asphaltene precipitated by n-C_7. Lian *et al.* (1994) performed nC_5 precipitation tests from asphaltene/toluene solutions and found as well that addition of resins to the solution decreased the amount of asphaltene precipitated. Hammami *et al.* (1998) measured the onset point of asphaltene precipitation at ambient temperature and high pressure (690 kPa) and found that addition of resins with high content of basic functions to the petroleum fluid increased significantly the onset point of asphaltene precipitation by nC_5. Recently, Carnahan *et al.* (1999) reported that resins from Boscan petroleum fluid could increase considerably the onset point of asphaltene precipitation from Hamaca petroleum fluid, suggesting that resins from Boscan petroleum fluid are more effective than resins from Hamaca petroleum fluid. However, the reasons underlying this phenomenon were not discussed.

Structural investigations of the resin fractions have not been carried out to the same extent as those of asphaltene fractions. Because asphaltenes and resins are two contiguous classes of components separated from a continuum of molecules, they may have a similar structure. However, the difference in size, aromaticity, polarity, and physical appearance confer to asphaltenes and resins different properties (Speight, 1999). Spectroscopic investigations indicate the presence of hydroxyl groups, as well as ester, acid, and carbonyl functions in the resin fractions (Speight, 1999). It has been postulated that resins contain long paraffinic chains with naphtenic rings and polar functions (Wu *et al.*, 1998; Firoozabadi, 1999). This might confer to resins some of the properties of surfactants. By definition, a surfactant is a substance that lowers the surface tension of the medium in which it is dissolved (Hiemenz, 1986). Amphiphiles are the surfactants with molecules consisting of two parts: a polar head and a nonpolar long-chain hydrocarbon tail, each part has an affinity for different phases (Hiemenz, 1986). There have been several studies on the effect of amphiphiles on asphaltene precipitation. Chang and Fogler (1994) analyzed the effect of the structure of amphiphiles such as p-nonylphenol (NP) and dodecyl benzene sulfonic acid (DBSA) on asphaltene stabilization. They found that the polarity of the head and the length of the tail affect the effectiveness of the amphiphile and selected DBSA as the most effective stabilizer for asphaltenes. The effect of DBSA on asphaltene precipitation has been reported to be successful in some studies (Permukarome *et al.*, 1997; Rogel *et al.*, 2001; Al-Sahhaf *et al.*, 2002) and not so successful by others (Clarke and Pruden, 1998). Recently, Al-Sahhaf *et al.* (2002) investigated the effect of resins and various amphiphiles on the onset point of asphaltene precipitation. They confirmed the observations of Chang and Fogler and reported the effectiveness of dodecyl resorcinol (DB) and DBSA amphiphiles. The same authors also reported that larger amounts of resins are required to produce the same effect on the onset point as low concentrations of amphiphiles.

In a previous work (Goual and Firoozabadi, 2002), eight petroleum fluids were separated into asphaltenes, resins and oils. Asphaltenes were precipitated by nC_5 according to a modified Syncrude analytical method. The choice of nC_5 is preferred to nC_7 because the latter would leave the nC_5–nC_7 fraction of asphaltenes soluble with resins. The resins were separated using two different methods: 1) propane precipitation, and 2) ASTM D2007 adsorption method on attapulgus clay with different nC_5/toluene ratios to elute oils. The dipole moment was used as a criterion for the determination of resins in petroleum fluids. Results showed that propane precipitation separates only part of the resins (the most polar portion). The adsorption method gives true amount of resins provided no toluene is used to elute oils. Material balance calculations reveal that the total amount of losses including the resins irreversibly adsorbed on the clay is less than 1 wt%. Because the clay may cause chemical modification of the resin constituents, we have compared the resins adsorbed on clay and on silica gel and found that the resins recovered have the same properties. A full description of the separation procedure is provided in our previous publication (Goual and Firoozabadi, 2002).

In a previous work (Goual and Firoozabadi, 2002), the dipole moment (a measure of polarity) of asphaltenes, resins and oils was investigated for eight petroleum fluids. The dipole moment was found to increase sharply from oils (0-1 D) to resins (2.4-3.2 D) to asphaltenes (3.3-6.9 D). The measurements show that asphaltenes are more polar than resins in the same petroleum fluid, however resins of one petroleum fluid can be more polar than the asphaltenes in another petroleum fluid. Polar species with a high

dipole moment (greater than 2 D) affect molecular interactions in the petroleum fluid and result in the formation of micelles.

The main objective of this work is to examine the effect of resins with different concentrations and dipole moments on asphaltene precipitation from three petroleum fluids using nC_5 as a precipitant. Due to the complexity of interactions between asphaltenes and resins in a petroleum fluid, this study is conducted by keeping asphaltenes in their natural environment (i.e. in the petroleum fluid). We also study the effect of DBSA on asphaltene precipitation from the same petroleum fluids at different concentrations. The effects of resins and DBSA are compared and discussed. Another objective of this work is to unveil the differences between asphaltenes and resins in a petroleum fluid. Accordingly, we perform solubility tests on resins in different media and examine the effect of asphaltene addition to a petroleum fluid on precipitation from the same petroleum fluid.

Experimental

We used three different petroleum fluids (data are listed in Table 1) to investigate the effect of various resins and DBSA on asphaltene precipitation. The three petroleum fluids are medium mixed-base type and their chemical composition is provided in our previous paper (Goual and Firoozabadi, 2002).

Table 1. Petroleum fluids

Petroleum fluid	Density at 20°C (g/cc)	API gravity at 20°C	Asphaltene wt%	Resin wt%	R/A
U	0.8550	34	2.5	8.6	3.4
TK	0.8520	35	1.3	7.5	5.6
C	0.8588	33	2.3	6.5	2.8

The resins are separated by adsorption liquid chromatography (ASTM D2007) from petroleum fluids C, TK, U and are named after the respective petroleum fluids. Table 2 presents the dipole moment of the resins and the corresponding nC_5 asphaltenes. Resins C have the highest dipole moment while resins U have the lowest dipole moment. The effectiveness of resins is evaluated from the onset point of asphaltene precipitation as well as the precipitation amount.

Table 2. Dipole moment (in D) of asphaltenes and resins

Petroleum fluid	U	TK	C
nC_5 Asphaltenes	4.4	5.2	6.7
Resins	2.4	2.8	3.2

Precipitation data are measured with nC_5/petroleum fluid ratios varying from 1 wt/wt to 20 wt/wt. The resins are added to the petroleum fluids at three different concentrations. Prior to the precipitation tests, we measure the solubility of resins C in nC_5, oils C and petroleum fluid C, as well as the solubility of resins TK and C in petroleum fluids TK and C, respectively. The effect of asphaltenes U on precipitation by nC_5 from petroleum fluid U is measured and compared to that of resins U. In addition, precipitation measurements are performed with DBSA at concentrations of 0.3, 0.5, 1, 3, and 5 wt% in the petroleum fluid. We could not determine the dipole moment of DBSA by dielectric spectroscopy because of strong association in toluene even at very small concentrations.

Chemicals. The data for the chemicals used in this study are listed below.

- n-Pentane (nC_5): J. T. Baker, HPLC grade, MW = 72.15, purity > 99%, density at 25°C = 0.63 g/cm^3, water content = 0.01%.
- Toluene: J. T. Baker, HPLC grade, MW = 92.14, purity > 99.5%, density at 25°C = 0.87 g/ cm^3, water content = 0.05%.
- DBSA: TCI, MW = 326.5, purity = 95%, density = 1.0 g/ cm^3.

Equipment. The asphaltene filtration set-up consists of a filtration flask and funnel connected to a vacuum pump through rubber tubings. To avoid solvent infiltration into the pump, a trap is used at a temperature of –60°C to liquefy n-pentane in the air. Asphaltenes are filtered using a Whatman glass microfibre filter paper (7 mm diameter and 1.5 μm pore size). The weight is measured with a Sartorius analytical balance with an accuracy of 0.001 g.

Procedure. Resins and DBSA are first transferred in equal amounts into eight different flasks. The weight of resins and DBSA is measured and an appropriate quantity of petroleum fluid is added to each flask. The mixture is left for 24 hours then nC_5 is added in different proportions. The concentration of nC_5 is varied to provide the nC_5/petroleum fluid ratios of 1, 2, 4, 6, 8, 10, 15 and 20 wt/wt. After standing overnight, the mixtures are filtered and asphaltenes are washed extensively with nC_5 then dissolved in toluene. Once the solvent is evaporated, asphaltenes are dried and weighed. The procedure used to measure the amount of resins soluble in different fluids consists of mixing resins with each fluid at various concentrations (from 1 to 20 wt%) and recording, after several days, the amount of resins soluble in the fluid as a percent of total resins. The amount of insoluble resins is measured by taking into account the portion of resins that remain on the wall of the test tube as well as the amount filtered from the petroleum fluid. Note that the filtrate had the appearance of resins (brown, shiny and non-friable).

Results

We first present the results of resin solubility in different fluids. Once the solubility behavior of resins is defined, the effect of resins U, TK and C on precipitation from petroleum fluids U, TK and C at three concentrations is presented. To better illustrate the difference between asphaltenes and resins, the effect of asphaltenes U on nC_5 precipitation from petroleum fluid U is also described. We also measured, the effect of DBSA amphiphile on precipitation from all the petroleum fluids; the results are discussed and compared with those obtained with resins. All precipitation measurements are repeated a minimum of three times.

Resin solubility tests

Figure 1 presents the solubility of resins C in three different fluids: nC_5, oils C, and petroleum fluid C. The oils C represent the non-volatile fraction of saturates and aromatics in petroleum fluid C; this fraction is only 40% of the total oils. For all the three fluids, the amount of soluble resins increases with the fluid concentration. The measurements were repeated twice and the average value is plotted in Figure 1. For concentration higher than 90 wt% in the petroleum fluid and oils, resins are completely soluble, however resins become partially soluble for lower petroleum fluid and oils concentrations. Data show that when resins are mixed with a petroleum fluid or with oils at a concentration of 20 wt%, 14% of the resins are insoluble in the petroleum fluid and 6% are insoluble in oils. Resins are generally believed to be soluble in nC_5 but our results show that this is not the case even at a low resin concentration. Indeed, when 80 g of nC_5 is mixed with 20 g of resins, about 70% of the resins are soluble, that is only 14 g.

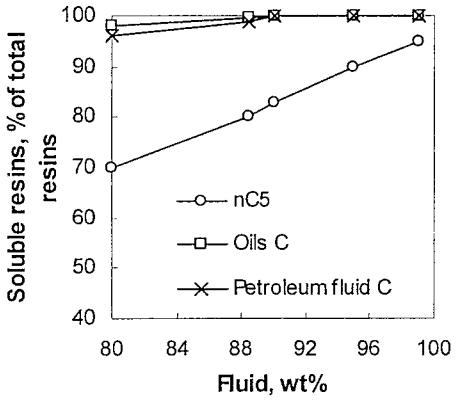


Figure 1. Solubility of resins C in nC_5, oils C and petroleum fluid C.

Figure 2 depicts the solubility of resins U, TK and C in petroleum fluid TK as well as the solubility in petroleum fluid C. Resins C are more soluble in the petroleum fluids than resins TK and U. In addition, resins U show the same solubility behavior as resins TK. This may imply that resins with a high dipole moment are more soluble in petroleum fluids than resins with a low dipole moment. In all cases, additional resins revealed to be completely soluble in the petroleum fluid at a concentration lower than 7 wt%.

Effect of resin concentration on asphaltene precipitation

Figures 3, 4 and 5 show the effect of resin amounts on precipitation by nC_5 from three different petroleum fluids. Resins are added to each petroleum fluid at three concentrations (see Table 3). In Figures 3-5, the thick solid curves represent the precipitation of asphaltenes from the petroleum fluids without resin addition.

Table 3. Concentration of additional resins in petroleum fluids U, TK, and C

Additional resins, wt%			Total resins, wt%		
U	TK	C	U	TK	C
0.0	0.0	0.0	8.6	7.5	6.5
1.9	1.7	1.6	10.5	9.2	8.1
3.8	3.4	2.9	12.4	10.9	9.4
14.7	13.0	11.5	23.3	20.5	18.0

Examination of the data in Table 3 and Figure 2 suggests that resins added at the first two concentrations are completely soluble in the petroleum fluid while resins added at the highest concentrations are partially soluble in the petroleum fluid. Indeed, asphaltene precipitated upon addition of low resin concentration do not have the same appearance as asphaltene precipitated upon addition of high resin concentration. In the first case, the precipitate is black, shiny and friable and resembles the asphaltenes precipitated from the petroleum fluids without resin addition. In the second case, the precipitate is brown, shiny and non-friable which reveals the presence of some resins with asphaltenes. Nevertheless, high resin concentrations are considered in order to examine the effect on the onset point of precipitation and the amount of precipitate. The main observation from Figures 3-5 is that the additional resins at low concentration increase the onset point of precipitation as well as the amount precipitated. The effect of resins on the onset point of precipitation at low concentration is in line with published data (Hammami *et al.*, 1998; Carnahan *et al.*, 1999). However, the increase in the amount of precipitation was not expected and has not been reported in the literature, to the best of our knowledge. Previous studies (Murzakov *et al.*, 1981; Lian *et al.*, 1994) examined the effect of resins on solutions of asphaltenes in aromatic solvents. In this study, we examine the effect of additional resins on precipitation

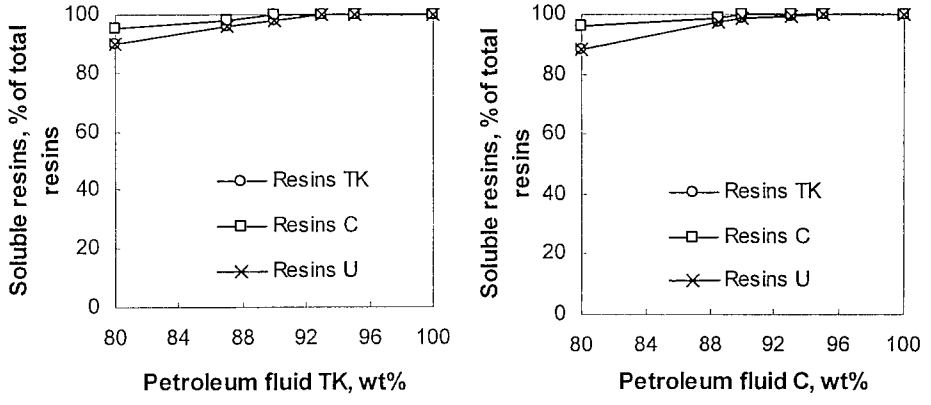


Figure 2. Solubility of resins in petroleum fluids TK and C.

from petroleum fluids. Our results reveal that asphaltenes interact differently with resins according to the medium in which they are present.

Figure 3 shows the effect of different concentrations of resins U on precipitation by nC_5 from petroleum fluid U. The increase in the amount of precipitation is proportional to the concentration of additional resins and becomes substantial (about 89% difference) when the total concentration of resins in the petroleum fluid is 23.3 wt% instead of 8.6 wt% in the original petroleum fluid. On the other hand, the high resin concentration causes early precipitation. The precipitate is mainly composed of resins that are not soluble in the petroleum fluid (see Table 4).

Figure 4 portrays the effect of different concentrations of resins TK on precipitation by nC_5 from petroleum fluid TK. The same behavior as in Figure 3 is observed; the maximum precipitation of 3.3 wt% occurs with 13 wt% additional resins TK as compared to 1.3 wt% in the original petroleum fluid. At the high concentration, precipitation occurs upon resin addition.

Figure 5 depicts the effect of different concentrations of resins C on precipitation by nC_5 from petroleum fluid C. One can observe the high slope of the precipitation curve with the addition of small concentrations of resins, which increases the uncertainty in the reading of the onset points. Nevertheless, the effect of resins in increasing the onset point of precipitation is not substantial at low resin concentration. Also, the amount of precipitation does not increase appreciably with the addition of 11.5 wt% resins. At this concentration, the percent of soluble resins in the petroleum fluid is 99% for resins C and 97.5% for resins TK and U, leading to 0.29 wt% precipitated resins TK and U and 0.115 wt% precipitated resins C in petroleum fluid C as shown in Table 4. In other words with low resin concentration, the onset is moved to the right in Figure 5, however at high concentration the onset is moved to the left, similar to the results in Figures 3 and 4. This is also the first report in the literature of the effect of resins at high concentration on the onset point of precipitation.

Effect of various resins on asphaltene precipitation

Figures 6, 7 and 8 present the effect of additional resins on precipitation by nC_5 from three different petroleum fluids at different concentrations (see Table 3).

Figure 6 presents the precipitation results for petroleum fluid U after addition of various resins at two concentrations. The maximum increase in precipitation amount is with resins U and the minimum increase is with resins C. Thus, resins with a high dipole moment result in less precipitation than resins with a low dipole moment. In addition, the onset point of precipitation is higher upon addition of resins C and it is lower upon addition of resins TK and U. This suggests that resins with high dipole moment are more effective than resins with relatively low dipole moment in increasing the onset point of precipitation at low resin concentrations.

Figure 7 presents the precipitation results for petroleum fluid TK by the addition of resins at two concentrations. The same correlation between the amount/onset point of precipitation and the dipole moment of resins is found as with petroleum fluid U. At the two concentrations of resins, comparable effects on the amount of precipitate are observed for resins U and TK and for resins C; the highest amount of precipitate corresponds to addition of resins with the lowest dipole moment (i.e. resins U). The effect of resin dipole moment on the onset point is also noted. A gradual increase in the onset point is obtained with increasing dipole moment of resins and a maximum value of about 1.8 wt/wt is found upon addition of 1.6 wt% of resins C as compared to 0.3 wt/wt in the original petroleum fluid.

Figure 8 depicts the precipitation results for petroleum fluid C after addition of resins at two concentrations. Petroleum fluid C contains approximately the same amount of nC_5 asphaltenes as petroleum fluid U; however, the effect of resins on the two petroleum fluids is different. The first observation is the contrast in the amount of precipitation between resins TK and U and resins C. Addition of 11.5 wt% resins C to petroleum fluid C slightly increases the amount of precipitation, however the amount becomes significant with resins TK and C and reaches 4.9 wt% with resins U. It is also found that resins U do not affect much the onset point of precipitation when added at low concentration.

Comparison of the results reveals that the difference in the amount precipitated with the addition of resins at low concentration increases from petroleum fluid U to petroleum fluid TK to petroleum fluid C as shown in Figure 9. Thus, the increase in precipitation is more pronounced when the dipole moment of asphaltenes in the petroleum fluid is high. On the other hand, resins C (with the highest dipole moment) are the most effective with respect to the change on the onset point of precipitation in all petroleum fluids, and result in the least increase in precipitation.

Effect of additional asphaltenes on asphaltene precipitation

Figure 10 shows the effect of adding asphaltenes U on precipitation from petroleum fluid U. Results are shown for two concentrations of additional asphaltenes: 0.6 wt% and 4.8 wt %. For comparison purposes, we also include in the same figures the results of resin addition at two concentrations: 1.9 wt% and 14.7 wt%. In Figure 10, the addition of 0.6 wt% of asphaltenes increases the amount of nC_5 precipitate from 2.5 to 3.3 wt%, which is 12% higher than the amount precipitated with the addition of 1.9 wt% of resins. For higher concentration of asphaltenes (i.e. 4.8 wt% asphaltene increase), results are substantially different. Prior to nC_5 dilution, only 44% of additional asphaltenes are soluble in the petroleum fluid, that is 2.1 wt%. The amount of precipitate by nC_5 is about 7.5 wt%, almost three times higher than the original amount in the petroleum fluid and considerably higher than the amount obtained with the addition of 14.7 wt% of resins. The addition of asphaltenes and resins at low concentration to a

Table 4. Resin precipitation from petroleum fluids U, TK and C

	Petroleum fluid U			Petroleum fluid TK			Petroleum fluid C		
	Additional resins			*Additional resins*			*Additional resins*		
	U	TK	C	U	TK	C	U	TK	C
Additional resins, wt%	14.7	14.7	14.7	13.0	13.0	13.0	11.5	11.5	11.5
Petroleum fluid, wt%	85.3	85.3	85.3	83.0	83.0	83.0	88.5	88.5	88.5
	Resin precipitate								
% of additional resins*	4.0	4.0	2.0	4.0	4.0	2.0	2.5	2.5	1.0
wt% "	0.59	0.59	0.29	0.52	0.52	0.26	0.29	0.29	0.115

* Determined from Fig. 2

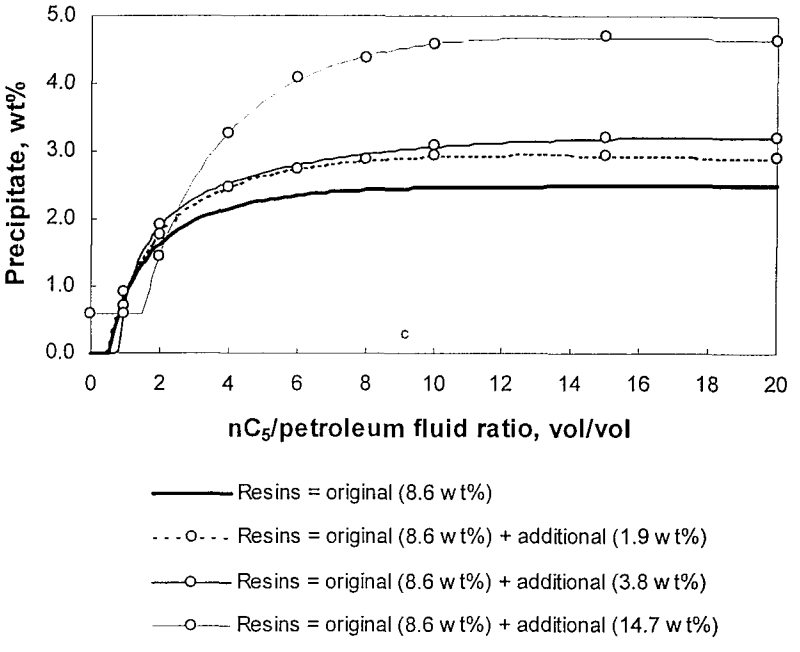


Figure 3. Precipitation by nC_5 from petroleum fluid U for various concentrations of resins U.

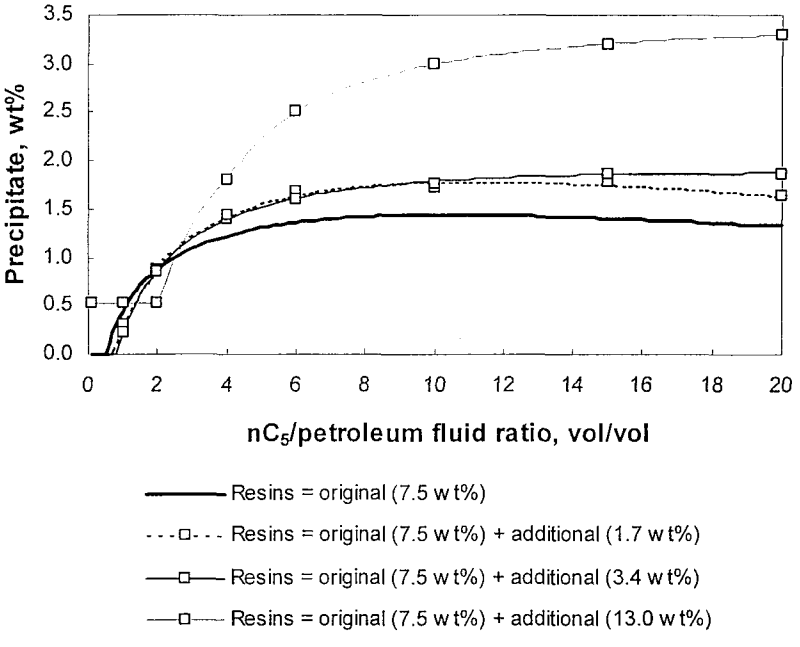


Figure 4. Precipitation by nC_5 from petroleum fluid TK for various concentrations of resins TK.

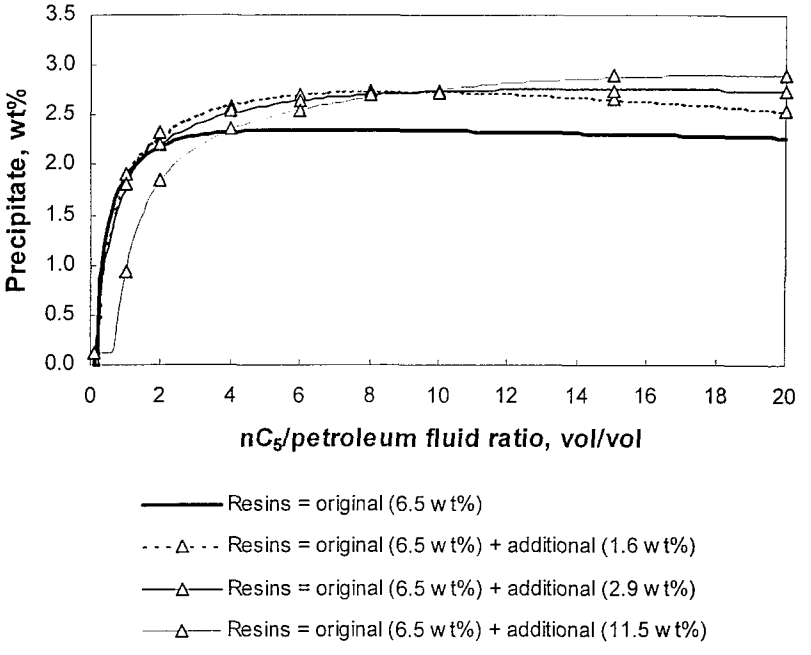


Figure 5. Precipitation by nC_5 from petroleum fluid C for various concentrations of resins C.

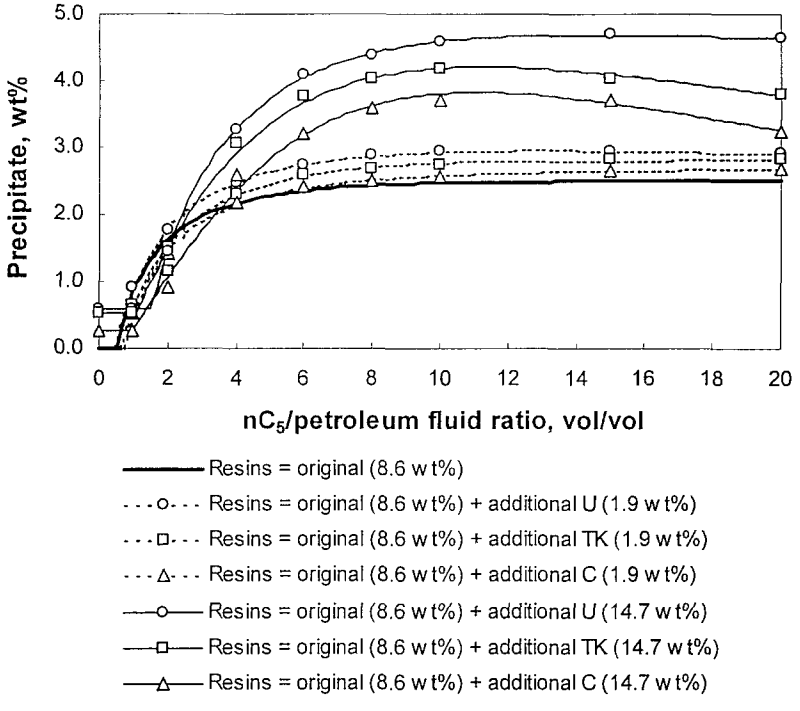


Figure 6. Precipitation by nC_5 from petroleum fluid U for various additional resins.

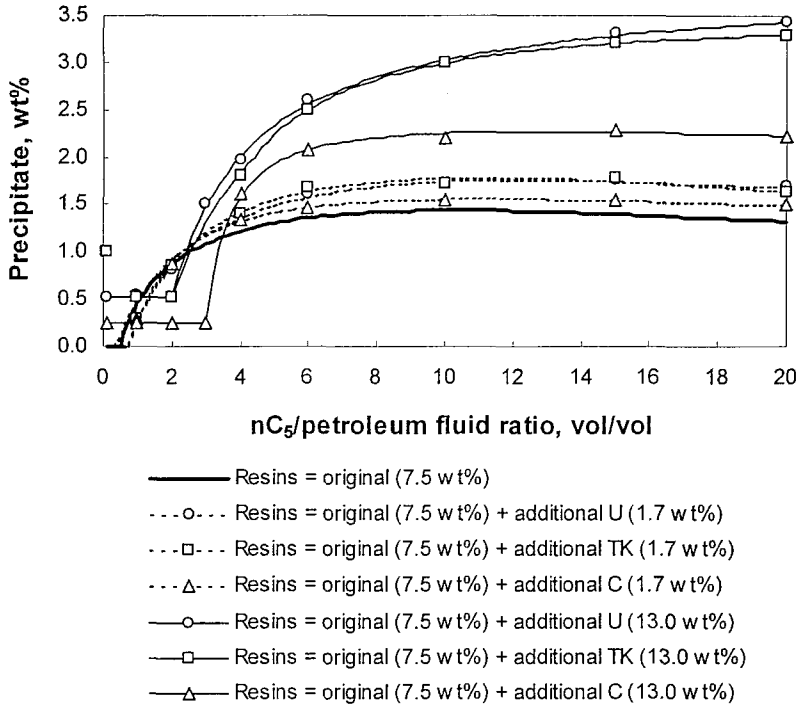


Figure 7. Precipitation by nC_5 from petroleum fluid TK for various additional resins.

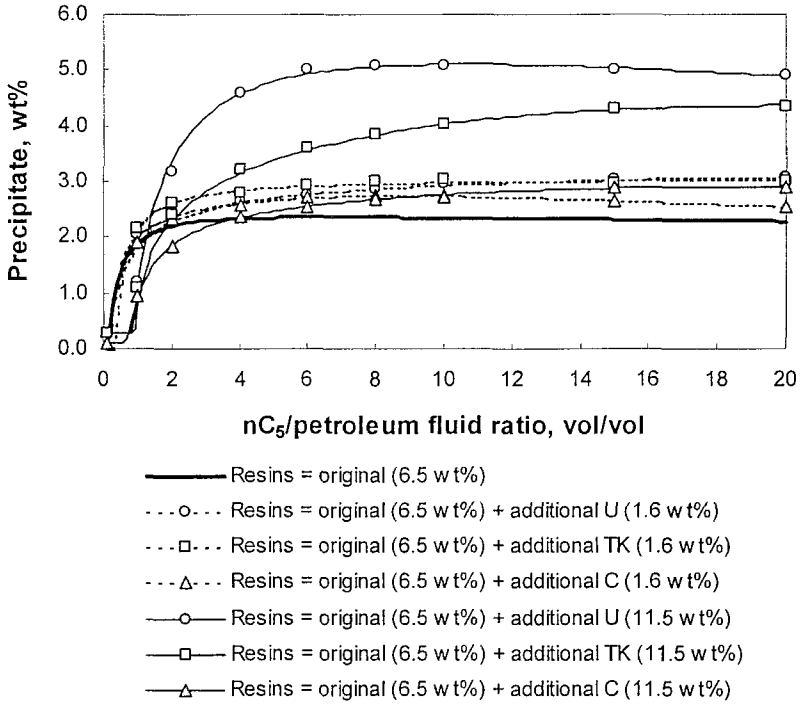


Figure 8. Precipitation by nC_5 from petroleum fluid C for various additional resins

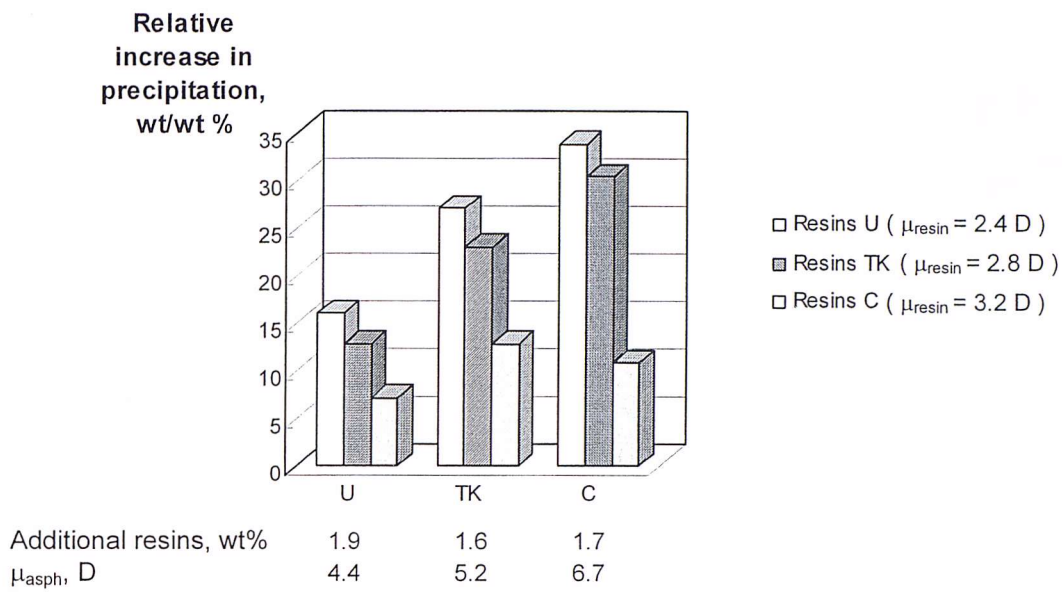


Figure 9. Relative increase in the amount of precipitation by nC_5 (nC_5/petroleum fluid ratio = 20 vol/vol) in petroleum fluids U, TK and C with additional resins. [Increase = 100 × (precipitate in fluid with additional resins – precipitate in original fluid) / precipitate in original fluid]

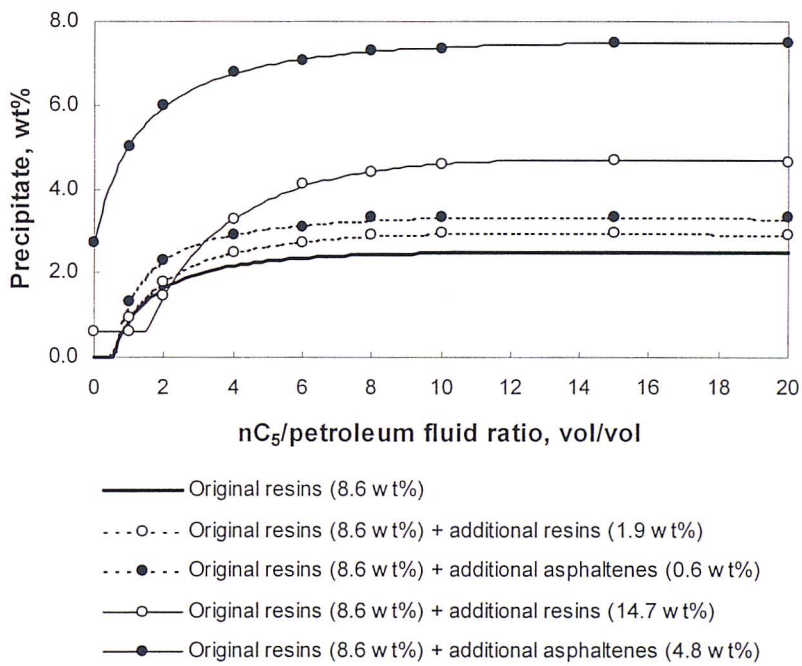


Figure 10. Precipitation by nC_5 from petroleum fluid U for various concentrations of resins and asphaltenes U

petroleum fluid has an opposite effect on the onset point of asphaltene precipitation. These observations along with solubility analyses corroborate the differences between asphaltenes and resins in the petroleum fluid.

Effect of DBSA on asphaltene precipitation

Figures 11–13 present the effect of DBSA on asphaltene precipitation from petroleum fluids U, TK and C, respectively. For each petroleum fluid, five precipitation measurements are made with nC_5 at different concentrations of DBSA. During our experiments, visual observations indicate that the amount of resinous material in the precipitate decreases when the concentration of DBSA is increased in the petroleum fluid. At 5 wt% DBSA in the petroleum fluid with an excess of nC_5, very small dark black and dispersed particles deposit on the bottom of the flask. The filtration of the precipitated solid does not require extensive washing with nC_5 indicating that the precipitate is almost resin-free.

Figure 11 presents the effect of DBSA on asphaltene precipitation from petroleum fluid U. It appears that the amount of precipitate depends on the concentration of DBSA in the petroleum fluid. At concentrations less than 1 wt%, the effect is similar to that of resins. Addition of 0.3, 0.5 and 1 wt% DBSA increases the amount of precipitate from 2.5 wt% to approximately 3 wt%. At these concentrations, the onset point of precipitation increases slightly with the concentration of DBSA. However, for concentrations above 1 wt%, the effect of DBSA on precipitation is different. The precipitation amount decreases with DBSA concentration to only 2.4 wt% when using 5 wt% amphiphile. Moreover, increasing the concentration of the amphiphile above 1 wt% has a significant effect on the onset point of precipitation. DBSA concentration of 3 and 5 wt% increases the onset point of precipitation from 0.4 wt/wt, to about 1.6 and 3.3 wt/wt, respectively. Thus, DBSA is a suitable stabilizer for asphaltenes at high concentrations.

Figure 12 presents the effect of DBSA on asphaltene precipitation from petroleum fluid TK, which follows the same pattern as in petroleum fluid U. At 1 wt% DBSA concentration in the petroleum fluid, the increase in the amount of precipitation is maximal and is almost two times higher than the original amount in the petroleum fluid. Conversely, a concentration of 5 wt% DBSA reduces precipitation considerably to 1.52 wt%, only 10% higher than the original amounts. As for the onset point of precipitation, DBSA shows high stabilization towards asphaltenes at increasing concentrations. The onset point increases significantly from 0.3 to 3.6 wt/wt at 5 wt% DBSA.

Figure 13 shows the effect of DBSA on asphaltene precipitation from petroleum fluid C. The effect of DBSA on precipitation is similar to that in petroleum fluid U. At different concentrations, the variation in precipitation is not high. The precipitation data are very close to each other especially when the concentration of DBSA is less than 1 wt%. In addition, the data show approximately the same onset point of precipitation. However at 3 wt% and 5 wt% DBSA, the onset point is increased from 0.05 wt/wt, to about 0.5 and 1wt%, respectively.

Comparison of the amount of precipitation from the three petroleum fluids is presented in Figure 14. One can observe the increase in precipitation with increasing concentration of DBSA amphiphile first and then decrease in precipitation. Differences with original amounts are approximately the same for petroleum fluids U and C, but much higher for petroleum fluid TK. Furthermore, for DBSA concentration less than 1 wt%, the effect of DBSA on precipitation is similar to that of resins and it is likely that the interaction of DBSA and resin molecules are the same with other species. However at greater concentrations, due to their high polarity, DBSA molecules may interact with themselves and with resins and asphaltenes through a different mechanism. The reasons underlying the effect of DBSA amphiphile on asphaltenes in petroleum fluids are the subject for future studies.

Electrostatic vs. London interactions

A new finding in this work from the effect of dipole moment of resins and asphaltenes on precipitation is that, the electrostatic interactions may not be negligible. Let us calculate the relative contribution of the electrostatic and dispersion interactions between asphaltene molecules in a solvent medium using the van der Waals interaction energy U given by (Israelachvili, 1991),

$$U_{a-a}(r) = -\left\{ 3kT\left(\frac{\varepsilon_a - \varepsilon_s}{\varepsilon_a + 2\varepsilon_s}\right)^2 + \frac{\sqrt{3}h\nu_e}{4}\frac{\left(n_a^2 - n_s^2\right)^2}{\left(n_a^2 + 2n_s^2\right)^{3/2}}\right\}\frac{R_a^6}{r^6} \quad (1)$$

and between asphaltene and resin molecules in a solvent medium given by (Israelachvili, 1991),

$$U_{a-r}(r) = -\left\{ 3kT\left(\frac{\varepsilon_a - \varepsilon_s}{\varepsilon_a + 2\varepsilon_s}\right)\left(\frac{\varepsilon_r - \varepsilon_s}{\varepsilon_r + 2\varepsilon_s}\right) + \frac{\sqrt{3}h\nu_e}{2} \frac{\left(n_a^2 - n_s^2\right)\left(n_r^2 - n_s^2\right)}{\left(n_a^2 + 2n_s^2\right)^{1/2}\left(n_r^2 + 2n_s^2\right)^{1/2}\left(\left(n_a^2 + 2n_s^2\right)^{1/2} + \left(n_r^2 + 2n_s^2\right)^{1/2}\right)}\right\}\frac{R_a^3 R_r^3}{r^6} \quad (2)$$

where the subscripts a, r, and s refer to asphaltenes, resins and solvent, respectively, ε is the dielectric constant, n is the refractive index, R is the molecular radius, r is the distance between polar molecules (asphaltenes or resins) and solvent interacting molecules, k is the Boltzmann constant, h is the Planck constant, T is the absolute temperature and ν_e is the absorption frequency. The product $h\nu_e$ is called ionization potential I, and a typical value of I in the UV range is 2×10^{-18} J (Israelachvili, 1991). We assume here that asphaltenes, resins, and the solvent medium have the same absorption frequency. In the brackets, the first term in the right-hand side of Eqs. (1) and (2) represents the electrostatic interactions and the second term represents the London dispersion interactions. We will calculate the contribution of each term in the total van der Waals interactions and compare them. At a temperature of 298 K, the dielectric constant of asphaltenes can be as high as 18.0, and the refractive index is approximately equal to 1.7, the dielectric constant of resins is about 4.5, and the refractive index is equal to 1.6, the dielectric constant and refractive index of the petroleum fluid are approximately equal to 2.0 and 1.49, respectively (Goual and Firoozabadi, 2002). If we consider these values in Eqs. (1) and (2) then the first term in the right-hand side representing electrostatic interactions is equal to 0.65×10^{-20} J in Eq. (1) and 0.26×10^{-20} J in Eq. (2), and the second term representing London dispersion interactions is equal to 1.96×10^{-20} J in Eq. (1) and 1.036×10^{-20} J in Eq. (2). The sum of these two terms is equal to 2.61×10^{-20} J and 1.29×10^{-20} J in Eqs (1) and (2), respectively, and the ratio of the first term (electrostatic interaction) to the sum of the two terms is 0.25 for Eq. (1) and 0.20 for Eq. (2). Thus, electrostatic interactions represent 25 % of the total van der Waals interactions between asphaltene molecules, and 20 % of the total van der Waals interactions between asphaltene and resin molecules; which is significant and cannot be neglected.

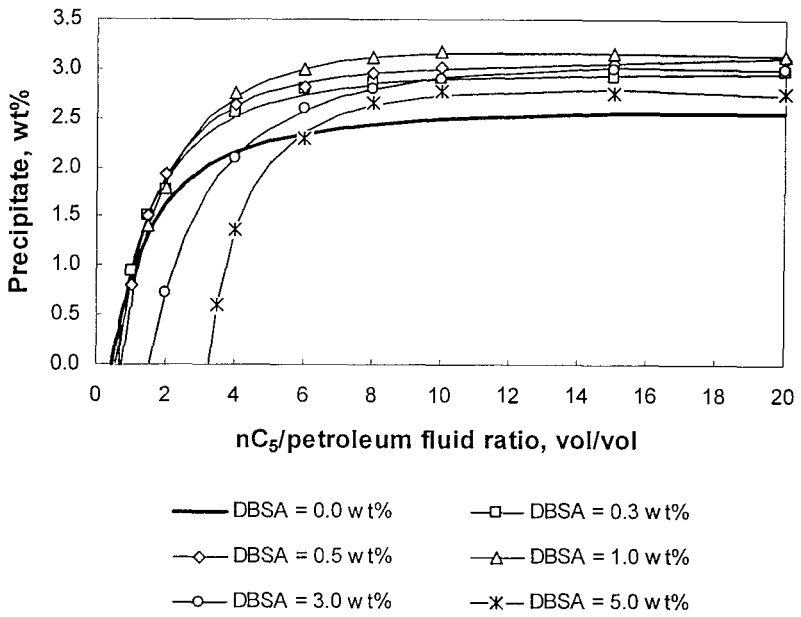


Figure 11. Precipitation by nC_5 from petroleum fluid U for various concentrations of DBSA.

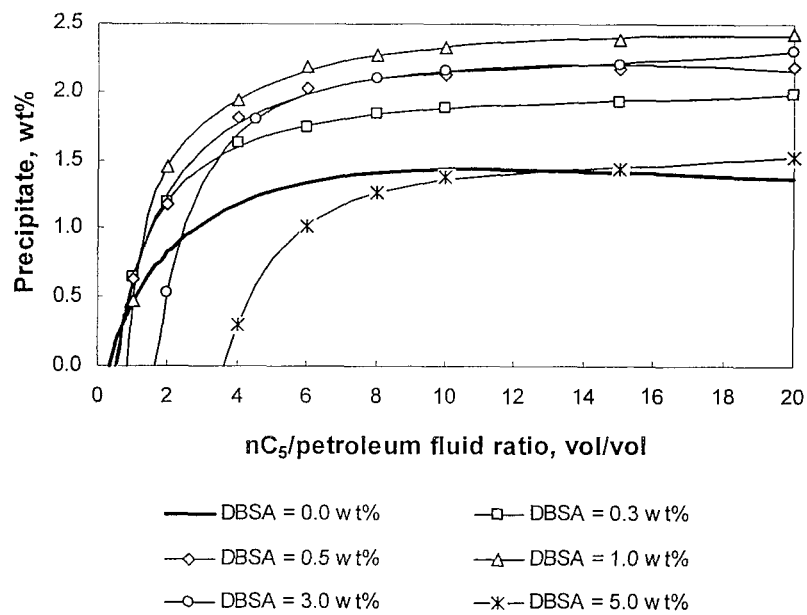


Figure 12. Precipitation by nC_5 from petroleum fluid TK for various concentrations of DBSA.

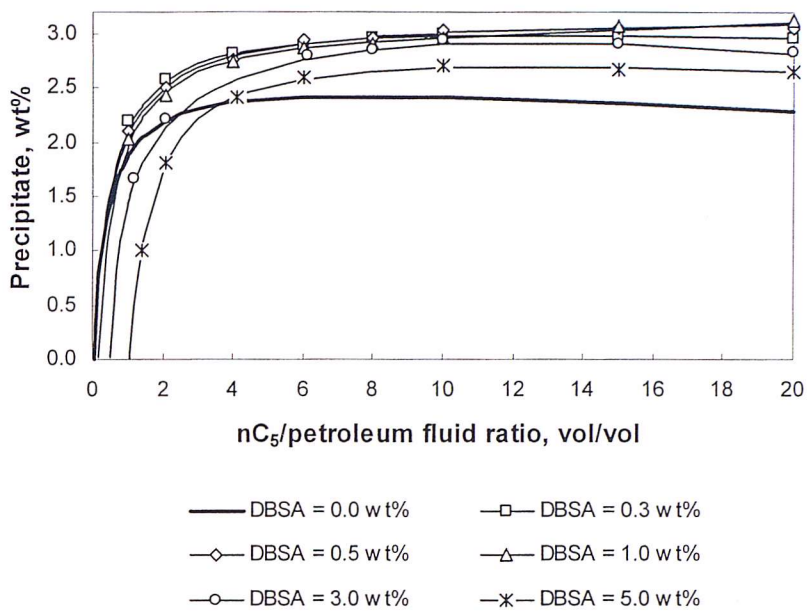


Figure 13. Precipitation by nC_5 from petroleum fluid C for various concentrations of DBSA.

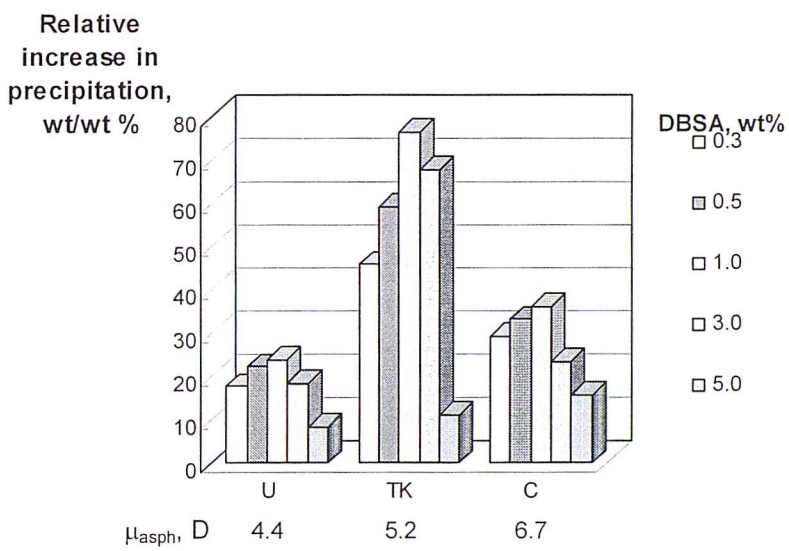


Figure 14. Relative increase in the amount of precipitation by nC_5 (nC_5/petroleum fluid ratio = 20 vol/vol) in petroleum fluids U, TK and C with various concentrations of DBSA. [Increase = 100 × (precipitate in fluid with DBSA – precipitate in original fluid) / precipitate in original fluid]

Conclusions

Based on the extensive and careful measurements reported in the paper, we draw the following conclusions.

1. Addition of resin to a petroleum fluid increases the amount of precipitation. Reported data in the literature indicate that resins decrease the amount of asphaltene precipitation. The effect of various resins on precipitation depends on the resin dipole moment. Resins with a high dipole moment do not increase the amount of precipitation significantly.

2. The increase in precipitation upon resin addition is more pronounced when the dipole moment of asphaltenes in the petroleum fluid is high.

3. The addition of the DBSA amphiphile on precipitation by nC_5 shows two different trends on the amount of precipitation. At low concentrations of DBSA, the amount of precipitation increases with increasing amphiphile concentration. This trend reverses with higher concentration (that is, as DBSA concentration increases, the amount of precipitation decreases). Therefore, before a certain concentration, the amphiphile is not effective.

4. Electrostatic interactions between polar molecules such asphaltenes and resins in a solvent medium may not be negligible in comparison to dispersion interactions.

Acknowledgments

This work was supported by the member companies of the Reservoir Engineering Research Institute (RERI). We thank Prof. J. M. Prausnitz (The University of California Berkeley) for his help and valuable comments during the course of this work.

Literature cited

Al-Sahhaf, T. A., A. F. Mohammed, and A. S. Elkilani, "Retardation of Asphaltene Precipitation by Addition of Toluene, Resins, Deasphalted Oil and Surfactants", *Fluid Phase Equilibria*, **194**, 1045 (2002).

Bardon, Ch.; L. Barre, D. Espinat, V. Guille, M. H. Li, J. Lambard, J. C. Ravey, E. Rosenberg, and T. Zemb, "The Colloidal Structure of Crude Oils and Suspensions of Asphaltenes and Resins", *Fuel Science & Technology International*, **14**, 1-2, 203 (1996).

Buckley, J. S., G. J. Hirasaki, Y. Liu, S. Von Drasek, J-X. Wang, and B. S. Gill, "Asphaltene Precipitation and Solvent Properties on Crude Oils", *Petroleum Science and Technology Int.*, **16**, 3-4, 251 (1998).

Carnahan, N. F.; J. L. Salager, R. Anton, and A. Davila, "Properties of Resins Extracted from Boscan Crude Oil and their Effect on the Stability of Asphaltenes in Boscan and Hamaca Crude Oils", *Energy & Fuels*, **13**, 2, 309 (1999).

Chang, C., and H. S. Fogler, "Stabilization of Asphaltenes in Aliphatic Solvents using Alkylbenzene-derived Amphiphiles. 1. Effect of the Chemical Structure of Amphiphiles on Asphaltene Stabilization", *Langmuir*, **10**, 6, 1753 (1994).

Clarke, P. F., and B. B. Pruden, "Asphaltene Precipitation from Cold Lake and Athabasca Bitumens", *Petroleum Science and Technology*, **16**, 3-4, 287 (1998).

Firoozabadi, A., *Thermodynamics of Hydrocarbon Reservoirs*, McGraw-Hill, New York (1999).

Goual, L., and A. Firoozabadi, "Measuring Asphaltenes and Resins, and Dipole Moment in Petroleum Fluids", *AIChE J.*, **48**, 11, 2643 (2002).

Hammami, A., K. A. Ferworn, J. A. Nighswander, S. Overa, and E. Stange, "Asphaltenic Petroleum fluid Oil Characterization: An Experimental Investigation of the Effect of Resins on the Stability of Asphaltenes", *Petroleum Science and Technology*, **16**, 3-4, 227 (1998).

Hiemenz, P. C., *Principles of Colloid and Surface Chemistry*, Marcel Dekker Inc., New York (1986).

Huyskens, P. L., W. A. P. Luck, and T. Zeegers-Huyskens, *Intermolecular Forces: An Introduction to Modern Methods and Results*, Springer-Verlag, Berlin (1991).

Israelachvili, J. N., *Intermolecular and Surface Forces*, Academic Press, San Diego (1991).

Li, S., C. Liu, G. Que, W. Liang, and Y. Zhu, "A Study of the Interactions Responsible for Colloidal Structures in Petroleum Residua", *Fuel*, **76**, 14/15, 1459 (1997).

Lian, H., J. -R. Lin, and T. F. Yen, "Peptization Studies of Asphaltene and Solubility Parameter Spectra", *Fuel*, **73**, 3, 423 (1994).

Maitland, G. C., M. Rigby, E. B. Smith, and W. A. Wakeham, *Intermolecular Forces: Their Origin and Determination*, Clarendon Press, Oxford (1981).

Moschopedis, S. E., and J. G. Speight, "Investigation of Hydrogen Bonding by Oxygen Functions in Athabasca Bitumen", *Fuel*, **55**, 3, 187 (1976).

Murgich, J., "Intermolecular Forces in Aggregates of Asphaltenes and Resins", *Petroleum Science and Technology*, **20**, 9-10, 983 (2002).

Murzakov, R. M., S. A. Sabanenkov, and Z. I. Syunyaev, "Influence of Petroleum Resins on Colloidal Stability of Asphaltene-containing Disperse Systems", *Z. I. Khim. Tekhnol. Topl. Masel*, **10**, 40 (1981).

Permsukarome, P., C. Chang, and H. S. Fogler, "Kinetic Study of Asphaltene Dissolution in Amphiphile/Alkane Solutions", *Industrial & Engineering Chemistry Research*, **36**, 9, 3960 (1997).

Ratajczak. H., and W. J. Orville-Thomas, *Molecular Interactions*, Vol. 1, John Wiley & Sons, Bath, UK (1980).

Rogel, E., "Simulation of Interactions in Asphaltene Aggregates", *Energy & Fuels*, **14**, 566 (2000).

Rogel, E., O. Leon, J. Espidel, and Y. Gonzales, "Asphaltene Stability in Crude Oils", SPE paper 72050 presented at the SPE Production & Facilities Conference (2001).

Speight, J. G., *The Chemistry and Technology of Petroleum*, Marcel Dekker, NY (1999).

Swanson, J. M., "A contribution to the Physical Chemistry of the Asphalts", *Journal of Physical Chemistry*, **46**, 141 (1942).

Wu, J., J. M. Prausnitz, and A. Firoozabadi, "Molecular-Thermodynamic Framework for Asphaltene-Oil Equilibria", *AIChE journal*, **44**, 5, 1188 (1998).